PLANT ROOT STUDY IN AGRICULTURAL SETTINGS WITH THE USE OF GEOPHYSICAL METHODS

By

ALEXANDRA GEORGIANA GEREA

A thesis submitted to
The University of Birmingham
For the degree of
DOCTOR OF PHILOSOPHY

School of Engineering
College of Engineering and Physical Sciences
University of Birmingham
May, 2022

ABSTRACT

The thesis represents a multidisciplinary approach to explore how geophysical methods can analyse plant roots in agricultural settings. It delves into the study of plant roots, examining their varieties, complexities, and significance in agriculture, as well as their behaviours. This is followed by an examination from the perspective of the geophysical methods, more specific ground penetrating radar (GPR) and resistivity, focusing on the methods themselves, the theoretical aspects, and a literature review of their application in agriculture, soil, and root studies.

The goal was to lay the groundwork for conducting geophysical surveys in actual agricultural contexts and to comprehend root behaviours through the lens of geophysical methods, taking into account their biological and physical complexity. The innovation comes from adapting the experimental settings so that they could come as close as possible to real-world agricultural environments and their specific characteristics, which could have practical applications in real world settings.

Direct measurements in the field were undertaken to understand the limitations and the behaviour of the environment and roots in a real world agricultural setting and thereby enhancing the application of geophysical methods. Both outdoor and indoor experimental surveys were conducted, under various conditions and types of plants using both the GPR and the resistivity methods.

Models were developed to not only understand the methods' limitations but also to simulate various conditions for better insight into root and soil behaviours when applying these

methods. A transparent soil was innovated and tested in the laboratory to improve correlation between objectives and data anomalies during resistivity surveys.

Various electrical devices were constructed and used, including the use of IoT sensors and a prototype for rapid resistivity surveys capable of collecting data from all the possible combinations of electrodes at different frequencies.

It has been observed that agricultural environments pose unique challenges and the use of high-frequency GPR antennas (1.5 GHz and 4 GHz) or small electrodes closely spaced entails limitations in real-world agricultural settings. However different areas have been highlighted and correlated with the root area but no individual roots of the agricultural plants with fine roots.

The models have allowed to understand how the resistivity areas modify the way root areas can be detected, and different arrays being more suitable for these kind of studies, whereas from the point of view of the GPR method the limitations appearing when the roots have closer permittivity values to the soil which represents a very plausible and common limitations.

The study suggests a shift in focus from individual roots to active root zones, understanding their dynamic behaviours influenced by environmental variables (e.g., watering or soil drainage). Roots are living objectives which grow, change paths, tend to absorb moisture around their roots, etc. all of these changing the way they can be identified with geophysical methods in different scenarios. More prominent observations have been made especially with the resistivity method where roots can change the resistivity values of the soil they grow in and its surroundings depending on watering time and drainage.

DEDICATION

To my family, my friends and my cats that have supported me in this journey so far away from home.

ACKNOWLEDGEMENTS

I would like to express my gratitude to my supervisor, Professor Phil Atkins, for providing me with the opportunity to study and conduct research at a renowned university. I am equally thankful to my co-supervisor, Dr. Farzad Hayati, for making this project possible and who has opened up the world of IoT devices and electronics to me. I am deeply grateful to Dr. Giulio Curioni for his support in learning to use new equipment and publishing new journal papers has been instrumental.

Many thanks to the management of the Winterbourne, Birmingham, and Bucharest Botanical Gardens for allowing me to conduct geophysical surveys on their grounds.

I would also like to acknowledge the GPR COST Action TU 1208 and all the individuals involved in the project and especially to Dr. Antonis Giannopoulos and Dr. Craig Warren, creators of the GPRMax software, for organizing invaluable GPR workshops and tutorials. My gratitude extends to Professor Andrew Binley from the University of Lancaster, the creator of the R2, R3 and reispy software for resistivity data processing and modelling, who has promptly answered my emails and questions.

Last but not least, Special thanks go to my colleague and partner, Dr. Andrei E. Mihai, who has supported me throughout my PhD journey. His help has been very important in improving my work and together, we have participated in numerous international conferences, created various projects, and contributed to journal papers. I extend my heartfelt thanks to my family for their support from afar. Even though they might not fully grasp the details of my work, their encouragement has been a cornerstone of my journey.

TABLE OF CONTENTS

TABLE OF FIGURES

LIST OF TABLES

Table 15. GPR models from A-H, and the parameters used in the models and their corresponding values: soil permittivity (ε) value, type of soil and its water content, root permittivity value, and the plant it belongs to, the root diameter and its water content, GPR antenna used, and the source of the parameter's information.

ABBREVIATIONS

GPR – Ground Penetrating Radar

TDR – Time Domain Reflectometry

ERT – Electrical Resistivity Tomography

C – Current electrode

P – Potential electrode

A, B – Current electrodes

M, N – Potential electrode

UTSI – UTSI Electronics Limited

BERT – Boundless Electrical Resistivity Tomography

NOTATIONS

α attenuation coefficient

ε dielectric permittivity

μ magnetic permeability

σ electrical conductivity

τ relaxation time

ω angular frequency

c speed of light in free space

D distance

f frequency

L length

R electrical resistance

t time

T temperature

v velocity

ρ resistivity

ρ_a apparent resistivity

1. INTRODUCTION

1.1 BACKGROUND

According to the latest UN projections (United Nations, 2022), the world population is expected to grow to 10 billion people by 2050, a significant change compared to the present population number of 7.9 billion people. This growth will bring major challenges for the agricultural sector, which will need to produce more food to feed these extra people. In addition, factors such as climate change or soil erosion will put even more pressure on global agriculture. Solutions such as indoor farming and precision agriculture are already developing, but it is unclear whether these efforts will be sufficient to feed the world's growing population.

Various multidisciplinary efforts are underway to address specific parts of this challenge, and geophysics can also play a role in improving agricultural outcomes (Allred *et. al*. 2010). In the past century, geophysical methods have been widely used in resource exploration (Reynolds, 1997; Telford, 1990) and in the study of the physical processes and properties of the Earth. Often, geophysical methods focus on large-scale geological structures (Elias, 2013) in the deeper parts of the Earth. However, in recent years, geophysics has diversified its scope and range of applications, increasingly focusing on near-surface objectives (Reynolds, 1997). Near-surface geophysics has been applied in a number of different applications, ranging from geo-hazards to archaeology as well as agricultural studies (Allred *et. al*. 2010).

By combining geophysical methods with soil studies and plant biology, agricultural studies can offer previously unavailable insights in agriculture and plant root studies. This work represents an interdisciplinary incursion into this field which tries to find and understand possible solutions to further explore this area of interest.

1.2. AIM AND OBJECTIVES

The main focus was to offer a better understanding of how geophysical methods can be used on a very small scale to explore the plant root extent and the area surrounding it in agricultural environments. For this to be achieved, the following main objectives have been identified and assessed:

- Choosing the geophysical methods that suit the target and objective of the study and adapt them to the target (size, physical parameters, geophysical parameters, etc.);
- Investigating and exploring the current knowledge through literature review on properties and techniques used in agricultural environments and in plant root studies from both the perspective of geophysical applications;
- Creating an experimental controlled environment, which can mimic as much as possible conditions from agricultural settings, allowing for flexibility in terms of data collection at any time;
- Developing necessary electrical equipment, with focus on low costs, which will aid the surveys and can also be applied in practical scenarios – the practical aspect would also

be able to help communities in lower developed countries to carry out surveys and study plants in agricultural environments;

- Creating models for the geophysical methods used for a better understanding on how to apply the methods and to highlight any limitations;
- Conducting surveys in both experimental settings and real world settings to understand limitations and how to better apply the methods to offer a practical solution for real world applications.

1.3. LAYOUT OF THE THESIS

The thesis is structured in five major chapters. The first chapter starts with the introduction, and lays out the aims and objectives of the paper and the layout of the thesis. Chapter 2 is mainly divided in three larger sections covering the literature review and fundamentals about the two chosen geophysical methods (ground-penetrating-radar and resistivity); continues with notions on plant roots and soils, covering fundamental notions about root biology, agriculture and soils, including aspects about the novel use of transparent soils; the last part of the chapter focuses on the use of geophysical methods applied in agricultural and plants studies. Chapter 3 focuses on the methodology, which includes the choice of sensing technology, descriptions of the direct measurements and more details about the experimental settings used in the study for both outdoor and indoor surveys. The electrical equipment which was developed and used for this study is presented, followed by more details and description of the transparent soil and its use in the experiments. In chapter 4, aspects of the

data acquisition, processing and results are presented, from the surveys carried out in both experimental settings and real world settings, with resistivity and GPR methods. Synthetic models for both GPR and resistivity data were developed and further described. The final chapter, number 5, ends the thesis with the the discussion, conclusions and aspects related to future work.

2. THEORY AND LITERATURE REVIEW

2.1. INTRODUCTION

This chapter provides an overview of the theoretical foundations, the selection of sensing technologies, and the modern applications of the two geophysical methods used in this study: the resistivity method and ground-penetrating radar (GPR). Both sections follow a similar structure, covering relevant theoretical principles, equipment types, field methodology, elements of data processing and analysis, data interpretation, and conclude with notes on the methods' limitations, which are particularly relevant to this research. Following the theoretical aspects of the geophysical methods, the chapter proceeds to introduce fundamental concepts in plant root biology, soil studies, and agricultural settings. Additionally, it details more on the novelty of the transparent soils explored and utilized in this research. The final section delves into the application of geophysical methods within agricultural contexts and plant root studies. This section is treated distinctly, synthesizing concepts from the preceding discussions on geophysics, agriculture, and plant root biology. It serves as a literature review, presenting the current state of the art in the field.

2.2. GEOPHYSICAL METHODS

Throughout their history, geophysical methods and the equipment used to carry out these surveys have undergone a series of developments and changes, owed to better sensing

equipment and, more recently, to advancements in computational power and technologies. These developments have enabled the progress of geophysics at multiple levels (acquisition, processing, interpretation), even as the underlying physical processes have remained largely unchanged. These developments have also enabled geophysicists to apply these methods on smaller scales, pushing the methods to their physical limits and enabling them to draw even more information in a variety of environments, including environments not traditionally considered suitable for geophysics, while making the entire process faster and more reliable. For example, in the civil engineering sector, GPR is widely used in urban environments for locating pipes, cables, cracks in concrete, for inspecting the quality of roads and bridges etc. (Reynolds, 2011; Daniels, 2009; Benedetto *et.al* 2016; Annan, 2009; Jol, 1995); in archaeology, the geophysical methods (especially magnetic, resistivity, and GPR) are successfully used to detect buried features, walls, kilns, and other historical features at a much faster pace compared to traditional archaeological methods (digging); finding water beds in areas affected by drought and severe climate conditions (usually with the help of resistivity surveys), etc.

Nowadays, geophysical methods represent one of the most reliable, non-invasive, and non-destructive way of measuring and scanning the underground for a variety of sectors with a scale ranging from kilometres to centimetres (Reynolds, 1997).

Despite all this progress, however, there are still significant challenges when it comes to adapting and using geophysical methods -- and one such example is the use of geophysical methods in the agricultural sector (Allred *et.al* 2016). While a variety of methods have already been used and adapted to detect and map water coverage in agricultural fields, the

spread of fertilizers and the quality of soils, etc. (Allred *et.al.* 2016), numerous challenges still remain. In addition, there is an impetus to stretch the applicability of the methods to even more areas, as it is the case of studying the plant roots and plant root areas of the plants and crops in general.

A key advantage of geophysical methods, especially in the context of agricultural measurements is that they are non-invasive and non-destructive. In addition, that data collection is relatively fast compared to traditional methods and results (Allred *et al.*, 2016).

In general, geophysical methods rely on detecting physical contrasts between the physical properties of the objectives (resistivity, magnetic susceptibility, permittivity, etc.) and the surrounding subsurface of the materials in the subsoil (Reynolds, 2011). A stronger contrast is desirable for a better imaging of the subsoil and understanding of the internal structure and objects, but in practice, this is not always the case.

Because each method measures on one physical parameter, it has become relatively common for more than one method to be used (Reynolds, 2011), to complement each other and to offer a better interpretation of the data representing the information from the underground.

According to Allred et al (2008) the geophysical methods that have been used successfully and widely in the agricultural sector is represented by the following:

- ***The geolectrical method***: typically uses electrodes to inject current into the ground and measure the potential difference between specified electrodes, being dependant on resistivity contrasts between the objects into the ground and the surrounding environment, and the configuration of the electrodes at the surface.

- ***Electromagnetic induction methods***: measures the conductivity of a shallow area beneath the surface using the electromagnetic induction between two small wire coils at a fixed distance between them.
- ***Ground penetrating radar method***: transmits a signal into the ground with the help of a transmitting antenna and records the signal which is reflected from the objects in the ground with different permittivity values, while the antennas are pulled over the ground.
- ***The magnetic method***: focuses on contrasts of specific magnetic susceptibilities of the objects into the ground.
- ***Self-potential method***: measures the natural electric potential in the area of interest.
- ***Seismic method***: transmits elastic waves into the ground which are generated by a source (explosive, impact, or vibratory). Similar to the GPR method, receptors (geophones) record the signal reflected from the objects with different elastic parameters.

From the variety of methods that are used in agricultural studies, in the following chapter, only the ground penetrating radar and resistivity methods will be described in full detail, as they represent the methods which were found to be best suited for the subject of this thesis, based on the literature review. They were also chosen based on the literature review described in chapter 2.4. These methods proved to have a good enough resolution to address the problem of the root area in agricultural plants and they are not only efficient in ideal settings but are also efficient in real world settings. Another advantage is their reliability and the fast pace at which the surveys are executed; in addition, they appear suitable for the detection of the type of contrasts that root areas produce compared to their surroundings.

2.2.1. GROUND PENETRATING RADAR

While Ground Penetrating Radar method has its roots in the 1960's where it was used mostly in glaciological applications (Milsom, 2011), it has flourished in the past years with the development and availability of new technology and more programming power.

Now it is already a successful and widely used geophysical method in civil engineering surveys (Allred *et al.*, 2016), road assessments and utility detection (Annan, 2009). More recently it became a method of interest in studying soil quality in different agricultural environments (Benedetto, 2010) and even mapping tree roots in urban environments or orchards (Zhang *et al.*, 2019).

With the high availability of different types and variations of the equipment, the GPR method looks very promising in the agricultural studies as well, where it has application in vineyard soil variation distribution mapping for example (André *et al.*, 2012).

2.2.1.1. INTRODUCTION

GPR uses an electromagnetic signal that travels within the ground, which at the interference with an object or boundary with a different permittivity value one part of the signal reflects, and the remaining part of the energy travels further, following the same pattern until it attenuates. There are different types of equipment for GPR but in general, they all work on the same principle. The equipment is formed of two antennas, a transmitting and a receiving

antenna and a console that records the received signals. Signal processing in GPR is somewhat similar to seismic data processing, and sometimes, the same software can be used to process both types of data. The field methodology (Milsom, 2011) for GPR, like any other geophysical method, depends on the objective, environment and degree of detail required. In principle, there is a trade-off between the investigated depth and the level of resolution (Annan, 2009).

Using GPR for plant root detection and characterization in agricultural environments is challenging and there is much room for improvement and innovation. GPR is one of the methods which usually produce much subsurface detail, as long as there is a good contrast in permittivity values, but this is not always the case in an agricultural setting. Below is a thorough description of the basic physical and mathematical principles of the method, continuing with general information regarding the equipment, followed by data processing, interpretation methods, which are generally used in GPR studies but with a focus on the aspects that are used and described in this project.

2.2.1.2. BASIC PRINCIPLES

The radiation of the GPR is electromagnetic and the propagation of the waves is described by Maxwell's equations, where the electric component $\boldsymbol{E}$ and the magnetic component $\boldsymbol{H}$ are orthogonal, and the specific shape and size of the directivity pattern lobes are represented by functions of the dielectric constant of the medium in which the waves propagate (Jol and Smith, 1995).

Maxwell's field equations describe the physics of the electromagnetic fields, which describe the variation in time and space of the coupled electric and magnetic fields and also their interdependence. These equations describe the electro-magnetic energy storage and the dissipation process of the materials. The equations, in the differential form in time domain are as follows (Jol and Smith, 1995):

$$\bar{\nabla} \times \bar{E} = -\frac{\partial \bar{B}}{\partial t}$$

$$\bar{\nabla} \times \bar{H} = \bar{J} + \frac{\partial \bar{D}}{\partial t}$$

$$\bar{\nabla} \cdot \bar{D} = q$$

$$\bar{\nabla} \cdot \bar{B} = 0$$

Where:

- $\bar{E}$ represents the electric field strength vector ***(V/m)***;
- q is the electric charge density ***(C/m^3)***;
- $\bar{B}$ represents the magnetic flux density vector ***(T)***;
- $\bar{J}$ is the electric current density vector ***(A/m^2)***;
- $\bar{D}$ is the electric displacement vector ***(C/m^2)***;
- t is time ***(s)***;
- $\bar{H}$ represents the magnetic field intensity ***(A/m)***; (Daniels 2006)

$$D = \varepsilon E$$

$$J = \sigma E$$

$$\boldsymbol{B = \mu H}$$

Where $\boldsymbol{\varepsilon}$ is the permittivity of the materials, measured in ***F/m***; $\boldsymbol{\sigma}$ is the conductivity of the material in ***S/m*** and $\boldsymbol{\mu}$ is the permeability of the material in ***H/m*** (Jol and Smith, 1995).

An electromagnetic wave is transmitted from the antenna into the ground, and propagates over time in the form of a spherical wave front. The velocity at which the wave propagates into the ground is dependent on the electrical permittivity property of the material type in which it propagates, different materials having specific permittivity values. When it encounters a layer or an object/material that has a different permittivity (sometimes called different dielectric constant value in GPR practice), the wave changes direction and character, which is usually called scattering. The scattering of the energy depends not only on the specific dielectric values but also on the shape and size of the object, part of the wave reflecting back to the surface where the transmitting antenna receives the signal, while another part of the energy continues traveling further with a velocity depending on that specific object's material permittivity value.

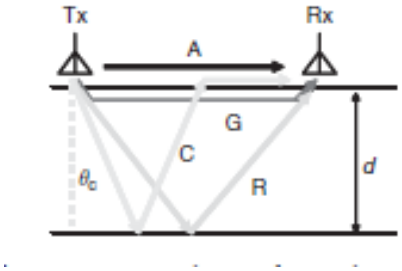

Figure 1. Signal paths between the transmitter and receiver (Jol and Smith, 1995).

The most important types of changes that the energy of the wave suffers at the incidence of two objects of materials with different permittivity values are (fig. 1): reflection, refraction, diffraction and resonant scattering (Allred *et al.*, 2016).

2.2.1.2.1 DIELECTRIC PROPERTIES OF THE MATERIALS

The properties of soils which affect the propagation and the attenuation of the electromagnetic waves are dependent on their composition and in particular, water content. The speed of the radio waves, $\boldsymbol{c}$, depends on three elements in a good conductor: the relative magnetic permeability $\boldsymbol{\mu_r}$ which has the value 1 for non-magnetic materials and the relative dielectric constant $(\boldsymbol{\varepsilon_r})$. This is independently on the type of the medium in which the radio waves are propagating. The real and imaginary components of the permittivity can be separated and result in the following equations, which results in the complex permittivity of the water (Jol and Smith, 1995):

$$\boldsymbol{\varepsilon'} = \boldsymbol{\varepsilon_\infty}^{\mathbf{1}} + \frac{\boldsymbol{\varepsilon_s} - \boldsymbol{\varepsilon_\infty}}{\mathbf{1} + \boldsymbol{\omega^2\tau^2}}$$

$$\boldsymbol{\varepsilon''(\omega)} = (\boldsymbol{\varepsilon_s} - \boldsymbol{\varepsilon_\infty}) + \frac{\boldsymbol{\omega\tau}}{\mathbf{1} + \boldsymbol{\omega^2\tau^2}}$$

First equation describes the permittivity real component and the second one the imaginary component, where:

-$\boldsymbol{\varepsilon_s}$ – is static, very low-frequency value of the permittivity;

-$\boldsymbol{\varepsilon_\infty}$ - very high-frequency value of the permittivity;

-$\boldsymbol{\tau}$ - permittivity relaxation time;

-$\boldsymbol{\omega}$ – angular frequency.

For GPR to be effective, the ground must be capable of supporting the propagation of radio waves. While some objects or layers may produce strong contrasts, other media like ice, can be "invisible" to the radio waves. Meanwhile, other types of environment like clays with a high degree of humidity or seawater can greatly attenuate the radio waves, up to the point where they become "opaque" to the radio waves (Daniels, 2006).

The amount of reflected energy is dependent on the radio wave velocity contrast and thus the contrast in the relative dielectric constant of two adjacent media. This ratio is the reflection coefficient $\boldsymbol{R}$.

The amplitude reflection coefficient is given by the following relations, where $\boldsymbol{V_1}$ *and* $\boldsymbol{V_2}$ are the velocities of the radio waves and $\boldsymbol{\varepsilon_1}$ *and* $\boldsymbol{\varepsilon_s}$ represent the relative dielectric constant, each corresponding to layers 1 and 2:

$$\boldsymbol{R} = \frac{(\boldsymbol{c_1} - \boldsymbol{c_2})}{(\boldsymbol{Vc_1} + \boldsymbol{Vc_2})} \; ; (\boldsymbol{V_1} > \boldsymbol{V_2})$$

$$\boldsymbol{R} = \frac{\sqrt{\boldsymbol{\varepsilon_2}} - \sqrt{\boldsymbol{\varepsilon_1}}}{\sqrt{\boldsymbol{\varepsilon_2} + \sqrt{\boldsymbol{\varepsilon_1}}}} \; ; \; (\boldsymbol{\varepsilon_1} < \boldsymbol{\varepsilon_2})$$

2.2.1.3. EQUIPMENT

Even though there is a great variety of equipment available on the market, the basic principle of operation is similar for all the GPR units. Usually, the differences between equipment from one company to the other amount to different materials for the antenna, and different data display and visualization capabilities (some units even allow the user to apply filters and gain functions from the recording stage). Some units have their own display system, while others rely on tablets and laptops for controlling the data acquisition and the parameters for data acquisition.

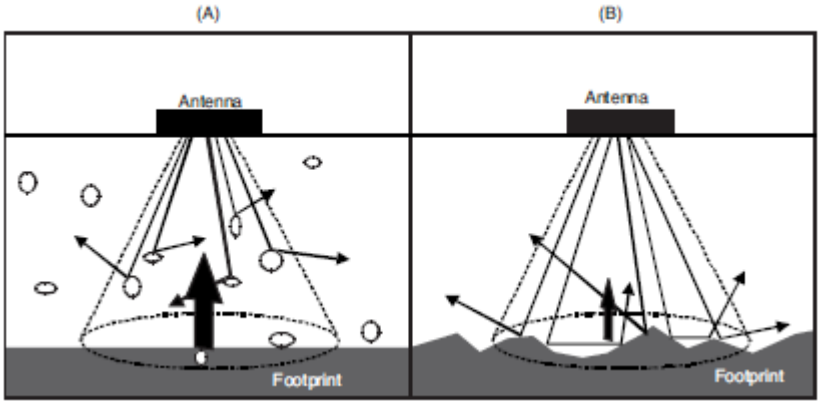

Figure 2. The antenna footprint and cone of influence. Details about the differences in reflection characteristics. A – scatterers are present, B – no scatterers. (Reynolds, 2011).

In general, the equipment can be divided in four parts: the antenna enclosure (containing the transmitter and the receiver), the console, the control unit, (sometimes the control unit and console are integrated) and a wheel equipped with an odometer-type sensor. Using accessories is common, and such accessories are chosen depending on the type of the surface, taking into

consideration different parameters of the survey: the shape and size of the surface area that needs to be prospected, the objective of the study, antenna type, etc., as well as environmental aspects (i.e. a solar or rain screen may be needed in some instances).

The antenna has a predefined central frequency and is usually slid over the ground with the minimal contact-gap (any pockets of air can create noise) (Conyers, 2004). For this type of survey a bow-tie antenna is used to maximise bandwidth. For antennas that take measurements above the ground (usually used for road or rails infrastructure measurements) the most commonly used type is a horn antenna (Rasol *et.al*. 2022).

The pre-set frequency of the antenna generally varies between 200 MHz and 8 GHz, and a general rule regarding antenna choice for a survey is that a higher frequency offers better resolution but lower depth of penetration, whereas a lower frequency offers a deeper depth of penetration at the expense of resolution (Daniels, 2006), and these aspects are related to the antenna footprint and cone of influence (fig. 2). The antenna footprint refers to the surface area on the ground directly above where the radar waves are being transmitted and received and determines the resolution and the extent of the ground surface that the radar can scan at any given moment (Conyers, 2011). The cone of influence, on the other hand, describes the shape and size of the subsurface volume that the radar waves penetrate and from which they can collect data. Shaped like an inverted cone, its size varies with the antenna's frequency and the permitivity of the ground; higher frequencies have narrower cones that are suitable for detecting smaller objects at shallower depths, while lower frequencies penetrate deeper but with less resolution (Conyers, 2004).

Figure 3. Example of a survey using a 400MHz antenna and a cart with 3 wheels. The console is covered with a plastic foil for protecting the console from rain.

The penetration depth and quality of the data are not only influenced by specific types of the antenna, but also by local environmental conditions. For example, a moist clay area will greatly attenuate the GPR signal, making the quality of the data much poorer, as will an imperfect soil-antenna coupling in the case of a bow-tie antenna (Conyers, 2011).

The console's role is usually for visualization purposes while recording the data, and most of the equipment systems offer real-time visualization of the data. The console is sometimes replaced with tablets or laptops for some systems, which tends to offer the advantage of lowering the cost of the overall system. Some display systems offer the possibility of changing different parameters before or during, the data acquisition process for visualization purposes or sometimes the data is even filtered during the data acquisition. However, it is not

necessarily advisable to apply permanent filters and gain function on the data at this initial stage, as it will affect the raw data in a way that cannot be undone at later stages (Conyers, 2011). It is good practice to have data in a raw form as much as possible, as filters and functions can always be applied after acquisition (Conyers, 2011). However, visualizing data at the acquisition stage can be useful for defining some acquisition parameters (fig. 3). Most of the times, the console and the control unit are in the same place.

Figure 4. Example of a survey using a 200MHz antenna and a single wheel. One person drags the antenna and the other is controlling the console.

The role of the control unit is to communicate and control the antenna, being responsible of collecting and storing the data.

The survey wheel varies in shape and size, and it usually has an odometer attached to it, for registering the distance of the surveying profile (fig. 4). Different types of wheels are usually chosen based on the type of surface on which the surveys are carried on, rougher surfaces needing larger wheels for example. Some devices even allow the addition of more than one wheel, in the form of a cart with 4 wheels attached at each corner. The wheel is usually calibrated before every survey, as the different types of surfaces will have a different impact on the rotations of the wheel and small positioning errors may emerge, especially on rougher surfaces (Conyers, 2011).

2.2.1.4. FIELD METHODOLOGY AND DATA ACQUISITION

2.2.1.4.1. FIELD METHODOLOGY

One of the first steps when it comes to planning a GPR survey (fig. 5) is obtaining a good understanding of the type of objective that needs to get detected or surveyed and its expected parameters (shape, size, depth, material type/composition) as well as any information regarding the surrounding material's parameters (soil type, composition, humidity, etc.). A good understanding of the parameters of the objects and materials that might interfere with the quality of the survey (pipes, rocks, metallic objects, rebar etc.), is also important, as these might introduce unwanted noise or might overshadow the response we get from the object of interest.

Figure 5. Planning the survey grid using measuring tapes, with a 400MHz antenna.

Understanding the dimensions of the objective, its properties, as well as the properties of the environment in which the survey will be carried out, represents an important step in choosing the type of the antenna and planning the profiles. The antenna beam resolution (fig. 6) which determines the system's ability to distinguish between closely spaced objects or features within the subsurface is primarily influenced by the frequency of the antenna. Higher frequencies produce a narrower beam, which offers greater resolution and enables the detection of smaller features, albeit at a reduced penetration depth (Reynolds, 2011), whereas, lower frequencies have a wider beam, increasing the penetration depth but at the expense of resolution, making it challenging to resolve smaller details. The beam resolution is also affected by the permittivity of the soil or material being scanned, as this impacts the speed and attenuation of the radar waves (Reynolds, 2011).

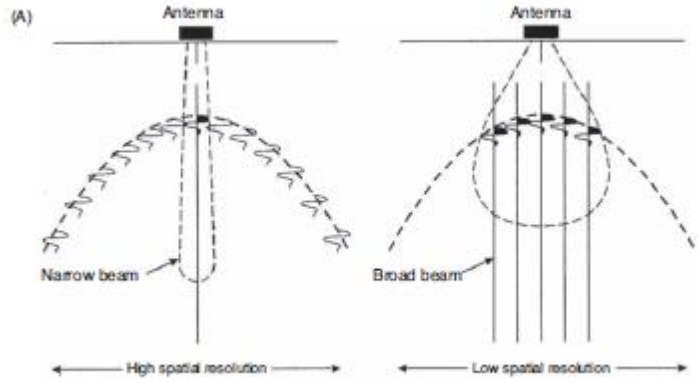

Figure 6. Image representing the horizontal resolution due to the beam width. (Reynolds, 2011).

Another important consideration before starting the survey is represented by the type of surface on which it will be carried out. Usually, a flat surface is desirable; if the measurements are going to be carried out over soil/grass, it is very important to ensure that the grass is short enough so it allows a good coupling of the antenna onto the soil surface and that the soil surface doesn't have any significant micro-topographical differences. If the survey takes place on concrete or other types of man-made materials, it is important again that the surface is smooth and any objects on the surface (like twigs or small rocks for example) be removed so they don't interfere with the antenna's coupling. A good antenna-surface coupling is essential for the signal to better penetrate the underground.

Regardless of the chosen or available type of GPR equipment, there are some pre-setup parameters that should be verified and potentially adjusted before starting a survey. In most of the modern equipment, these parameters are adjusted using software provided by the manufacturer. Doing these set-ups before starting a survey should take into consideration all of the above parameters, the objective of the survey, and should consider that some of the

changes made during this step might interfere with the data in a way that that cannot be undone later in the processing step. Some of these parameters will later be used in the data processing, therefore will be described further.

- ***Header information*** **-** includes elements such as date, site name, grid name/number, and other related information;
- ***Time window*** - represents the amount of time (measured in nanoseconds) in which the radar energy travels from the transmitter, reflects from the object and is recorded by the receiving antenna, and is usually referred as the two-way travel time. The window is open from the moment the electromagnetic pulse is transmitted until all the reflections of interest from the ground are received;
- ***Samples per reflection trace*** **–** represents the number of samples necessary to record a reflected waveform, where one sample is a digital value which defines a portion of the reflected waveform (Conyers, 2004). Therefore, more recorded samples generally result in an increased accuracy of the reflected wave that is recorded;
- ***Trace stacking*** - is a process that could be done either before the recording phase or later in the processing stage (which is generally recommended). This method arithmetically averages reflected traces at a specified distance along the profile;
- ***Transmission rate*** - this feature is important for the determination of the horizontal resolution of the recorded reflections. Due to the high degree of pulses transmitted by the radar systems and the speed at which the antennas must record each individual reflected trace by each transmitted pulse, the systems have the ability to sample incrementally (one pulse must be transmitted for each sample that is recorded);

- ***Time zero position -*** adjusting the time zero position represents an important step when setting the parameters for starting a new survey. For most GPR systems the direct wave, or the first reflection from the ground surface, when displayed, appears as the first large-amplitude wave after a period of no data recording (Conyers, 2004);
- ***Range gains*** – *(*can also be used in the processing stage) this function amplifies the recorded signal for better highlighting areas of interest;
- ***Vertical filters*** – (or bandpass filters) are applied in order to remove high and low frequency noise from the recorded information;
- ***Calibration - refers*** to the calibration of the wheel, which allows for better recordings of the distances of the profiles, based on the different types of surfaces on which the surveys are carried out.

2.2.1.4.2. DATA ACQUISITION AND VISUALISATION

After all the previous details have been established, the next step is represented by the data acquisition process itself. With the whole equipment set and ready to go, it's time to carry out profiles, usually in a straight line or a pre-defined grid (though other geometries can also be used, especially if high-precision, real-time positioning equipment is available). It is useful to mark the pre-established profiles either by marking it with paint, measuring tapes, laser levels etc. Usually, the data acquisition process requires two people for a survey, but some types of equipment allow one user to carry both the console and to drag or push the antenna on the surface of the ground. The surveys are carried out by controlling when to start and stop

recording, and the antenna is dragged or pushed on the ground. If the surveys are carried out in time mode, the speed at which the antenna is moved should be constant in order to allow for an accurate recording of the distance of the profile, if the survey is in distance mode (using the survey wheel), the antenna should move at a constant speed depending on the parameters previously described and established in the previous subchapter. However, surveys carried out in distance mode avoid this challenge.

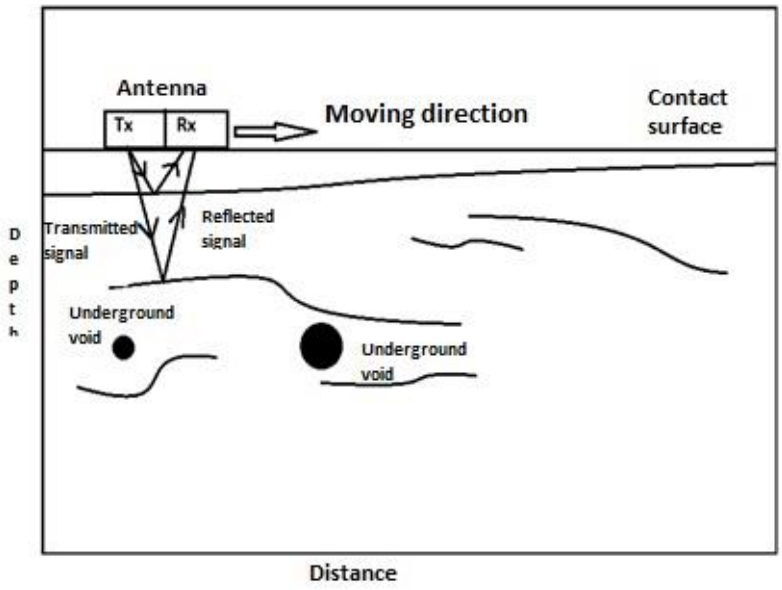

Figure 7. Representation of an antenna moved on a surface and the signal transmitted and recorded by the antenna. Reproduction after (Reynolds, 2011).

Fig. 7 highlights the way in which the surveys are carried out, with the transmitting and receiving antenna moving in a certain direction, having a good contact with the surface. The transmitted signal meets a boundary of two types of material with different permittivity values, and the signal reflects and is recorded by receiving antenna.

Fig. 8 highlights the antenna's cone of influence footprint, which has an ovoid shape (Jol and Smith, 1995). As a result, when the antenna is dragged on the surface, the cone of influence transmits and receives signal at different angles when the signal reaches an underground object.

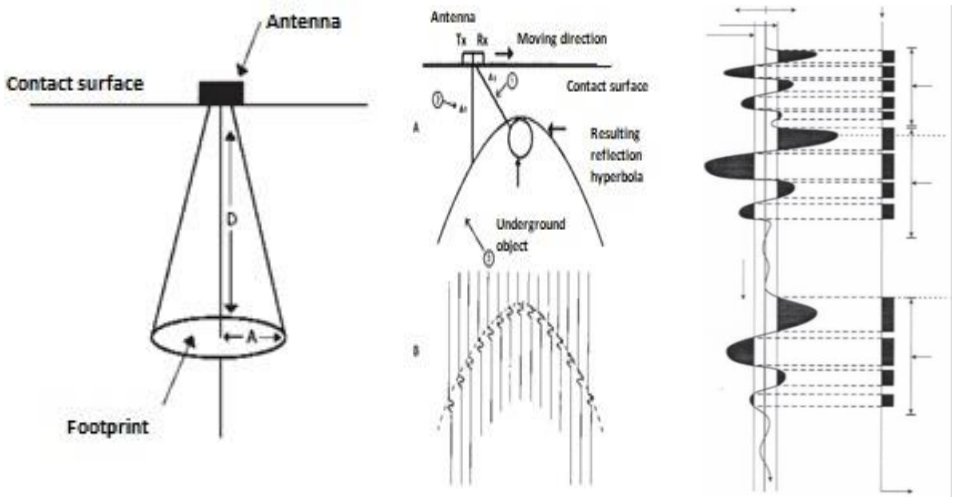

Figure 8. Left – the antenna with the cone of influence, and footprint; middle – the hyperbola resulted from moving the antenna on the surface; right – a recorded trace.

Therefore, most of the times the type of response that can be visualised on the registered radargrams, involve a variety of hyperbolas, and a distorted visualisation of the actual shape and size of the buried object. The recorded signal comes in the form of a trace, and more traces together are able to image features from the underground. These recorded traces altogether, on a profile are called radargrams. These represents the most used visualisation method of the GPR surveys, even though singular traces can be analysed individually, depending on the purpose of the study.

2.2.1.5. DATA PROCESSING

While data processing may share some similarities to the above-mentioned aspects, it is a separate stage. There is no “one size fits all” approach to GPR data processing, the filters and values of the applied processes applied are usually unique to the data set and dependant on the quality of the data (noise, interferences from unwanted or unknown objects, metallic objects, etc.), the type of the environment in which the surveys were carried out, and the objective of the survey. In order to obtain a qualitative interpretation, all the data must be processed in a way that improves the signal-to-noise ratio and removes unwanted types of noise, thus improving the overall quality of the radargram.

There are many types of algorithms and software available that make GPR data processing easier and faster. One of the widely used software for GPR data processing is ReflexW, a potent processing tool which is also the software used in this study.

An important factor regarding data processing is represented by the order in which the filters, corrections and other processing steps are applied, because some of these functions are used to remove information, while others are used to amplify the data, therefore it is very important to make sure that no important data is deleted and in the same time that the unnecessary data is not amplified.

The type of filters and functions applied depends on the type of data, the objective, the level of noise appearing in the data, etc. For example, features of interest in civil engineering projects (pipes, humidity, metallic objects, etc.) that usually need to get highlighted during

processing might be features that are intended for removal if the objective of the project is the detection of archaeological features.

There is a variety of ways in which these steps would be applied, but as a general rule of thumb, the following steps presented in figure 9 represent the most common order in which the raw radargrams are processed, even though these steps might change depending on the type and quality of the data:

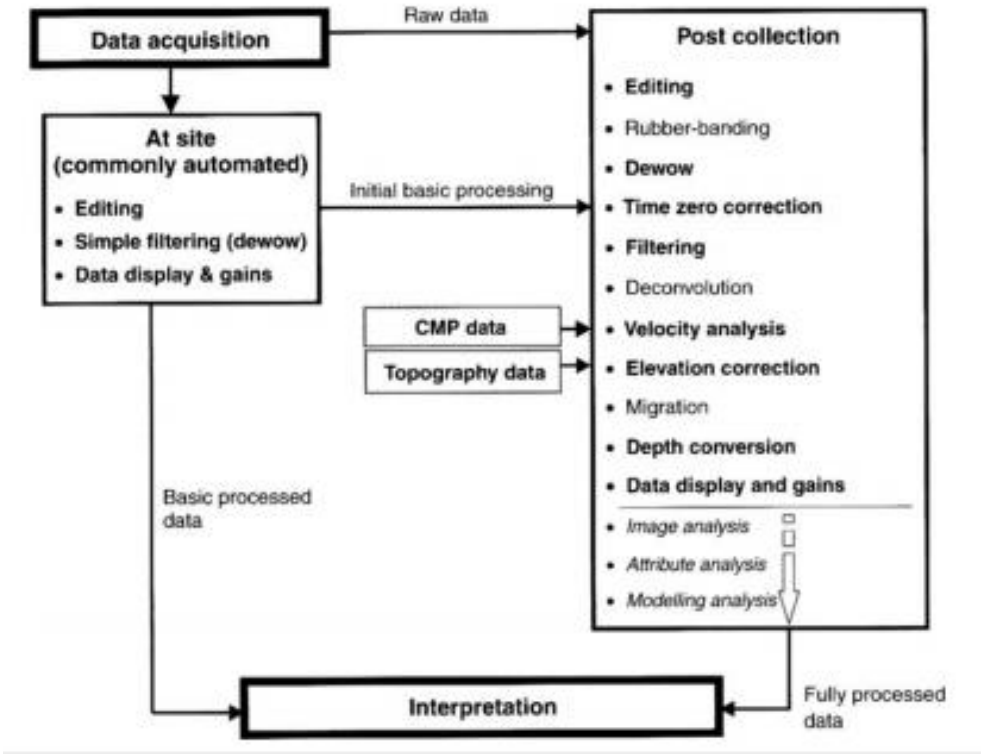

Figure 9. Example of data processing work-flow for GPR (Cassidy, 2009).

There is no specific workflow when it comes to data processing in GPR measurements, but there are some features that are widely used in many types of surveys (fig. 9). Some common

processing flow functions that have also been used very frequently in this study are described below:

- ***Time-zero correction*** – before all the processing methods will be applied, it is important to adjust the traces to a common time-zero position. Different factors like the length of the cable, electronic instability and variations in the antenna air gap might cause 'jumps' in the first arrival times. (Jol and Smith, 1995);
- ***Band-pass filtering*** – this type of filters work in the frequency domain (Conyers 2004), removing information from unwanted frequencies (noise);
- ***Background removal*** – this filter uses the mean of all the traces in a GPR section and subtracts it from each trace, thus removing the background mean trend (Jol and Smith, 1995);
- ***Dewow*** – represents the subtraction of the DC signal component and application of a median filter in order to remove the effect which is caused by the saturation of the recorded signal of the early arrivals and also inductive coupling effects (Daniels, 2005);
- ***Gain function*** – has the ability to improve visually the details and information of the GPR sections, amplifying information is usually desired. The gain function is usually applied after the other filters have been applied, in order to reduce the amount of amplification carried out on noise (Annan, 2009);
- ***Migration*** – this function usually helps with improving the resolution of the section and to develop a more realistic image of the environment in which the measurements (Daniels, 2005) were conducted. The most common migration types used in GPR are:

stack migration, F-K migration, Kirchhoff migration and finite-difference modelling algorithm (Özdemir *et al.*, 2014).

Most of the data is analysed and processed using the normal 2D radargrams but there are advantages of using the depth slices at pre-defined points, depending on the type of survey and on the desired type of outcome (Benedetto, 2010).

2.2.1.6. INTERPRETING THE DATA

The final step of a survey is represented by the interpretation of the data. This usually occurs after the raw data has been analysed, amplified, migrated and the signal to noise ratio has been improved and finessed as much as possible. The resulting information, in the form of a radargram, should represent the objective as close as possible to how it might look in reality. For example, in a geological study, the layers and limit of the layers should be very well delimited and highlighted whereas if the objective is a pipe, the dimensions and shape should be highlighted.

More often, the resulting radargrams still contain a degree of complexity and uncertainty, and the interpretation may not be effective without integrating additional information including utility maps for example, or information from boreholes, or from other geophysical methods.

The interpretation of the GPR data depends on several factors, including the quality of the acquisition data, the effectiveness of data processing, the additional information regarding the area, the type of objective, and the experience of the person conducting the interpretation.

This should take into consideration all the information available, in the form of maps of sketches from the field work. The interpretation of the data can be done on either individual profiles, or on sets of parallel profiles, a feature which is possible in the ReflexW software as well.

2.2.1.7. MODELLING GPR DATA

Modelling GPR data represents a potentially important but often overlooked tool that can enable a better understanding of the GPR data. For this project, the GPR data modelling was created with the use of open-source software called GPRMax. This software represents a valuable modelling tool based on the Finite-Difference Time-Domain numerical method (Warren, Giannopoulos and Giannakis, 2015).

GprMax simulates electromagnetic wave propagation, with the help of Yee's algorithm to solve Maxwell's 3D equations using the Finite-Difference-Time-Domain method. (Warren C., 2016).

The software does not have GUI interface and works with inputting the variables in a text-based file, in which the user defines various parameters in order to create the model: geometry, discretization, model size, permittivity values, etc. It also allows the user to choose between different types of commercial antennas models, which resemble GSSI and MALA models.

It is possible to create models of the soil with more realistic characteristic including dielectric values and geometry, by relating the relative permittivity of the soil to its sand particle density, sand fraction, clay fraction, volumetric water function and bulk density. For expressing the topography of soils, fractals – scale invariant functions, have been used by generating the convolution of Gaussian noise with the inverse Fourier transform of $1/k^b$ (k-wavenumber, b-constant dependent on the fractal dimension).

The latest version of the software allows for anisotropic objects to be modelled and simulated, including wood and fibre-reinforced composites, and it makes this possible by enabling every volumetric geometry object to specify up to three material identifiers (Warren C, 2016).

2.2.1.8. LIMITATIONS

As with all the other geophysical methods, the GPR method also has its own limitations. Some of these limitations are given by the properties of the environment (Quinta-Ferreira, 2019), as described above. Some classic examples of unsuitable environments for GPR are wet clays or soils near coastal areas that have seawater infiltrations. In these types of environments, the radio waves are either highly absorbed or reflected to such a degree that the ground becomes opaque to the radio waves, therefore limiting the ability of the GPR method to deliver good quality data (Daniels, 2005). Another limitation is given by the lack of contrast between the relative dielectric permittivity values of the objective that needs to be studied and the environment.

2.2.2. ELECTRICAL RESISTIVITY METHOD

2.2.2.1. INTRODUCTION

The electrical resistivity method was developed at the beginning of the 1900s by two French brothers named Conrad and Marcel Schlumberger (Reynolds, 2011). The method, as it is the case with most of the geophysical methods, was originally used and developed for the exploration of minerals and hydrocarbon reservoirs of economic interest. In the past century, the resistivity method has become more robust and is increasingly used in areas including environmental, geotechnical, and agriculture and archaeological studies (Allred *et.al.* 2016).

The basic principles on which the resistivity method operates are largely unchanged compared to when the Schlumberger brothers developed it. However, technological improvements of the method have made the data acquisition faster and more flexible. Another improvement is made by the availability of inversion and modelling software which improves the speed of the data processing, whilst providing a higher degree of information and mapping of underground objectives.

2.2.2.2. RESISTIVITY – BASIC PRINCIPLES

The basis of the resistivity method lies in understanding Ohm's law and the relationship between resistance and resistivity. In order to explain resistivity, let us consider a block with length $\boldsymbol{L}$ and cross section area $\boldsymbol{A}$, composed of a homogenous material (fig. 10).

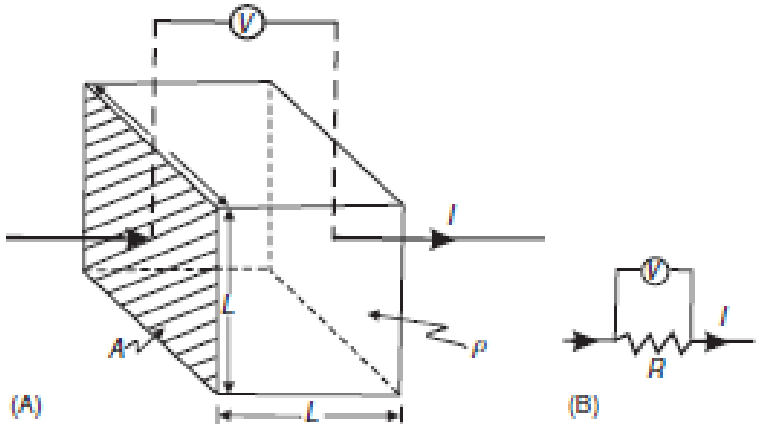

Figure 10. A - the resistivity across a block of side length ***L*** *with an applied current* ***I*** *and potential difference between opposite faces of* ***V****. B - the electrical circuit equivalent, where* ***R*** *is a resistor. (Reynolds, 2011)*

An electric current of intensity ***I*** is applied at one end of the cylinder and exits at the other end. The block opposes the flow of the current and causes a drop in electric potential $\Delta \boldsymbol{V}$ between the opposite ends. Therefore, the resistance ***R*** is represented by the proportionality to the length ***L*** of the material and inversely proportionality of the cross-sectional area ***A***. The resistivity, $\boldsymbol{\rho}$, on the other hand is represented by the constant of the proportionality and is a property of the material.

$$\boldsymbol{R = \frac{\rho L}{A}}$$

Considering Ohm's law where the resistance ***R*** is defined as the ratio of the potential drop to the applied current, both expressions can be combined in order to define the resistivity as the product between the resistance ***R*** and a distance (area/length), and the measuring unit *in ohm-meters* $\boldsymbol{\Omega m}$, this is mathematically demonstrated below:

$$R = \frac{V}{I}$$

$$\rho = \frac{VA}{IL}(\Omega m)$$

$$\rho = \frac{E}{J}(\Omega m)$$

where J is the current density in $amps/m^2$ and E is the electric field strength in $volts/m$.

2.2.2.2.1. CURRENT FLOW AND APPARENT RESISTIVITY

The apparent resistivity is defined as the product between a measured resistance **R (Ω**) and a geometric factor **K (m)** which is specific for different types of electrode arrays and takes into account the number and spread of the electrodes (Reynolds, 2011). Similarly, the apparent resistivity is measured in units of ohm-meters (**Ωm**)**.** It is important to differentiate between both types of resistivity (true and apparent) and to understand that the type of resistivity measured in a natural environment is always an apparent resistivity (Reynolds, 2011). The 'true' resistivity is calculated (or rather, estimated) using a method called inversion, a complex mathematical process of calculating cause from a set of observations. There are multiple types of inversion methods that can be used, and usually different types of software use different inversion methods (more on this subject in chapter 2.2.2.5.1.Inversion and Forward Models).

The propagation of the current through a homogenous medium is described by a considered point source, through a hemisphere with equipotential lines perpendicular on the lines of equal current (fig. 11).

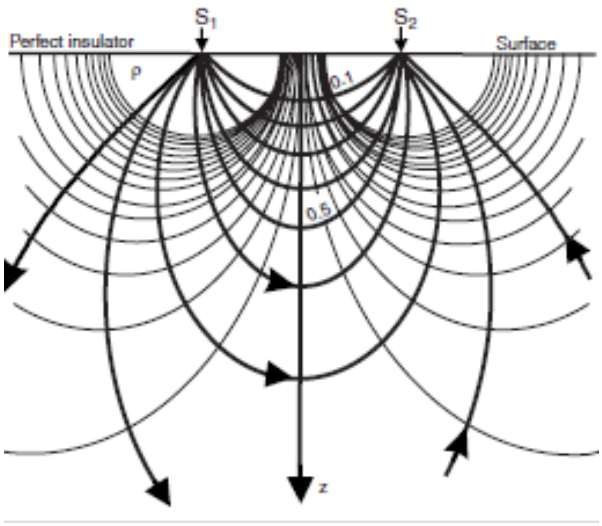

Figure 11. The image represents the current and equipotential lines produced by a current source and sink (Reynolds, 2011).

2.2.2.2.2. ELECTRODE ARRAYS AND PENETRATION DEPTH

Because calculating resistivity is dependent on the geometric factor ***K***, for a better understanding on how this factor is affecting the resistivity the following substitutions and rewriting of the equations was carried out:

$$\frac{\delta V}{\delta I} = -\rho \times J = -\rho \frac{I}{2\pi^2 r}$$

$$V_r = \int \delta V = -\int \rho \times \frac{I\delta r}{2\pi r^2} = \frac{\rho I}{2\pi} \times \frac{1}{r}$$

For a better understanding of the dependency of the geometric factor (Reynolds, 2011) when defining the apparent resistivity, a mathematical approach is presented below:

$$V_M = \frac{\rho I}{2\pi}\left[\frac{1}{AM} - \frac{1}{MB}\right],\ V_N = \frac{\rho I}{2\pi}\left[\frac{1}{AN} - \frac{1}{NB}\right],\ \rho V_{MN} = V_M - V_N = \frac{\rho I}{2\pi}\left\{\left[\frac{1}{AM} - \frac{1}{MB}\right] - \left[\frac{1}{AN} - \frac{1}{NB}\right]\right\}$$

$$\rho = \frac{2\pi\rho V_{MN}}{I}\left\{\left[\frac{1}{AM} - \frac{1}{MB}\right] - \left[\frac{1}{AN} - \frac{1}{NB}\right]\right\}^{-1}$$

$$K = 2\pi\left[\frac{1}{AM} - \frac{1}{MB} - \frac{1}{AN} + \frac{1}{NB}\right]^{-1}$$

Where in order to represent the geometric factor and what role it plays in defining the apparent resistivity, the demonstration starts with defining the potential at each electrode, depending on the position of the distance between the current and potential electrodes, the resistivity, the current and the half sphere of the current equipotential lines.

After describing the geometric factor ***K***, apparent resistivity can be defined thusly, depending on the resistance and geometric factor:

$$\rho_a = RK$$

$$R = \frac{\delta V}{I}$$

According to (Szalai and Szarka, 2008) there are around 100 types of electrode arrays or configurations available, but only a small number of them are widely used. The array

selection is made based on aspects such the type of objective, the desired lateral sensitivity, the desired vertical sensitivity (Reynolds, 2011).

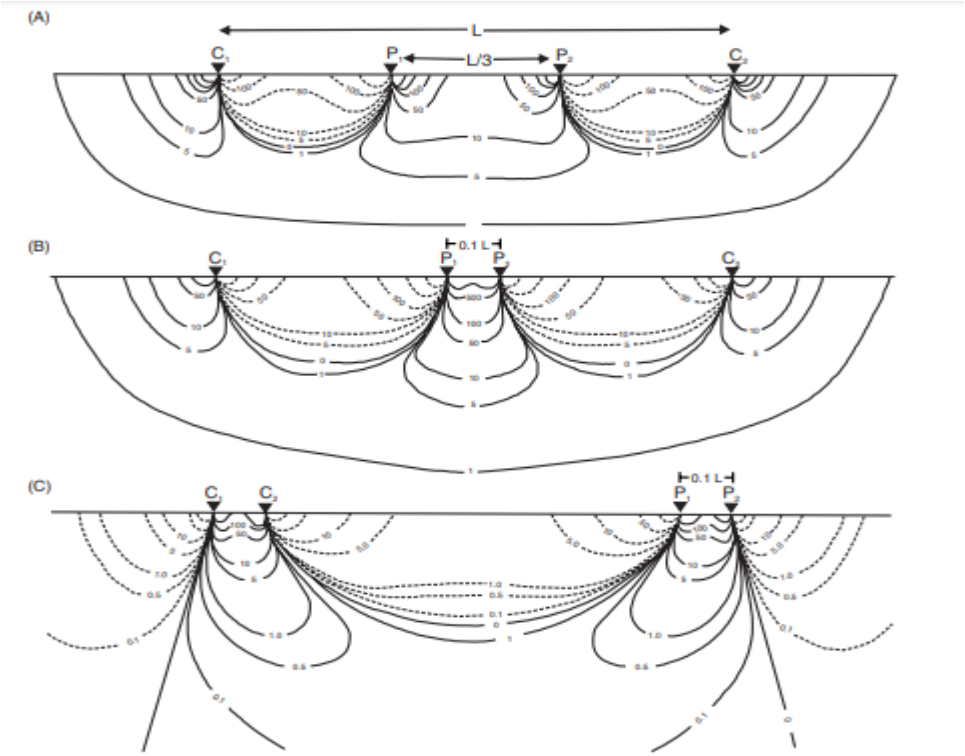

Figure 12. Representation of signal contribution sections depending on the electrode array type: A- Wenner array, B- Schlumberger array and C-dipole dipole array (Barker, 1979).

The most common types of electrode arrays are the following, considering that A and B are the current electrodes and M and N represent the potential electrodes (fig. 12):

- ***Wenner***: 4 electrodes are inserted into the ground with an equal distance between them - AM=MN=NB;
- ***Schlumberger***: also requires 4 electrodes but the distance between M and N is smaller than the distance between A and B, which increases for the same point so it can penetrate to higher depths - AB>MN; MN=n; AM=NB=n*a;

- ***Dipole-dipole***: the current electrodes are on opposite sides of the potential electrodes, and the distance between them increases for every measurements - AB=MN=a; BM=n*a;
- ***Square array***: a square array requires 4 electrodes which are inserted into the ground at an equal distance between them in the form of a square. The measurements for one point require the square to become smaller or larger by increasing the distance between the electrode - AB=BM=MN=NA=a.

These arrays each provide their own benefits and shortcomings.

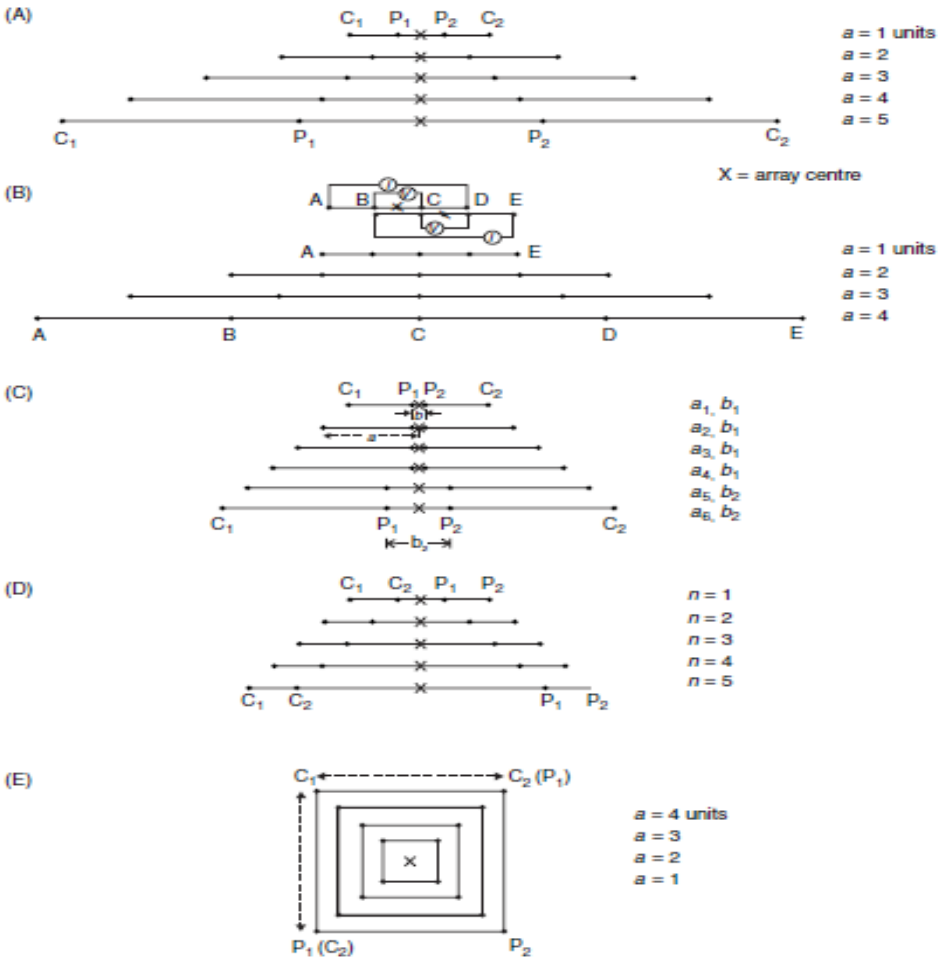

Figure 13. Representation of resistivity arrays with successive positions. (Reynolds, 2011).

2.2.2.2.3. ELECTRICAL RESISTIVITY TOMOGRAPHY

Electrical resistivity tomography (ERT) is perhaps the most convenient and probably the most used variation of the electrical resistivity method. The electrical resistivity tomography works on the same principles as the resistivity method, the only difference, as it was previously mentioned, is that with ERT all the electrodes are inserted into the ground at the same time and the systems is switching electrodes between potential and current, starting with a fixed distance **a** between the electrodes (fig. 14). When it reaches the end of the profile, the distance between the electrode increases in incremental steps of 1, and this process repeats until it reaches the maximum length of the profile (Reynolds, 2011).

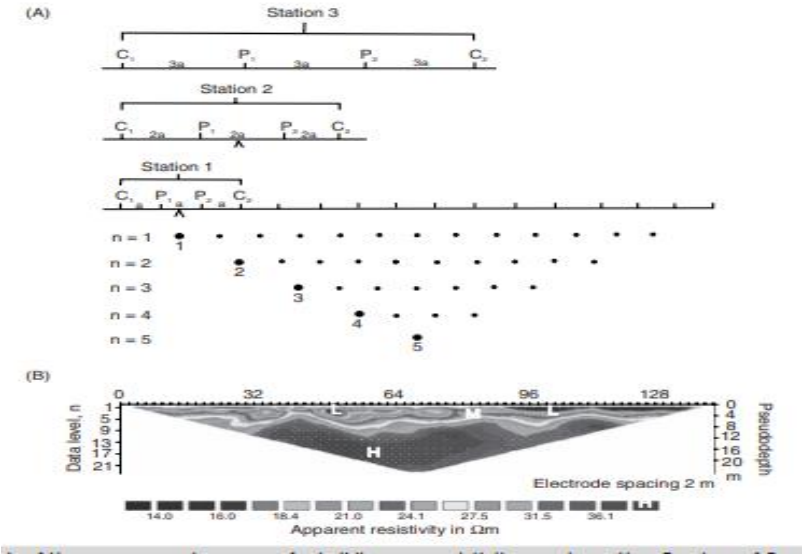

Figure 14. Electrical resistivity tomography. A- all the electrodes are inserted into the ground (Loke, 2013).

By doing this, it is possible to carry out several types of electrode arrays on the same profile, which represents a great advantage by shortening the amount of time it takes for a survey to

be carried. It is also more user friendly, as it can be done by only one surveyor, and takes far less time than moving electrodes manually. With the ERT the data is displayed in the form of vertical sections, where the length of the section is given by the actual length of the profile and the depth is given by the type of electrode array used. The basic principle of the ERT method (fig. 14) involves inserting 16 electrodes into the ground at equal distances ***a***, and when utilizing a Wenner array for example, where the distance between electrodes remains constant, the measurement process begins with alternating electrodes between current and potential roles, moving along the profile until the end is reached. Upon completion, the electrode spacing doubles to ***2a*** for a new measurement line, repeating this process with increased distances to vary the depth of investigation. In this context, the depth measurement changes proportionally with the electrode spacing, where, for instance, ***n=1*** indicates a depth with electrode distance ***a***, and ***n=2*** indicates a depth with distance ***2a***, and so on.

2.2.2.3. EQUIPMENT

There are two types of surveys often used when it comes to resistivity prospection. There is the “classical approach” and the electrical resistivity tomography, or ERT method. The basic physical principle is essentially the same for both methods, they both have advantages and disadvantages and different applicability. The classical method usually needs only 4 electrodes and the measurements are conducted along a linear profile. The electrodes are inserted at pre-defined points, where a measurement occurs, and then they are removed and

inserted at the next point. This is a very effective method, for ground water detection, or geological and or mining studies, as the length of the profiles could be between several hundred meters up to kilometres. It takes a long time depending on the length of the profile, but it gives information from larger depths.

The equipment used for resistivity surveying consists of the following:

- ***Electrodes***: which are usually made of a solid and conductive material like copper or stainless steel;
- ***Console*** which has the ability to inject the current, measure the potential difference, and display the data (most types of equipment are also able to store the data);
- ***Cables***: having the role to connect the console or resistance meter to the electrodes.

In the case of an ERT, a switchbox (or multiplexer) is typically used to pass current to the desired electrode positions. This can be integrated into the measuring console or can be separated. Some systems also require an external battery for additional power.

2.2.2.4. FIELD METHODOLOGY

Most of the resistivity equipment is usually straightforward and doesn't require much preparation, compared to other methods (ground penetrating radar e.g.), and allow the user to just start collecting data, with the possibility of the user to write the values down and all the information about the position of the electrodes (fig. 15), or the equipment will be able to record the measured values. Other newer equipment including the multielectrod types of

equipment, on require the user to insert more data and information regarding the project, like number of electrodes used, distance between electrodes, type of array used, and even allowing a combination of multiple types of arrays.

Figure 15. Image showing a resistivity survey using an ABEM Terrameter equipment which uses the classical method with 4 electrodes .

Before starting a survey, it is important to understand what the objective is (size, shape, material, etc.) and to plan accordingly. Different types of objectives require different distance values between the electrodes, electrode array and the maximum spread of the electrodes. Most of the times the surveys are carried on long linear profiles, but depending on the purpose of the study, square arrays are also an option, while for some other studies (Reynolds, 2011),

where two electrodes (one potential and one current electrode) are mobile, while other two electrodes are fixed, and the surveying is carried out in a grid pattern (in archaeology e.g.).

Planning the field surveys usually requires other types of field equipment like wooden pegs to mark the corner of profiles, measuring tapes in order to ensure the position of the electrodes , etc.

Figure 16. Example of a survey using multielectrode equipment, which requires all the electrodes to be inserted into the ground at the same time, while the equipment automatically carries out the survey.

If a multielectrod (fig. 16) unit is used, all the electrodes will be inserted into the ground and, as mentioned before, all the parameters set and adapted for the required project. After the equipment has stopped recording the data, these will be available for downloading and using

for processing. The data resulted from this type of survey comes in the form of apparent resistivity values, which the equipment is already able to calculate.

If a classical equipment with 4 electrodes is used, depending on the type of array required, 2-4 surveyors will need to make sure that they constantly move and insert the electrodes at the desired position, using the measuring tape, while one other surveyor will control the unit and choose when to start injecting the current and when to record the values. After the recording for one position stopped, the electrodes are moved to the next position where the process of injecting current and recording repeats until all the required positions of the electrodes have a value recorded. After the data was collected, the information and values are usually inserted in a spread sheet after which they are ready to be processed. The data resulted from this type of equipment is in the form of a resistance value, which needs to be transformed in apparent resistivity values based on the position of the electrodes and the ***K*** factor described earlier.

2.2.2.5. DATA ANALYSIS AND PROCESSING

There is a variety of software packages for processing the resistivity data and carrying out the inversion of the data; as with GPR, both commercial and open-source options are available. Some software packages require specific formats of the files in which the data (including the position of electrodes, distance between electrodes, type of array and apparent resistivity or resistance values) follow a required pattern.

As a general rule, the processing of the resistivity data can be organized in four stages:

- ***In the first stage*** – points outside reasonable value ranges, are removed. This is site and survey specific, and this is a behaviour that might appear in the data due to a number of situations in the field (electrodes not inserted properly, no good contact between the electrode and the soil, etc.);
- ***The second stage*** **-** involves preparing the files with the appropriate format for the specific inversion software used, checking the type of parameter recorded in the data (resistance/resistivity) and making topographic corrections (the inversion models are significantly are influenced by the relative position of the electrodes);
- ***The third stage*** - involves using specialized software to calculate an inversion model, which converts apparent resistivity values into actual resistivity values and allows adjustments like cell discretization and iteration numbers. Different software may use varied inversion methods, and while inversion models provide real resistivity estimates, they represent an approximation of the actual environment based on the resistivity of subsoil objects and materials (more on the subject in chapter 2.2.2.5.1). It's important to note that multiple models might fit the observed data well. For studies aiming to generate 3D images or horizontal slices, the inversion file must include comprehensive data from parallel profiles, accurately reflecting electrode positions and patterns;
- ***The fourth stage*** **-** usually consists of analysing and interpreting the resulted inversion models. The format of the data resulted after the inversion is in the form of vertical resistivity pseudo-sections. If a 3D model was to be processed, it is possible to visualise horizontal slices at different estimated depths. The interpretation of the data represents a challenging process, and it requires taking into consideration all the available

information on the surveys, type of survey, and meteorological conditions at the time of surveying, the objective and its characteristics and many other features presented in the previous sections.

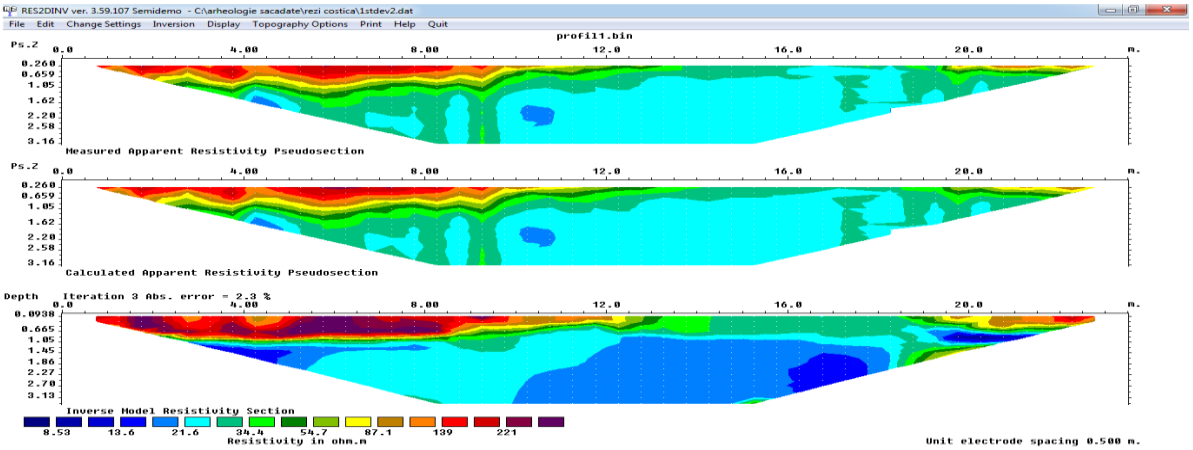

Figure 17. Image showing an example of resistivity surveys using multielectrode equipment, in a grassy-marsh type of environment. Data processed using RES2DINV software. The last pseudo-section represents the final itteration of the ivnersion model.

For assessing layers and features from the subsurface and transforming from apparent resistivity values to real resistivity values, the data goes through a process called inversion (Kohlbeck and Mawlood, 2009), as mentioned in the previous sections, there is a variety of software which can be used for processing the resistivity data, and the software used for processing the data in this paper are RES2DINV, ResiPY and BERT.

Fig. 17 is an example of resistivity data using multielectrod equipment in an area with grass and high humidity levels in parts of the surveying area. After the data were downloaded from the equipment, and processed with RES2DINV, the software carried out the data inversion and the last iteration represents the model that is the closest estimate to the observed data,

compared to the first image which represents the actual measured values of apparent resistivity. Based on the result (and with the aid of observations from the field and information regarding the objective), the data interpretation was carried out.

2.2.2.5.1. INVERSION METHODS AND FORWARD MODELS

RES2DINV represents probably the most common software used in commercial resistivity data processing, for the determination of 2D resistivity models resulted from 2D resistivity surveys (Dahlin, 1996).

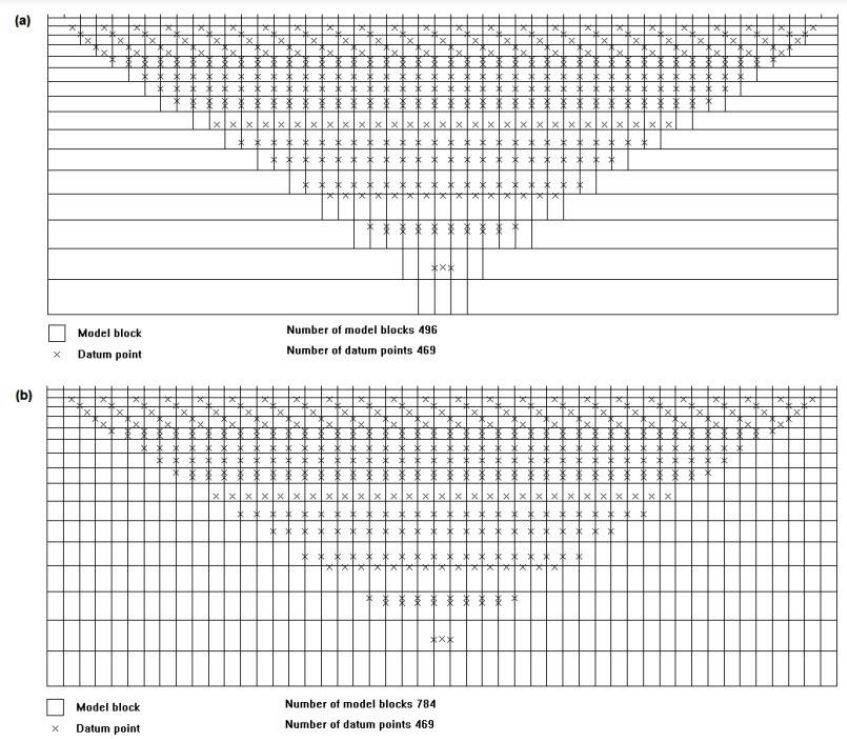

Figure 18. Two examples of blocks used for creating the models and their position related to the actual data points (Aarhusgeosoftware, 2020)

In order to create the models (Loke, 2013), the inversion program uses a large number of rectangular blocks (fig. 18), for which size and distribution are generated automatically, taking into consideration the distribution of the actual data points (Aarhusgeosoftware, 2020). The depth of the bottom row is normally set to represent an approximation of the median depth of the investigation (Edwards, 1977) of the data points from the largest electrode spacing (Aarhusgeosoftware, 2020). For calculating the apparent resistivity values, RES2DINV uses a finite-element (Silvester and Ferrari, 1996) modelling routine and for calculating the resistivity values for the model blocks, it uses a non-linear smoothness-constrained least-square optimization technique (Degroot-Hedlin and Constable, 1990; SASAKI, 1992; Loke, Acworth and Dahlin, 2003), which is based on the following equations:

$$(\boldsymbol{J^T J} + \boldsymbol{\lambda F})\Delta \boldsymbol{q_k} = \boldsymbol{J^T g} - \boldsymbol{\lambda F q_{k-1}}$$

where:

$$\boldsymbol{F} = \boldsymbol{\alpha_x C_x^T C_x} + \boldsymbol{\alpha_z C_z^T C_z}$$

and:

$\boldsymbol{C_x}$ is the horizontal roughness filter and $\boldsymbol{C_z}$ is the vertical roughness filter

$\boldsymbol{J}$ is the Jacobian matrix of partial derivatives with $\boldsymbol{J^T}$ represinting the transpose of $\boldsymbol{J}$

$\boldsymbol{\lambda}$ is the damping factor

$\boldsymbol{q}$ is the model vector

$\boldsymbol{g}$ is the data misfit vector

$\boldsymbol{\alpha_x}$ is the weight for horizontal filter while $\boldsymbol{\alpha_z}$ represents the weight of the vertical filter

$\boldsymbol{k}$ is an iteration number

The modelling process begins with a homogenous earth subsurface as the initial model, and then the software adjusts the model parameters $\Delta \boldsymbol{q_k}$ to minimize the discrepancy between calculated and measured apparent resistivity values $\boldsymbol{g}$. Adjustments to the model's resistivity are based on smoothness constraints (Aarhusgeosoftware, 2020). The root-mean-squared (RMS) error measures this discrepancy, with the software providing multiple iterations featuring different RMS values which enables users to select the model that most accurately reflects field reality, guided by these RMS error comparisons.

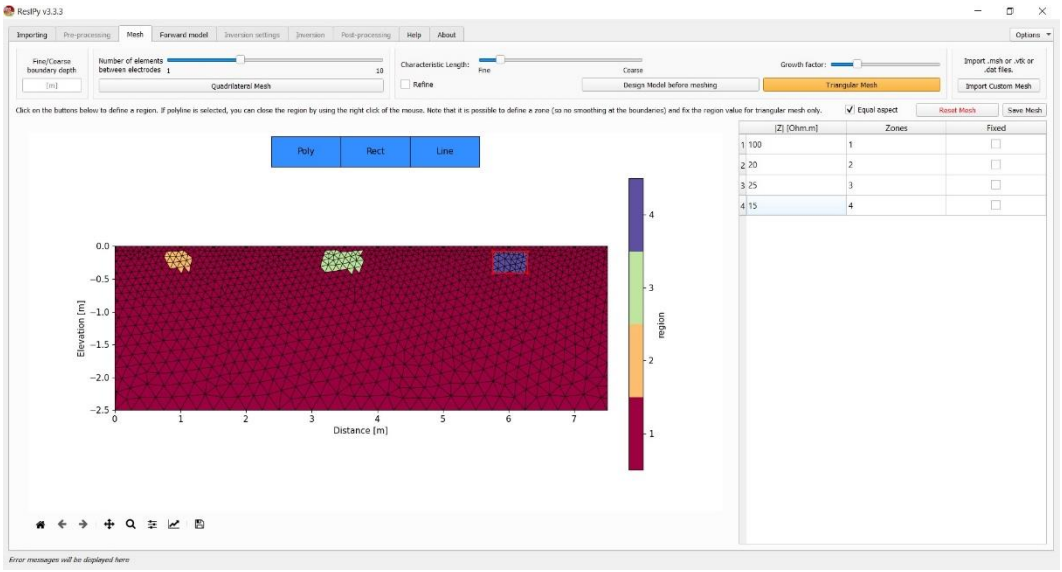

Figure 19. ResIPy example of creating a forward model, with the options of creating objects in the form of polygons, rectangles and lines, and choosing different resistivity values for each object.

ResIPy is an open-source software designed to simplify the inversion process for resistivity data through a user-friendly graphical interface and a Python API (Blanchy *et al.*, 2020), incorporating codes from R2 and R3 software that solve forward and inverse models for resistivity data. Despite R2 and R3 requiring users to input parameters via a text file, ResIPy offers a more accessible interface, with all three tools sharing the same underlying algorithm.

Both ResIPy and R2/R3 utilize Gmsh software (Geuzaine, 2009) for mesh generation in models, supporting both triangular and rectangular meshes (fig. 19). The inversion solution (fig. 20) integrates a regularized objective function with Occam's solution approach and weighted least squares (Binley and Kemna, 2005), streamlining the inversion process and enhancing user experience.

BERT (Boundless Electrical Resistivity Tomography) is, similar to ResIPy, an open source resistivity forward and inversion software. The software represents a flexible solution that works on all types of geometries, notably including arbitrary geometries as well (Gunther and Rucker, 2019). It uses unstructured finite element meshes (triangles for 2D and tetrahedrons for 3D) for forward calculations and for the parameter identification, an important aspect which makes it suitable for any kind of geometry, probe or structural information from the subsurface (Gunther and Rucker, 2019).

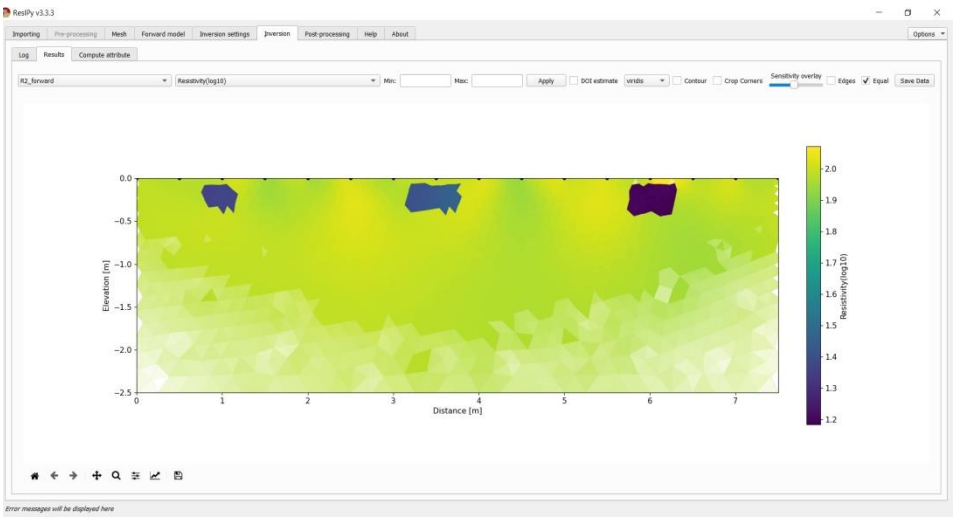

Figure 20. Example of the inversion of a forward model in ResIPy. The forward model from fig. 19 inverted in ResIPy

For forward and inverse models, BERT uses the technical solutions described by Gunther (2006) and Rucker (2010) and comprises a triple-grid inversion technique based on finite-element forward calculation and unstructured tetrahedral meshes. For fitting the data within error bounds, it uses a Gauss-Newton method with inexact lines search, and a global regularization scheme using special smoothness constrains is also applied (Gunther *et al*, 2006). The regularization parameter compromises model roughness and data misfit is based on an L-curve method and evaluated by the discrepancy principle, and for solving the inverse problem it uses a form of least-square method (Gunther *et al*, 2006).

2.2.2.6. LIMITATIONS

Like any other geophysical method, the effectiveness of the resistivity method is dependent on the contrast between the resistivity values of a subsurface object and its surroundings (Reynolds, 2011). Without such contrast, the method cannot differentiate the object from its environment, necessitating the use of alternative geophysical methods. Weather conditions, particularly variations in moisture content within surficial pores (Archie, 2003), significantly influence resistivity measurements; thus, conducting surveys under consistent conditions is ideal. For instance, during dry summers, lower water content leads to reduced soil resistivity, poor electrode contact, and restricted current flow, adversely affecting data quality. Electrode spacing is another critical factor, with a minimum distance of ***AB/2*** (where ***A*** and ***B*** are the current electrodes in configurations like the Schlumberger array) required for effective subsurface exploration. However, practical challenges such as vegetation or obstructions can

complicate survey deployment. Additionally, the sensitivity of different electrode arrays to various orientations highlights the importance of selecting the appropriate array type for the survey's objectives (table 1).

Criteria	Wenner	Schlumberger	Dipole-dipole	Square
Vertical resolution	√√√	√√	√	√√
Depth penetration	√	√√	√√√	√√
Suitability to VES	√√	√√√	√	×
Suitability to CST	√√√	×	√√√	√√√
Sensitivity to orientation	Yes	Yes	Moderate	No
Sensitivity to lateral inhomogeneities	High	Moderate	Moderate	Low
Labour intensive	Yes (no*)	Moderate (no*)	Moderate (no*)	Low
Availability of interpretational aids	√√√	√√√	√√	√

√ = poor; √√ = moderate; √√√ = good; × = unsuitable.
* When using a multi-core cable and automated electrode array.

Table 1. Sensitivity details about different types of arrays (Reynolds, 2011).

2.2.2.7. 2D AND 3D SURVEYS DATA

Most resistivity measurement arrays present data in 2D as apparent resistivity pseudo-sections or depth-specific maps, offering a unique flexibility in visualization compared to other geophysical methods like GPR (which provides only vertical profiles) and magnetometry (which provides only horizontal maps) for example. This 2D format allows for horizontal (***xy*** plane) or vertical (***xz*** plane) visualizations, depending on electrode positioning and array type. For instance, Wenner arrays can produce maps across a surveyed area using parallel profiles

in a rectangular grid, while twin-probe arrays, commonly used in archaeological geophysics, are supported by both classical and modern resistivity equipment (e.g., RM Frobisher).

For 3D visualizations, combining multiple profiles or pseudo-sections can create comprehensive 3D models, enabling the generation of horizontal slices at various depths, similar to GPR 3D imaging techniques. Both 2D and 3D approaches offer distinct advantages depending on the survey's goals and objectives.

2.3. NOTIONS ON PLANT ROOTS AND SOILS

2.3.1. INTRODUCTION

Agricultural fields represent around 37.6% of the Earth’s total land area, from which 28% is used for crops, according to the United Nations Food and Agricultural Organization (FAO), in 2019. Agricultural systems for crop fields represent complex systems, which are characterized by soil type, terrain, and climate limitations. Besides the environmental conditions, crop growth is highly dependent on nutrients and water. These factors therefore mean that there are physical constraints when it comes to the productivity level of the fields.

2.3.2. PLANT ROOTS

In order to better understand the functionality and structure of a root, it is important to understand the differences between plant root and the general classification of plant roots.

This also helps in understanding how to better use and apply the geophysical methods in a more effective manner. The following does not intend to provide an exhaustive or comprehensive classification of roots, but merely to present aspects regarding plant roots that are significant in geophysical measurements.

2.3.2.1. PLANT ROOT SYSTEM ARCHITECTURE

There are several classifications when it comes to the roots of the plants (de Dorlodot *et al.*, 2007). The root architecture embodies the spatial configuration or the geometry of the root system without including the microscopic details of the root such as the root hairs, and there is such variation that multiple types of classes have been derived.

The distribution of roots represents the existence of the roots in a positional gradient and studies concerning this matter usually focus on root biomass, depending on factors like depth in soil and position between neighbouring plants.

These types of studies are significant in agricultural environments where the focus is usually on more than one plant or species. Root topology (Lynch, 2016), another aspect which may influence the result of geophysical surveys, focuses on how individual root axes are connected to each other through branching. Studies concerning this factor are made possible by measurements of excavated roots.

2.3.2.2. ROOT MORPHOLOGY

Root morphology refers to all the details of the structure of the plant root, including features like root hairs and the root cap (fig. 21). Usually, studies regarding root morphology focus on anatomical features, cell type and tissue organization (Lynch, 2016).

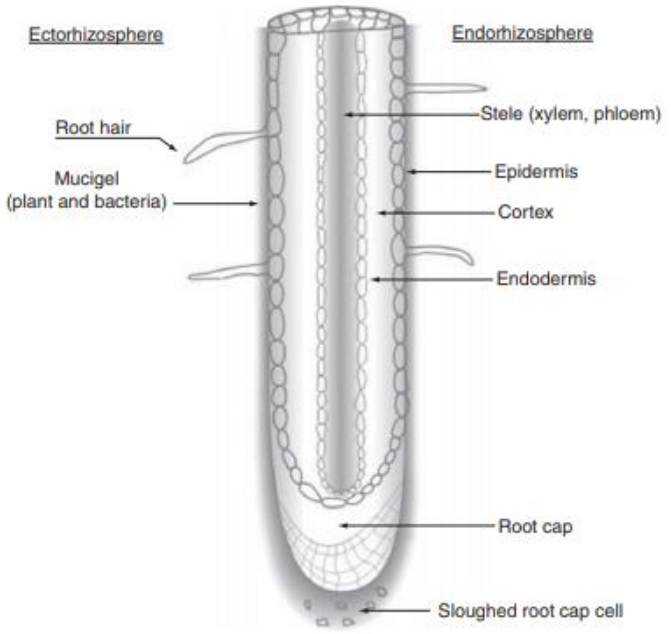

Figure 21. Root cross section showing ecto- and endorhizosphere (Fageria, Baligar and Li, 2008).

Other functions linked to the root system architecture are represented by the water and mineral uptake, where the shape of the root system has the role of determining the length of transport pathways of the resources, as well as the permeability of the root surface. The transportation within the plant depends on the conducting capacity of the branching system. The anchorage of the plant depends on both the geometrical and mechanical properties of the root system.

There are different classifications of root system architecture based on the diversity of the root system the morphology and the growth strategy (Lynch, 2016).

From a morphological point-of-view, root systems are generally classified as:

- ***Fibrous***: are mainly formed by a very large number of equivalent roots connected to the stem;
- ***Taproot***: consist of a central, vertical main root, from which numerous lateral roots originate at different depths.

This classification is not fixed during the plant's evolution. Often, plants will start growing as a taproot and later develop into fibrous systems (Lynch, 2016).

From a developmental point-of-view, according to Cannon (2014) the root system architecture (fig. 22) can be classified depending on:

- ***The primary root system,*** which originates from the radicle that grows downward and starts branching from the base to the tip. This system is very common in dicotyledonous plants (e.g. all legumes), and gymnosperms (e.g. conifers) where the radial growth of the roots and storage functions are significant.
- ***The secondary root system*** originating from the shoot system, where the radical only develops a small and temporary root system. The roots emerge continuously during the shoot development. This system is common for monocotyledonous plants that have no radial growth.

There is another category, which is described by a combination of the two systems described above where the primary root system is predominant in the early stages of the plant

development, followed by dominant secondary root system occurring during the later stages (fig. 23). This aspect was observed and described by Krasilnikov (1968).

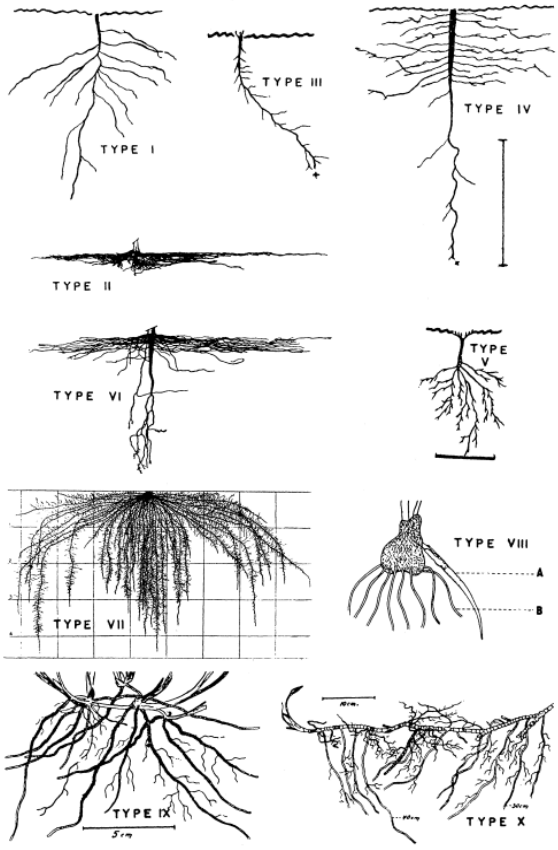

Figure 22. Classification of root systems (Cannon 1949). Types 1-6 represent the primary root systems (taproot developed from the radicle). Types 7-10 represent the secondary root systems (main roots emerge from the shoot system).

Some root system architectures are frequently modified depending on special adaptations of the roots especially when considering the anchorage function of the roots. Typically, two types of roots can be depicted: buttress (which develop along the base of the trunk providing

good stability in shallow saturated soils) and stilt roots (which grow down from lateral branches and then branch further into the soil). Another special adaptation is dependent on the nutritional aspect.

Some other types of roots modified by nutritional aspects are the tuberous roots, which work as storage organs that keep the nutrients for later – this type of roots has a lateral development. In the case of a parasitic plant, the roots are developed to obtain their water and nutrients from another plant, these types of roots are called haustorial roots.

For a better understanding of the root system architecture, it is also important to consider the properties of the main components and developmental processes.

Branching represents one of the main processes when it comes to root number, length and surface. This is described by lateral roots that develop from their 'mother root' in a certain time and space (Loic Pages, 2011).

Dicotyledonous plants have secondary meristems (plant tissue), which add layers of vessels and stiff tissues to the root, to make the roots become thicker, are highly sap conductive, and develop a better capacity for protecting against other organisms or mechanical damage. The monocotyledonous plants have roots where the original tissues are complemented by protective substances (lignin, suberin, etc.), but compared to the dicotyledonous, there are not secondary meristems as no additional tissue is produced. (Loic Pages, 2011). Many roots have a short lifespan but represent a large surface area that has a transient role of nutrient exchange with the medium.

The properties of the soil highly affect and influence the development of the roots. For example, the temperature of the soil and it's variation have an influence on the kinetic development of the roots, whereas mechanical factors affect aspects like elongation and branching, thus affecting the whole root system architecture.

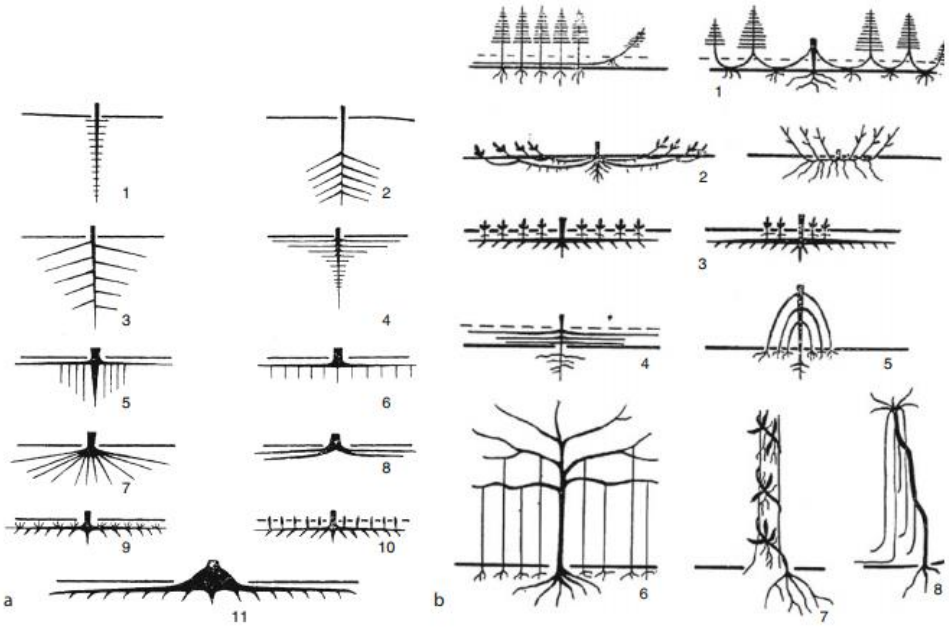

Figure 23. Root systems classification of trees and shrubs (Krasilnikov, 1968). Left side, (a) represent the primary root systems and different forms. Right side (b), represents secondary and mixed root systems with eight different varieties.

2.3.2.3. THE WATER UPTAKE OF THE ROOTS

Water represents one of the main elements that the plant needs in order to develop and grow healthily, along with other nutrients from the soil. According to Martin et. al (1976), cropped plants transpire around 200-1000 kg of water per kilogram of dry matter produced, with most

of this water coming from the soil. Therefore, understanding the plant water uptake represents an important factor when it comes to agriculture, where factors like yield predictions and irrigation management are highly affected and influenced by this property of the plants. Understanding processes related to water uptake is also important from the perspective of precision agriculture. Developing sustainable techniques to ensure that the crop uses less water without affecting the productivity of the yield requires the use of sensing equipment and modelling approaches that are not yet fully developed. According to Steudle and Peterson (1998), the water uptake process of the roots is of passive nature and is described by the water potential gradient between the soil surrounding the root and the xylem. Thus, knowledge of the hydraulic properties of the soil and the root is important for the physical characterization of the roots and their environment.

From a geophysical standpoint, the water uptake of the plant is important in the determination of methods used and the outcomes desired. Due to the hydraulic properties of the soil, the area surrounding the roots sometimes has a higher humidity level compared to average value of the humidity in the soil. This creates a contrast of humidity which alters the electrical and electromagnetic properties of the soil including the resistivity and the relative permittivity.

2.3.2.4. AGRICULTURAL PLANT ROOTS BEHAVIOUR

As was discussed in previous chapters, the roots represent an essential part of the plant, with the roles of absorbing water and minerals from the soil, keeping the plant anchored and enabling it to develop properly and produce a healthy crop.

Root architecture is a parameter that addresses the structure, geometry, and development of the plant root. Understanding the root architecture of the agricultural plants enables not just an understanding of the plant, its surrounding environment, and the interactions between the two, but can also pave the way for selective breeding or genetic modifications, developing favourable traits of the plant such as water uptake or fertilizer need.

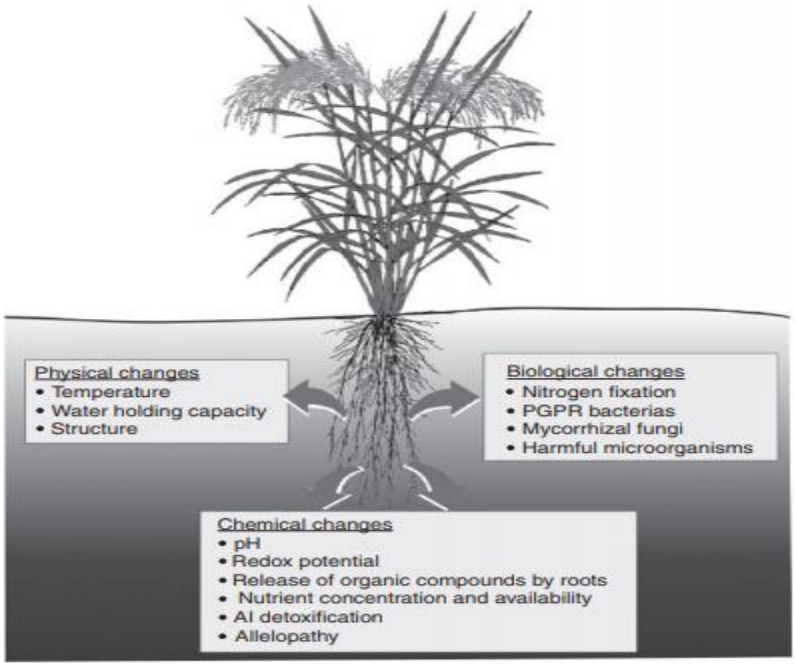

Figure 24. Major physical, chemical, and biological changes in the rhizosphere (Fageria and Stone, 2006)

It appears that lateral roots represent the most common type of branching, and in many cases the lateral roots represent the majority of root length (Lynch, 2011) The development of the roots is affected by the mineral and nutrient content of the environment For example nitrate and phosphorus modify the branching pattern of the lateral roots. The roots are highly affected

by the distribution of the nutrients as well, but according to Lynch et al. (2011) there are still significant knowledge gaps in this field, even in regards to relatively simple plants. This produces difficulties for controlled experiments, suggesting that there are many inputs that should be taken into consideration.

There are many biotic and abiotic factors that modify the pattern of root branching and the plasticity of the roots represents a very challenging subject.

Lateral roots (fig. 25) are not the only roots affected by the environment and the physical (stress, compactness, etc.) and chemical (nutrient content, water content, etc.) parameters of the environment.

Much of the work done on the physical parameters of crop roots focuses on a set of standard root parameters such as the root length of the dry root and the dry weight. For instance, in Barber and Silberbush (1984), where the relationship between root length and soybean yield was studied, it was concluded that the yield was related to the total root length at the full seed stage of the plant. When the roots of oat and barley crops were studies, it had also been concluded that the growth of the root is very important when it comes to determining the supply of nutrients to the shoot (Fageria, Baligar and Li, 2008), which also affects the crop yield (fig. 24). Leon and Schwang (1992) determined that root system length was strongly correlated with the yield stability.

When it comes to cereals for example, in the first weeks of development, the roots are represented by nodal roots, which are a type or shoot-borne root. (Leon, 1992)

The relationship between maximum root length, root dry weight and grain yield of rice was also discussed by Leon (1992), and it was concluded that the grain yield increased quadratically with the increase in root length or root dry weight, where the second factor represented a better predictor than root length of the yield. Other work from the same author concluded the same results when it came to tropical legume cover crops. For example, in order to reduce plant root water uptake and save water for later stages of development, modifications on the xylem vessel diameter have been made in order to reduce the root hydraulic conductance.

Agricultural root architecture is influenced by: genetics, plantic density, plant size, intercropping patterns, agronomic practices and seasonal weather patterns (Meister *et al.*, 2014).

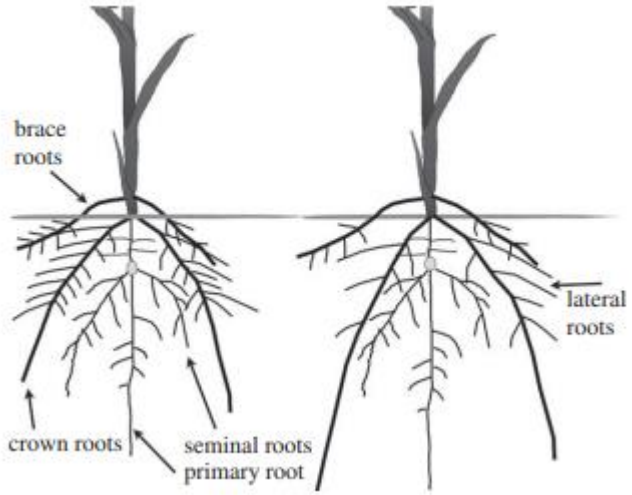

Figure 25. Maize root system showing lateral root development. The root system on the right has greater axial (Lynch and Brown, 2012).

Modifications of root functions also represent an area of current interest, and this may grow in importance given the challenges facing modern agriculture. As much of the work carried out in this field is done in situ, the ex situ work generally involves invasive methods and plants being dug out so that the roots can be measured and analysed. Better ex situ imaging techniques would represent an important step towards helping with developing better crop roots that will use less nutrients and water in a way that can still keep the plant healthy.

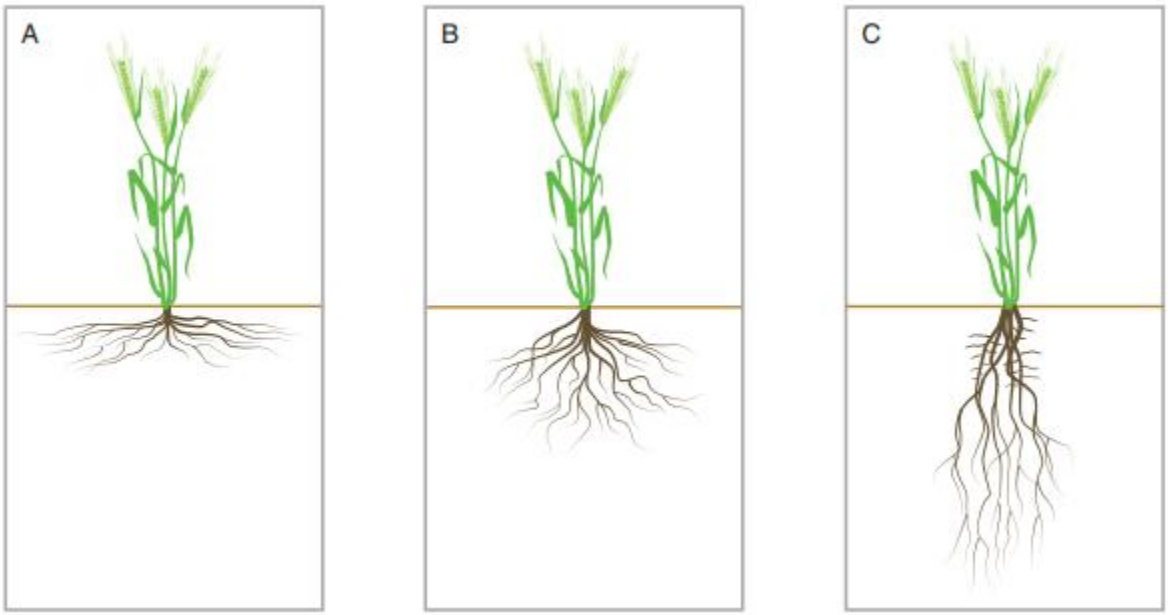

Figure 26. Example of root system engineering for different types of roots and their properties (White et. al., 2014).

2.3.2.5. GENERAL OUTCOMES

In general, from the existing literature, it can be concluded that the most important aspects of the root characteristics that affect the crop yield are represented by the root dry weight and

maximum root length (fig. 26), two factors that are also expected to be significant in geophysical surveys, thus suggesting that geophysical methods may eventually act as a proxy for predicting or estimating some characteristics regarding crop yield.

2.3.3. ROOTS PROPERTIES FROM THE GEOPHYSICAL PERSPECTIVE

So far, in the previous chapter, the properties described were presented in terms of biology or functionality, but when it comes to geophysics, the focus on the roots comes from a different perspective.

Resistivity perspective

A thorough analysis on the resistance values in laboratory, throughout different sections of the maize roots, suggest that the resistance values vary in the longitudinal direction, it appears that the xylem (fig. 21) resistance is larger than the resistance of the rest of the root (Ginsburg and Laties, 1973), and there appear to be variations in terms of resistance throughout different sections of the root as well (Anderson and Higinbotham, 1976). Absolute values were not determined, as the roots had been treated with a variety of solutions in order to prepare them for experiments, which may influence the absolute values of resistance and resistivity of the roots. Even though these studies are carried out on very specific areas of the roots, it gives a point of view in terms how the roots are perceived from a geophysical point of view. Roots are complex and variable systems, and the variability in physical parameters throughout different type of roots as well as different sections of the roots creates complexity when it

comes to understanding how to better apply the geophysical methods in a real setting environment for the best outcome possible.

From the point of view of resistivity, when it comes to classifying the plant roots, the electrical properties of the root zone would be determined by the type of root (young and fine roots or more mature, woody roots) , the sap content, and the histologic capability or the cells with pronounced anisotropy, in order to conduct currents (Petersen and al Hagrey, 2009). The classification is simplistic but robust, and it represents an interdisciplinary pathway for bringing two domains together.

It has been observed (Petersen and al Hagrey, 2009) that fine roots, which are usually young and sap-absorbing, are electrically conductive or have a lower resistivity compared to the wooden type of roots, which are usually older roots that transport sap. These coarse, woody roots are usually found on more mature plants, whereas young plants tend to have the younger finer types of roots, changing their property and functionality in time.

In terms of resistivity, it has been observed that roots exhibit a broad range of values which represents an aspect that brings more complexity in terms of surveying the roots and geophysical data interpretation. The water filled conductive tissues of the roots would present values around 50 Ωm whereas the more wooden roots, are a bit more resistive with values of around 104 Ωm (al Hagrey, 2007) when it comes to tree roots. However, these values are still just estimates based on observed samples; to date, there has not been a large-scale classification and estimation of resistivity values for multiple types of plants.

The root-soil relationship represents another important consideration for the geoelectrical imaging of roots. The range of permittivity values for soils can vary greatly depending on

properties like clay content, porosity, water content, and so on. These parameters strongly influence the resistivity properties of the soil and have a great impact on the ability of the resistivity method to find a contrast between the roots and the surrounding soil. As mentioned before in chapter 2.2.2 , the resistivity contrast represents probably one of the most important aspects when it comes to the efficiency of the resistivity method and applicability. It has been observed that soil volumes high in root content, appear as more resistive usually with an increases of the order of 10 to 102 Ωm (Weihs et al. 1999).

When it comes to the spatial resolution in resistivity, this is determined among other aspects, by the space between the electrodes and the type of array used (Dahlin and Zhou, 2004), but when it comes to roots the situation is a bit more complicated due to the overlapping of the resistivity properties of different materials and soil changes induced by the roots (Amato *et al.*, 2011).

Ground penetrating radar perspective

When it comes to the GPR method and applying it in plant root studies, the method is able to differentiate between the root and soil if there is a contrast and the permittivity value of the root is different than the permittivity value of the surrounding soil.

Measuring the permittivity value of the plants raises inherent difficulties due to the nature and size of the specimens which are usually not suitable, but it has been observed on measurements carried out on the *Casuarina* needle-shaped leaves, rubber wood and rubber leaves, that there seems to be an usual correlation between increased permittivity values and moisture content (Tan, 1981). This is also consistent with what is known regarding other materials.

Recently, it has also been observed (Mihai *et al.*, 2019) that even across similar-looking roots in the same soil unit, there can be great variation between permittivity values. This variation is not only related to water moisture and in some instances, can be very close to the permittivity value of the soil, making detection difficult or even impossible. The same work of Mihai et al (2019) notes that roots can exhibit both a positive and a negative permittivity contrast compared to their surrounding subsurface.

When it comes to choosing the right type of equipment it appears that high-frequency antennas (e.g. 1.5 GHz) are more suitable for detecting the roots and even finer roots as they provide higher resolution, and there is often no need for a large depth of investigation. The bark coverage of coarse, woody roots may play a role in how the response appears in the radargrams, especially when it comes to roots with a thinner bark layer (1-2mm), which can exhibit a double hyperbola response which makes them slightly easier to detect usually when the roots appear in soils with higher permittivity values (Mihai *et al.*, 2019).

When it comes to agricultural plant roots, the situation is even more challenging compared to that of tree roots. Even though agricultural plant roots could denote a variety of plants (from vineyards and alfalfa to maize, wheat, tomatoes etc.), the two categories are based on root size. For agricultural plant root studies in general, finer roots are more important than coarse roots due to their water and nutrient uptake abilities (Liu, Dong and Leskovar, 2016).

In general, the root diameters of the most common types of agricultural plants with fine roots, wheat, corn and soybean is relatively small. In the case of wheat plants for example the root diameter could range between 0.25 mm to 0.33 mm, with the higher values for the sole wheat plants and the lower values for intercropped wheat (Wang *et al.*, 2014). Fine corn roots

diameter would be a bit larger than the soybean plants', at around 0.5mm, and their number of fines roots would depend on agricultural practices, with some practices having a lower number of roots than others (Wang *et al.,* 2015). This makes it virtually impossible to resolve individual roots with today's geophysical capabilities, and suggests that geophysical studies would yield better results when focusing on the root area or other aspects of interest.

The position of the roots, especially of the fine sap transporting roots, represents another important feature when it comes to geophysical surveys, as this allows for a better selection of the type of antenna in the for GPR surveys, and a better decision regarding the right distance between electrodes and the array of electrodes that would give the best imaging results in the case of resistivity surveys, for example. It appears that in some agricultural settings (for example when studied in a maze field) the root lateral distribution would be more concentrated in the 0-10 cm from the stem base, with the area below 20 cm depending on the type of agricultural strategies used, but differences would be much higher in terms of concentration of the lateral distribution of the roots (Wang *et al.*, 2015).

2.3.4. AGRICULTURAL SOILS

2.3.4.1. INTRODUCTION

From the point of view of agriculture and plant growth, the soil represents the environment that provides plants with mechanical support and elements vital for the growth of the plants including water, oxygen and nutrients. Soil is not a static unit, but rather a dynamic body

existing at the surface of the earth whose properties and composition are in a state of continuous changed due to natural factors like climate and living organisms.

2.3.4.2. SOIL PROPERTIES OF INTEREST IN GEOPHYSICS

The physical and chemical properties of the soil influence the growth of the plants, through their water and nutrient supplying capacity. Soils with suitable physical and chemical properties aid vertical and lateral development of the plant roots, which represent an important aspect in plant stability in agricultural environments, by making plants resistant to drought and severe weather (for example high intensity winds). The quantity and variety of available nutrients might increase due to the development of deeper and lateral expanse of the roots, as they will be able to get their nutrients from a larger volume rather than being dependent on a small and localized area.

Poorer quality soils which feature a high degree of compactness, a lack of organic and mineral nutrients, a low degree of soil moisture and higher quantities of chemical elements that inhibit plant growth and development (high levels of soluble salts for example) represent physical and chemical properties that inhibit plant growth and development.

Another important aspect regarding the quality of an agricultural soil comes from the air-water relationship. The pores in the soil are filled with both of these elements in varying amounts, and the ratio should be optimal in order to benefit the prosperity of the plant roots. In some situations, the water cannot penetrate the deeper parts of the soil in order to make way for air to fill the pores, and prolonged exposure of the plant root to this kind of

environment can result in oxygen shortages, which can also be combined with accumulations of metabolic waste products which are very toxic for the plant. Situations like this result in weed problems and nitrogen-deficient crops as well.

Besides the air and water, the plants also accumulate mineral elements like nitrogen, phosphorus and sulphur from the soil.

The presence of salts in soils is usually a cause of concern due to the negative effect they have on plant root water absorption from the soil (Berge *et al*, 2017).

Soil texture represents an important feature when it comes to agriculture. For instance, clay particles are generally smaller and more conductive compared to other materials like silt and sand particles. This feature is important when it comes to the productivity of the crop, in terms of the soils ability to hold water, drainage capabilities, and the soil's ability to hold nutrients or lose them and some of these aspects could be mapped and analysed with geophysical methods. Some of the nutrients described earlier, like nitrogen for example, can be leached through light soil and are more mobile compared to fixed nutrients like phosphorus which tend to be more stable.

From a geophysical point of view, when it comes to soil texture, compactness and porosity are important features which have a significant effect on the resistivity values. It has been observed that soil resistivity decreases significantly with the increase in density and typically for water contents less than 0.25 g g-1, and this is more pronounced for the drier soils which indicates a strong impact of the surface conductance in agricultural soils (Seladji *et al.*, 2010).

Organic matter. The organic matter percentage in the soil usually influences the soil structure, including the ability of the soil to hold water and nutrient availability and influences the effects of the chemical solutions added to the soils in the form of fertilizer, pesticides etc.

The organic matter content of the field usually develops over time and mapping this feature is important in terms of understanding the past productivity of the fields in order to assess and predict for future crops. Because organic matter is so important in the productivity and the quality of the soil, mapping its content, especially when manure or other types of organic matter are added on the field, could provide information regarding which areas are not very well covered and needs more adding for a healthy development of the plants throughout the whole field.

It has been observed that permittivity values are usually higher for organic matter (vermicompost e.g.) compared to that of inorganic matter like calcium carbonate e.g., and also that variation in dielectric permittivity is approximately linear with increase in percentage volume of the organic and inorganic matters (Navar khele et al., 2009).

Soil pH has an impact on nutrient availability and microbial activity as well as the herbicide use, and not only these but different types of crops require different pH levels for them to be able to grow at a healthy rate. The soil's pH varies primarily depending on the mineral content of the parent material of the soil. Usually, in dry climates where soil weathering is less intense, the soil's pH is usually either neutral or alkaline, compared to the areas where the parent material has gone through more weathering, especially in humid environment, where soils acidify over time (van Breemen et al., 1983). When testing permittivity values on different types of soils with different pH values, it has been observed how wide the variation

is and how hard it is correlate these two parameters (Lawal et al., 2019). For example it appears that Cambisols (pH acidic) generally have low dielectric constant values of 5.01±0.37 while Acrisols which are also acidic but slightly more compared to Cambisols were found to have higher values of dielectric constant of 7.95±1.64 (Lawal et al., 2019). For different types of Arenosols, for example, with acidic and neutral pH it has been observed that the range of values is really large from 3.90-25.60 and Fluvisols which are even more acidic than the previous types, have a range of 5.13-5.70 (Lawal et al., 2019). These differences are so wide that is difficult to conclude that certain pH levels correlate with certain permittivity values, but this information is important in terms of understanding the large variation in the soils with same permittivity value, and how this affects the way we see the roots, as well as the difficulty to pinpoint on specific values or ranges.

Soil moisture and soil temperature also represent important factors, especially in regards to sowing, where having suitable temperature and humidity in the soil enables the plants to have a healthy and productive start. Soil moisture represents one of the most important features in crop production. This parameter is in a strong relationship with air, heat, and mechanical resistance for plant root growth, acting as the main feature in transporting nutrients to the plants (Boone, 1986).

In terms of resistivity, and the relationship between water content and compaction, when laboratory experiments carried out with the aid of models based on Archie's law (Archie, 1941), it has been observed that models of soils with water content of $> 0.2\ m^3m^{-3}$, usually lead to higher values of water content for the same value of resistivity , whereas in models with water content below that value, the opposite situation occurred (Melo *et al.*, 2021). It has

also been observed that resistivity is more impacted by the water content than the compaction level (Melo *et al.*, 2021).

Besides soil pH, soil moisture, and soil temperature, another important feature is represented by the local ***topography.*** Topographical variations, even small in size, will have an effect on the water flow, and the soil content might also vary due to natural erosion processes from wind or water flowing on the surface.

In terms of electrical surveys, soil resistivity values could range from as low as 1 Ωm or even less (when saline water is present) to 105 Ωm in permafrost (Palacky, 1987). Clay content and soil porosity are among the most important features, in terms of resistivity values for the soil (Besson *et al.*, 2004). Overall, however, soils exhibit a great range of resistivity variation.

2.3.5. NOTES ON PRECISION AGRICULTURE

Precision agriculture is represented by a set of technologies which combine sensors, information systems, enhanced machinery and informed management in order to optimize production by accounting for variability and uncertainties in the agricultural systems. (Gebbers & Adamchuk 2019). The concept of precision agriculture started to materialize in the 1980's under the idea of applying the right treatment in the right place at the right time. In the beginning, it mainly focused on adapting the fertilizer distribution depending on different soil conditions in agricultural fields. The technologies used were the global navigation system or GNSS, platforms like geographic information systems or GIS and microcomputers, but

since then, with the evolution and availability of technology and sensors, precision agriculture has flourished. More devices have emerged, including cheap and robust sensors, autonomous machinery, and automatic vehicles.

The use of precision agriculture very diverse and depends on many factors that include but are not limited to crop type, area, resources and available technology in the area. Even though the concept is broad, it can be said that the main goal of precision agriculture is to optimize the use of available resources and to increase the productivity of agricultural operations in a sustainable manner (Gebbers and Adamchuk, 2010).

2.3.6. TRANSPARENT SOILS

Using transparent soils for geophysical studies represents a novel approach and it is believed that this paper represents the first attempt to use this type of soil for imaging plant growth environments with the use of geophysical methods. Using transparent soil in an experimental setting would allow for a direct correlation of the data with the actual position in real life of all the roots and changes in the soil.

Transparent soils have been used in biological research as they provide a good growth environment for the plants, and allow flexibility in terms of adding nutrients and modifying and controlling the growth environment (Downie *et al.*, 2012). Some transparent soils are used in geotechnical studies, even though this represents an innovative approach as well, there are situations in which solutions have been found to mimic the geotechnical properties of soils (Iskander, 2010).

For this study, three types of transparent soil have been found and tested and will be described as follows.

Agar transparent soil – probably the most used type of transparent soil, as it is commonly used in biological studies as growth material for studying plants. Agar-agar is a powder made from algae which becomes gelatinous at certain temperatures. It is a product widely used in food industry in some parts of the world. In terms of biological studies, it is also a very common material used for bacterial and plant growth due to its pH neutral properties.

Because it is routinely used in biological studies, there are certain protocols that need to be used in order to create the agar transparent soil, and one of them is represented by the protocols used for growing the *Arabidopsis thaliana*, one of the most widely used for plant experiments in a variety of studies worldwide. In order to create the transparent soil, a solution of MS salts, sucrose, and distilled water is mixed. After mixing the ingredients, a solution of NaOH or KOH is added to lower the pH level of the solution to 5.7, the agar powder is added, after which the whole solution is inserted into an autoclave for 20 minutes at 120°C. The solution is afterwards cooled down to 50°C, and kanamycin added to it for preventing bacterial growth.

Following the protocols is important as the agar gel is a great environment for bacterial and mold development, and this is also one of the aspects that makes the use of agar in geophysical experiments a bit more complicated.

Nafion polymer transparent soil – this is a type of material used in recent studies that mimics the properties of the soil better than agar-agar, allowing for a more natural development of the plant roots. Nafion represents a transparent synthetic polymer with ionic properties which has

the ability to adapt from a physical and chemical point of view. In order to create the actual transparent soil, the nafion material comes in the form of pellets (4 mm x 3 mm) and is freeze-milled to create smaller particles (350 to 1600 mm), after which the particles are washed repeatedly in a variety of solutions (KOH, dH_2O) and treated with sulphuric acid, until the solution reaches a neutral pH, after which they were sterilized as a final step, for preparing them for use (Downie *et al.*, 2012).

As this type of soil has been proved to be a great environment for root growth, and allowing for changes in chemical and physical properties, as well as adding and controlling microbial growth (Downie *et al.*, 2012), it has some limitations in terms of costs and production facilities. Because for geophysical studies, there is a need of large amounts in terms of volume (e.g. 60 L, 90 L) in order to fill the tanks for allowing the geophysical methods surveying, this type of soil even though a great option for the plants, would be very difficult to use in a real experimental setting for geophysics. Therefore, it represents an excellent material to be used in future studies for experimental use.

KI-gel 201KA (aquabeads) transparent soil –a type of material used in geotechnical studies, and could mimic very well a variety of soil properties. Plastic beads or aqua beads represent a strong water adsorption polymer sold under the commercial name KI-GEL 201K. The beads are composed of isobutylene and maleic anhydride copolymer with the same refractive index as water, and come in the shape of light-yellow spherical particles, with density of 980g/l, water content of 7%, and a pH of 9-10. After absorbing water, the beads change their appearance and transition from yellow to a very clear transparent gel-like material (Iskander, 2010).

Figure 27. Example of a plant immersed in a transparent soil type created by grounding KI-gel 201KA aquabeads granules. This represents the type of soil used in the case study which will be presented at the methodology section.

Some features regarding aquabeads include good durability and stable water absorption under different temperatures and can absorb water up to 200 times their own weight (Tabe, Iskander and Honma, 2011).

The advantages of using this type of material relies on their level of transparency (fig. 27), which is much higher than the usual type of silica gel which is normally used in geotechnical studies (Tabe, Iskander and Honma, 2011), and this represents a feature that could offer advantages for plant root study. Also, from a geotechnical perspective, aquabeads have similar hydraulic characteristics to natural sands and silts, and are compatible with water, oil, surfactants and alcohols (Tabe, Iskander and Honma, 2011), which allows for adapting the

environment or modifying it without degrading the “soil” environment. In terms of permeability, it appears that the hydraulic conductivities are similar to those of fine and silty clays, and compression and recompression indices are similar to the ones for natural soils, and porosity structure close to many peats and organic clays (Tabe, Iskander and Honma, 2011).

Even though this type of transparent soil is not necessarily a perfect replacement of agricultural soils, it appears to be the closest out of everything that was tested so far, with similarities related to a variety of sands, peats and clays. Another advantage of this material is the low cost of the material necessary for the study, and “imperfect” gel aspect (compared to agar e.g.), with porosity and different granule sizes which seem ideal for allowing roots to develop in a more natural pattern throughout the transparent soil.

2.4. THE USE OF GEOPHYSICAL METHODS IN AGRICULTURAL AND PLANT ROOT STUDIES

2.4.1. INTRODUCTION

The previous chapters have described the theoretical aspects of the geophysical methods used in this study, as well as elementary notions relevant for the objective of the study, such as the understanding of plant root biology, agricultural plants and their behaviour and agricultural soils and their composition, highlighting notions that are relevant from a geophysical point of view as well.

This chapter will focus on the existing literature on the applications of geophysical methods in agricultural plant root studies, plant roots and agricultural settings, which offered support and played an important role in starting and working on the case study and practical applications of this project.

As was described in the previous chapters, there is vast usability and potential of geophysical methods in agriculture, but as the paper focuses on only the resistivity method and the ground penetrating radar method, only studies involving these two methods will be discussed.

This literature review studies enables a better understanding of how the geophysical methods should or would be applied and what limitations should be expected – many of which are discussed in this type of study.

2.4.2. GPR IN AGRICULTURAL STUDIES

As mentioned in the chapter 2.2.1.8. on the limitations of the method, in order to obtain the most from GPR data, a very good coupling between the survey surface and the antenna is essential. This represents a particularly important aspect for GPR agriculture, as the surface could be quite rough due to micro topographical differences, and a good contact can be difficult to achieve in real world settings.

Another important aspect is represented by the clay content, as mentioned before due to the nature of clays, they absorb the energy from the antenna and affect the level of reflections into the underground and the quality of the data altogether. This means that the effectiveness of

the GPR method will depend on local site conditions (Goodman *et al.*, 2006), and soil maps with information regarding clay content would represent a great tool to understand how to better apply the method and if this would be a feasible method to use.

A previously mentioned, another important feature of interest in agriculture is represented by the soil water content, and GPR represents a method that can be used for the detection of this parameter in soils.

Various GPR approaches have been proven to offer significant information in agricultural studies, in terms of soil water. After analysing two variations of the GPR method, the WARR (Wide Angle Reflection and Refraction) method and STA (Single Trace Analysis) for testing their accuracy on measurements of soil water content, it has been observed that GPR represents a more practical approach in terms of large scale surveys compared to TDR (Time Domain Reflectometry) surveys (Huisman *et al.*, 2001). Different from the classical GPR surveys, the WARR method usually consists of having one fixed antenna and one mobile antenna, and increasing the distance between them stepwise, and for the identification of the ground wave, the path of the ground wave between the emitting antenna and the receiving antenna results in a linear relation between travel time and antenna separation (Huisman *et al.*, 2001). For the STA method the separation between the antennas is fixed. TDR represents a very efficient method and highly accurate and automatable for the determination of porous media water content and electrical conductivity (Jones, Wraith and Or, 2002). Compared to GPR which uses antennas for surveys, the TDR uses a variety of multi-wired probes which are able to take only localized measurements in certain points when they are inserted into the ground, therefore making it inappropriate for large scale surveys. This represents one of the

advantages of the GPR systems, as they offer comparable results to the TDR method but are able to offer this information on large areas (Huisman *et al.*, 2001). It appears that when tested on 25 different site locations with a variety of soil types textures, especially varieties of loamy sands, loams, silt loams and sands, the GPR method is still limited when it comes to heavier textures because of the high conductivity of the soils (Huisman *et al.*, 2001).

Borehole GPR and off-ground GPR surveys represent two other methods used for the determination of soil water content (Klotzsche *et al.*, 2018). Vertical radar profiling or VRP, is primarily used to derive 1D velocity models by inverting the arrival times of direct waves, and represents a single-borehole geophysical technique, in which the receiver antenna is located inside hole and the transmitter antenna is placed at various offsets from the borehole (Tronicke and Hamann, 2014).

The off-ground GPR method uses measurements in the time domain for estimating soil water content using the surface reflection method, which compared with on-ground GPR systems, has limitations in terms of getting information from deep soil horizons due to the strong dielectric contrast at the soil–air interface, and is more sensitive to the soil surface roughness (Klotzsche *et al.*, 2018).

In terms of practical applications for agriculture, using the GPR WARR method along with TDR proved to be a great way to monitor and estimate soil water content during both the irrigation process and the drainage phase (Galagedara *et al.*, 2005).

All of these methods and variations on GPR rely on the use of two separate antenna systems, one receiving antenna and one transmitting antenna.

In terms of how the water changed the permittivity value of fine silt soils, using a GPR system that has both the receiver and transmitter fixed, it has been observed that for fine silt soil, with lower water content (less than 6%), the dielectric constant values were found to be around ***9*** when using a 400 MHz antenna, and ***8*** for higher frequency antennas (1 and 1.8 GHz) (Cigna *et al.*, 2012). It appears that these values would increase gradually with the increase in water content, for example, for water content above 12%, the values are around ***18*** for the 400 MHz and ***15*** for the higher frequency antennas (Cigna *et al.*, 2012).

For estimating water content with a GPR system that has fixed receiving and transmitting antenna, has its advantages in terms of large surface areas and usually being much faster.

It has also been observed that compaction of the soil helped by the level of water content also increases the permittivity value of the soil (Cigna *et al.*, 2012).

The organic matter component in the soil also affects the permittivity values of the soil. When tests were carried out on a type of humid tropical soil with organic fractions between 4% to 7% it has been observed, that the organic matter component in the soil decreases the dielectric constant of the tested soil (Zhou *et al*, 2019).

2.4.3. RESISTIVITY IN AGRICULTURAL STUDIES

As mentioned in the chapter 2.2.2, the classical resistivity surveys are very time consuming, as they require the surveyor to insert the electrodes for measuring only one data point, and having to move and reinsert the electrodes every time for a new data point. Even the

multielectrod systems can be time consuming. These limitations of the method have led to some adaptations and improvements which are applicable in the agricultural sector, as it is the case of the galvanic contact resistivity, which allows for measurements to be taken continuously, this way speeding up the process of data collection (Allred *et al.*, 2016).

Figure 28. Image showing an example of a resistivity equipment using disks as electrodes developed by Veris Technologies (Binley and Slater, 2020)

One of the first systems using galvanic contact with continuous resistivity measurements was developed by (Christensen and Sørensen, 2001) and consisted of a line of cylindrical steel tubes with current and potential electrodes connected via a multicore cable (Allred *et al.*, 2016). The way the system was designed, it allowed for measurements for apparent resistivity values to be collected using the Wenner array at two depths (one system was 30 m long while another one was 90 m long), which according to Loke (2004) would correspond to an approximate depth of 5 m respectively 16 m. The systems have suffered modification and

adaptations for it to be more suitable for agricultural settings, as it is the case of Veris 3100 Soil EC Mapping System by Veris Technologies, which uses electrodes composed of steel disks mounted in a steel frame, with diameter of 43cm and are pulled along by a vehicle (fig. 28) at a constant speed of 25 km/h. This shape and feature allow a depth of penetration from approximately 2.5 to 7.5 cm. Compared to the previous example, this system uses 6 disks (electrodes) with two electrodes acting as current electrodes and the other two pairs as potential electrodes. The surveys carried out with this method are very useful in mapping soil water content in dry land fields (McCutcheon *et al.*, 2006), and how the data changes aspect when surveys are carried on same areas but in different periods of time.

The method has been proven to be useful in the prediction of crop yields due to the soil water differences (Corwin and Lesch, 2005). In another recent study, it was found that this method helps with the mapping and highlighting of the cation exchange capacity of the agricultural fields, an important soil property which influences the soil's ability to hold essential nutrients (Koganti *et al.*, 2017).

2.4.4. GPR IN PLANT ROOT STUDIES

When it comes to studying roots with the use of GPR surveys, the majority of the studies focus on tree roots most of the times or plants with woody roots of significant size. Even so, the methods used and the way it was applied (in terms of type of antenna, types of profiles, etc.) represent a good starting point for the understanding on how to apply the method in this study to get the most out of it.

Tree roots have been found in GPR surveys for a long time, but for most of times the registered data from them was considered noise and wasn't given much attention (Butnor *et al.*, 2001), but have started to gain more attention in the past years with the development of newer types of equipment, and with people focusing more on the wellbeing of the plants in terms of urban landscaping, forestry (Butnor *et al.*, 2003), and agriculture.

In terms of detecting smaller roots, high frequency antennas (in this case, 2 GHz) on tree roots proved effective in detecting roots as small as 0.5 cm, when the roots of a Siberian elm tree (*Ulmus pumila*) were analysed (Cui *et al.*, 2010). Even though it has been showed that tree roots and tree branches and twigs present different permittivity values (Mihai *et al.*, 2019) and they have been used in studies as if they were presenting similar characteristics, it has been showed that in sandy soils it is possible to detect roots (twigs) of as low as 2 to 3 mm in diameter when antennas of 1.5 GHz were used (Wielopoiski *et al.*, 2000), if there is a sufficient permittivity contrast.

However, when analysing the roots of a Japanese cedar (*Cryptomeria japonica*) with a relatively lower frequency antenna of 900 MHz, it was found that the detection of the roots greater than 19 mm was possible in some instances, but not for any roots below that size, as shown by the analysis of roots with diameters going as low as 10 mm (Hirano and Dannoura, 2009). It also appears that other limitations have occurred in terms of distinguishing between roots that were close together (less than 20 cm), especially if the roots were smaller, even though the surveys were carried out in a controlled environment using sand, which is great for GPR data (Hirano and Dannoura, 2009).

When it comes to analysing agricultural plant roots with GPR, most of the times the focus is on the whole root biomass rather than individual roots as it is the case with tree roots. Cassava *Manihot esculenta Crantz*) is one of the most important sources of starch (Delgado *et al.*, 2017), and is therefore an important type of agricultural plant, of which the roots biomass was studied with the use of GPR. It has been shown that the GPR was not only able to detect the root biomass, but through monitoring, it was possible to detect when the root biomass was increasing, and all this with the help of a 700 MHz antenna (Delgado *et al.*, 2017) which has much lower frequency than the previously described ones used in the detection of finer tree roots.

2.4.5. RESISTIVITY IN PLANT ROOT STUDIES

As is the case with GPR studies, much of the literature discussing geoelectrical methods applied to plant studies focus on trees and their roots, and plants with very coarse woody roots, which are more likely to be resolved compared to the roots of smaller agricultural plants. In a study on tree roots it was observed that the root biomass of the trees or really woody roots, exerts a strong effect on resistivity value of 40 Ωm, and it was hypothesised that if the values get lower than this, the resistivity method will have difficulties in differentiating between the roots and other properties of the soil (Amato *et al.*, 2008). This aspect represents a very important information when it comes to applying the resistivity method, especially in real outdoor environments, where soil parameters change due to their variation in minerals, water content and soil porosity.

A study carried out on an alfalfa (*Medicago sativa*) plant (Amato *et al.*, 2009), which has a complex root system involving both branched and fibrous roots (Bucciarelli *et al.*, 2021), has showed promising results in terms of highlighting root zone areas with the resistivity method. The experiments were carried out indoor for a better control of the environment, using containers and different types and mixtures of soils for each container. The resistivity array used was a combination of Wenner and dipole-dipole, but borehole resistivity surveys were also carried for allowing the visualisation of the data in 3D sections. It was observed that even though root biomass was highlighted with the use of the resistivity method, it seems that in some situations it is difficult to differentiate between the root area and the water content, with this method.

Root water uptake is another important feature when it comes to agricultural plants in general, and it appears that there are variations in terms of root water uptake throughout the day (Werban, Al Hagrey and Rabbel, 2008). During the experiments, daily patterns in root absorption were observed; for example, it was found that the water content increases continuously from dawn to noon, while during the afternoon there was an irregular increase and decrease. The study combined TDR (time-domain-reflectometry) surveys with ERT surveys for monitoring the root water uptake in a controlled environment, using an already grown 40 cm lupine plant (*Lupinus polyphyllus)* with developed roots approximately 25 cm in diameter (for the whole root area) and instead of soil, the container used for the experiment was filled with a sand material (Werban, Al Hagrey and Rabbel, 2008). One of the findings from the study was the identification of a zone of lower resistivity at a depth of approximately 4-5cm which coincides with the zone with the highest root content (Werban, Al Hagrey and

Rabbel, 2008). As it is the case with the alfalfa plant study, described earlier, this work uses another plant with a complex and significant system of roots of multiple orders with a variety of sizes as well as larger roots, with a very thick and central tap root which branches into other smaller roots (Leitner *et al.*, 2014).

In another study, the ERT method was combined with borehole resistivity surveys for imaging the root zone area of a hibiscus plant (*Hibiscus rosa-sinensis*), and the container containing the plant was filled with a type of soil consisting mostly of sand (Petersen and al Hagrey, 2009). The hibiscus plant has mostly horizontal and surficial roots. From a root architecture classification point of view, this is classified as H-type root system (Fan and Chen, 2010). This marks a different type of root than the previously discussed studies, but this work also shares a similarity with previous work in that the roots are well-developed, coarse, and woody.

These surveys were carried out using a system of two perpendicular resistivity profiles of 16 electrodes each, on the diagonals of the experiment box, and four vertical borehole profiles with 12 electrodes each (Petersen and al Hagrey, 2009). Prior to the resistivity surveys, resistivity models were created which helped with the understanding of how to maximize the outcome from the actual resistivity surveys. The electrode spacing is 1 cm, except for the central electrodes closest to the root where the distance has been increased to 2 cm, and the electrodes used are 2 mm and 3 mm stainless steel, which were chosen to be smaller than the distance between the electrodes for ensuring good coupling, and the distance between electrodes was chosen to be far smaller than the root size, in order to ensure a good tomographic coverage (Petersen and al Hagrey, 2009).

Having the ability to control the environment in which the resistivity surveys are carried out represents a significant advantage. Experimental settings (which offer the advantage of controlling parameters like temperature, water content, type of soil etc.) represent ideal situations, which are great for highlighting features of interest and understanding how to better apply the methods in the real world. But oftentimes, the situation in the real world is very different from the ideal scenario of a laboratory experiment, and when trying to apply what has been learned and applied in a controlled environment, it is important to keep in mind that real surveys will face a number of limitations and challenges in an actual, active agricultural environment.

When vineyards were studied with the use of resistivity method for the purpose of understanding the relationship between the plant and the soil water content and uptake (Brillante *et al.*, 2015), petrophysical models had to be created for describing and understanding the properties of the soil in order to highlight root water uptake areas. As is the case with the plants used for the experiments, vineyards represent plants that also have much coarser roots compared to the roots of wheat (and most other types of plants with of agricultural interest). For vineyards, the soil water content, availability and uniformity across the area represents an important aspect which affects the quality of the yield, and this was studied by taking into consideration uncontrollable aspects like rainfall and temperatures (which were measured) for highlighting differences in soil water depletion.

Applying the resistivity method in a coffee plant (*Coffea arabica L.*) plantation (Paglis, 2013), showed that the roots were able to affect the soil electrical resistivity, and found that there are difficulties in terms of highlighting and differentiating the length of the roots from the soil in

terms of resistivity values, but highlighting root biomass was possible. The root system of the coffee plant usually involves a tap root (ranging between 68-104 cm) with developing lateral roots (ranging between 20-120 cm), out of which between 7-15 are large coarse roots, a similar number for medium roots and the fine roots are in the range of 11-30, and an average root volume would be in the range 300-560 cm^3 (Kufa and Burkhardt, 2013). These elements are important when taken into consideration as again, the resistivity method is applied on a plant with a significant volume of roots among which there is a combination of both fine roots and coarse roots which are usually a lot easier to highlight.

Overall, while the application of geophysical methods in agriculture is receiving more attention in recent years, there are still substantial knowledge gaps; one such gap is represented by the existing literature's focus, which falls more on coarse, woody roots, than on fibrous roots – which is the principal aim of this work.

3. METHODOLOGY

3.1. INTRODUCTION

For a better understanding of how to use geophysical methods for plant root detection and analysis, the study comprises two parts: an indoor experimental setting and field measurement in natural environments. The final focus being to apply these lessons and notions in real world agricultural settings, it was important to understand limitations and applications from both points of view.

The field measurements helped with understanding the limitations of both GPR and resistivity methods, and also helped with shaping the experimental environment in the laboratory.

Using the information from the observations and measurements in the natural field, the experimental settings were created in a way that closely mimics natural factors. A variety of boxes have been used with different parameters, tubes, plates created to hold electrodes for resistivity surveys, transparent soil has been developed, and a variety of plants tested.

This chapter will explain the methodology used for both categories of measurements, indoor experimental setting and field measurements, describing different parameters specific to the setting, equipment used including a resistivity prototype equipment and a variety of electrical devices, created specifically for this study and the way the equipment was used including specific details about positioning, types of profiles and arrays, etc.

3.2. CHOICE OF SENSING TECHNOLOGY

Based on the literature review which is presented in chapter 2 and the observations and measurements in the agricultural field which will be presented at the beginning of this chapter, the resistivity method and the GPR were chosen for this study. These methods could provide the most degree of information and a higher quality of the subsurface imaging regarding plant roots detection and analysis (Zhang *et al.*, 2019). The electrical resistivity method required adaptations and modifications in order to achieve the degree of imaging desired, by building electronic equipment and attaching it to the pre-existing commercial.

Because the parameters of the GPR antenna, affect the depth of penetration and horizontal spatial resolution, choosing higher frequency antennas was appropriate keeping in mind that the objective regarding plant roots study requires a spatial resolution of centimetres and the depth of penetration is also quite small in the range of tens of centimetres (Daniels, 2005).

High frequency antennas are successfully used in geotechnical studies for imaging and estimating the quality of concrete and other building materials. The range of the antennas used for high spatial resolution in these types of studies goes up to 8 GHz. These work very well in homogenous environments where there is a greater contrast between concrete and metallic materials for example, whilst the water quantity in the medium would usually reduce the quality of the imaging and the depth of penetration. A 4 GHz antenna provides an acceptable compromise by doubling the size of the minimum resolvable horizontal spatial feature whilst

increasing the depth of penetration. As the 4 GHz antenna gets easily affected by any inhomogeneity and has a very low depth of penetration, another smaller frequency antenna was chosen, 1.5 GHz.

The GPR antenna transmits short pulses of high frequency electro-magnetic energy, depending on the antenna type and frequency, into the subsurface (Jol and Smith, 1995). The electromagnetic wave is dispersed while traveling downwards, and its velocity suffers modifications due to its encounters with materials of different electrical properties (Neal, 2004). Due to the changes in the dielectric constant, part of the energy is reflected and detected by the receiver of the antenna, while some part of the energy is scattered.

The two-way travel time is a function of reflector depth and the electromagnetic velocity of propagation (Neal, 2004; Jol and Smith, 1991). The resulting data from this kind of surveys it's given by a continuous profile of the subsurface, displaying horizontal survey distance against vertical two-way travel time, which is converted to depth if the propagation velocity is known;$d = vxt/2$; where d is depth, v is velocity and t is two-way travel time.

The resolution and zone of influence represent two important factors when choosing geophysical methods for a particular study. The GPR's resolution is dependent on two components longitudinal or the range or depth resolution length and the lateral or the angular or sideways displacement resolution length (Jol and Smith, 1995). As the GPR is a system that generates a pules and detects their echoes, it is possible that these echoes might arrive simultaneously, in which case they might overlap. Therefore, characterizing a pulse by its width at a half amplitude, W, two pulses might be differentiated if they are separated by half their "half width" (fig. 29). If the pulses are however separated in time by less than this

amount, it is usual to interpret the pulses as a single event (Jol and Smith, 1995). This temporal pulse separation represents the spatial resolution. The factors that influence the resolution length are the pulse width and the velocity in the material, whereas the radial resolution length is affected by pulse dispersion and attenuation, at larger distances.

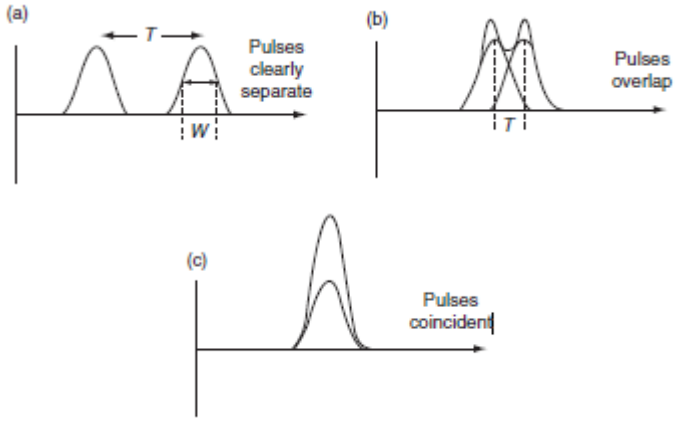

Figure 29. Image representing: a - Temporal pulses with half width. B - Two pulses are distinguishable until T W. c – When T much smaller than W the two events are not distinguishable (Jol and Smith, 1995).

The lateral resolution therefore depends on the velocity, the pulse width and the distance which as it increases it improves the lateral resolution. The pulse width in GPR, W, in time is directly related to the bandwidth, B, which is also directly related to the central frequency (Jol and Smith, 1995).

The resistivity method represents a flexible geophysical method which can be used in almost every kind of environment and on every kind of scale if the proper equipment is provided. The electrical resistivity method, works very well in environments, where there exists a contrast in resistivity values of the materials. As the water content in a porous material affects

the conductivity and resistivity of the material (Munoz et al. 2012), and understanding that root water absorption area is usually higher in water content compared to the surrounding environment, it is possible to see the change in resistivity throughout profiles close to the plants and their root areas. Using the right parameters for the surveys in a way that will allow the increase in data points close to the surface and covering the deeper parts of the roots, as well as having an understanding of the environment type and conditions in which the plant grows, represent important factors that need to be considered and assessed before starting the surveys in order to offer a higher degree of imaging quality of the root zone area, from a resistivity point of view.

As the current source is considered a point, and in this kind of surveys the objective is very close to the surface, as it is described in the next chapters, choosing the right size of distance between electrodes and the size of the resistivity probes will present another important factor that will need to be considered and changed in order to create good imaging versions of the resistivity contrast in the environment containing plant roots.

3.3. DIRECT MEASUREMENTS AND FIELD OBSERVATIONS

The initial step in understanding the challenges and limitations of applying geophysical methods in agricultural settings, particularly focusing on the root zones of crops, involves a thorough understanding of the specific characteristics of the subject in real-world environments. Therefore, field observations across various crop fields provided valuable information, which facilitated the design of indoor experiments. This approach enabled the

replication of the environmental conditions and plant growth parameters in experimental settings, closely recreating field conditions. It facilitated the collection of extensive data within a controlled environment, free from the limitations imposed by weather or other unpredictable external factors. While many studies using geophysical methods on plant root areas concentrate on idealised conditions and plants with coarser roots (Hagrey et al., 2009; Amato et al., 2009; etc.), this paper aims to evaluate the methods' applicability in actual agricultural settings, taking into account their specific characteristics.

Direct measurements and observations were conducted near Chirnogeni village, Constanța County, Romania, involving the excavation of small trenches alongside plant roots to create a vertical cross-section for photography. This helped in understanding the soil layers present (fig. 30 - a). Fields covered by wheat (*Triticum aestivum*) and rapeseed (*Brassica napus*) crops were selected for these observations based on site availability, local council permissions and on their status as some of the world's most extensively cultivated crops (Tang *et al.*, 2011). After taking several pictures in different areas, several plants were taken from the field to be photographed, measured and analysed in more detail.

The observations revealed that plant roots tend to lie close to the surface, and in most cases the top 10 cm layer represents the layer with the highest root density. In terms of depth of the roots for the rapeseed plants the roots vary approximately between 10-15 cm in depth, whereas the wheat roots appear to not go below 10 cm (fig. 30 – a), or at least the top 10 cm layer appears to have highest root density after which, due to the nature of the wheat roots (very fine white roots, less than 1 mm diameter) is not as clear if they also continue to grow

further down. This tendency is likely influenced by irrigation practices in agriculture, as root growth and distribution are closely linked to water availability (Robbins and Dinneny, 2018).

Figure 30. Visualizing the wheat plant root areas and the different layers with changing parameters in a soil cross-section (a); location of the main samples and and state of the field (b); focus on the layer with high root content (c); focus on the short distance between individual plants in the field.

Consequently, regular irrigation diminishes the need for roots to extend deeply in search of water and nutrients (Guo *et al.*, 2022).

In terms of physical parameters of geophysical interest, the rapeseed plants present thick roots close to the surface with a diameter of approximately 1 - 2 cm (fig. 31), a situation similar to those found in the literature review where the GPR and resistivity methods have been applied to tree roots of similar sizes, and even though challenging their detection was possible (Borden *et al.*, 2014; Delgado *et al.*, 2017; Zhang *et al.*, 2019). In the case of the wheat plants on the other hand, due to their small diameter (less than 1 mm) and their density throughout the soil, delimiting individual roots is very difficult, however the fine roots appear to create a layer with distinctive parameters (fig. 30 – a). The layer can be described as a mix of roots and soil which at least visually appears to possess different parameters, like higher moisture content and darker colour (fig. 30 – c), creating a contrast between this layer and the layer below which appears to look dryer (fig. 30 – a), lighter in colour and doesn't appear to contain any roots, consisting mainly of soil. The appearance of the contrast in physical parameters should allow for both GPR and resistivity methods to detect change from one layer to another.

The close proximity of the plants, often around 5 cm apart (fig. 30 – d; fig. 31), complicates the identification of individual roots, posing significant challenges for the application of geophysical methods in terms of identifying specific roots from each plant when grown in a real world agricultural setting.

These observations have been made only on the plants on the edges of the fields, as the fully grown plants posed an impediment in trying to access the field on foot (fig. 30 – b), an aspect

which would also poses a practical limitation in terms of applying the GPR and resistivity surveys in a conventional way.

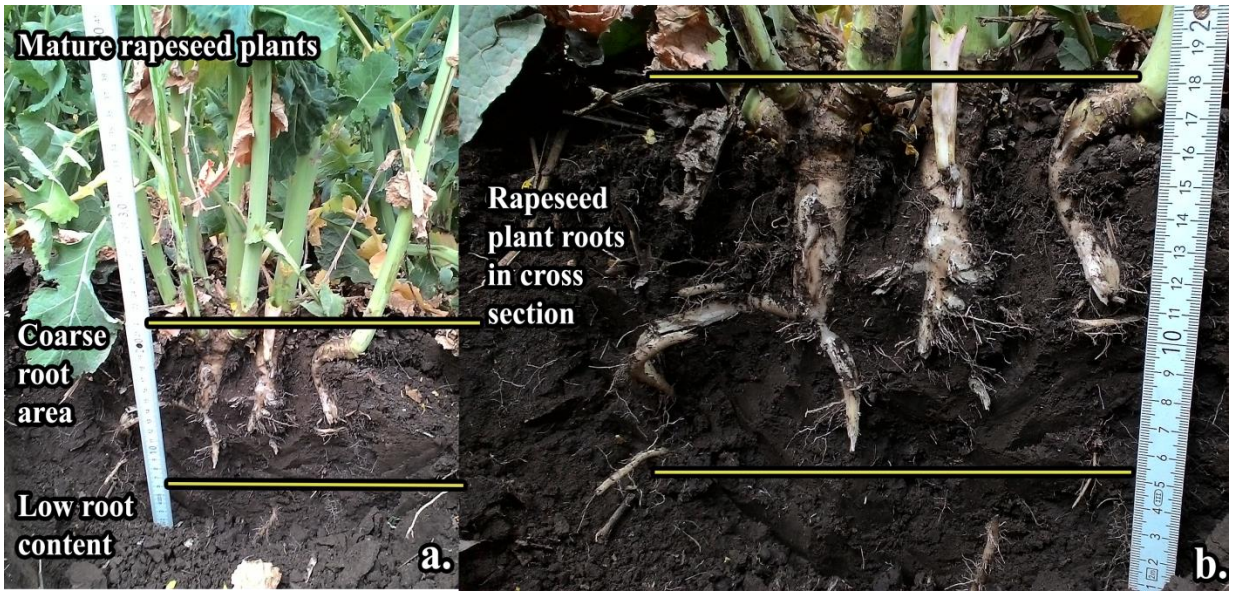

Figure 31. Image from a rapeseed field, representing the root zone layer in the soil in a csoil unit cross-section (a) and focus on the root area (b).

The observations indicate potential limitations when applying geophysical techniques, like GPR and resistivity surveys, especially when the crops are fully grown and access to the field becomes restricted. Surveys are still possible at other stages of the plant growth, until they reach a point at which the person that is handling the geophysical equipment is no longer able to walk without physical restrictions in the field. For instance, resistivity surveys can be conducted using tractors where this method would allow for a faster data collection, however it would unfortunately have an impact on the health of the plants and these might be damaged by the weight of the machines (Shima, Sakashita and Kobayashi, 1996). The soil's surface roughness and irregularities can also challenge GPR applications, where optimal soil-antenna

contact is crucial for signal penetration and for quality data collection, especially when the objectives are of the order of centimetres.

These findings underscore the importance of real-world observations in guiding the development of synthetic models and experimental setups, ensuring they mimic natural conditions as closely as possible, including spatial distribution, soil layers, and surface characteristics.

3.4. EXPERIMENTAL DEVELOPMENTS

This chapter will explore various experimental setups and containers utilized in indoor geophysical surveys, detailing their sizes, soil types or material composition, and plant quantities, among other variables. It will also introduce a range of electrical and electronic devices designed to support these experiments, such as small automated irrigation systems for example.

Furthermore, the chapter will discuss the development and application of transparent soils, alongside the rationale and considerations behind the selection of plants for these experiments.

3.4.1. INDOOR EXPERIMENTAL SETTINGS

Following the field observations, indoor experimental setups were established to create a controlled environment where geophysical surveys could be conducted at any time,

incorporating insights gained from the field. An advantage of these controlled environments is the ability to not only regulates the conditions under which the surveys occur but also to directly correlate survey results with specific features directly. Additionally, these settings eliminate the dependence on specific weather conditions for conducting the surveys.

In an indoor setting, parameters such as humidity levels, soil type, and surface characteristics can be easily managed. Several trials were conducted within this indoor experimental framework, leading to gradual improvements. This process culminated in the development of a final version that was employed for the majority of the forward or synthetic models and indoor surveys.

3.4.1.1. INDOOR SETTING NO. 1 – TRANSPARENT CONTAINER

Setup description

The first indoor setup included four transparent containers measuring 59 x 30 x 47 cm with a volume of 90 litres, each filled with different materials (see fig. 32-33) as detailed below:

- Container no. 1 contained 4 layers of soil (compost and organic soil) with 3 tomato plants in the middle of the box (fig. 32 – 1). From top to bottom the types of materials used are: root boosting compost, moisture control compost, organic blend top soil and John Innes no. 2 compost (table 2).
- Container no. 2 (fig. 32 - 2)featured only 3 layers of soil, and in terms of the tomato plants, only one was planted exactly in the middle of the box. From top to bottom the

materials used in the box are: John Innes no. 2 compost, followed by organic blend top soil, and the bottom layer is made of the same John Innes no. 2 compost.

- Container no. 3 (fig. 32 – 3) consisted of no plant but one layer of top soil at the top, followed by sand in the middle and ballast at the bottom of the container.
- The 4th container consisted of only one tomato plant inserted into the box filled with water and added fertilizer only (fig. 33-34, table 2).

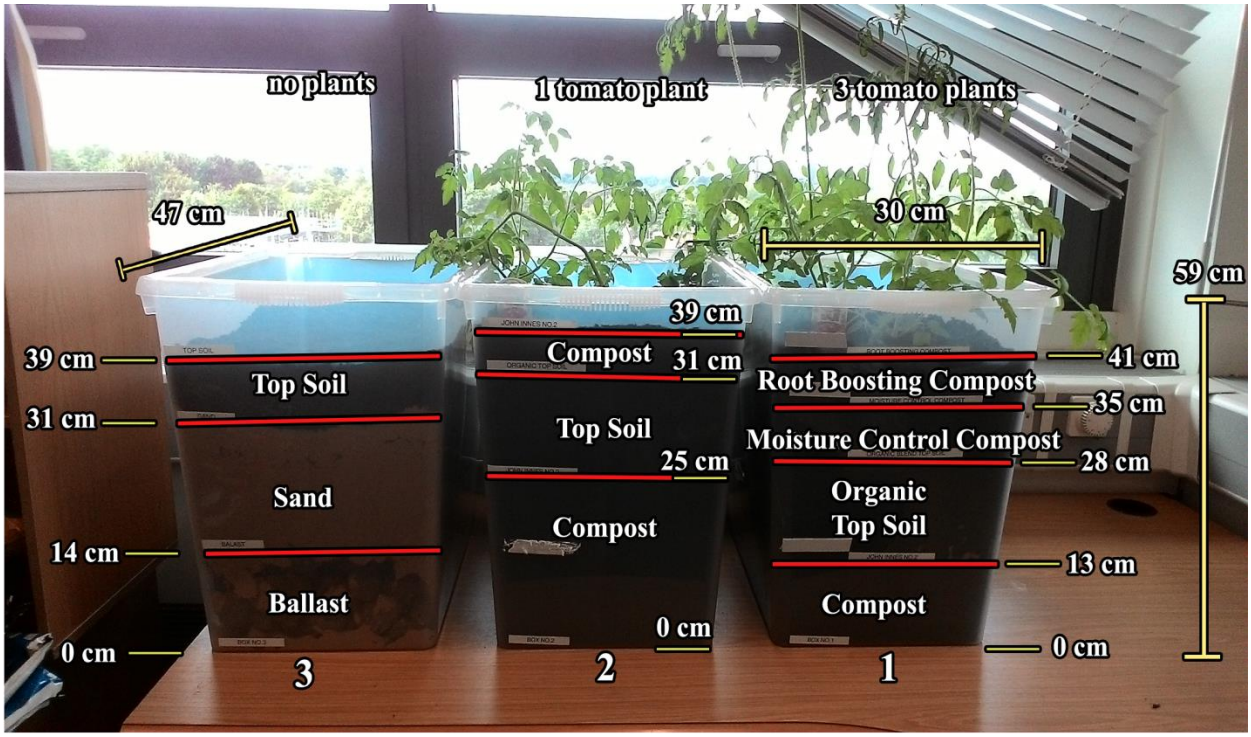

Figure 32. The first three containers with different types of soil and layer thickness numbered from 1 to 3 with details about composition and dimensions.

For container no. 4 (fig. 33), to secure the plant in position, an acrylic plate was designed to facilitate the insertion of both the electrodes and the plant, preventing them from falling. This arrangement allowed for placing the electrodes in 6 profiles, 3 on each side of the plant, with

a uniform distance of 5 cm between each profile and electrode. The plate was cut in the middle to enable the plant's insertion, which was then stabilized with sponges.

		Composition		
No.	**Material Name**	**Base**	**Additions**	**Fetilizer**
1	Root Boosting Compost	peat-free, organic loam-based	N, PsO5, K2O, B, Cu, Fe, Mn, Mo, Zn	NPK ratio of 0.03-0.03-0.03
2	Moisture Control Compost	coconut fibre	mixture of organic ingredients: kelp, earthworm castings, feather meal, and bone meal	NPK ratio of 0.18-0.10-0.10.
3	Organic Top Soil	peat-free, organic, rich, loam-based soil	N/A	N/A
4	Compost	peat-free wood fibre, mixture of loam and sand or grit	N/A	organic N
5	Sand	fine washed silica sand	N/A	N/A
6	Ballast	granite	N/A	N/A
7	Water	tap water	N/A	N/A
8	Fertilizer	N(12%), P2O5(4%), K2O (8%), Mn (0.05%), Zn (0.05%)	N/A	N/A

Table 2. The description and composition of each individual material used in all of the four containers.

The irrigation of the boxes filled with soil (fig. 32) occurred at irregular intervals and the water was manually spread throughout the surface of the soil in the box.

The electrodes consisted of stainless steel tent pegs with a length of approximately 150 mm and a diameter of 4 mm and were inserted manually at every 5 cm. For conducting the measurements, electrodes were placed for each profile, and after completing a survey, they were removed and reinserted at the next row for the subsequent profile.

Various methods were developed to insert the electrodes into a regular grid, including using a tape measure for simple displacement measurements and attaching line gauges to the box's four sides.

Observations and limitations of the setup

After using the setup to conduct several surveys (which will be described in later chapters) a couple of observations and limitations have been noted as follows.

- The acrylic plate, important for measuring a plant in water, lacked precision (fig.33-34). Its design did not ensure consistent positioning on the box upon removal and reinstallation for measurements. Since the electrode holes were manually drilled, a slight tilt occurred during insertion, altering the distance between electrodes by up to 2 cm. This issue arose because, unlike soil, water does not provide mechanical support to secure the electrodes.
- The irregular irrigation system proved to influence the anomalies and include ambiguity in interpreting the data, discussed in the following chapters, also affecting the repeatability and the imaging quality.
- The short length of the box didn't permit any useful data collection with the GPR unit.
- Even though the boxes were deep enough to permit unrestricted growth of the plants vertically, in terms of horizontal dimensions the containers didn't allow for a spread of electrodes which would've been able to get information from much deeper layers (even though theoretically maximum depth achievable AB/2 would've been approx. 25 cm - this was not achieved).
- The water filled container, even though the plant was fixed at the stem, would've have the position of the roots moved with any slight movement of the box or the elimination and insertion of the electrodes, which made it hard for the anomalies in the data to be compared to the actual position of the roots.

Overall these experiments and the trial-and-error approach led to a better understanding and enhancement of the new experimental setup and the accuracy of geophysical measurements. It also facilitated the testing of various plants, including wheat, rapeseed, and tomatoes and testing a variety of types of soils for their properties and suitability.

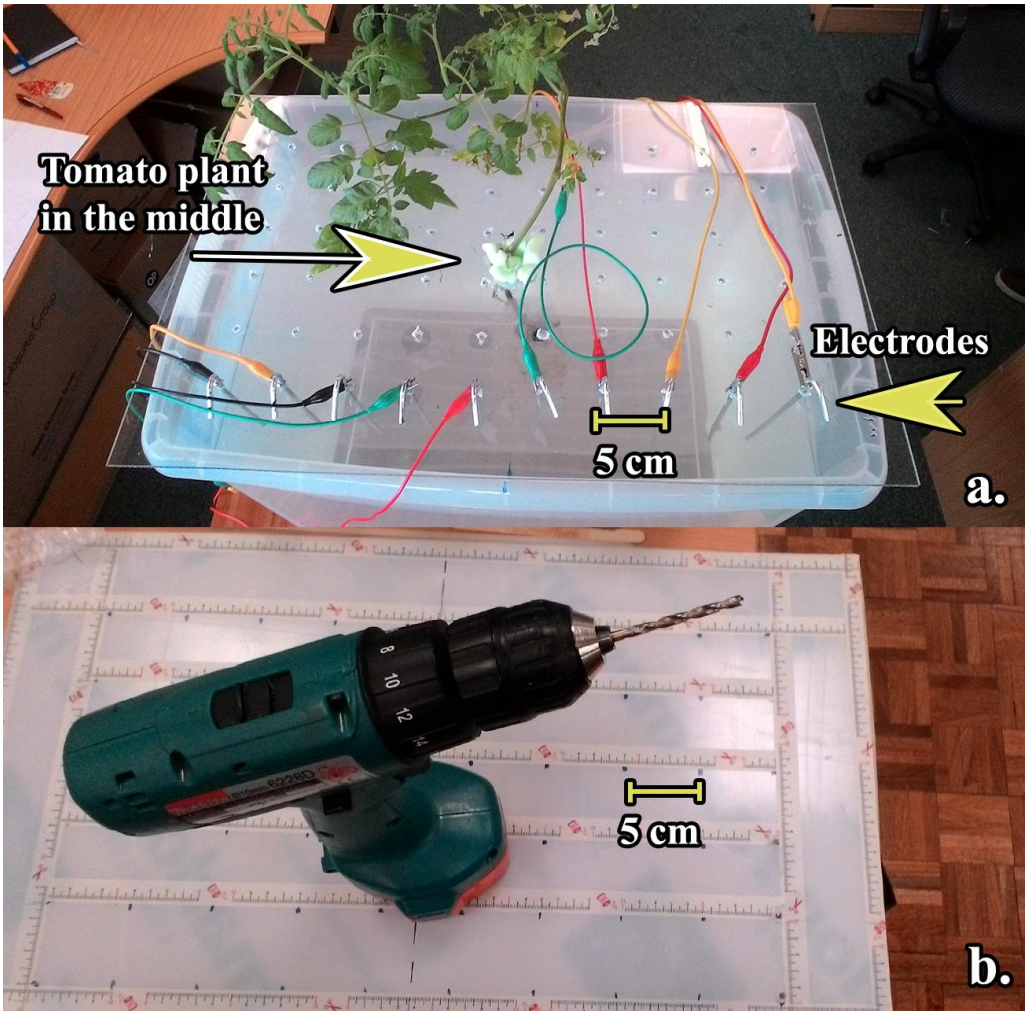

Figure 33. The system used for the surveys in the container no. 4 which involves a mixture of water and fertilizer (a); and the process of creating the acrylic plate used on top of the box (b).

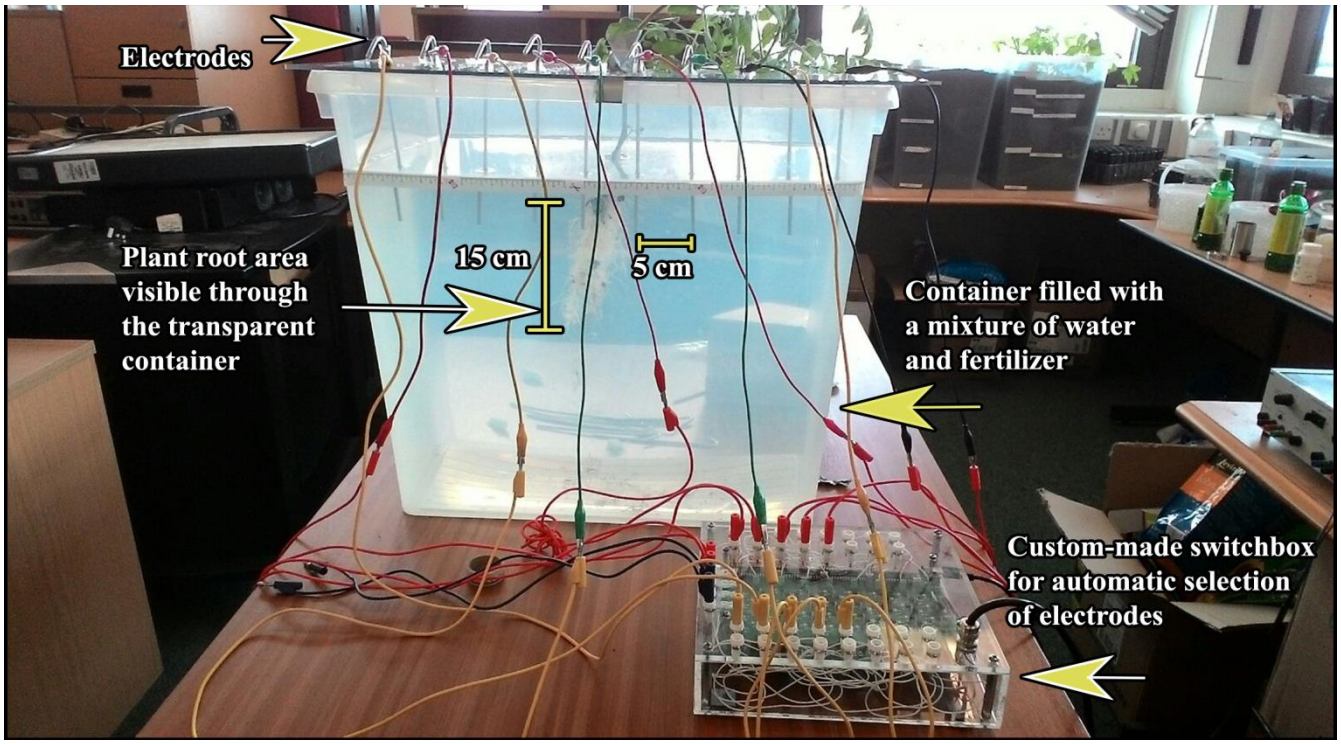

Figure 34. The container no. 4 with the water-fertilizer mixture, where the root area can be seen immersed into the solution and the inserted electrodes used for the resistivity surveys.

3.4.1.2. INDOOR SETTING NO. 2 – LARGE TRANSPARENT CONTAINER

Building on the insights gained from the initial experiments, the second experimental setup was comprised of two containers, shorter in height but longer in length compared to the ones previously described, measuring 100 x 40 x 42 cm with a volume of 133 litres. These dimensions were selected to better facilitate the collection of both GPR and resistivity data. For the GPR data collection the container would be long enough to allow for both the

insertion in the box of the antenna and to collect data in profiles which would cover both the plant area and the areas without plants, which would allow for better contrasts. In terms of the resistivity surveys these containers would allow for data collection at greater depths, a factor influenced by the distribution of electrodes on the surface.

Figure 35. Tomato plants used in experiments and their roots: a- 90 days old plants and b- 35 days old plants.

Setup description

To mimic the natural agricultural environment as closely as possible, and informed by insights from direct field surveys, all three boxes were planted with three tomato plants, spaced equally at approximately 20 cm apart (fig. 37).

- Unlike the previous setups, which featured various levels and types of soil, the first container was filled with organic topsoil. This soil, a loam-based topsoil without added lime and rich in organic matter, represents the same top soil used earlier experiments and is detailed in table 2. The plants were grown separately and transplanted into the containers after approximately 90 days of growth from seed (fig. 35 - a).
- The second container employed considerably younger, 30-35 days old plants, also grown from seed (fig. 35 – b). This approach was chosen to give the plants more time to naturally develop their roots within the container and soil. The aim was to achieve a root spread more similar to that found in natural environments, ensuring the data collection methodology could be applicable to real agricultural settings without necessitating outdoor surveys, which was shown to be limited and very difficult to conduct as described in the field observations subchapter. The soil selected for this container was multi-purpose compost, characterized by the manufacturer as a balanced peat blend. However, the manufacturer does not provide detailed information on the exact composition and quantity of ingredients. Compared to the first box, this soil visibly contains a higher amount of organic matter.
- The third box contained an experimental type of soil, described as a transparent soil (later described in subchapter 3.4.3), chosen for its unique mechanical and opacity

properties, which would allow for a direct visualization of the root areas and facilitating data correlation and interpretation. However, due to the soil's low nutrient content, maintaining the plants for more than a few days proved challenging. Consequently, plants were placed in the soil for a couple of days before surveying, after which they have been removed and replaced with new ones for subsequent surveys.

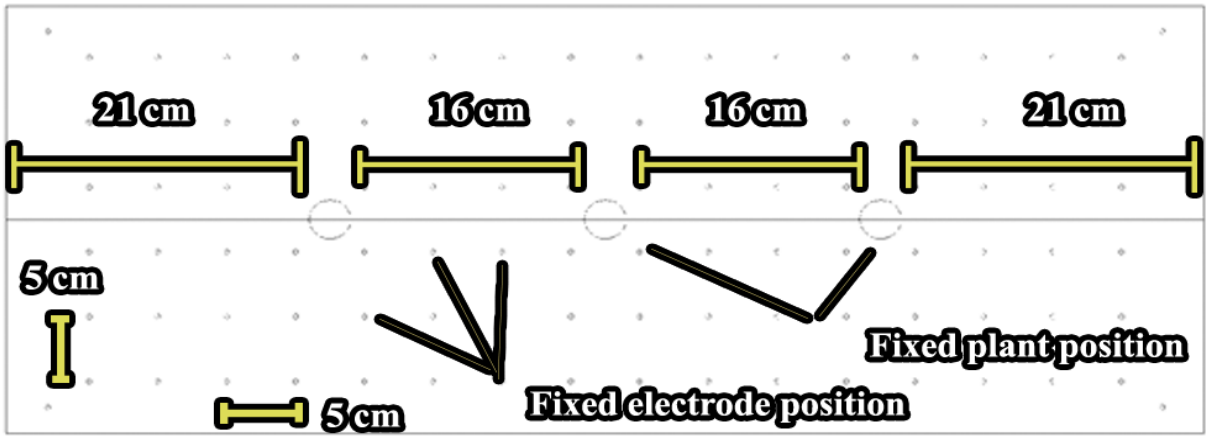

Figure 36. The design of the new acrylic plates, created in LibreCAD.

The adaptations and improvements made in terms of the resistivity surveys include four acrylic plates, designed in LibreCad and created using laser-cutting technology (fig. 36), to enhance the precision of the electrodes' positioning by keeping them securely fixed at all times (fig. 38). This improvement significantly increased the accuracy of the electrodes' placement, effectively minimizing their tilting (a challenge encountered in the previously described setup) and maintaining a consistent distance of 5 cm between electrodes across the surface. The introduction of these four mobile plates made it possible to remove and insert plates effortlessly without causing any harm to the plants. Consequently, the setup and

arrangement of electrodes in all containers were consistently uniform, enabling more accurate comparative analyses, correlations, and interpretations of the data.

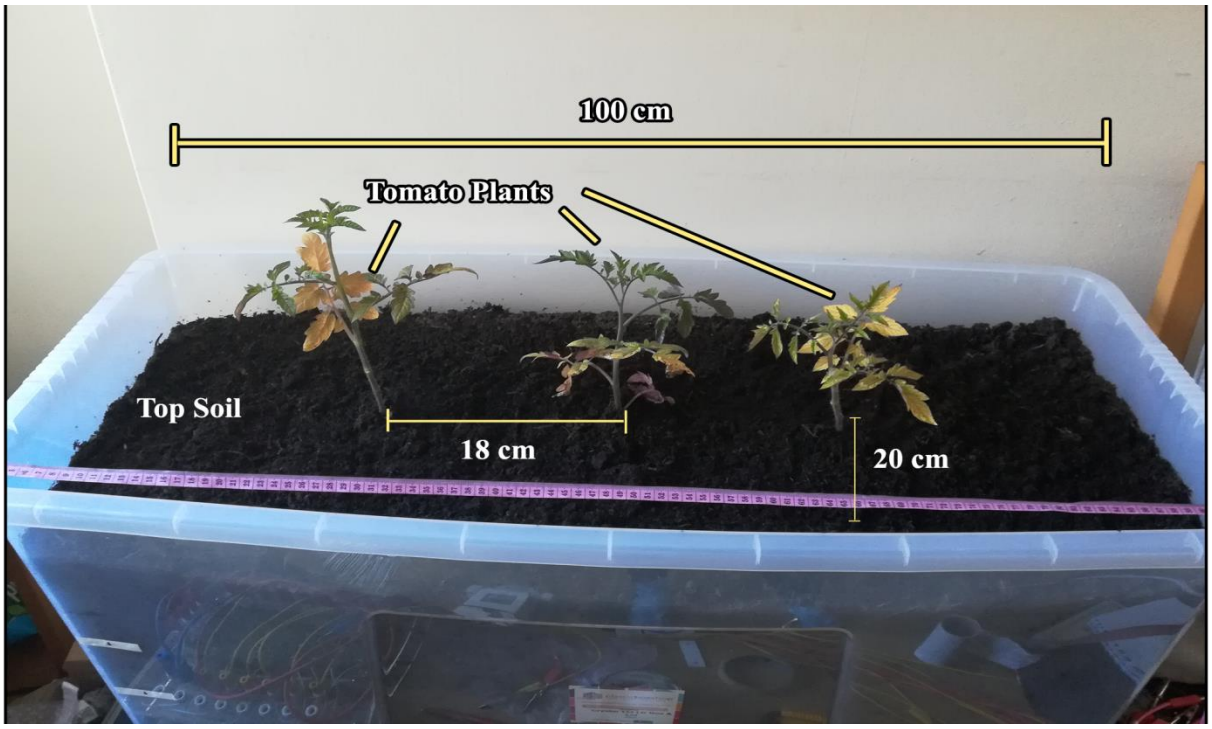

Figure 37. Image representing tomato plants in one of the large containers and information related to their position and setup.

The electrodes utilized comprised of two sets of knitting needles: one set with a diameter of 3 mm and a length of 40 cm, and the other with a diameter of 2.5 mm and a length of 15 cm. The 40 cm needles were found to be significantly more effective due to a 10 cm gap between the soil's surface and the beginning of the acrylic plates, which meant that the shorter 15 cm electrodes would only make minimal contact with the soil (fig. 38). The aeration and unevenness commonly found in natural soil environments often resulted in poor contact between the shorter electrodes and the soil, leading to the equipment's inability to record the

measured data accurately. For the resistivity measurements, electrodes for all six profiles were inserted simultaneously; however measurements were conducted one profile at a time.

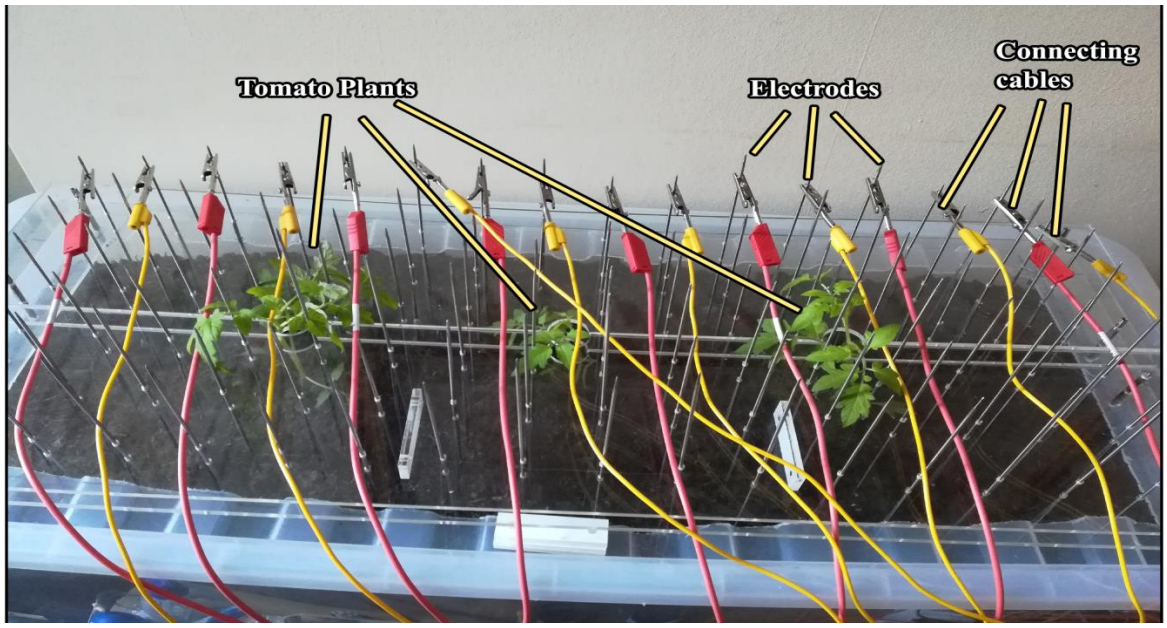

Figure 38. Representation of the resistivity system in the container using the acrylic plates.

In order to have an equal spread of moisture content within the soil and to minimize the anomalies affected by the uneven distribution of the water when irrigating the plants (issue addressed with the previous setting), an automatic electronic system using IoT devices was designed and created, which is described in the 3.4.4. chapter.

3.4.1.3. INDOOR SETTING NO. 3 – TRANSPARENT TUBES

The third indoor setup included three transparent tubes, theoretically enabling vertical root development of the plants (Schiefeibeina and Benfeyb, 1991). Excessive water and inadequate

drainage systems can harm the plant's health, a topic thoroughly discussed in chapter 2.3. Another reason for adopting this setup was to simulate a borehole survey, thereby enhancing the accuracy of resistivity measurements and the precision of the results. Therefore, the arrays employed for the tubes incorporated both traditional and unconventional types. (Petersen and al Hagrey, 2014).

The tubes were selected from various materials and tested, including acrylic and polycarbonate. Polycarbonate was chosen for its material flexibility, ease of machining, and high shock resistance, as opposed to acrylic, which was found to be fragile and prone to breaking during drilling.

Setup description

The tubes were uniformly cut to 50 cm lengths. Their design included holes drilled every 5 cm to securely position the electrodes, reducing their tilt, with nine electrodes per profile (fig. 39).

- One tube served as a control with only one profile, utilizing stainless steel electrodes 15 cm in length and filled with organic compost (described in table 2).
- The remaining two tubes featured four profiles arranged orthogonally. These tubes used copper rods as electrodes, each 5 mm in diameter and 15 cm long, which were permanently attached to the tube, eliminating the possibility of removal. While this setup might lessen survey flexibility compared to the removable acrylic plates in boxes, ensuring consistent electrode positioning across different surveys and conditions enhanced data correlation.The second tube was also filled with organic

compost, whereas the third tube was filled with transparent soil (described in chapter 3.4.3.)

The plants deployed in all the three tubes were inserted in the middle of the tube and only resistivity measurements were conducted (fig. 39).

The equipment for the tube measurements, included the RM Frobisher resistance meter and the switch box created. This setup facilitated adjustments to the electrode arrays for these surveys.

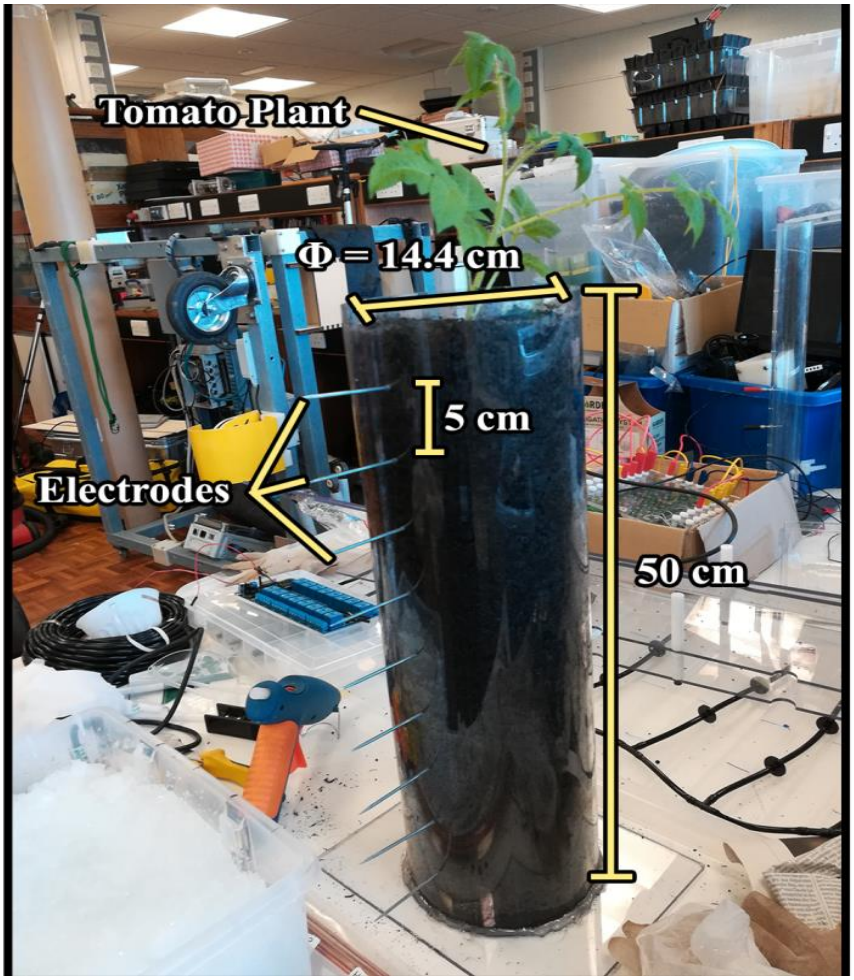

Figure 39. Representation of one of the tubes used in the surveys.

3.4.1.4. INDOOR SETTING NO. 4 – WOODEN CONTAINER

This experiment features a wooden box measuring 1.2 x 0.6 x 0.6 meters, filled with weed-free topsoil, characterized as natural loam mixed with nutrient-rich organic matter (fig. 40). Three tomato plants were placed in the box, spaced 20 cm apart. The larger size of the box, compared to typical plastic containers, facilitates the distribution of electrodes and enables GPR surveying.

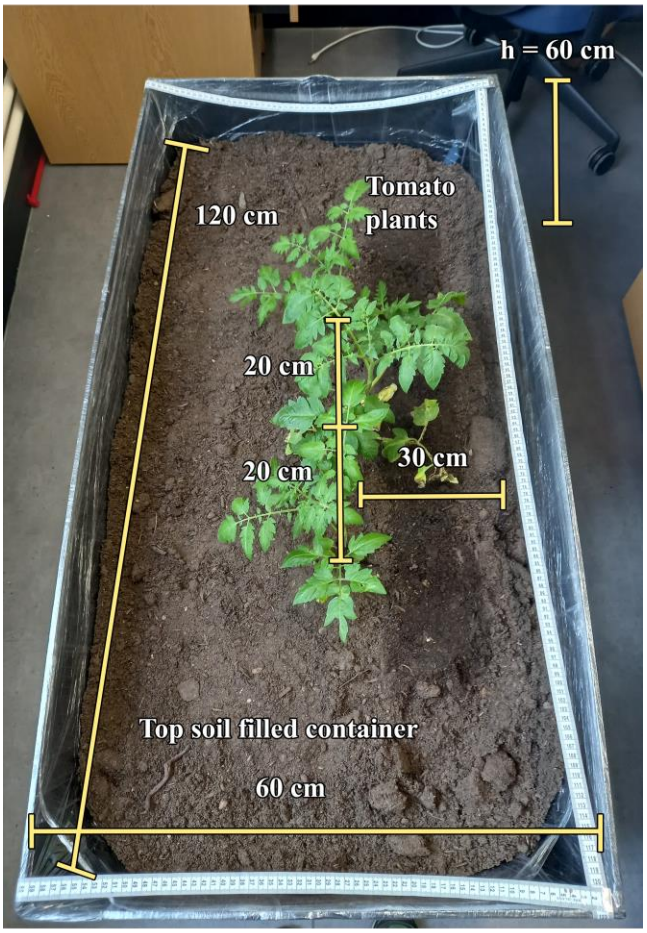

Figure 40. Image representing the wooden container with 3 tomato plants and information about dimensions.

3.4.2. PLANT SELECTION FOR EXPERIMENTAL USE

Tomato plants (*Lycopersicon esculentum Mill*.) were chosen for these experiments after several trials with different plants grown in the laboratory (fig. 41), like wheat (*Triticum aestivum*), beans (*Phaseolus vulgaris*) and even onion plants (*Allium cepa*) have been and tested.

Figure 41. Wheat plant grown in the laboratory for experiments and dimensions of the root area.

While *Arabidopsis thaliana*, a Brassicaceae family member related to cabbage and mustard, is frequently used in plant biology studies, (Szymanski, 2013), obtaining Arabidopsis seeds can be challenging and its small root size and sensitivity to various conditions make it less suitable for our purposes, especially considering the commercial soils employed in this thesis's experiments (Drake *et al.*, 2016), which are used in the experiments from this thesis.

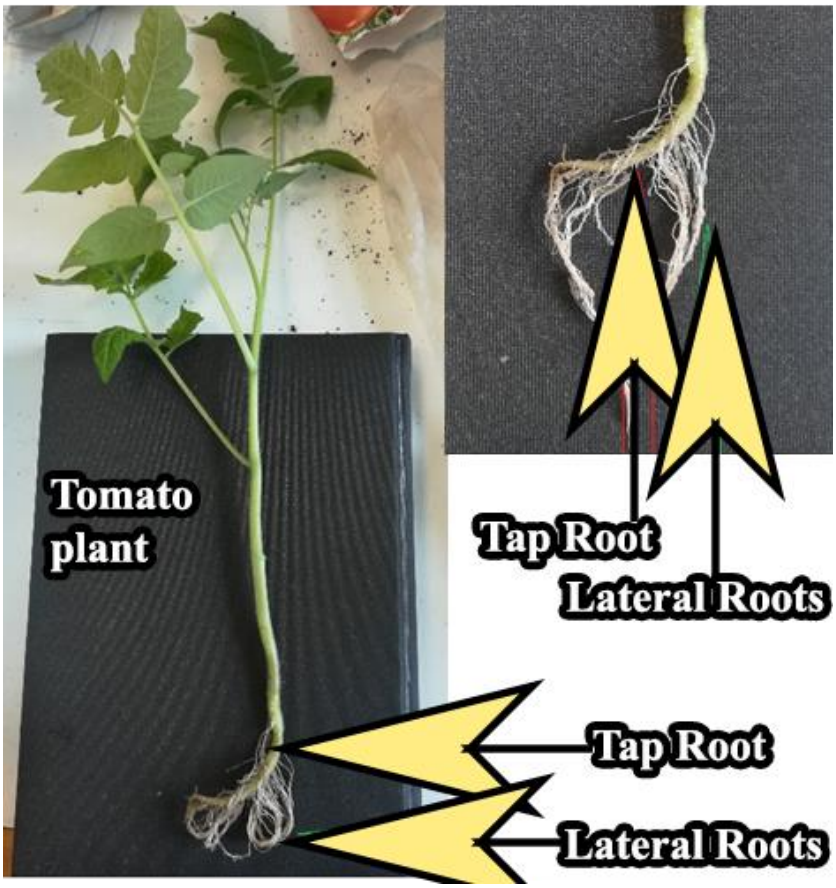

Figure 42. The root system in a young tomato plant root grown from seed, with tap root and lateral roots highlighted.

In contrast, tomato plants, are agricultural plants and are robust in general -- they don't depend on the length of the day, as it is the case with wheat for example (Friend et al., 1966)--

and are resistant to a variety of conditions of temperature and drought as well (Naika et.al., 2005). When grown in the laboratory, wheat plants were found to be vulnerable to existing conditions and did not survive long, despite their rapid growth. This vulnerability makes them less suitable for the task at hand.When using bean plants (*Phaseolus vulgaris*) in the laboratory, the mature bean plants' stems presented challenges in maintaining a straight, upright position suitable for surveying around the plant. Bean plants require support as they grow, necessitating a more complex experimental setup that could potentially affect the results, despite their rapid growth advantage (Castro-Guerrero et al., 2016). The onions (*Allium fistulosum*) have only been used occasionally for the experiments in the transparent soils in order to test different types of roots.

Therefore based on these considerations, tomato plants appear to be the most suitable for this type of work.

Figure 43. Tomato plants grown from seeds in the laboratory to be used in the experiments.

Tomato plants are usually a good choice for experimental indoor settings in biological studies (Schwarz, Thompson and Kläring, 2014), and some of the characteristics that made tomato plants an excellent subject for the experiments in this paper include:

- ***The root type***. According to Rost (1996), the tomato plant can have two types of roots, both a taproot system and a fibrous system which basically represent most of the plants, depending on how it's grown (fig. 42). This aspect made it suitable and representative for a large variety of agricultural plants. Its vigorous tap root system can grow to a depth of 50 cm or even more depending on the soil and environmental conditions (Naika et.al., 2005), with the main root produces dense lateral and adventitious roots.
- ***It is an agricultural plant***. The tomato plant is one of the most important vegetables worldwide (Schwarz, Thompson and Kläring, 2014). It belongs to the Solanaceae family, which also includes other well-known species, such as potato, tobacco, peppers and aubergine (Naika et.al. 2005).
- ***It can be cultivated all year round***. With the help of greenhouses (Kumar *et al.*, 2005), it can be cultivated year-round, offering flexibility in scheduling experiments without the need to wait for a specific season.
- ***It is resilient in a variety of climates and types of environment***. The tomato plant usually requires a relatively cool, dry climate for high yield, but it adapts easily to a variety of climatic conditions from temperate to hot and humid tropical, and temperatures between 21 and 24°C for optimum growth but can survive between 10°C and 38°C as well (Naika et.al., 2005).

- ***The suitability for indoor growth.*** The tomato plants thrive in indoor settings (Schwarz, Thompson and Kläring, 2014) an important aspect, as the plants will mostly be used in indoor experiments in this study (fig. 43).
- ***Fast growth.*** Another advantage is the fast growth rate of the tomato plants (Naika et.al., 2005), which allowed for multiple trials of experiments without wasting much time waiting for the plants to grow.
- ***Suitability for most types of soils***. The tomato plants can grow well in most mineral soils with really good water holding capacity and aeration (but free of salts), and prefer deep and well drained sandy loam soils, but can also thrive in clay rich soils if the appropriate agricultural methods are used to allow the roots to penetrate deeper into the soil (Naika et.al., 2005).
- ***Suitability for growing in hydroponic systems***. An aspect which was tested in the experiments (Verdoliva *et al.*, 2021) but also an important feature in terms of using the plants in the transparent soils created in the laboratory.

3.4.3. TRANSPARENT SOILS

Transparent soils, as discussed in earlier subchapters, have been utilized in various containers for the experiments. Employing transparent soils to image plant roots using geophysical methods is an innovative strategy and the primary reason for choosing these “soils” is to enable the accurate correlation of anomalies in resistivity sections with root positions, eliminating the need to remove the plants to observe their root patterns.

From the types of transparent soils documented in the literature chapter of this thesis, only two types have been tested, and eventually only one type has been used for the actual experiments.

The first type of soil tested is represented by the agar gel. The protocol for creating the agar can be done in a laboratory with minimum equipment, but it seems more unstable and allows for mould bacteria to grow really quickly if not treated in sterile conditions. In addition, the agar gel seems unstable for a longer period of time at room temperature, changing its texture and colour.

The second type of soil represented by the Nafion polymer and used in biology studies had its limitations in terms of costs. Even though the right equipment and space was found for the transparent soil to be created in the laboratory, the Nafion beads cost at around 100-150 £ for only 10g of product. In terms of quantities needed for the experiments planned in this project, the transparent soil needs to fill up a volume between 90 to 120 L approximately. This would be a very useful type of soil to test and use for future projects but so far for this project it seemed that other alternatives could provide similar advantages. According to the producer, for each gram of aquabeads, 100ml of water was needed for them to absorb the water and expand.

The third type of soil tested and used in the actual experiment is represented by the transparent soil made of aquabeads. Aquabeads come in a range of shapes and sizes, but the ones used for this experiment are the clear type, which would allow for greatest transparency level. There is a variety of brands and packaging available, but the ones that proved to be more approachable in terms of price and volume are represented by the crystal pearls under

the APAC Packaging branding (fig 44 –a). Two types of beads size have been used under the codes FL3038 and FL3040. The difference between them lies in size differences as the FL3040 type has much larger beads. As these needed to be grinded (fig. 44 b-c) for preparing the soil the size of the beads was not of importance.

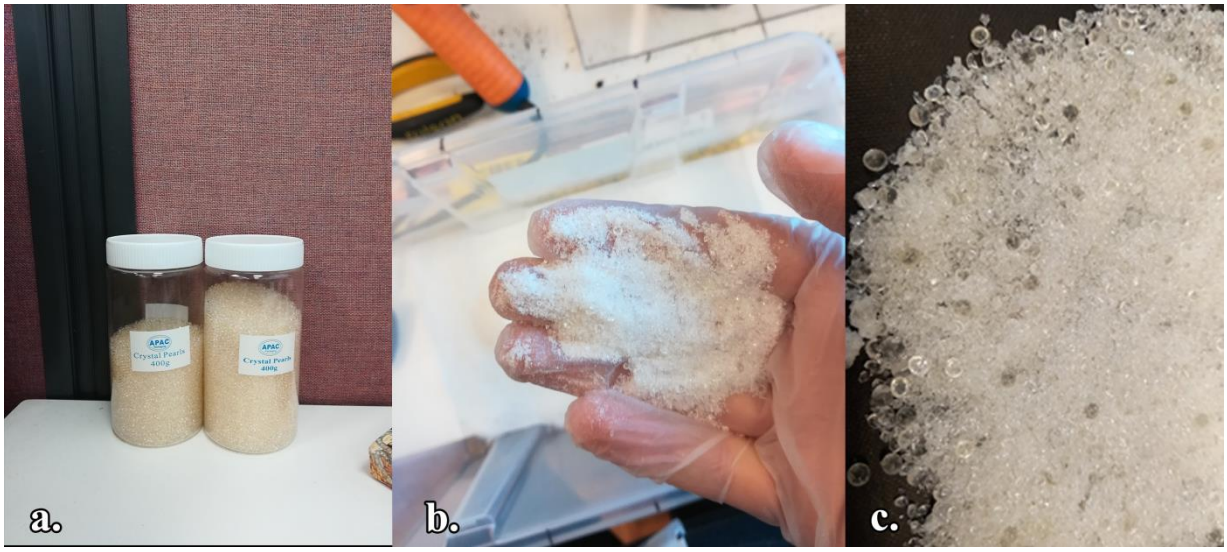

Figure 44. A– aquabeads in brute form; b - close up on the different sizes of the particles of grinded aquabeads; c – grinded aquabeads powder before adding water to expand into a gel like material.

3.4.3. CREATING THE TRANSPARENT SOIL FOR THE EXPERIMENTS

In preparing the "transparent" soil, a process not documented in the literature, numerous trials were conducted. The material needed to be ground into a gel-like transparent solution to mimic the mechanical and physical properties of natural soils, facilitating more natural root

development in the experimental containers and to increase transparency levels which would allow for a better visibility of the exact position of the roots.

- ***Grinding the beads*** proved to be challenging because grinding raises the temperature of the beads, making them more elastic and thus more difficult to pulverize into powder. Careful experimentation led to a solution: freezing the beads before grinding, enabling them to maintain their pre-elastic state for an extended period.
- ***Particle size and distribution.*** The intent with the sizing of the particles was to have the particles in uneven sizes to better resemble the natural environments in which plants grow (fig. 44 –b,c), which usually have a variety of different particle sizes. Keeping the size of the beads uneven would create a texture closer to the natural soils in terms of putting resistance in some areas and allowing the roots to develop in a way that would resemble the conditions in a natural environment. As plants usually develop their roots on the path of least resistance pattern (Bengough *et al.*, 2006), this is an aspect that was followed with keeping the size of the particles uneven and allowing the plants to follow root growth patterns closer to what can be found in natural environments and soils. When it comes to tomato plant roots in particular, it has been showed that the effects on root morphology were more pronounced in the coarse textured loamy sand than in the finer-textured clay loam soil (Tracy *et al.*, 2012), which represents the importance of taking into consideration different particle sizes.
- ***Hydration***. The material keeps its properties in time and at room temperature as long as the material is topped with water regularly (as water naturally evaporates). If the water evaporates, the beads simply return their initial form before the water absorption

process, and will start expanding as soon as water is added again. It takes about eight hours for the beads to expand at their maximum size and level of transparency.

- ***Transparency***. As the transparency of the beads is dependent on the quantity of water added, the level of transparency for the transparent soil used was changed usually by the addition of more water to the solution (fig. 45 - 47).

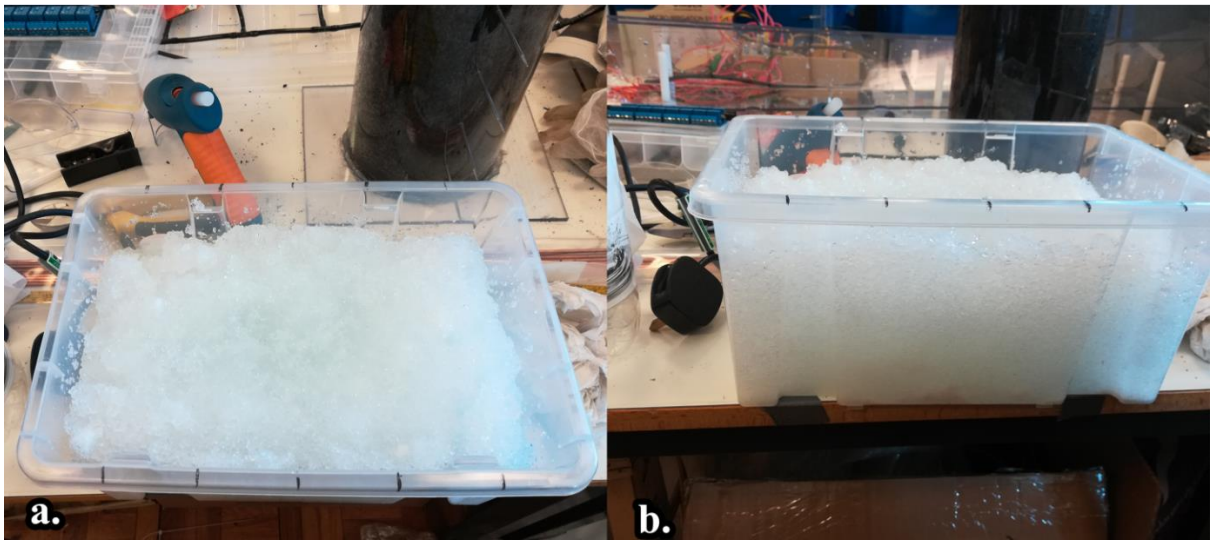

Figure 45. In both images, the transparent soil from different angles, after water has been added.

- ***Fertilizer use.*** During experiments, when different types of fertilizers have been added to the gel, a chemical reaction took place caused the gel to lose its form and the particles separated from water this way transforming from gel to liquid phase, rendering the entire transparent soil unusable. This represents one of limitations which will probably need further research in the future, to assess if this could be prevented with the use of other types of fertilizers or solutions. Therefore, this transparent soil has been used in the experiments with no addition of fertilizers or other chemicals. No other limitations

have been observed during testing and using this type of transparent soil in these conditions.

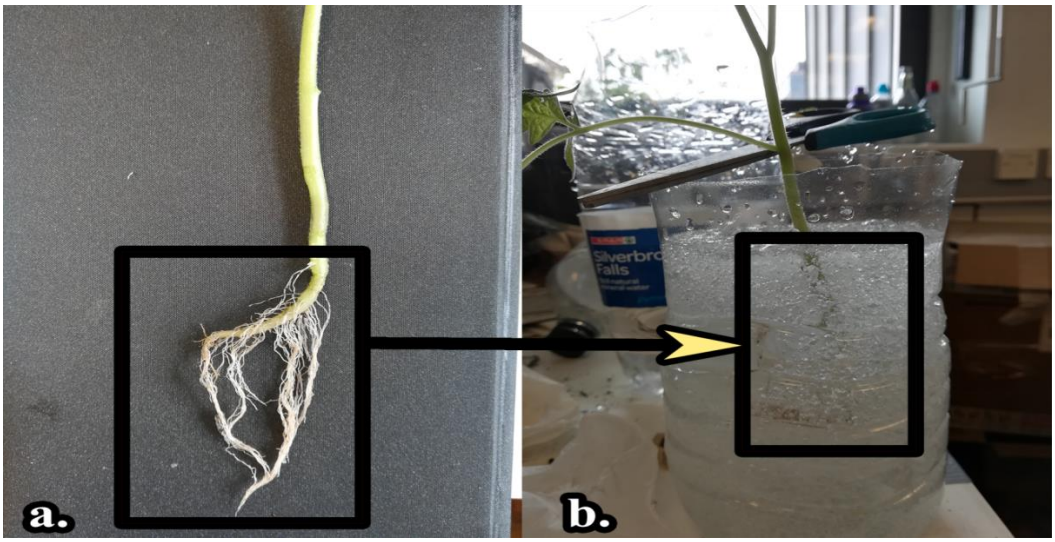

Figure 46. A– the roots of a tomato plant grown in the laboratory from seed; b– the tomato plant root placed into the transparent soil, to test the soil's transparency level.

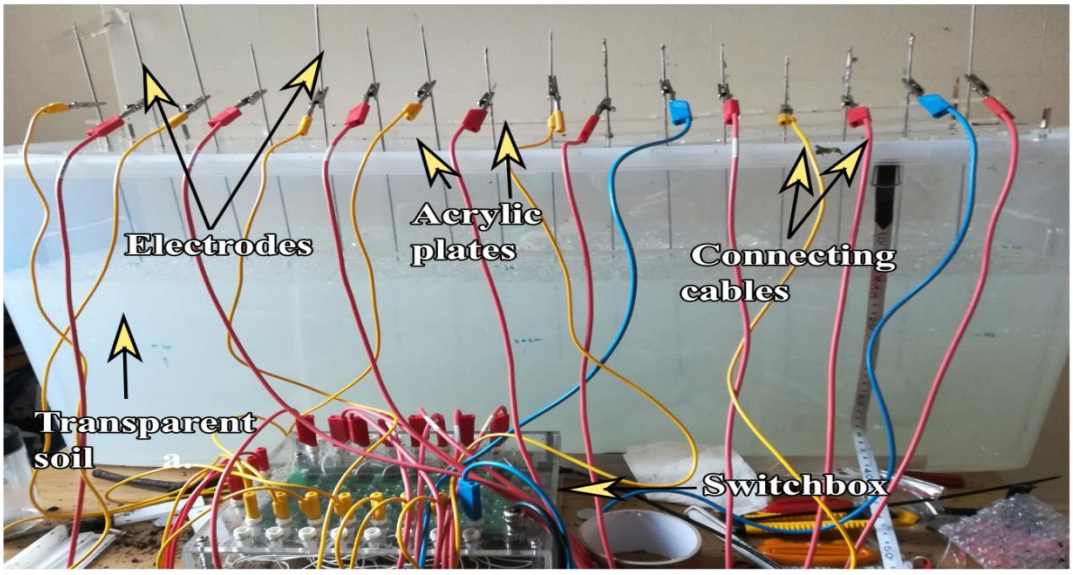

Figure 47. Example of how the transparent soil has been used in the experiments. The electrodes were not normally inserted that far down for the actual experiments, they have been pushed down for assessing the transparency of the soil.

3.4.4. SENSORS AND ELECTRONIC DEVICES CREATED

To support the surveys, various types of electrical equipment were developed, including custom-built devices, IoT gadgets, and environmental sensors. Initial experiments and field trials in agricultural settings revealed that soil moisture content varied unevenly due to irrigation, affecting both resistivity and GPR surveys by altering soil properties.

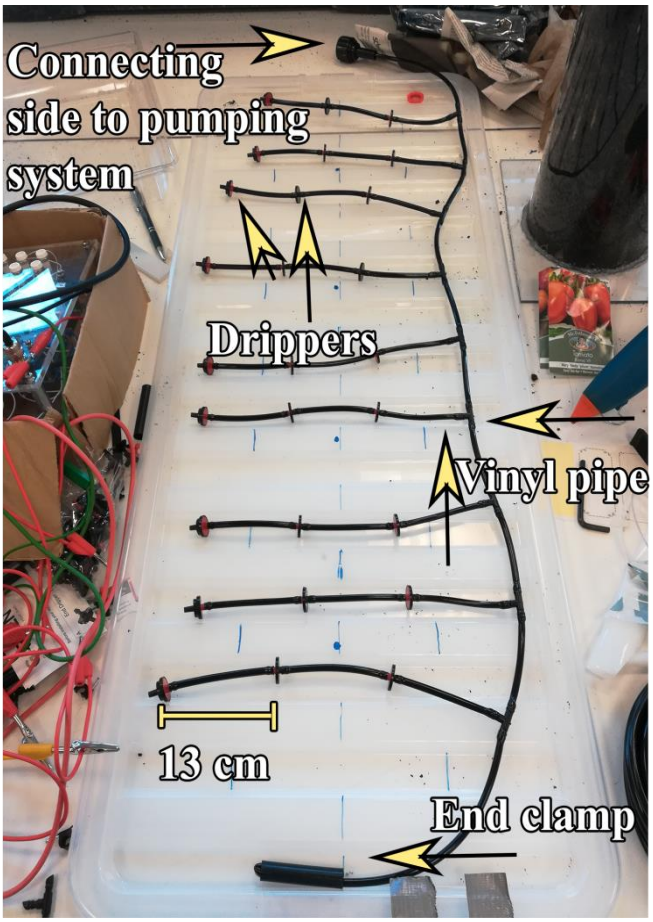

Figure 48. The irrigation system and its components without the electrical attachments.

In response, an automated watering system capable of evenly distributing water was developed (fig 48 - 49). Environmental sensors played an important role in this irrigation system by monitoring soil humidity and triggering the automatic watering mechanism. The system, assembled from a garden drip kit – customized to fit in the experimental container (described in chapter 3.4.1.2.) - featured hoses cut to equal lengths to ensure full coverage of the surface area and equal spread throughout the whole surface at all times (as shown in figure 48). It included an Arduino Uno board, a 4-relay board, an LCD screen to control the immersive pump, and a moisture sensor (fig. 49).

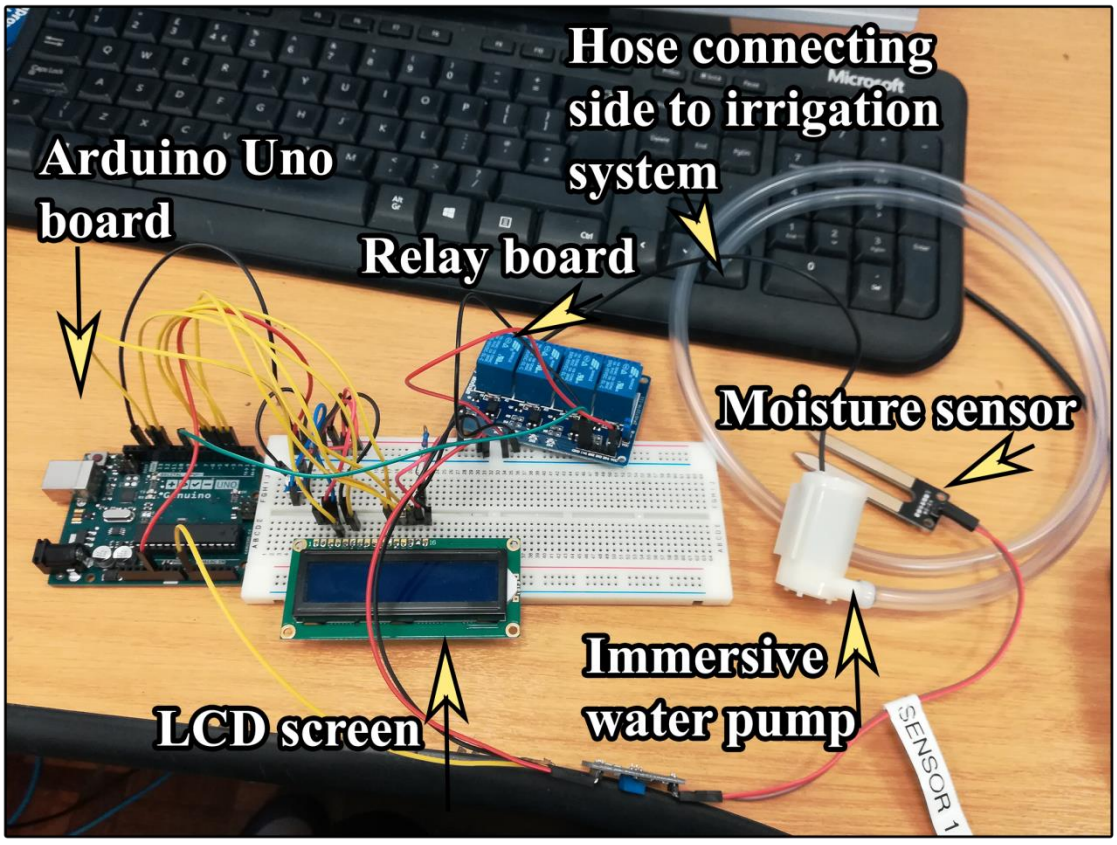

Figure 49. Image representing the environmental sensors and irrigation system created with IoT devices and its components.

This sensor not only measures the soil's water content (where the sensor was calibrated for very dry soil to have a 0% value, and water to have 100% value) but also activates the pump to draw water from a container and distribute it through the hose into the containers used in the experiments, maintaining optimal moisture levels and providing this information which is accessible before the geophysical surveys (fig. 49).

3.5. EQUIPMENT USED FOR GEOPHYSICAL SURVEYS

The two methods used for both indoor and outdoor surveys are represented by the GPR methods and the resistivity methods. Some equipment represents commercial readily available equipment, while for other surveys some types of equipment have been developed to attach to the commercial equipment.

There is a variety of ready available geophysical equipment on the market, but focusing on lower cost alternatives provide a great opportunity for this methods and lessons presented in this thesis to be applied in a larger variety of settings by more people, especially in least developed countries. Least developed countries struggle the most in terms of agriculture and with the increase in population there is more demand and more pressure on the agricultural sector (Cuffaro, 2001). For geophysical applications to be applied, offering solutions for lower cost alternatives in terms of equipment represent a great advantage which can aid with faster and reliable applications of the methods.

3.5.1. GROUND PENETRATING RADAR EQUIPMENT

For the GPR method an UTSI Groundvue 3 system was used with two different and separate antennas of 1.5 GHz and 4 GHz (fig. 50 – b). Both antennas can be used both in distance and in time mode. For the distance mode they both use wheels adapted to their size to measure the distance. The GPR console controls the antennas and is connected to a laptop or tablet for visualizing and controlling the surveying.

3.5.2. RESISTIVITY EQUIPMENT

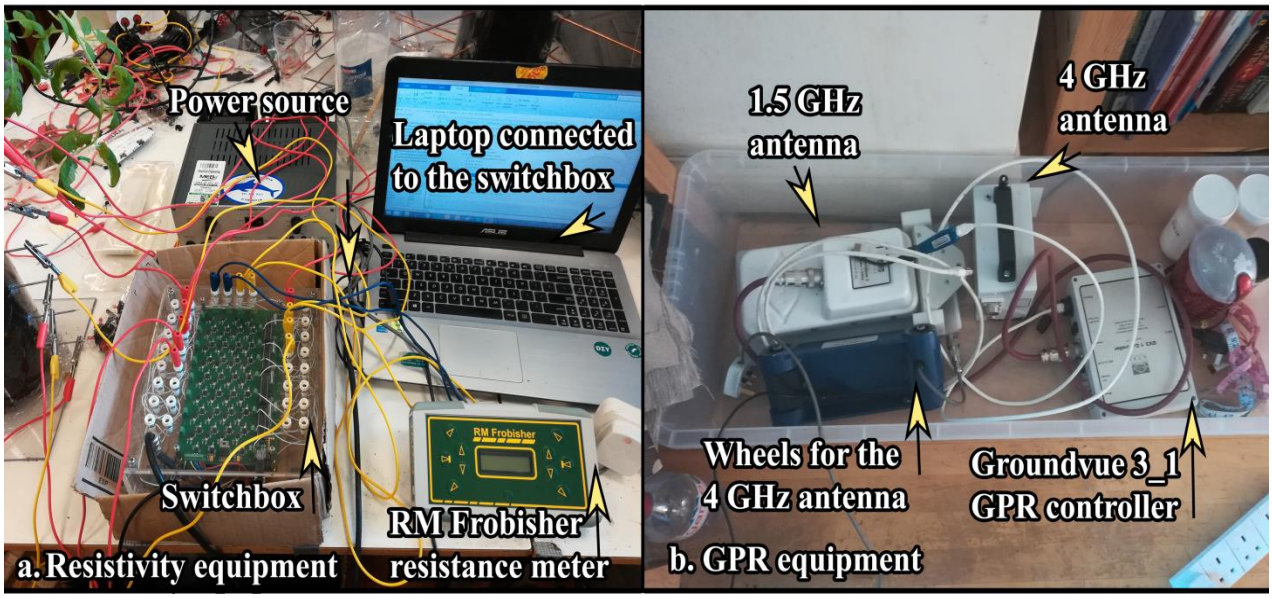

Figure 50. A- representation of the resistivity equipment and it somcponents; b – the GPR equipment and its components.

The resistivity equipment consists of an RM Frobisher TAR-3 Resistance Meter which uses four electrodes, two for injecting the current and the other two for measuring the potential

difference. The RM Frobisher TAR-3 has other accessories, like electrodes, cables and a frame that can be used for fixing electrodes and moving them with an ease on the field, but these elements have been changed with other types of electrodes which have been previously described, depending on the type of application the equipment was used on (fig. 50 – a). Most of the surveys are carried with electrodes represented by knitting needles made of stainless steel with various sizes, and copper rods (e.g. in the case of the transparent tubes – chapter 3.4.1.3).

3.5.2.1. THE SWITCHBOX USED FOR ELECTRICAL RESISTIVITY TOMOGRAPHY

As highlighted in the literature review, the ERT method needs inserting all electrodes into the ground simultaneously during surveying. This method, which involves having all electrodes in place and automatically selecting which to use for current injection and voltage measurement, improves flexibility in array types and significantly shortens data acquisition time. This advancement aligns with features already available in commercial equipment. To offer a cost-effective solution, a switch box was developed that can be connected to any equipment, whether commercial or lab-made by facilitating automatic electrode switching during surveys.

This device also allows for array type control and customization which is compatible with any laptop or tablet running MATLAB code, or a standalone app has been created which can be added to any windows device. The switchboard operates on relays—devices that

mechanically or electronically open and close circuits to control an electrical circuit by opening and closing contacts in another circuit. The creation of this equipment can vary in method and cost, from relay boards to individual relays, impacting the overall expense. However, this innovation significantly reduces costs for geophysical equipment while providing the benefits of multielectrode systems. It even offers greater flexibility by allowing customization of both conventional and unconventional electrode arrays for various survey types, including boreholes.

3.5.2.2. PROTOTYPE ELECTRICAL RESISTIVITY EQUIPMENT

The equipment uses a laptop to manage the acquisition process and the electrode arrays, using MATLAB written software for control. An important component is represented by the switch box (described in the previous subchapter), which controls the electrode arrays and alternates between current and potential electrodes based on the chosen array. The system is powered by two 12 V batteries, which are needed for running the entire setup, including the laptop. The measurement unit consists of a National Instruments (NI) CDAQ 9184 4-Slot Ethernet Chassis connected to the laptop, capable of measuring up to 128 channels across various signals. It includes two modules: an analog-to-digital and a digital-to-analog (a NI 9263 module, ±10 V, analog output, 100 kS/s), which delivers a sine wave signal through a 1:1 non-grounded transformer (fig. 51).

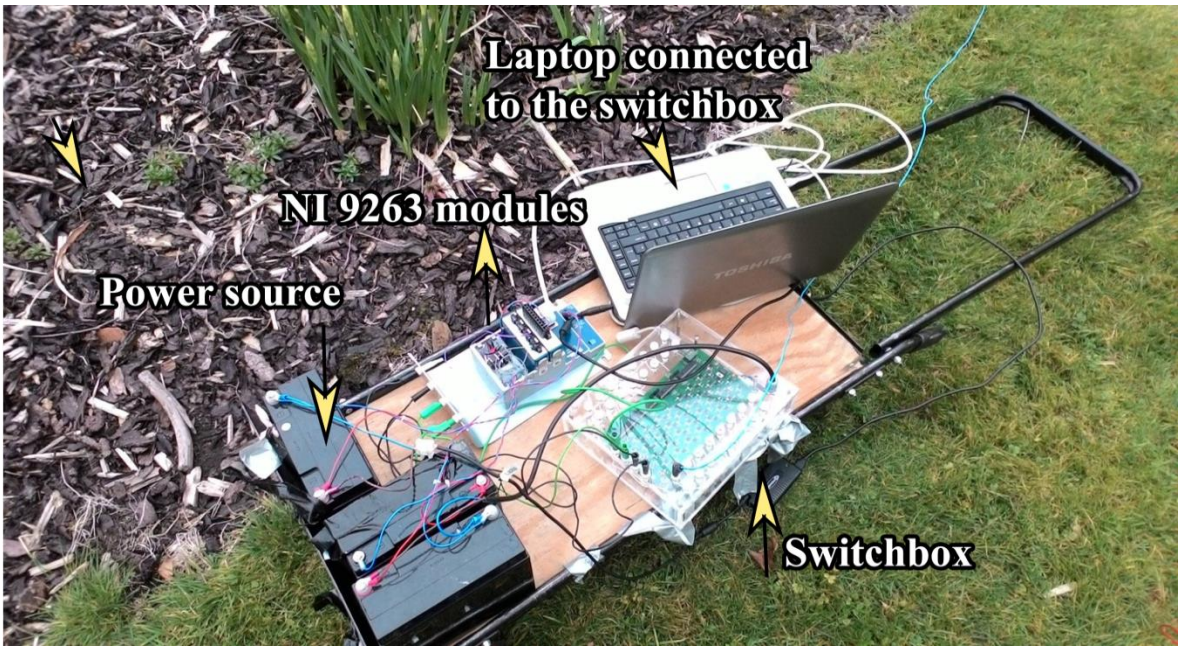

Figure 51. The prototype electrical equipment with the laptop, switch box, chassis and batteries.

After the sine wave signal passes through the transformer, it enters a 10k resistor and divides into two branches, each amplified. One branch, linked to the batteries, controls the current electrodes. The current sensing branch, after a 100 ohm resistor, connects to an analog-to-digital module, the NI 9239, with a 24-bit resolution, supporting the potential electrodes. The data frequency is 775 Hz.

This setup's advantage, beyond lower costs compared to commercial multielectrode systems, is its ability to use a higher frequency for quicker data acquisition, allowing for comprehensive tomography by utilizing all electrode combinations more rapidly.

4. DATA ACQUISITION, ANALYSIS AND RESULTS

4.1. INTRODUCTION

This chapter details the surveys conducted throughout the study, divided into subsections covering both indoor experimental and outdoor settings. Each scenario is addressed individually, including information on survey locations, data processing, and analysis. As the number of surveys was very high due to the experimental approach of the study, only the most representative and repeatable data are included, highlighting the setting of each survey type and processing details.

The chapter is organized into two main sections according to the geophysical method employed—GPR or resistivity. It encompasses discussions on outdoor and indoor surveys, the equipment used, setting descriptions, synthetic models, and data processing and analysis.

4.2. GPR SURVEYS AND DATA

The GPR surveys presented in this chapter represent the surveys from both indoor and outdoor surveys and the setting will be described for each data set. Synthetic models have also been created and are presented in more detail at the end of the chapter.

All the data has been collected with the use of the UTSI Groundvue 3_1 GPR system, with two separate antennas of 1.5 GHz and 4 GHz. For some sites both antennas have been used and for some others only one of each has been used depending on site conditions.

The data processing for all the surveys were carried out in ReflexW and the following filters and functions have been used for the majority of the data, adapted to each set of files:

- ***Move start-time*** –this function was used for the zero time adjustment, where the parameter was chosen for every set of using the wiggle window tool;
- ***Dewow –*** used for the mitigation of low-frequency noise;
- ***Bandpass butterworth filter*** – was used for eliminating frequencies outside the antenna's operation range targeting both low and high frequency ranges. In general, where the lower cutoff and upper cutoff depend on the frequency of the antenna, 2000-8000 MHz was used for the data collected with the 4GHz antenna and 750-3000 MHz for the data collected with the 1.5GHz antenna;
- ***Background removal –*** was applied to reduce the systematic coherent noise or ringing, which involves subtracting an average trace;
- ***Energy decay/manual gain*** – used for the signal amplification where necessary and increase the visibility of the reflections;
- ***Trace stacking*** – where several traces are stacked and average usually with the purpose of providing a better resolution for weaker reflections; this function was used only when necessary;
- ***fk-Stolt migration*** - tool was used only in particular instances, and the velocity used was usually based on the hyperbola fitting tool, for transforming data from time domain to distance and reducing the appearance of the hyperbolas.

4.2.1. GPR - OUTDOOR SURVEYS

The GPR surveys discussed in this chapter took place outdoors at the Birmingham Botanical Gardens and Winterbourne House and Garden in Birmingham, UK. These surveys aimed to test two types of high-frequency antennas, 1.5 GHz and 4 GHz, in a realistic outdoor setting. The goal was to assess the method's applicability in real-world environments, taking into account realistic conditions and the method's limitations in actual settings.

A variety of different plants have been chosen for this, with different types of roots, different types of surfaces (soil, grass, e.g.), single plants as well as a multitude of plants close together (an aspect of interest in agricultural settings), humid soils, dry soils, etc. The botanical gardens offer a good environment for this type of approach, due to the variety of plants on a small area, and because the information regarding the recent use of irrigation or fertilizers (or other man-made arrangements) that could affect GPR surveys was readily available.

A multitude of profile arrangements have been used, to find the approach that provides the best information in the least amount of time, so that the method could be used efficiently in the future in real world (non-experimental) settings. For example, one question that was considered was how far away from the plant can the surveys be carried so that the antenna will still catch information from the roots or their effect? As in agricultural settings, particularly when plants are fully grown, as shown by the direct field measurements presented earlier, approaching the actual stem of the plant with the GPR unit can be challenging.

This chapter will also compare the results from data collected with a 4 GHz antenna to those from a 1.5 GHz antenna, to assess whether one antenna is more suitable for the majority of the

surveys, or if there is one antenna that would be more suitable in certain settings. Testing if there are any ideal conditions in which one or both antennas could offer more information is also an aspect of interest for which this chapter tries to address.

In terms of similarities or differences with the agricultural plant roots, there are some reasonable differences that need to be considered. As it has been described in previous chapters, there is a variety of types of plants which can be called agricultural plants; there is not only one type, when it comes to the plant root area, which can universally describe agricultural plants. In some instances, the focus of the GPR profiles would be to try to identify individual roots, for example aflalfa plants (*Medicago Sativa.)* which are widely cultivated have long taproot roots which might get close in physical parameters (length, diameter, sap-absorbing, or anchoring properties, etc.) to the ones of tree roots. Whereas in some instances, where we deal with plants like wheat (*Triticum aestivum*), or barley (*Hordeum vulgare*) for example, which have fibrous root systems, due to the size of individual roots, the focus would be to identify a root area described as an area with a higher root density in the soil. As well as observing and analysing their behaviour in a way that would make their detection visible in the GPR data, and taking into consideration different parameters and conditions of the soils which might allow for their detection (humidity, soil type, etc.).

Increasing the antenna frequency has the potential to help with identifying smaller objects or smaller changes in the soil properties from soils with or without higher root density volumes, but at the same time, will increase uncertainty as other smaller changes in the soil, unrelated with the roots, would also be more visible (uneven soil compactness, uneven water content in

the soil, any other types of materials present in the soil matrix, like sand, small pebbles and rocks, other organic matter).

On some sites, it was possible to test both antennas for the same plant, but due to spatial limitations (such as the dimension of the antenna not allowing to get close enough to the plant, or the surface being very uneven, which is common in agricultural settings) some areas have been tested with only one of each antennas.

The findings from these surveys also helped with shaping the indoor experimental settings as well.

Every group of plants or single plant that was surveyed will be described separately with all the information about the antennas used, details about the roots of the plant, information related to the type of surface or humidity.

4.2.1.1. TREE ROOT

The first site chosen for carrying out GPR surveys in outdoor real environments (non-experimental settings), is represented by a tree root visible at the surface. The rationale behind this choice was to start surveying in an easy setting, understanding the limitations when we already know the position of the root and having a significantly larger root would allow for more understanding in more difficult settings. This would help with understanding the method's limitations as well, and the idea was that, if there are features which can't be seen or detected when we know certain parameters, then what would be the likelihood of detecting

plant roots in natural environments when dealing with smaller objective of unknown position. This represented a good starting point for using the 4 GHz antenna as well, as the subject is not very well covered in the existing literature.

Therefore, the tree root belongs to a Sycamore (*Acer pseudoplatanus*) tree, with root visible at the surface, approximately 10 m away from the tree trunk. The soil conditions at the time of survey were dry, without any prior irrigation taking place or any rain in the previous days. Two surveys were carried out, one with the 1.5 GHz antenna (fig. 53) and the other one with the 4 GHz antenna.

Acquisition parameters			
Site name	Tree root		
Antenna frequency	1.5 GHz	4 GHz	4 GHz
survey conditions	dry	dry	dry
no. of profiles	13	15	3
direction of profiles	perpendicular to root	perpendicular to root	parallel to root
distance between profiles	10 cm	10 cm	5 cm
profile length	190 cm	80 cm	140 cm
samples per line	512	512	512
scan frequency	50 Hz	50 Hz	50 Hz

Table 3. GPR data acquisition parameters for the Tree root site.

The geometry of the 4 GHz survey, is represented by a number of 15 profiles perpendicular to the root, with a distance between the profiles of 10 cm, making sure that the first 2 and the last 2 profiles are in the area where the tree root is no longer visible at the surface, in order to allow for contrasts and understanding of the continuity of the root when it is no longer visible at the surface, and a length of 80 cm another 3 profiles perpendicular on the previously mentioned, were carried out with the same antenna, parallel to the tree root this time, with the

middle profile exactly on the tree root and the other 2 profiles on each side of the root, with a distance of 5 cm in-between (fig. 52) and a length of 140 cm . The data acquisition parameters can be found in table 3.

The geometry for the survey carried out with the 1.5 GHz antenna (fig. 53), consisted of 13 parallel profiles perpendicular on the tree root, with a distance between the profiles of 10 cm (fig. 52) and a length of 190 cm.

Data processing parameters			
Site name	Tree root		
Antenna frequency		1.5 GHz	4 GHz
move starttime	manual input	-0.833	-0.52632
dewow	timewindow [ns]	0.66	0.25
bandpass butterworth	lower cutoff	750	2000
	upper cutoff	3000	8000
background removal		yes	yes
gain function	linear gain	0.1	0.2
	exponent	2	2
fk migration Stolt	velocity [m/ns]	0.065	0.065

Table 4. Data processing parameters for the GPR surveys at the Tree root site with both of the antennas.

All of the profiles have been imported in ReflexW and have been processed in batches based on the antenna frequency used. The data processing has been carried out in a trial and error manner, and a multitude of filters and functions have been applied in different order with the purpose of highlighting areas of interest in a way that the data would still be kept true to reality. Therefore the data presented here, represents the version of the data which had minimal processing but highlighted areas of interested the most. The data processing flow is presented in the table 4.

As parallel profiles were collected in the surveys, the data from all of the profiles has been interpolated to generate and represent horizontal slices at different depths into the ground.

Figure 53. The tree root was partially visible at the surface; a- total length of the root visible at the surface; b- 4 GHz antenna survey profiles; c – 1.5 GHz antenna survey profiles.

4.2.1.1.1. TREE ROOT SITE RESULTS

After the data has been processed, a distinct anomaly appears in the data horizontal slices described as ait appears that the tree root creates a contrast with the surrounding material, and the dimension of the anomaly appears as larger than the one of the tree in width (fig.54) (ranging from 10-20 cm), which indicates that this is an actual effect of the root with the surrounding soil not the actual tree root itself. In general when detecting tree root what is important is the lateral continuity of the root, which is also visible in this data.

Figure 54. Example from surveying on the tree root, in this case with the 1.5 GHz antenna.

The appearing anomaly correlated with the tree root, appears as a positive anomaly closer to the surface changing into a negative anomaly, and there appears to be another negative anomaly close to the positive anomaly closer to the surface (fig. 54). However, it can't be said that this is the actual root itself but more like its effect on the data, as mentioned previously.

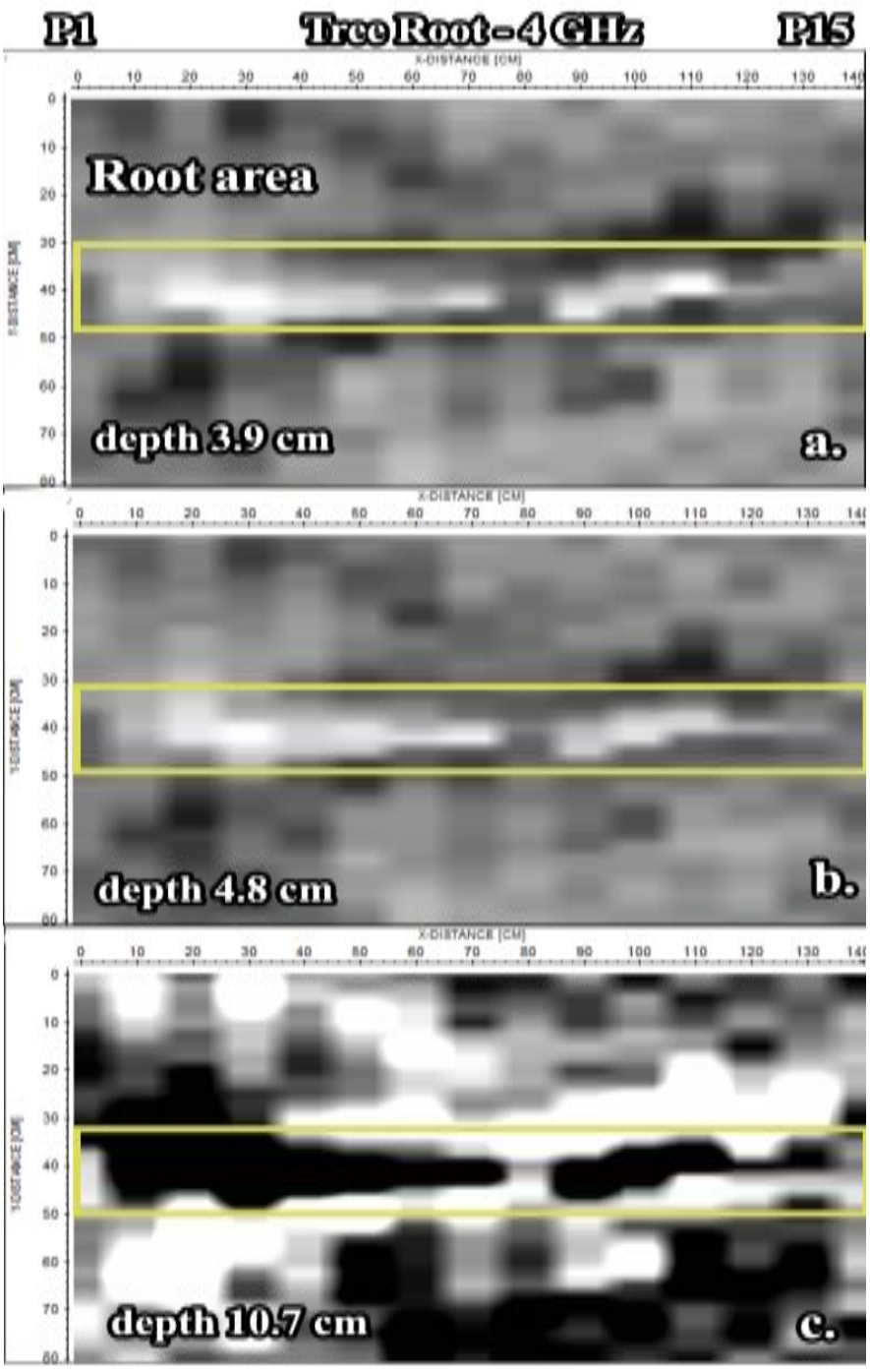

Figure 55. Processesd GPR 4 GHz antenna data, interpolated with slices extracted at: a – 3.9 cm depth, b – 4.8 cm depth and c – 10.7 cm depth.

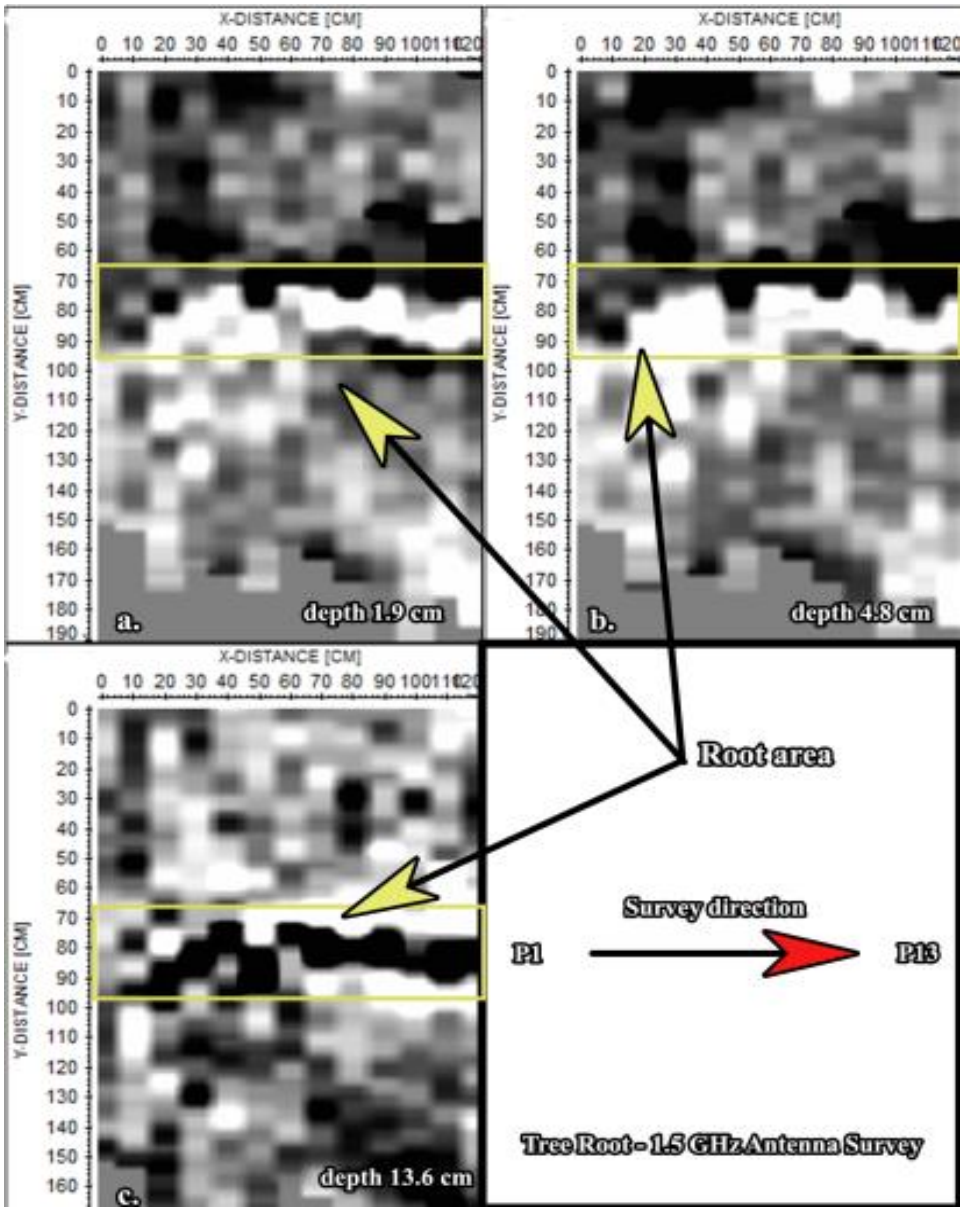

Figure 56. Processed GPR slices from the data with the 1.5GHz antenna at different depths: a- 1.9 cm depth, b- 4.8 cm depth and c – 13.6 cm.

Integrating the data is more difficult with the 1.5 GHz antenna as the profiles are longer and is difficult for the antenna not to be affected by microtopography (fig. 55), and this aspect affects the way we see the data and the lateral continuity of the root effect on the data, and other anomalies. Having all of these difficulties with a root of this size and known location,

the lessons learned from this test which would help with the future more specific surveys is that, it appears to make smaller types of roots even more difficult to survey and detect and even reduce the certainty when correlating the anomalies in the data with the known actual position of the plants. As this is a soil from a real world environment, the soil is not homogeneous; therefore other anomalies are appearing in the data, which interfere with the clarity of the anomalies and with the certainty of correlating the anomalies with the roots.

4.2.1.2. RHODODENDRON *(Rhododendron Markeeta's Prize)*

This site was chosen due to the Rhododendron's root type, which is much smaller compared to the previously mentioned survey on the tree root, with many fine fibrous roots held in a compact clump, which develop close to the surface of the soil (Douglas et al., 1990).

Acquisition parameters	
Site name	Rhododendron
Antenna frequency	4 GHz
survey conditions	dry
no. of profiles	5
direction of profiles	parallel to root area
distance between profiles	5 cm
profile length	130 cm
samples per line	512
scan frequency	50 Hz

Table 5. GPR data acquistion parameters for the Rhododendron site.

Rhododendrons are woody plants from the Ericaceae family, and they thrive in acidic soils (Turner, Arzola and Nunez, 2020), which can grow roots from stems (Pierik and Steegmans,

1975). There was also enough space from this plant to the next ones, which means that the plant was relatively isolated, and allowed for less interference from the roots of other plants. Only the 4GHz antenna was used on this site and details about the acquisition parameters are described in table 5.

Data processing parameters		
Site name	Rhododendron	
Antenna frequency		4 GHz
move starttime	manual input	-0.88
dewow	timewindow [ns]	0.25
bandpass butterworth	lower cutoff	2000
	upper cutoff	8000
background removal		yes
gain function	linear gain	0.1
	exponent	1
fk migration Stolt	velocity [m/ns]	0.07

Table 6. GPR data processing parameters for the Rhododendron site.

Even if the surface was covered with dried leaves and landscaping bark, stones and other man-made unconsolidated materials, everything has been removed prior to the survey, in order to allow for a good contact between the antenna and the surface of the soil. The survey grid contains a number of 5 parallel profiles at a distance of 5 cm between the profiles, positioned in from the plant, with the first profile being as close as possible to the stem of the plant and the last profiles 20 cm away from the stem of the plant (fig. 56). The profiles have been chosen in this particular pattern, because as can be seen in fig. 57, this area in front of the plant is clear of any other plants and would allow for the antenna to easily be pushed on the surface of the soil without anything to disturb its direction while carrying long straight profile lines. The soil also seems quite dry and no irrigation has taken place recently prior to the GPR surveying.

Figure 57. The GPR survey setup with details about profiles with the 4 GHz antenna.

4.2.1.2.1. RHODODENDRON SITE RESULTS

After the data has been processesd (table 6) and the profiles have been interpolated to create horizontal depth slices, there appears to be an area highlighted corresponding to the position of the plant at 60-80 cm on the profiles (fig. 56). The area appears to be around 20 cm in length and has a width of about 10 cm, a size that is significantly smaller than the size of the actual plant at the surface, with the base of the plant measuring approximately 10 cm. The anomaly seems to be changing polarity with depth (fig. 56), appearing as positive closer to the

surface, changing to negative, and turning into positive again. This is a behaviour similar to the one observed at the tree root from the previous survey.

Figure 58. Close up on the area near the plant where the first profiles were carried out as close as possible to the plant.

Data positioning is also an issue when it comes to interpolating the data. Doing surveys at only 5 cm distance between the profiles, has been proved to be very difficult to keep the correct distance at all times equal between the profiles.

The soil appears to also highlight other features, due to the nature of the setting and soil, therefore increasing the difficulty in highlighting clearly features related to the roots (fig. 58). The correlation between the roots and the highlighted anomalies in the data was based on the known position of the plant at the surface.

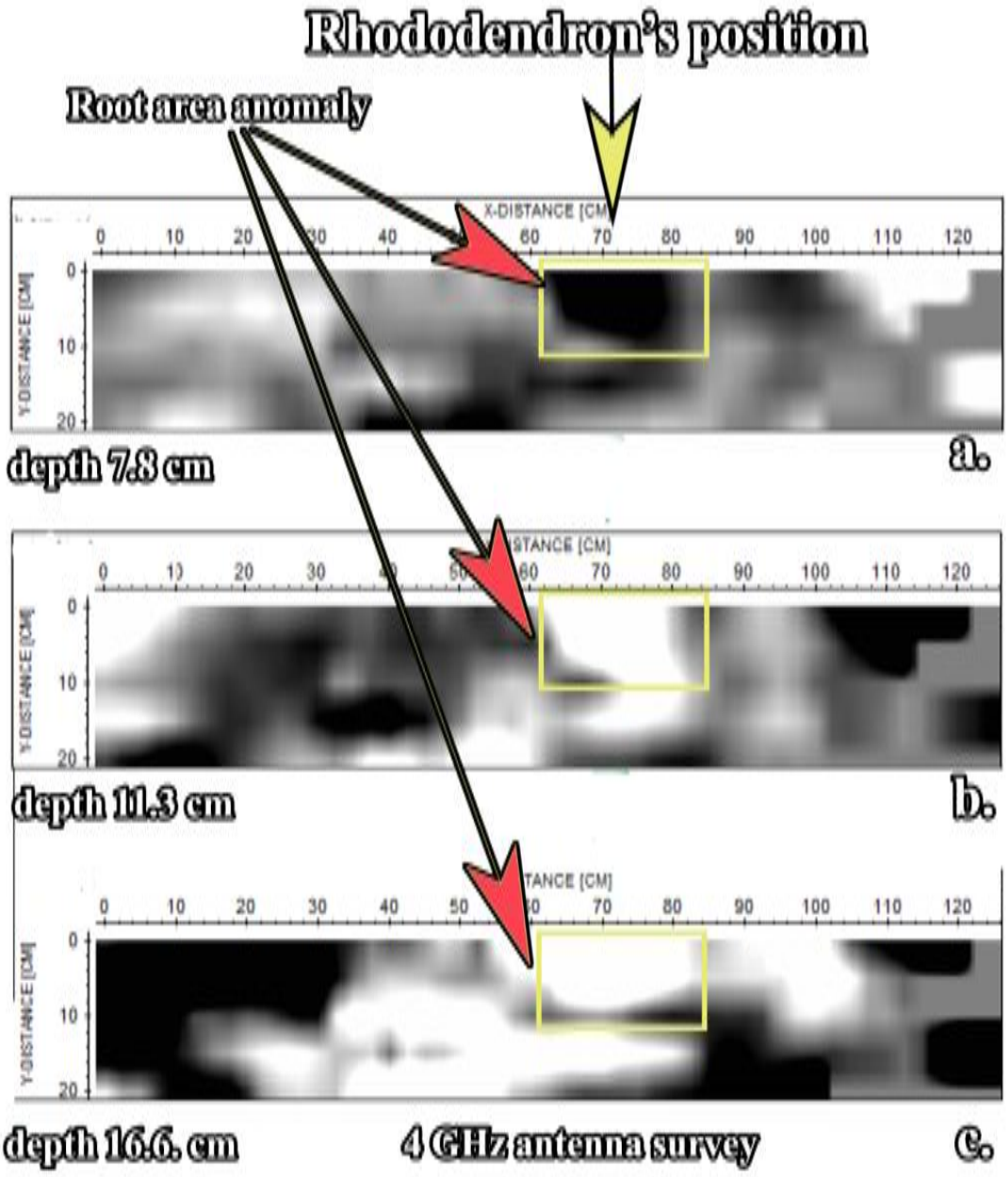

Figure 59. Horizontal slices resulted from the interpolation of the vertical GPR profiles, at different depths: a – 7.8 cm, b – 11.3 cm, c – 16.6 cm.

4.2.1.3. BRAZILIAN JOYWEED (*Alternanthera brasiliana Kuntze*)

Different than the previous settings, this area has been chosen due to its similarity in some of the parameters with those of agricultural plants. As it has been observed and described in chapter 3.3 in an agricultural setting, with fully grown plants it appears that it's difficult to identify individual plants from each other when it comes to their root area, as the plants are numerous and really close together, their roots appear to create a root dense layer inside the soil. Surveying an area like this might provide useful information regarding how to better apply the GPR method in an agricultural setting with high frequency antennas and if either individual roots can be distinguished, high moisture content area, or even if a layer can be distinguished which could represent where the roots are.

Figure 60. The GPR profiles for surveys with both 1.5 GHz and 4 GHz antenna on the Brazilian Joyweed site.

The Brazilian joyweed (*Alternanthera brasiliana Kuntze*) is part of the same family as spinach, beets, and chard, but the Brazilian joyweed is used most of times as an ornamental plant or in traditional medicine for a variety of uses (Duarte and Debur, 2004). The plant usually grows in moist but well drained soils, and the plant grows either from a seed or through the stems that come in contact with soil and start developing roots (Llamas, 2003).

Where the surveys were carried out, the soil appears to have higher moisture content visible from the surface. The surface of the area was also covered in grass which may represent a limiting factor in terms of visualizing the actual root area of the joyweed plants.

Acquisition parameters		
Site name	Brazilian Joyweed	
Antenna frequency	1.5 GHz	4 GHz
survey conditions	wet	wet
no. of profiles	4	5
direction of profiles	parallel to root area	parallel to root area
distance between profiles	5 cm	5 cm
profile length	140 cm	140 cm
samples per line	512	512
scan frequency	50 Hz	50 Hz

Table 7. GPR data acquisition parameters for the Brazilian Joyweed site with both 1.5 GHz and 4 GHz antennas.

Both antennas have been used on this site (4 and 1.5 GHz). The data set using the 4 GHz antenna contains a number of 5 parallel profiles at a distance of 10 cm in-between, whereas the set of data which used the 1.5 GHz antenna contains 4 parallel profiles with the same distance between them (fig. 59), and the acquisition parameters are described in table 7. The first profile in each set of data, goes parallel to the line of plants with the first profile getting

as close as possible with the antenna to the stem of the plants, and moving 10 cm away from the plants with each profile afterwards.

Data processing parameters			
Site name	Brazilian Joyweed		
Antenna frequency		1.5 GHz	4 GHz
move starttime	manual input	-1.34	-0.888
dewow	timewindow [ns]	0.66	0.25
bandpass butterworth	lower cutoff	750	2000
	upper cutoff	3000	8000
background removal		yes	yes
gain function	linear gain	1	0.07
	exponent	1	3
fk migration Stolt	velocity [m/ns]	-	-

Table 8. GPR data processing parameters for the Brazilian Joyweed site, for the data collected with both antennas.

4.2.1.3.1. BRAZILIAN JOYWEED SITE RESULTS

The data has been processed, with the parameters detailed in table 8, and the resulting data has been considered in the form of vertical profiles as the interpolation of the profiles, due to their reduced number, didn't seem to show conclusive results. It has been observed that the grass surface proved to be difficult for the 4 GHz antenna surveys, as it can be seen from the profiles, there are places where the poor coupling of the antenna affects the data (fig. 60).

The 1.5 GHz antenna is also affected by the surface but not as much as the 4 GHz antenna, probably due to the size of the antenna, making surveys much easier to be carried out and not as sensitive to any micro topography at the surface.

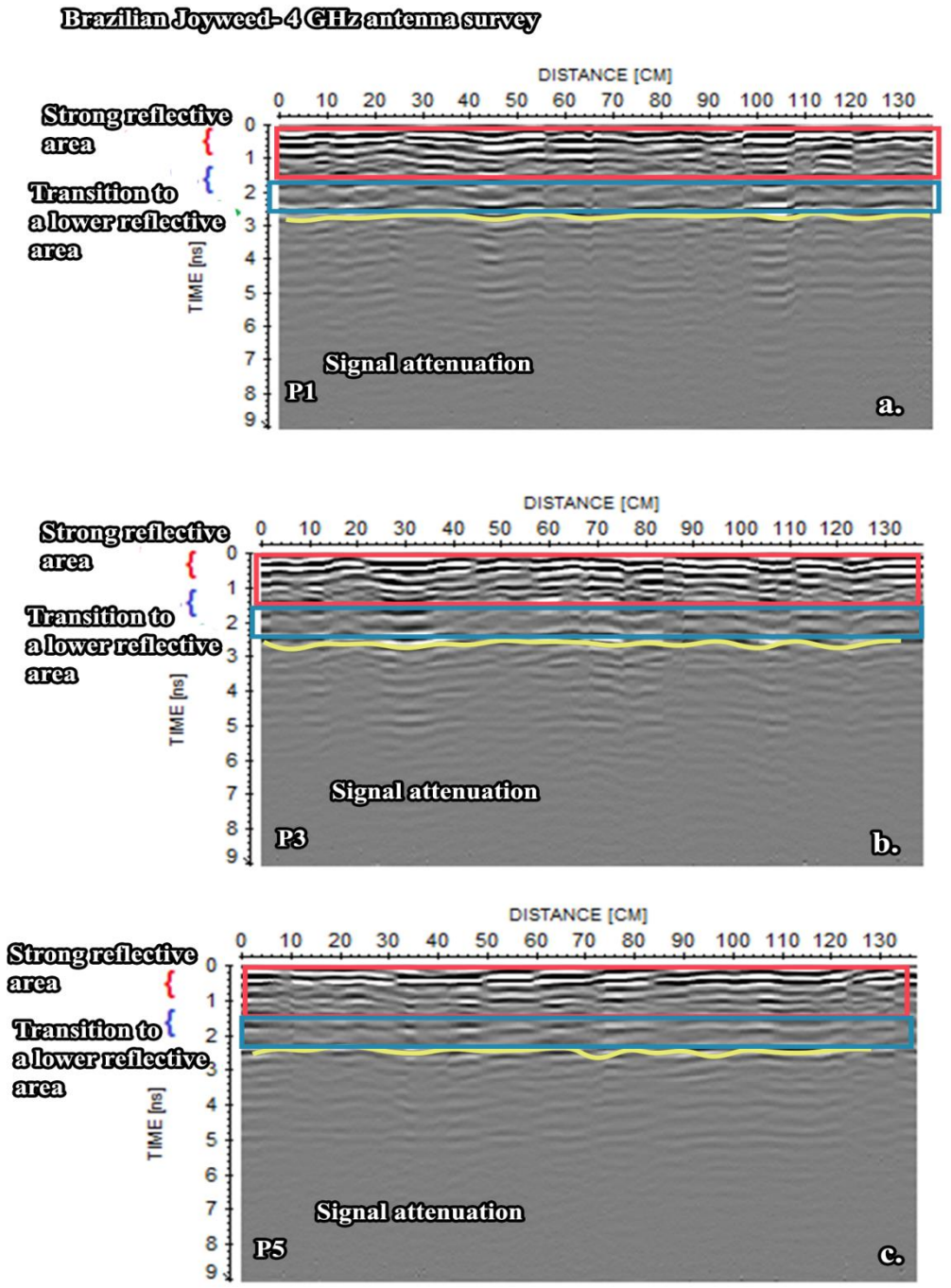

Figure 61. Processesd data from the surveys with the 4 GHz antenna; a – profile no. 1 closer to the plants; b- profile no. 3; c – profile no. 5 furthest away from the plants.

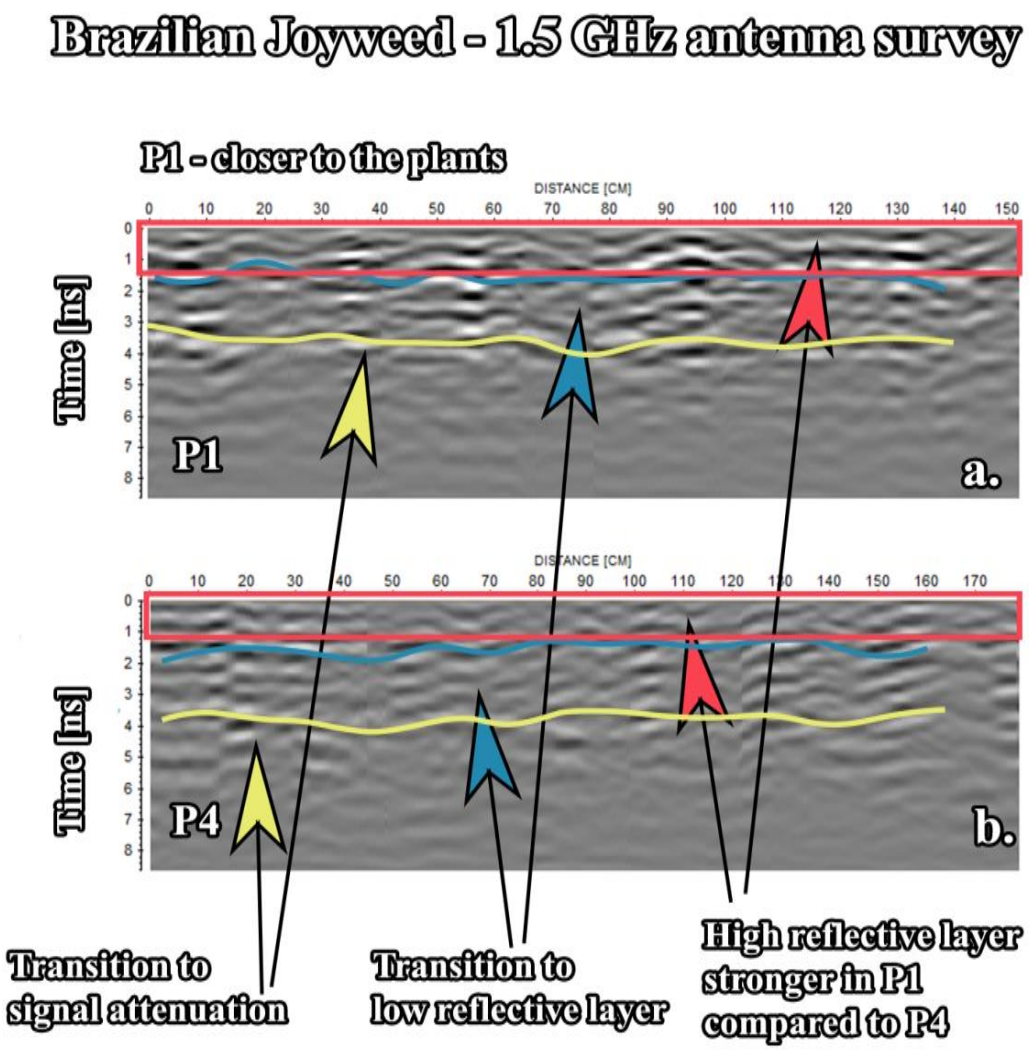

Figure 62. GPR processesd data for the surveys with the 1.5 GHz antenna; a- profile no. 1 closest to the plants; b – profile 4 furthest away from the plants.

It appears that dewow makes a great difference to the 4 GHz and is also useful for the 1.5 GHz antenna the difference is not as strong. It is very difficult to correlate 4 GHz antenna, and 1.5 GHz antenna data, as every cm counts and offset the profile. The surveys are very sensitive to positioning, which is also time consuming and great precision is hard to achieve in the field.

In the 4 GHz data, what can be observed is the appearance of three distinct features: two thick layers or areas marked with the red and blue arrow (and the curly brackets) and a continuous horizon appearing marked with the green arrow (fig. 60).

It appears that the top most layers, marked with the red (fig. 60-61) in data from surveys with both antennas are characterized by high reflectivity which might indicate higher water content.

The second layer marked with the blue rectangle in the 4 GHz antennas surveys (fig 60) and between the blue line and yellow line in the 1.5 GHz surveys (fig. 61) is characterized by a multitude of reflections but it appears as less intense compared to the previously described layer.

The horizon marked as a transition to a lowe reflective area (fig. 60), shows continuity from left to right, with small interruptions, and probably marks the change from one type of soil to another; maybe this represents a landscaping feature.

Another interesting feature is the intensity of all of these described layers and the way their intensity decreases with the profiles moving further away from the plants (fig. 60-61), which might indicate a correlation between these plants and their position to the appearance of all these highlighted features.

There are similar aspects appearing in the 1.5 GHz data (fig. 61), with the decrease in intensity of the contrasts and reflections as they the profiles are further away from the plants.

Due to the inability to dig and check details about where the roots are, it’s difficult to say where the roots are or a more general root area, and how this correlates with the data.

However there is a high probability that the top part of the profiles where the previously described layers are appearing down to the horizon marked by the green arrow, to be related to the effect the roots have on the soil and their ability of holding more moisture around them compared to the surrounding area. This is valid for the data collected with both 1.5 GHz and 4 GHz antenna.

4.2.1.4. IRIS PLANTS (*Iris pseudacorus L.*)

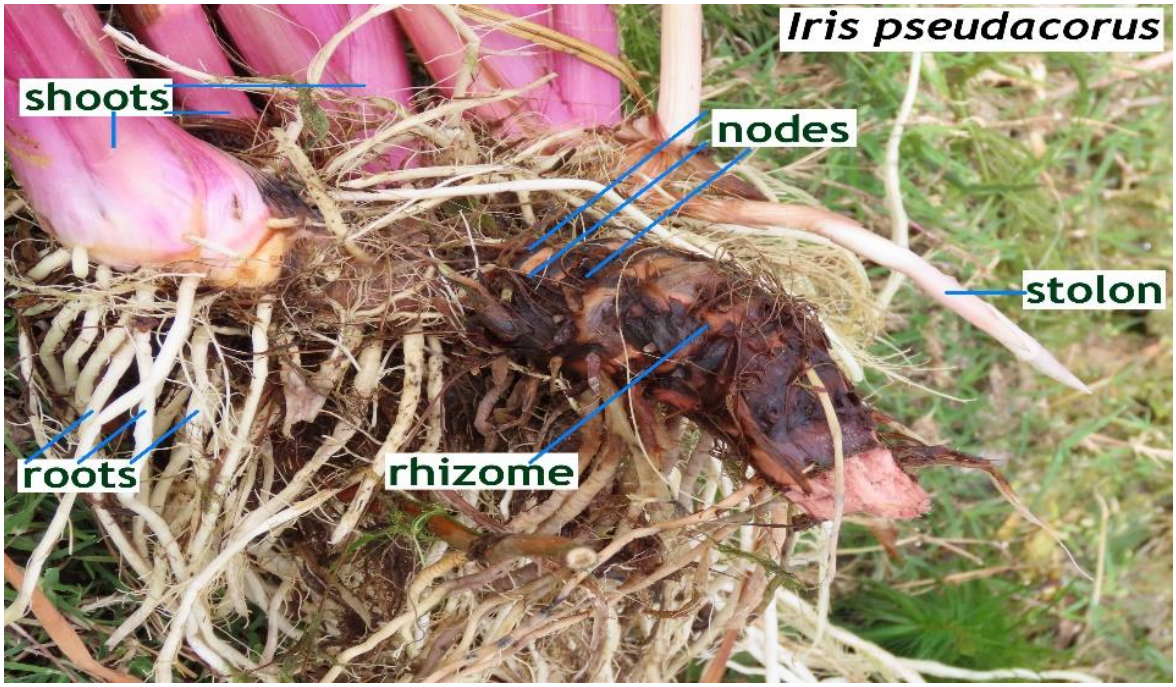

Figure 63. Image representing the complex root system of the Iris pseudacorus plants. Jon Richfield (2019).

This site was chosen based on the same principle as the last site (see 4.2.1.3 Brazillian Joyweed) however in this instance, not only that the plants are really close together (an aspect

that bears resemblance to the agricultural environments), but the roots of the iris plants (*Iris pseudacorus L.*) are quite complex (fig. 62), with a rhizome that could go up to 20 mm in diameter, from which fibrous roots are emerging (Mehdiyeva et al., 2017). They also prefer moist soils (Mehdiyeva et al., 2017)., and where the surveys were carried out the soil seemed to have high water content visible from the surface. The area is also covered with grass, which might interfere with the detection of the root area.

Acquisition parameters		
Site name	Iris plants	
Antenna frequency	1.5 GHz	4 GHz
survey conditions	wet	wet
no. of profiles	4	4
direction of profiles	parallel to root area	parallel to root area
distance between profiles	10 cm	5 cm
profile length	170 cm	140 cm
samples per line	512	512
scan frequency	50 Hz	50 Hz

Table 9. Acquisition parameters for the surveys at the Iris plants site using both 1.5 GHz and 4 GHz antennas.

Both antennas were used on this site, in a similar pattern to the previous site, with 4 profiles parallel to the line of the edge of the plants, and 10 cm between profiles for the survey carried out with the 1.5 GHz antenna (fig. 63 – a) and 5 cm for the surveys with the 4 GHz antenna (fig. 63 – b) and their acquisition parameters are detailed in table 9. Even though the area has a triangular shape due to landscaping reasons (fig. 64) in order to create the parallel profiles of 170 cm (fig 63 – a) and 140 cm respectively (fig. 63 – b) and area has been chosen for covering a large portion of continuous plant growth in the profiles.

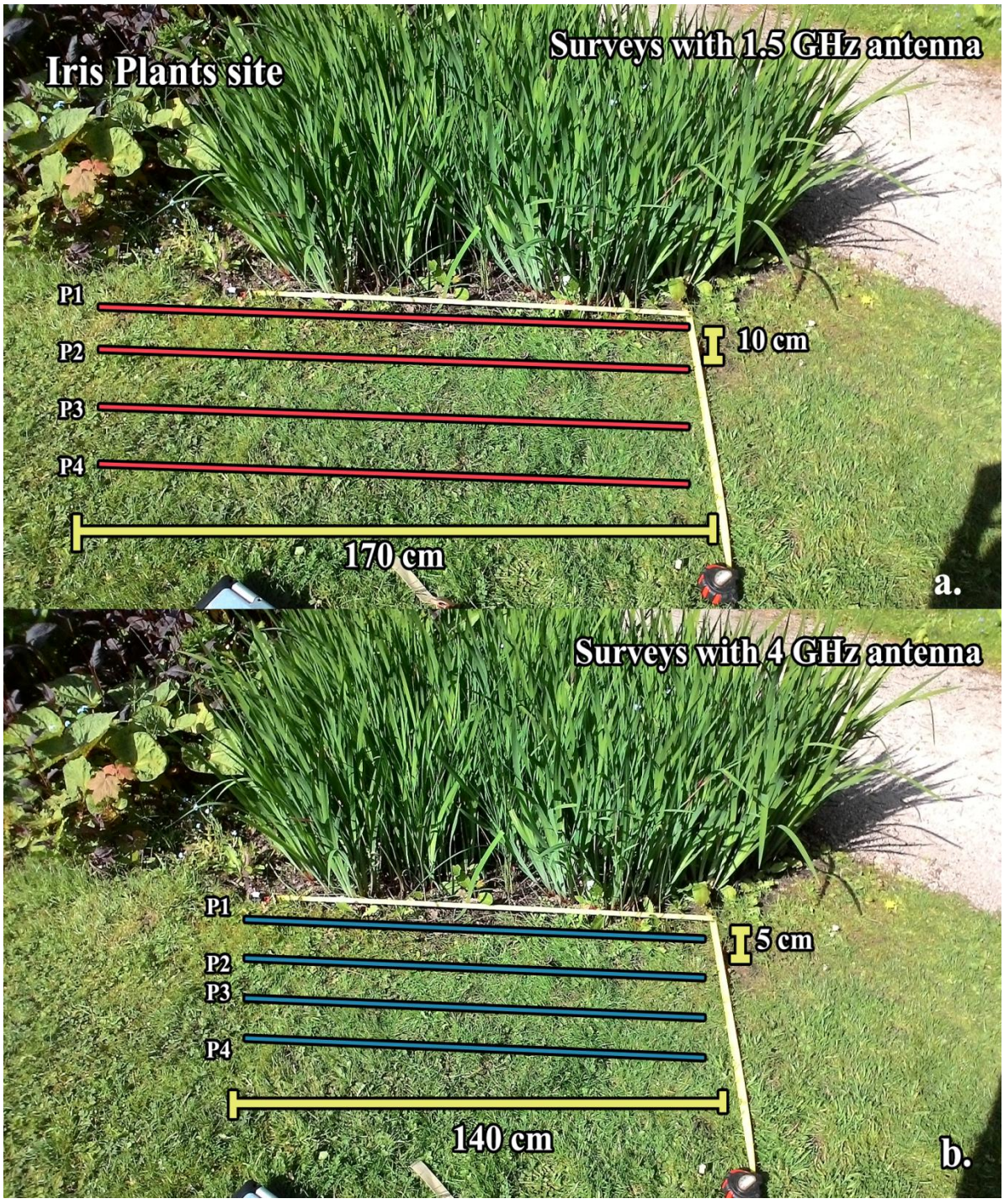

Figure 64. Details about the survey design at the Iris plants site using the 1.5 GHz antenna (a) and the 4 GHz antenna (b).

Figure 65. The Iris plants are planted in the form of a triangle due to landscaping reason, therefore a place was found to carry out the survey where parallel proviles to a continous line of plants could be found.

4.2.1.4.1. IRIS PLANTS SITE RESULTS

Due to the reduced number of profiles, after the data has been processed (table 10) interpolation of the data hasn't been carried out, therefore the analysis of the results was achieved through vertical radargrams only. Similar to the previous surveys, there appear to be 3 distinct features highlighted as well, with a top layer featuring a high reflective area (fig. 65) found between the top of the radargrams and going down to 1.5 ns, followed by a layer with a lower reflectivity between 1.5 ns to 2.5 ns (fig. 65 – c, d) much more clearly marked in the 4

GHz data, after which bellow 3 ns mostly (fig. 65) there is a higher attenation in the surveys with both antennas.

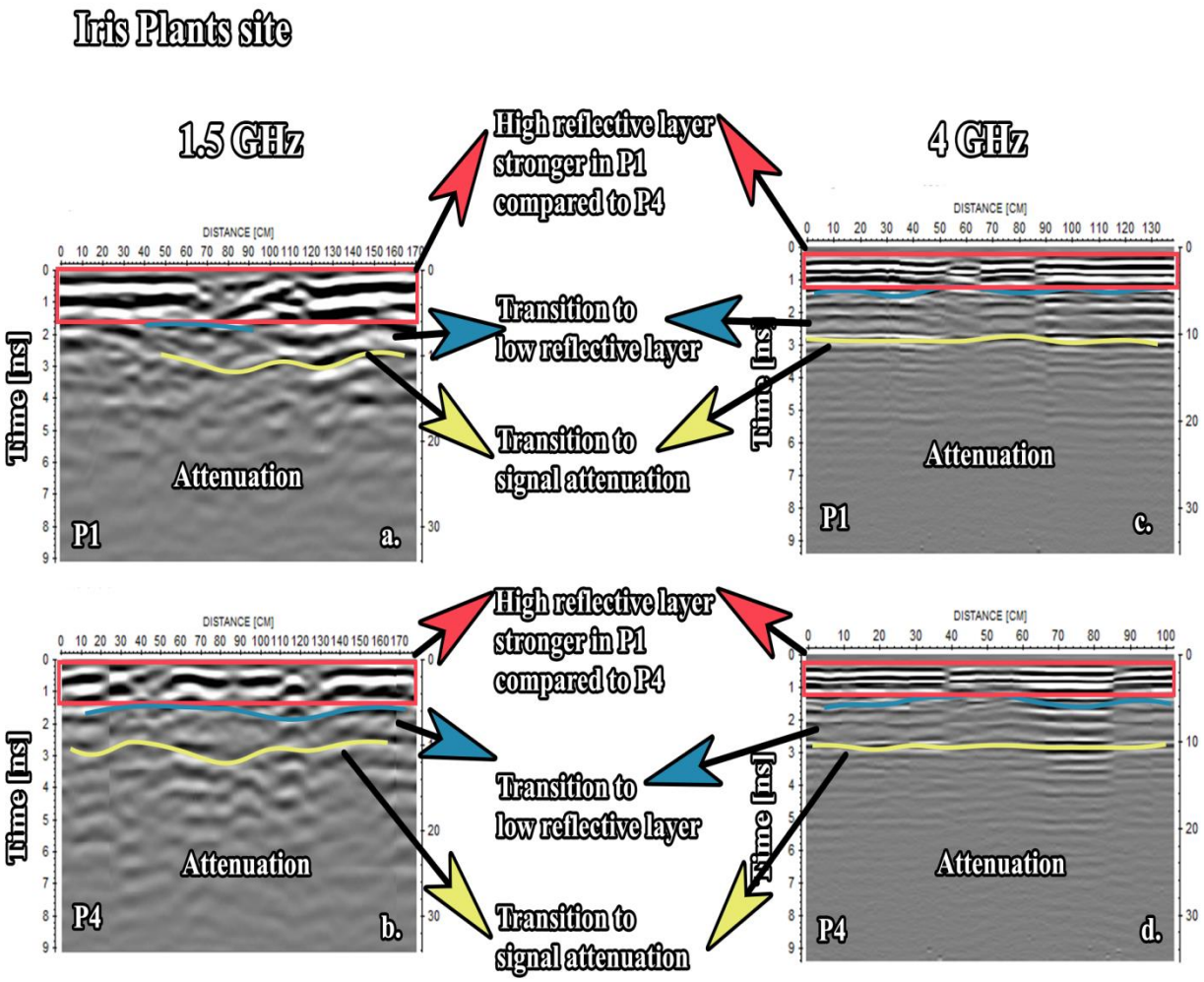

Figure 66. Processed GPR data with highlighted features of interest for: a – profile 1 for the surveys with the 1.5 GHz antenna; b – profile 4 with the 1.5 GHz antenna; c – profile 1 for the surveys with the 4 GHz antenna; d – profile 4 with the 4 GHz antenna.

Another similarity with the previous set of data is the fact that moving away from the plants, the intensity of the contrasts is fading. This aspect appears to be more prominent, in the 1.5

GHz data (fig. 65 – a, b), only because the distance between the profiles was greater (10 cm compared to the 5 cm of the 4 GHz surveys).

Data processing parameters			
Site name	Iris plants		
Antenna frequency		1.5 GHz	4 GHz
move starttime	manual input	-0.833	-0.52632
dewow	timewindow [ns]	0.66	0.25
bandpass butterworth	lower cutoff	750	2000
	upper cutoff	3000	8000
background removal		yes	yes
gain function	linear gain	0.1	0.2
	exponent	2	2
fk migration Stolt	velocity [m/ns]	0.065	0.065

Table 10. GPR data processing parameters for the surveys on the Iris plants site, with both 1.5 GHz and 4 GHz antennas.

As it is the case with the previous set of data, the top layer presents higher contrasts compared to the layer underneath, which might be related to the higher water content, and another similarity is the appearance of the horizon marked with green arrow.

Also similar to the previous survey, it is hard to identify and correlate the layers or data to any roots, but there is a possibility of these being between the surface and the horizon marked by the red rectangle (fig. 65).

4.2.1.5. PAMPAS GRASS (*Cortaderia sellona*)

The Pampas grass (*Cortaderia sellona*) is a plant in the Poaceae family, a family which includes plants like wheat, maize, rice, which are important agricultural plants, with a fibrous root system (Smith and de Smet, 2012), therefore this representing the main reason of

choosing to survey in this setting. Another reason was due to their shape and position which allowed for long profiles to be carried out on areas both with grass and no grass, allowing for contrasts and for highlighting the area of interest (the root zone area).

For this site, both 4 GHz antenna and 1.5 GHz antenna have been used in order to analyse the root area.

Figure 67. The Pampas grass site and details about the position of the profiles – they were the same for both of the antennas used.

Only three parallel profiles have been created with a distance of 5 cm in-between for the surveys with both antennas (fig. 66), however due to the long distance of the profiles (340 cm) the data collected with the 4 GHz antenna suffered more from the bad coupling of the antenna with the surface therefore the data hasn't been conclusive enough and only the data

collected with the 1.5 GHz antenna were analysed. The details about the parameters for data acquisition are presented in table 11.

Acquisition parameters		
Site name	Pampas grass	
Antenna frequency	1.5 GHz	4 GHz
survey conditions	very dry	very dry
no. of profiles	3	3
direction of profiles	parallel to root area	parallel to root area
distance between profiles	5 cm	5 cm
profile length	340 cm	340 cm
samples per line	512	512
scan frequency	50 Hz	50 Hz

Table 11. Acquisition parameters for the GPR surveys at the Pampas grass site using both 1.5 GHz and 4 GHz antennas.

Before the surveying, the ornamental bark which was covering the surface of the soil was removed in order to allow for a good contact between the antenna and the surface of soil.

Data processing parameters		
Site name	Pampas grass	
Antenna frequency		1.5 GHz
move starttime	manual input	-1.038
dewow	timewindow [ns]	0.66
bandpass butterworth	lower cutoff	750
	upper cutoff	3000
background removal		yes
gain function	linear gain	0.1
	exponent	2
fk migration Stolt	velocity [m/ns]	0.14

Table 12. Data processing parameters for the surveys at the Pampas grass site only for the 1.5 GHz antenna data.

4.2.1.5.1. PAMPAS GRASS SITE RESULTS AND GENERAL REMARKS

Due to the small number of parallel profiles no interpolation has been carried out, therefore the analysis of the processesd data (table 12) was done on the vertical radargrams of the data collected with the 1.5 GHz antenna (fig. 67).

It can be observed from the data that there are some anomalies appearing correlated with the position of the plants, where the profiles are closer to the plant (fig. 67 –a) show a higher contrast in that area, especially for the first plant, compared to what can be seen in the profile furthest away (fig. 67 - b).

Longer profiles are harder to be correlated and it is difficult to keep perfect distances between the profiles even with the 1.5 GHz antenna.

Some areas can be correlated with the position of the plants in both closer profiles and profiles at 15 cm away from the plants (fig. 67). Also, similar to previous sites, there appear to be a higher attenuation bellow the 3 ns level, with a high reflective area in the top layer going to approximately 1.5 – 2 ns (fig. 67). Another similarity to the previous site is that moving further from the plants the intensity of these high reflective top layer diminishes, and in this case this is mostly true for what appears to be the reflective effect created correlated with the position of plant (marked as) 1 (fig. 67 – a), however the plant marked as number 2 with the corresponding anomaly appears to be slightly shifted to the right and the effect slightly larger (fig. 67 – b). The 4 GHz antenna was very much affected in terms of data acquisition on the longer profiles, even though the surface of the soil has been “tidied up” of any unconsolidated elements. However the dry soil made the coupling of the antenna difficult.

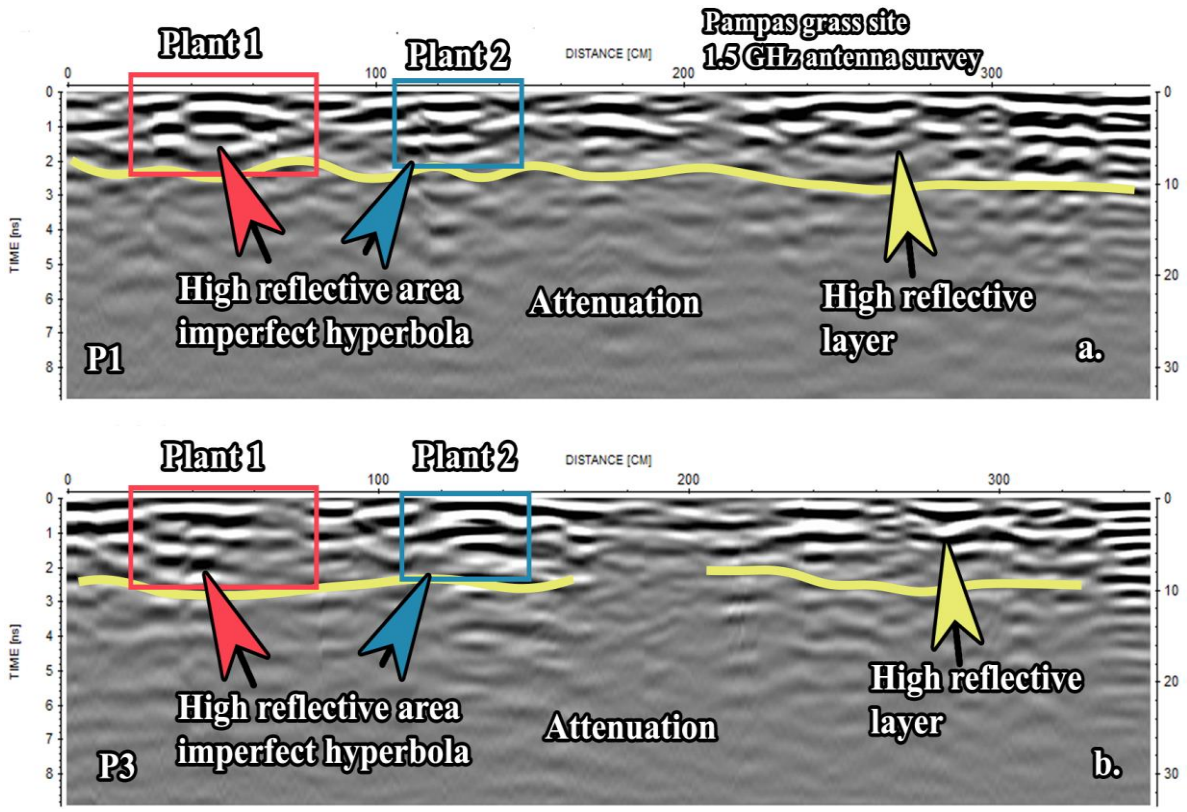

Figure 68. The vertical radargrams resulted from processing the GPR data with 1.5 GHz antenna at the Pampas grass site; a – profile no. 1 closest to the plants; b – profile no. 3 furthest away from the plants.

Generally it has been observed that both of the antennas, 4 GHz and 1.5 GHz, seem to make it difficult to correlate profiles in natural environments for detecting small targets into the ground, due to the small offsets created by small changes in the surface of the surveyed area. However the 4 GHz antenna seems to be even more affected due to its size and lightness by any uneven surfaces, and even non-compact dry soil at the surface of the survey area.

They both take a long time for data collection as the antenna needs to be moved slower to keep the profiles straight, and sometimes profiles need repeating. Even though the 1.5 GHz antenna is more robust and a bit heavier, both antennas are really difficult to be used when the

surface is not compact, and resembles characteristics of the agricultural fields with rougher and uneven surfaces.

It has been observed that in some cases, as it is the case described in chapters 4.2.1.3 and 4.2.1.4, there can be some layers or areas highlighted which have lateral continuity; however it's difficult to clearly correlate these with the position of the roots. These layers are described by high contrasts, which might indicate higher water content and lateral continuity, and are clearly separated from the environment below this horizon, in characteristics.

In terms of data processing, it has been observed that the 4 GHz antenna makes benefits very much from the application of the dewow filter, which was applied to the 1.5 GHz data as well, but the difference is significantly important for the 4 GHz antenna.

Migration was difficult to proceed with, due to the nature of the environment, as there appear to be too many unknown features into the ground, and due to the fact there didn't appear much clear hyperbolas around which could've allowed for calculating the velocity value needed for the migration**.**

4.2.2. GPR - INDOOR SURVEYS

4.2.2.1. LARGE TRANSPARENT CONTAINER SURVEYS

The indoor GPR surveys carried indoor were in the large experimental container with 3 tomato plants (fig. 68), setup fully described in chapter 3.4.1.2. Several trials have been done

and surveys have been carried in different conditions, using both the 1.5 GHz antenna and the 4 GHz antenna.

Figure 69. Example of GPR survey using the 4 GHz antenna in the large container with 3 tomato plants.

Because the area in the box is very limited the wheels have been removed and all the surveys were carried in time mode on known distances.

Due to the size of the antennas and the limited space, only 2 profiles were possible with the 1.5 GHz antenna, one on each side of the plants, and with the 4 GHz antenna, 8 profiles were possible at a spacing of 5 cm (fig. 69). Using threads and measuring tapes which were fixed on the edges of the box, helped with keeping the correct distance throughout collecting data on each profile.

A variety of surveys have been carried with different conditions but only the most relevant ones will be presented, and more details about these and specific data acquisition parameters are more detailed in table 13.

Acquisition parameters				
Site name	Indoor large container			
Antenna frequency	1.5 GHz	4 GHz	1.5 GHz	4 GHz
survey conditions	very dry	very dry	5 hours after watering with water and fertilizer	5 hours after watering with water and fertilizer
no. of profiles	2	8	2	8
direction of profiles	parallel to root area	parallel to root area	parallel to root area	parallel to root area
distance between profiles	20 cm	5 cm	20 cm	5 cm
profile length	55 cm	80 cm	55 cm	80 cm
samples per line	512	512	512	512
scan frequency	50 Hz	50 Hz	50 Hz	50 Hz

Table 13. Acquisition parameters for the surveys carried out in the large container with the 3 plants, for surveys with both 1.5 GHz antenna and 4 GHz antenna, before and after watering the plant with water and fertilizer.

In the large tomato container with 3 plants, where from left to right, the first two plants were still alive and the third plant was dead, a number of surveys have been carried out in different conditions. This situation was chosen to inspect whether the roots of the plants that were still alive would have different permittivity values and produce different GPR reflections compared to the roots from the dead plant. The living roots were expected to be, sap flowing roots, with higher moisture content and with closer permittivity values to the ones described by Ellis (2012) whereas it is expected for the dead roots, as they have lower moisture content, to behave more like woody roots with lower permittivity values. Observing if there are any contrasts between these different situations would allow understanding what kind of features can be seen and highlight in the control environment when it comes to plant roots with the use of high frequency antennas.

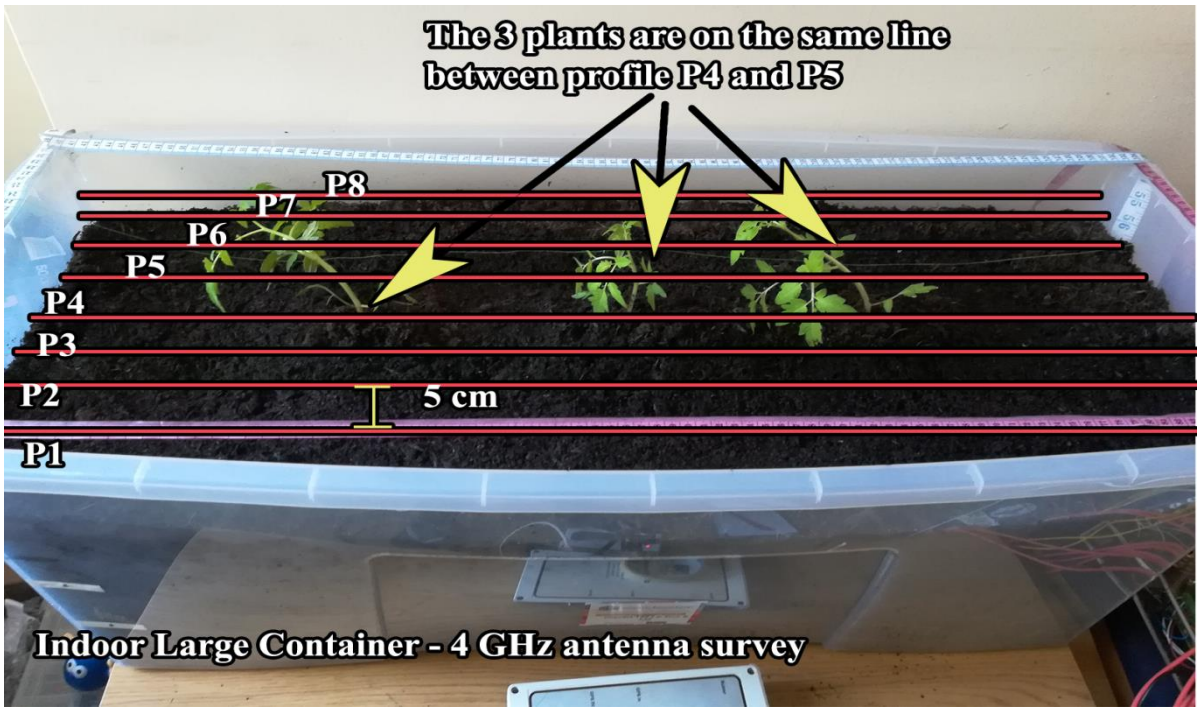

Figure 70. Representation of the profiles carried out with the 4 GHz antenna, four profiles on each side of the line of plants.

The first surveys took place before watering the plants, when the soil was very dry, and the second set of surveys took place at approximately 5 hours after watering the plants with both water and fertilizer. The period of time was chosen for allowing the plants to absorb water and for allowing the water to drain from the top layer. Using a transparent box, it was easily visible when part of the added water would reach the bottom of the box.

After processing the data, it was possible to use data from the 4 GHz antenna to create horizontal slices due to the large number of profiles. Specific details about data processing steps for both situations (before and after watering) resulted from the data collected with both of the antennas are detailed in table 14.

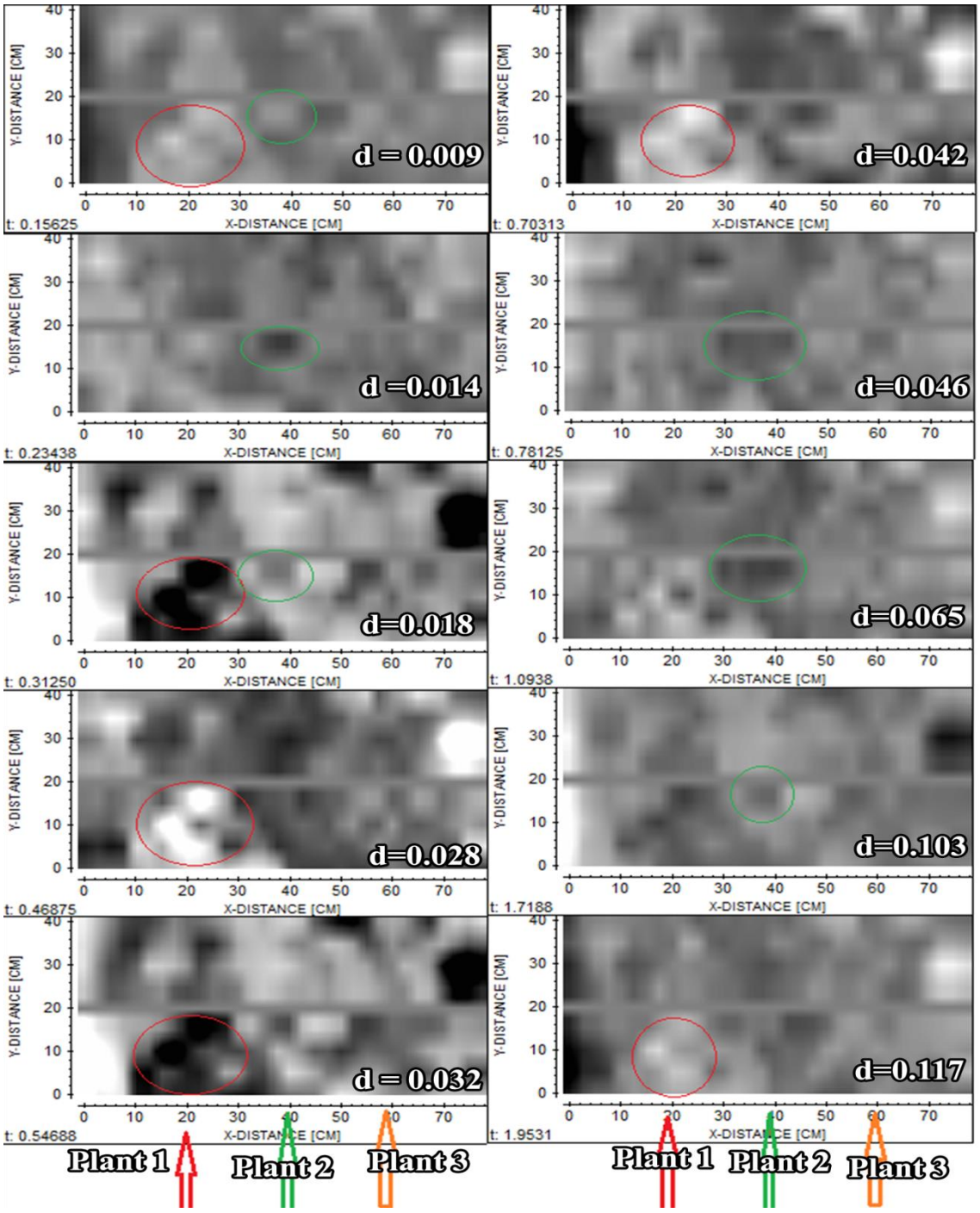

Figure 71. Horizontal 4 GHz antenna GPR slices at different depths in cm (d) for the data that took place after the plants ware watered, with red, green and orange arrow are represented the location of the known position of the plants.

4.2.2.1.1. INDOOR TRANSPARENT CONTAINER RESULTS

Data processing parameters					
Site name	Indoor large container				
survey conditions		before watering		after watering	
Antenna frequency		1.5 GHz	4 GHz	1.5 GHz	4 GHz
move starttime	manual input	-1.206	-0.732	-1.187	-1.3604
dewow	timewindow [ns]	0.66	0.25	0.25	0.25
bandpass butterworth	lower cutoff	750	2000	2000	2000
	upper cutoff	3000	8000	8000	8000
background removal		yes	yes	yes	yes
gain function	linear gain	0.1	0.25	0.2	0.35
	exponent	1	3	2	3
fk migration Stolt	velocity [m/ns]	-	-	-	-
stack traces	nr. of traces	-	-	4	3
	nr. of tr./ensemble	-	-	0	1

Table 14. Data processing parameters for data collected with both 1.5 GHz and 4 GHz antenna, before and after watering the container with 3 plants.

In the data from the surveys, which took place after the plants have been watered with both water and fertilizer, several features stand out, including features which can be observed highlighted in figures 70 and 71. Knowing the exact position of the plants and keeping straight profiles on the small surface enabled the correlation of the position of the plants with some features appearing in those specific areas. What can be observed in figure 70, located where the plant 1 should be, a stronger reflective area with a diameter of approximately 20 cm appearing on the lower part which changes amplitudes from positive to negative and back to positive as the slices go deeper, untill is no longer visible bellow 0.042 cm. Slighlty lighter reflective area compared to the previously described appears in the middle as well, even though reduced in size at about 10 cm in diameter, changing from positive to negative amplitude as it goes deeper. However on the right side where plant 3 was supposed to be (the

dried plant) there doesn't seem to be anything specific. What can be observed in both slices and vertical radargrams is that the reflections around the first two plants are more visible contrasts than the reflections around the 3rd plant, after these have been watered. The features are more visible on the radargram closer to the centre of the box. The plant on the left side appears to produce a stronger anomaly compared to the one in the middle in the data from the surveys carried out with the 4 GHz antenna before water was added in the container as well. In the radargrams, there appear some reflections on the plant which is on the left side, but the reflections are really faint compared to the other two, and highlighting an area in the slices that would correspond to the 3rd plant is rather difficult.

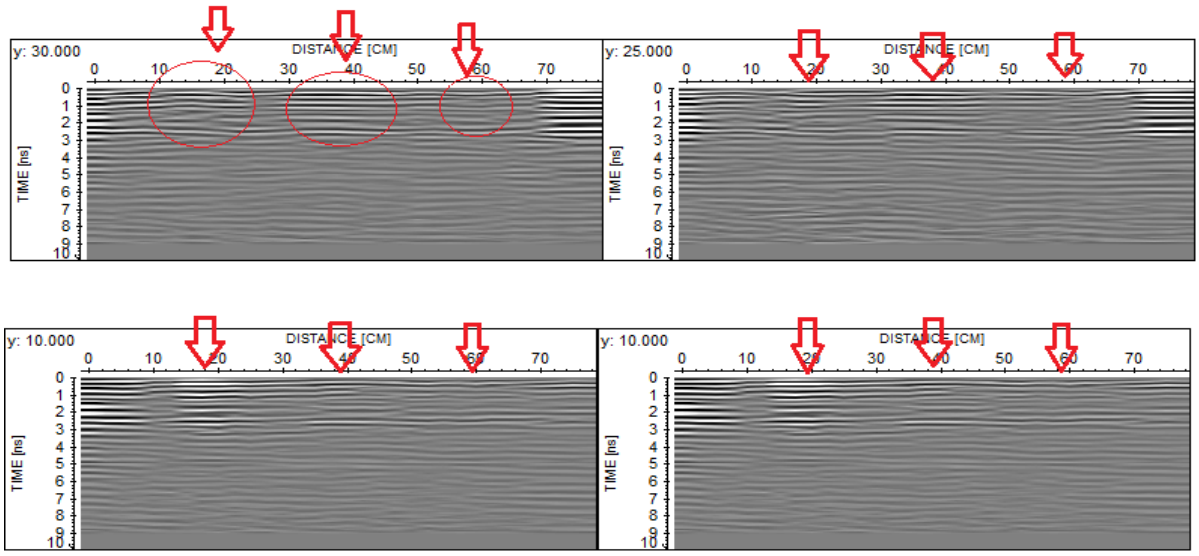

Figure 72. Vertical processed radargrams for the surveys that took place after the plants were watered, with red arrows highlighting the position of the plants.

The data from the 1.5 GHz antenna seem to show more reflections in the subsoil. In the image 72, the red arrows point to the position of the plants at the surface. It can be observed in the

profile no. 1 from the data, after plants were watered, that there are more reflections contouring in the data.

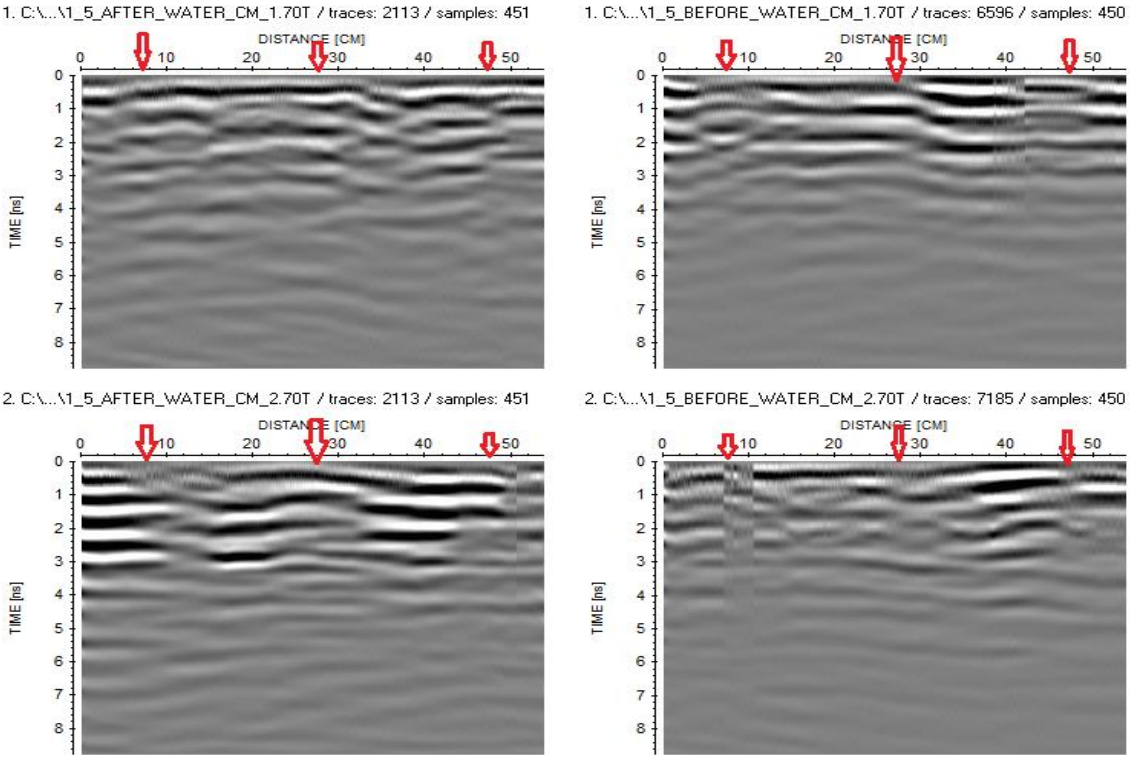

Figure 73. The processed data for the 1.5 GHz antenna surveys, before and after watering with fertilizer and water.

The reflections from the 3rd plant seem to have a different behaviour compared to the ones on the left side and the middle. There appear some stronger reflections where the first plant is on all the profiles. In the data before the watering (fig. 73), there seem to be similar aspects related to the presence of the anomalies related to the position of the plants, with high reflective areas changing from positive to negative amplitudes as the depth increases, however no significant anomaly is visible for the third plant (fig. 73 – orange arrow). It is more visible as well in the vertical radargrams (fig. 74) where from left to right it can be seen how the

intensity of the reflective areas coresponding to the plants' position, is significantly decreased in the third plant (orange arrow).

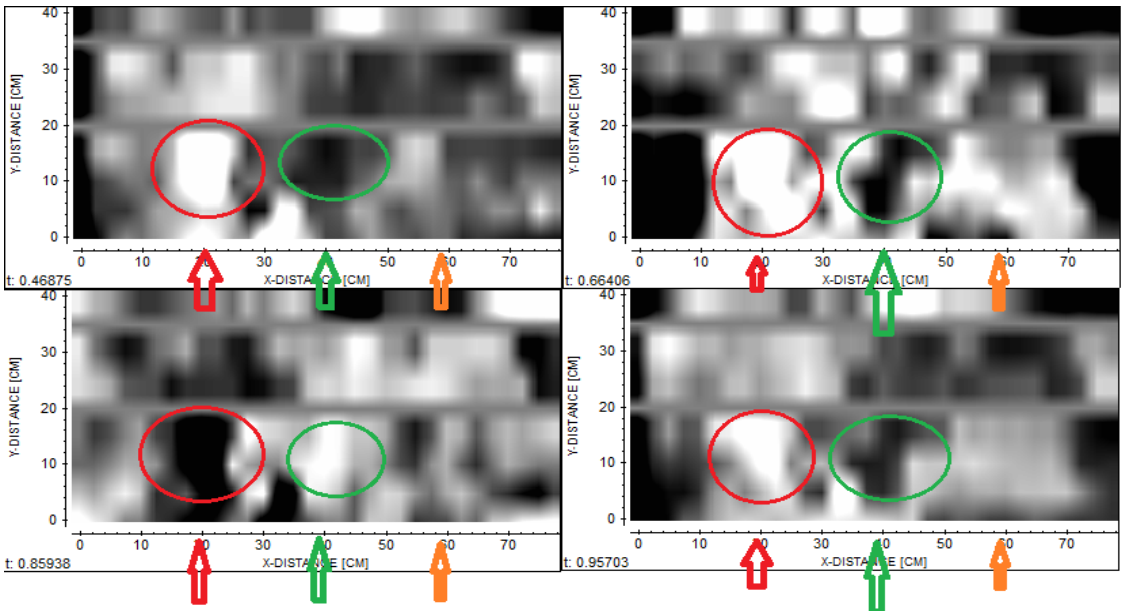

Figure 74. Figure representing horizontal slices from the data with the 4 GHz antenna before watering the plants. With arrows, the position of the plants is highlighted.

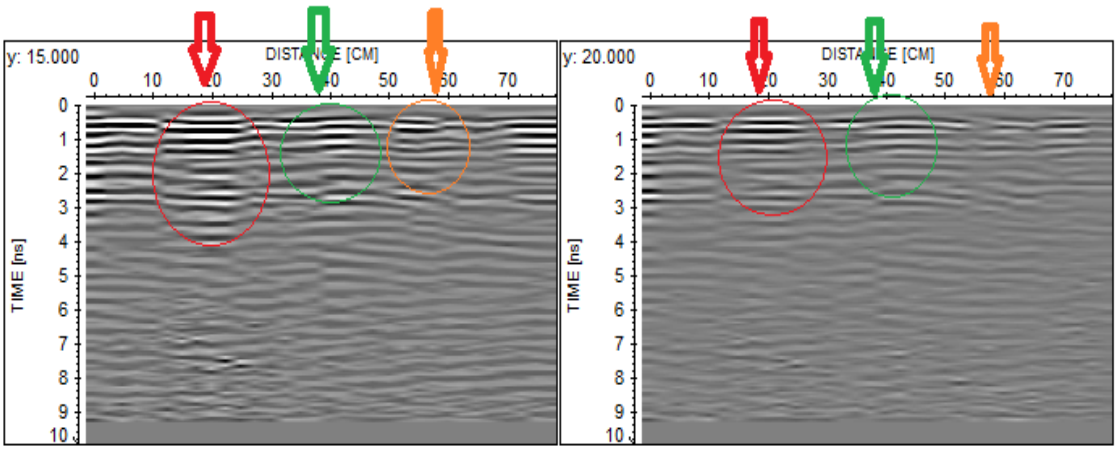

Figure 75. Image representing the vertical radargrams for the data with the 4 GHz antenna before watering the plants, profile P4 and P5. The position of the plants is represented with arrows, and with circles, areas of interest.

4.2.3. GPR SYNTHETIC MODELS

Another potentially useful source of information comes from GPR forward models. Here, 2D models were used for this purpose.

GPR forward (or synthetic) models represent an important approach in understanding what type of response the plant roots produce in different types of soils and with different type of antenna frequencies.

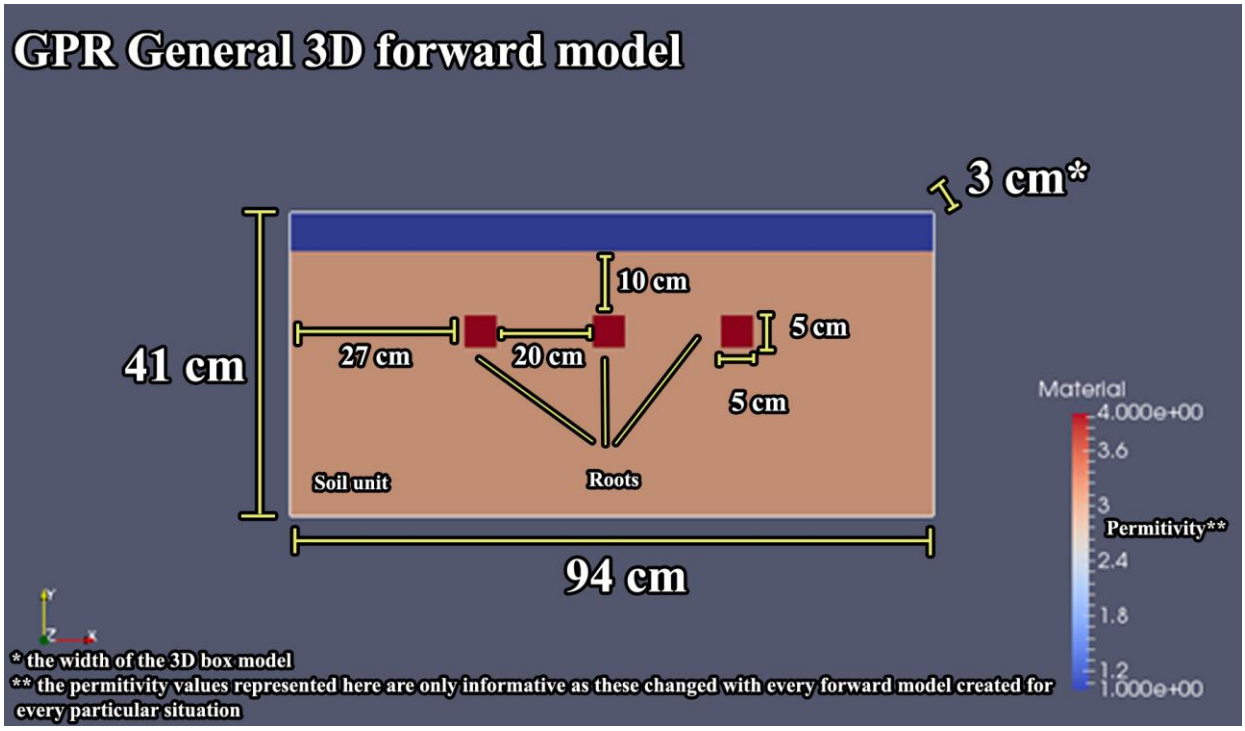

Figure 76. Example of the geometry used in the domain. The size of the objects remained the same throughout all of the models however the permittivity values changed.

Testing a variety of conditions for roots, soil and antenna frequencies helps with understanding the potential and limitations for different situations, which could further enhance the understanding of this type of response in real world settings. The permittivity

values used for the synthetic models are based on the literature review, and usually represent values resulted from experimental work on root and soil types. For example, in some studies the permittivity values of the roots have been measured on a variety of tests on different diameters and water content (Mihai et al., 2019) and some permittivity values for the roots have been calculated or approximated for specific fibrous roots (Ellis et al., 2012). While the real permittivity values of the roots modelled here may be different, these are the closest starting points mentioned in the literature. The antennas which are used in the models are the 1.5 GHz antenna and the 4 GHz antenna, which are the same antennas used in the experiments in this thesis. All the synthetic data is based on the same model domain, only changing the permittivity values roots and soil and the antenna configuration. The model consists of a rectangle-shaped box of 94 cm x 41 cm, and 3 5x5 cm rectangles which represent the roots (fig. 75). The box model is a modelled version of the actual box which was used in the experiments and has the same size. The rectangles are placed at an interval of 20 cm between them and 27 cm from the sides of the box, at a depth of 10 cm from the surface. Because the final applications of these data is to better understand behaviour of the plants in agricultural settings from the point of view of GPR data, the purpose of these models is to understand the potential and limitations in terms of GPR surveying focusing on permittivity values of the roots and the soil, especially when plants are relatively close together as it is the case with agricultural settings.

Three permittivity values have been chosen for the modelling the roots: 26.2, 15.3 and 68. According to Mihai (2019), the 26.2 permittivity value is the value resulted from the measurements on a Sycamore tree root with the diameter of 6 mm and 0.51% water content

and 15.3 is the value resulted from measuring the root of a Sycamore tree with 10 mm in diameter and higher water content at 0.54%, both values corresponding to measurements at 1.5 GHz (table 15). Even though the roots are quite large compared to plant roots, they were chosen based on size, trying to get the value for the smallest root in diameter, and water content, choosing the roots with higher water content, as these might get closer to the values of the agricultural plant roots.

Model	Soil ε	Type of soil	Water %	Source	Root ε	Plant type	Root Φ (mm)	Root water %	Source	Antenna (GHz)
A	4.54	brown soil, silty loam texture	18.01%	Zhou et al. (2019)	15.3	Sycamore	10	0.54 %	Mihai et al. (2019)	1.5
B	4.54	brown soil, silty loam texture	18.01%	Zhou et al. (2019)	26.2	Sycamore	6	0.51 %	Mihai et al. (2019)	1.5
C	4.54	brown soil, silty loam texture	18.01%	Zhou et al. (2019)	26.2	Sycamore	6	0.51 %	Mihai et al. (2019)	4
D	8	fine silt soil	6%	Chiara et al. (2014)	15.3	Sycamore	10	0.54 %	Mihai et al. (2019)	1.5
E	17.77	brown soil, silty loam texture	25.74%	Zhou et al. (2019)	26.2	Sycamore	6	0.51 %	Mihai et al. (2019)	1.5
F	17.77	brown soil, silty loam texture	25.74%	Zhou et al. (2019)	15.3	Sycamore	10	0.54 %	Mihai et al. (2019)	1.5
G	4.54	brown soil, silty loam texture	18.01%	Zhou et al. (2019)	15.3	Sycamore	10	0.54 %	Mihai et al. (2019)	1.5
H	17.77	brown soil, silty loam texture	25.74%	Zhou et al. (2019)	26.2	Sycamore	6	0.51 %	Mihai et al. (2019)	1.5

*Table 15. GPR models from A-H, and the parameters used in the models and their corresponding values: soil permittivity (**ε**) value, type of soil and its water content, root permittivity value, and the plant it belongs to, the root diameter and its water content, GPR antenna used, and the source of the parameter's information.*

In most studies, the permittivity values for the roots taken in consideration are simplified and treated as just bark or wood, which is gross simplification of the root aspects, and choosing values from actual measurements would allow for more reliable forward models. GPRMax forward model with permittivity values for roots of 15 and soil permittivity value 4.54. It was noted that if the time window is too long, then the domain edges can produce “multiples”, duplications of the signal. The first reflections marks the position of the simulated roots, the deeper hyperbolae mark these multiples. The time window was shortened in subsequent models to prevent this phenomenon. The third permittivity value, 68, is described by Ellis (2012) and unlike the previous two values; it was calculated and not measured (assuming roots were cylindrical capacitors and taking into consideration permittivity values for air, water, wax and cellulose). This value has taken into consideration the roots of a bean (*Vicia faba*) plant, which represents an agricultural plant with finer roots compared to those of trees.

The permittivity values for the soil are 4.54, 8, 15 and 17.77. Values of 8 and 15 have been chosen based on the experimental measurements in controlled environment described by Chiara et al. (2014), with permittivity 8 corresponding to a fine silt soil with low water content of about 6% measured with 1.8 GHz and 1 GHz antennas, and 15 corresponding to the same type of soil but with higher water content at about 12%.

Permittivity values of 4.54 and 17.77 have been chosen based on the laboratory measurements described by Zhou et al. (2019), with 17.77 corresponding to a brown soil with a silty loam texture and high water content (25.74%) and 4.54 corresponding to the same type of soil but with lower water content (18.01%) measured with a 2 GHz antenna. Among these parameters

the brown soil has an organic matter content of approximately 17.59 g kg^{-1}, salt content of 0.01%, pH value of 7.62, and consists of 66.4 % silt and 7.4% clay (Zhou et al., 2019).

Models have been created using a different root permittivity and a different soil permittivity value with either 1.5 GHz antenna or 4 GHz, as these are the types of antennas used in this study for the experimental settings and real world surveys described in previous chapters.

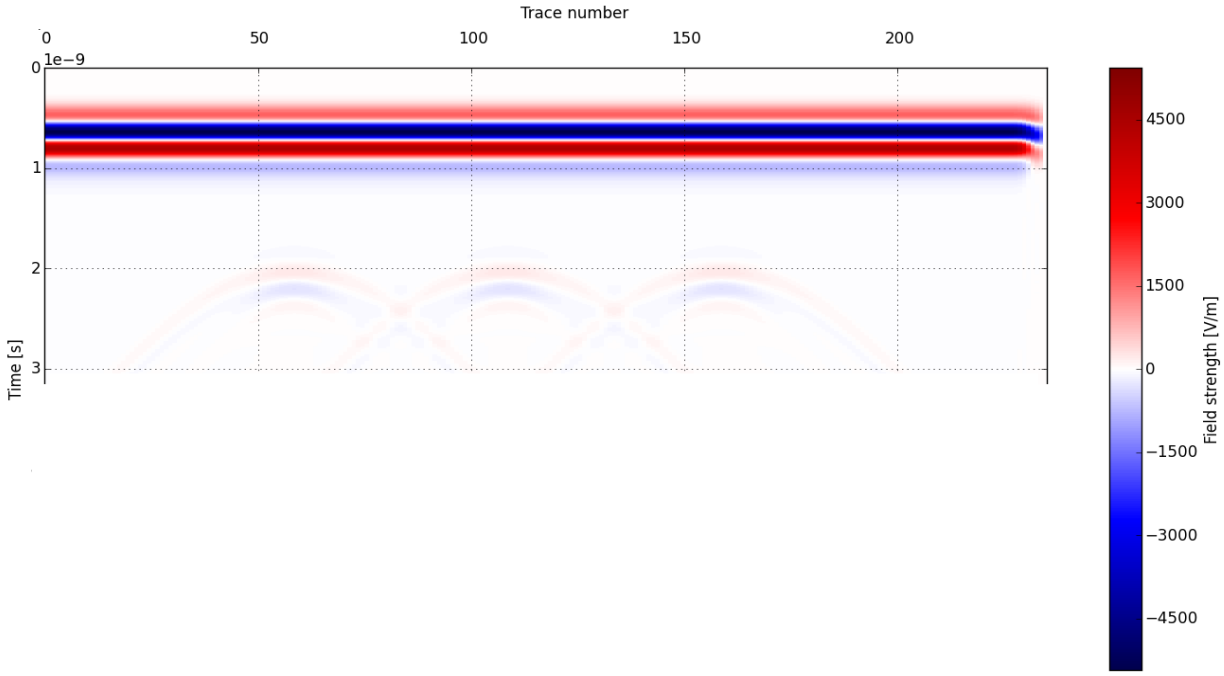

Figure 77. Model A - this GPR model was created with the following parameters: the soil has a permittivity value of 4.54 and the roots have a value of 15.3. The model is simulated with an antenna frequency of 1.5 GHz

For these models the soil was considered to be homogenous with the same value of permittivity throughout the environment and no other interferences, this way creating ideal environments which would help with understanding limitations in terms of hyperbolas, and their visibility in a variety of conditions related to water content of the soil, and different types of roots and soil.

4.2.3.1. GPR SYNTHETIC MODEL RESULTS

As expected, a significant permittivity contrast between the soil and the roots produces a detectable signal. In the figure 76, the soil has a permittivity value of 4.54 and the roots have a value of 15.3. The model is simulated with an antenna frequency of 1.5 GHz.

The same setup, but with a permittivity value of 26 for the roots (fig. 77), produces a very similar, but slightly more pronounced contrast.

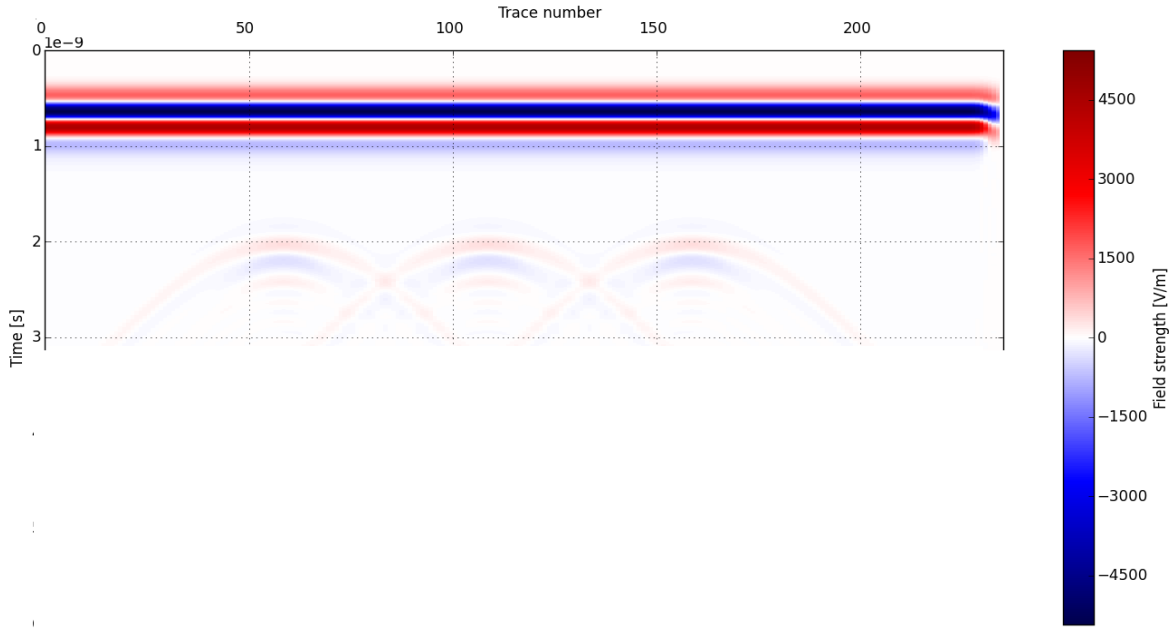

Figure 78. Model B - the GPR model which consists of a permittivity value for roots 26, uses a 1.5 GHz antenna and has a permittivity value of 4.54 for soil.

Meanwhile, the above-mentioned scenario (fig. 77), when simulated with a 4 GHz antenna instead (fig. 78), produces a different type of response. Already, this provides some useful information regarding the type of signal differences that can be expected with the two antennas.

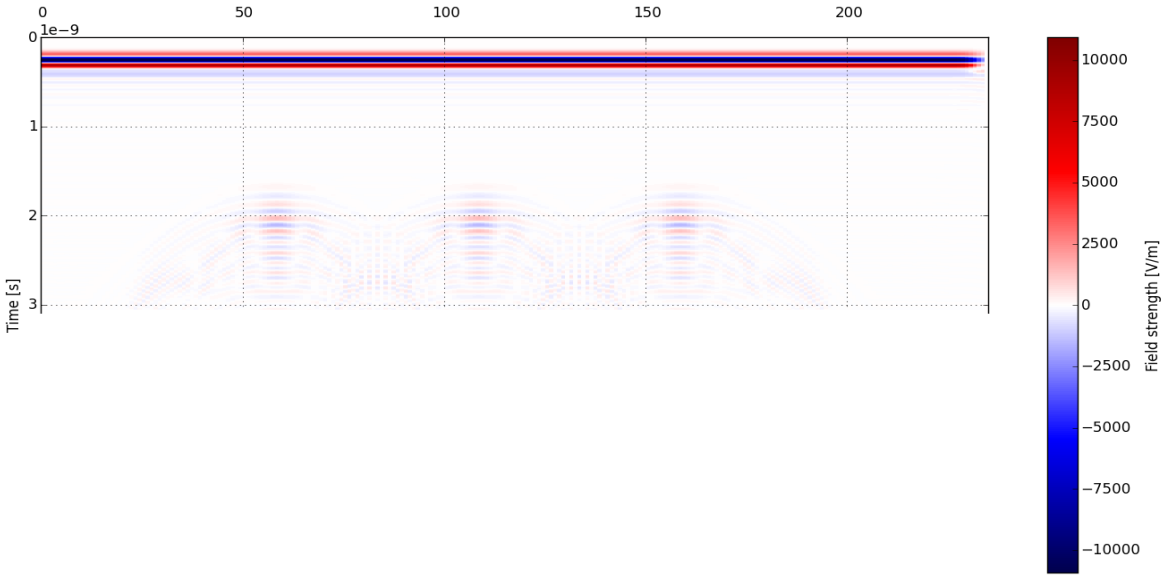

Figure 79. Model C - GPR model created with the following parameters: permittivity value for roots 26, 4 GHz antenna and 4.54 for soil.

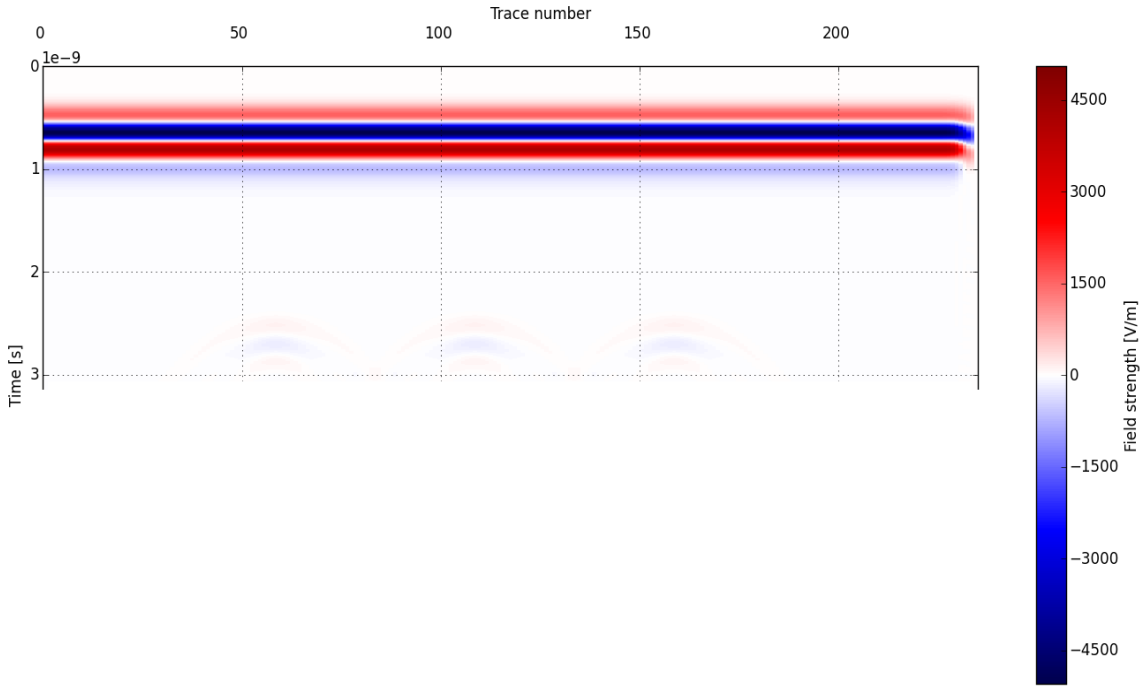

Figure 80. Model D - a soil unit with a permittivity value of 8 was simulated with a root with a permittivity value of 15 and a 1.5 GHz antenna.

However, as the permittivity contrast becomes less pronounced, the simulated signal becomes fainter. In the following figure (fig. 79), a soil unit with a permittivity value of 8 was simulated with a root with a permittivity value of 15. The signal is still detectable, but fainter.

The permittivity contrast is not the only aspect of interest though. A slightly stronger permittivity contrast (soil: 17.77; root: 26), but in a soil with higher permittivity, produces a fainter response (fig. 80) than in the above-mentioned situation (fig. 79).

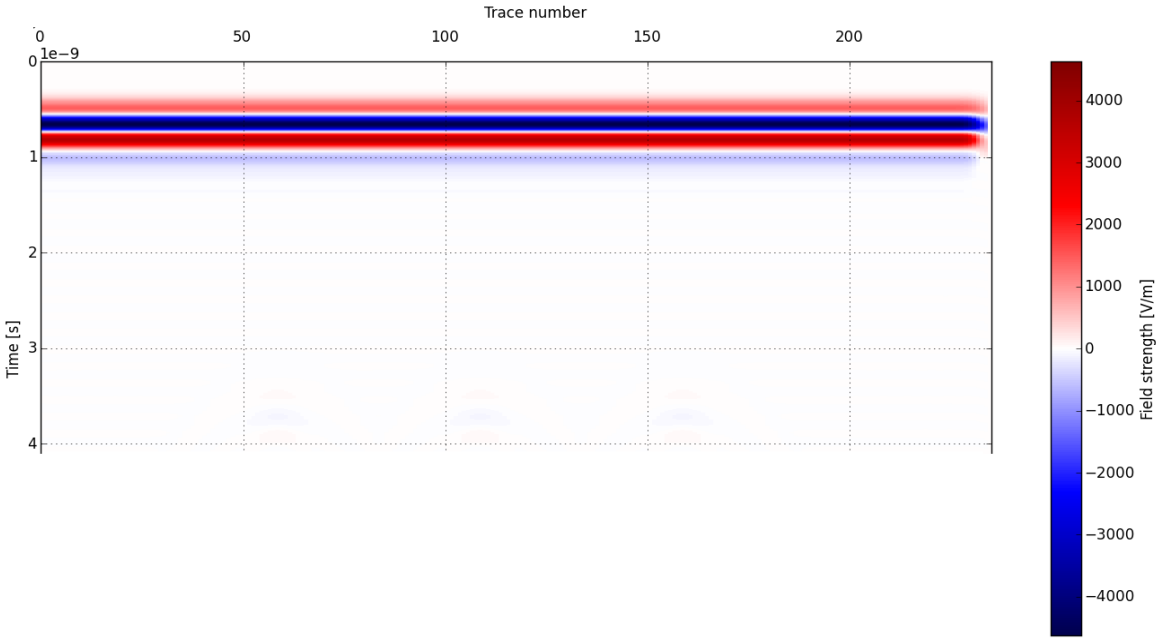

Figure 81. Model E - GPR model where the soil unit has a permittivity value of of 17.77, and a root value of 26 and a 1.5 GHz antenna.

As expected, when the permittivity contrast falls under a certain threshold, the objective may become undetectable. For instance, in the case of a soil unit with a permittivity of 17.77 and a root with a permittivity of 15, there is no detectable contrast. The following figure (fig. 81) is presented just as an illustration to that.

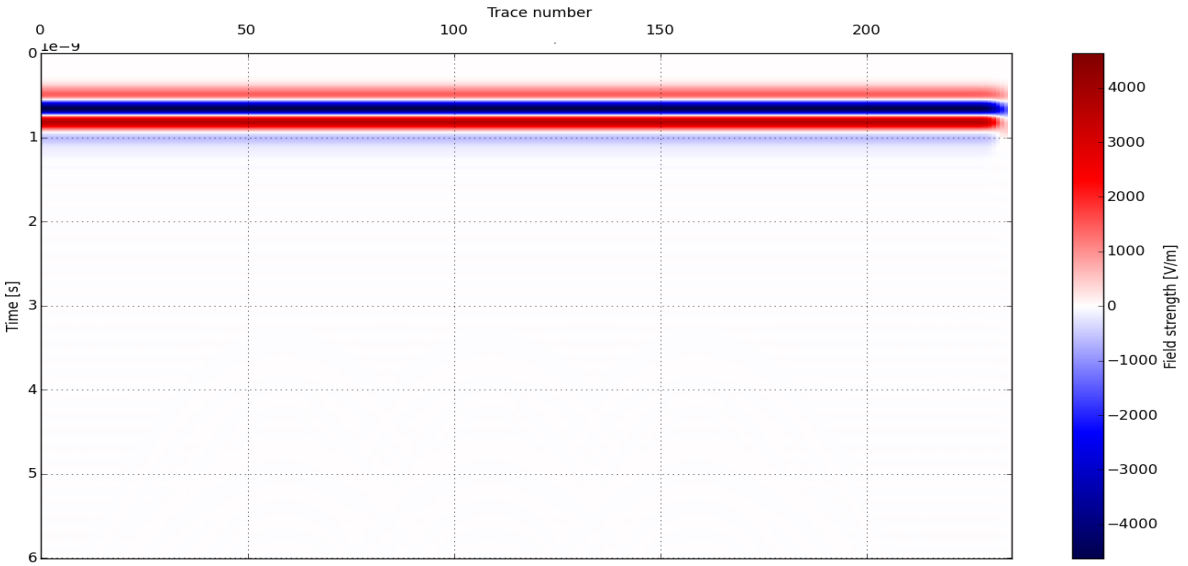

Figure 82. Model F - a GPR model consisting of a soil unit with a permittivity value of 17.77 and root permittivity value of 15. Model created with the 1.5 GHz antenna.

Figure 83. Model G - Soil permittivity value of 4.44 and a root permittivity value of 15, before and after adding noise, with a 1.5 GHz antenna

However, it should be noted that these are ideal cases, far from what can be expected from real life data. To make this data more realistic, the models were migrated from gprMax to

SegY format, which can be read and processed in ReflexW to image radargrams and to get them closer to radargrams resulted from surveys (fig. 82 -83). The following figure (fig. 82) presents such a case, with a soil permittivity value of 4.44 and a root permittivity value of 15, before and after adding noise, with a 1.5 GHz antenna, in the exact same domain box as above (fig. 81).

Several representative situations were simulated, to assess the type of GPR response that would be expected (in an ideal scenario), and to visualize the limitations of the method. Less emphasis was placed on cases where a strong contrast was evident (for instance, in the case of a root permittivity of 68, which may not even be realistic in some scenarios), and more focus was placed on situations where the contrast was not as pronounced, as is the above-mentioned case of the above-mentioned situation with a soil with a permittivity of 17.77 and a root of permittivity 26.2 (fig. 83). The contrast, faint in the raw model, can be accentuated and gained in ReflexW.

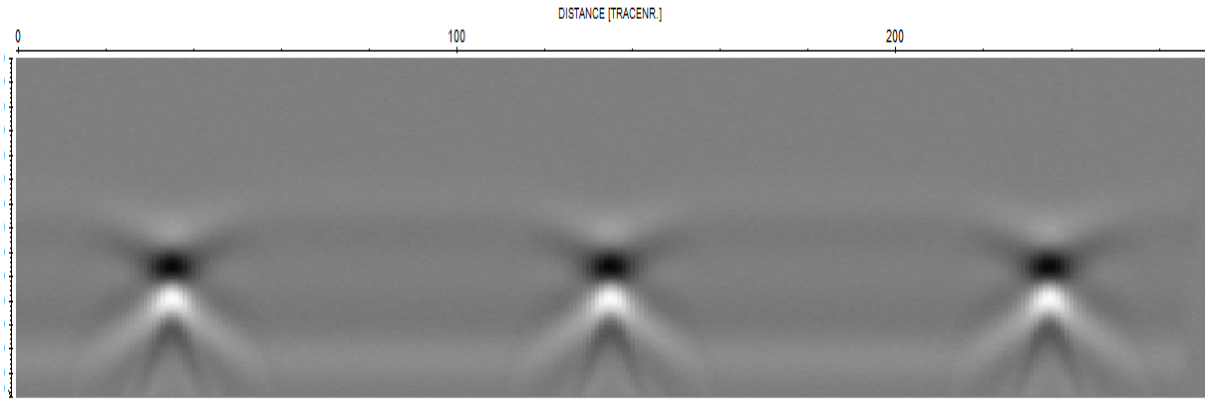

Figure 84. Model H - soil with a permittivity of 17.77 and a root of permittivity 26.2 and a 1.5 GHz antenna.

4.3. RESISTIVITY DATA

In the following section, the resistivity data will be presented from both indoor and outdoor surveys, with experimental equipment and with manual surveys, and also with different types of soils, conditions, including the transparent soil. At the end, synthetic models will be presented.

4.3.1. RESISTIVITY - OUTDOOR SURVEYS

The rationale behind the choice for this site is represented by the nature of the environment and the type and character of the plants growing in it. As one of the challenges and scopes of this thesis was to understand the limitations of resistivity method for detecting and analysing the roots of the plants in agricultural environments, this site posed potential for providing some answers to this challenge.

The outdoor resistivity surveys were carried out in a corn (*Zea Mays*) field and in a cabbage (*Brassica oleracea var. capitata*) field, in a real world agricultural environment. Both sites share similarities in terms of equipment used, but they share different aspects, besides the type of the plant, related to the surface roughness and the moisture content. The cabbage field was recently irrigated compared to the corn field soil which was a lot drier, for example, but their particularities will be described in the following chapters.

4.3.1.1. CABBAGE FIELD

The site represents a real agricultural environment, with uneven surfaces, irrigation system, soil has been subject to agricultural practices (ploughing, levelling, manuring, etc.), and cabbages (*Brassica oleracea var. capitata*) represent agricultural plants. As the cabbage plants in this field are quite young (fig. 84), at about 3-4 weeks from seeding, their root system will be represented by the developing roots, fine and sap absorbing roots with low resistivity. The electrodes used for this survey were made of thick copper wires, chosen for their easy availability and the good conductive properties of the material.

Figure 85. Image showing surveying with the resistivity method in a young cabbage field.

The nominal distance between the electrodes was set to be 5 cm (fig. 84). The number of profiles measured was 6 in total; with 3 on one side of the plants and another 3 the other side of

the plants row. The profile included 3 cabbage plants found at 7, 57 and 100 cm on the measured resistivity profile. The data was collected using the RM Frobisher equipment and was processed with Res2DINV and ResIPy following the standard protocol for preparing the files in the format necessary for each specific software.

4.3.1.1.1. CABBAGE FIELD SITE RESULTS

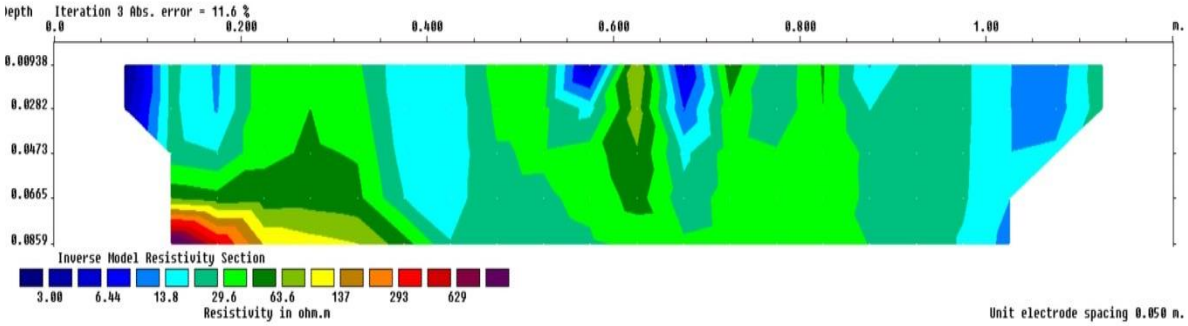

Figure 86. Cabbage field profile 1 processed with Res2DINV, using the Wenner array. This represents the profile furthest away from the plants

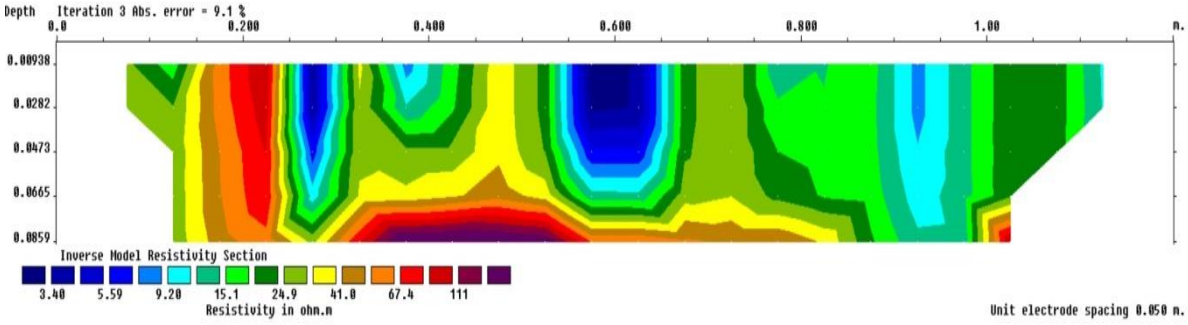

Figure 87. Cabbage field profile 2 processed with Res2DINV, using the Wenner array.

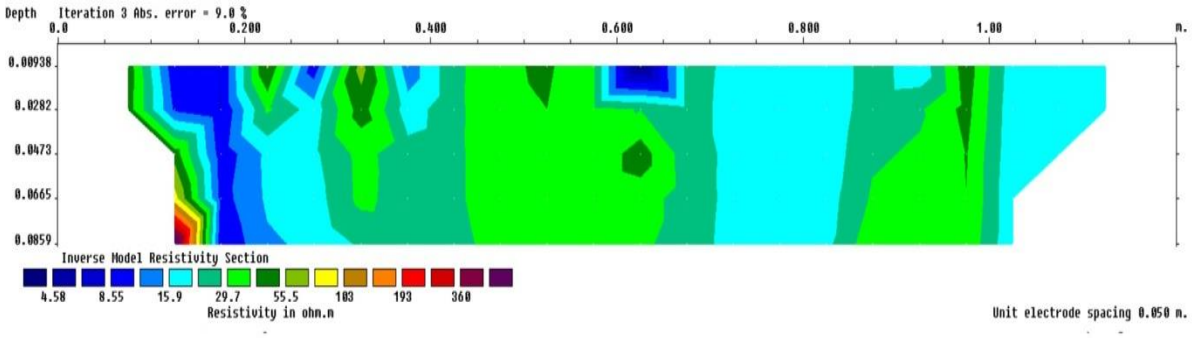

Figure 88. Cabbage field profile 3 processed with Res2DINV. This represents the profile closest to the plants.

It can be observed from the data, especially in the Res2DINV data with lower resistivity values corresponding to the position of the plants (fig. 85-87). As the plant have been recently watered, it is possible that the other similar lower resistivity values to correspond to patches of water or higher moisture content unevenly spread.

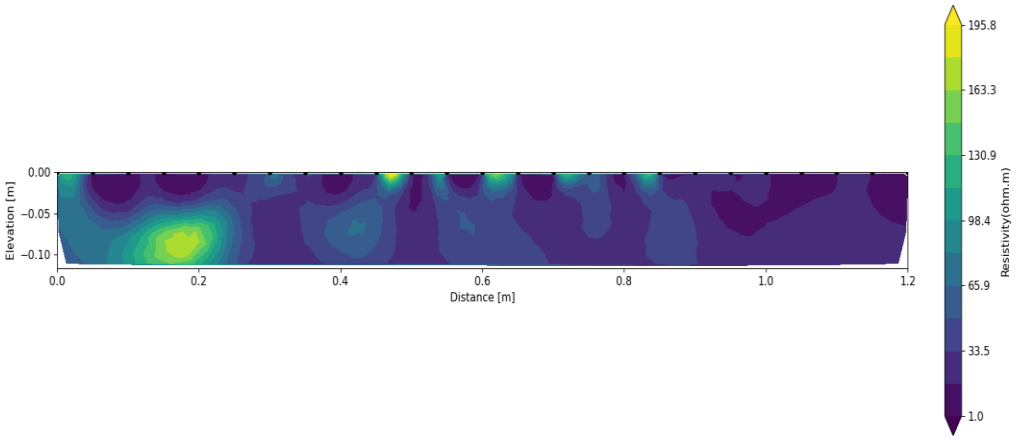

Figure 89. Cabbage field profile 1 processed with ResIPy. This represents the profile furthest away from the plants.

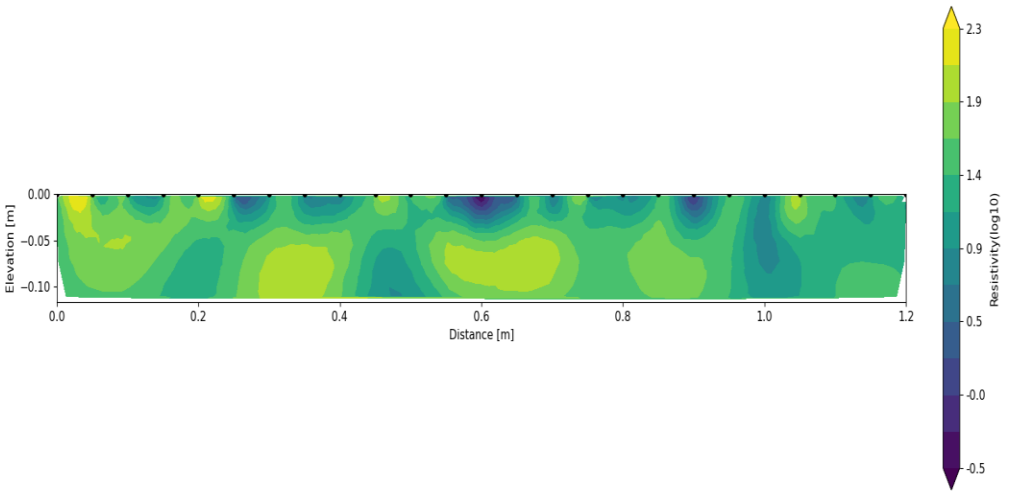

Figure 90. Cabbage field profile 2 processed with ResIPy.

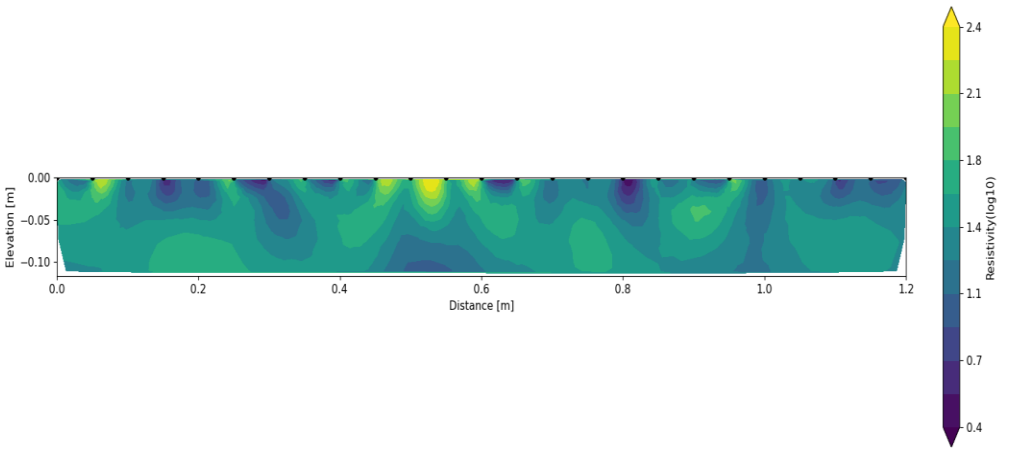

Figure 91. Cabbage field profile 3 processed with ResIPy. This represents the profile closest to the plants.

The data processed with ResiPy (fig. 88-90) look a bit different compared to the data processed in RES2DINV. For two of the profiles the logarithmic scale was chosen to

represent the resistivity section, as it allows for a better representation of the contrasts. It is noticeable that the ResIPy data is able to highlight more contrasts especially in the first level, top 5 cm (fig. 88-90), which are not as visible in the Res2DINV data (fig. 85-87). Even though it is much difficult to correlate the data with position of the plants, for example in profile 1 (fig. 88) the appear some features at 1 m which has a lower resistivity, but the effect from the electrodes seems more prominent in the fine mesh chosen for the inversion model of ResIPy to process the data, compared to the data from Res2DINV.

4.2.1.2. CORN FIELD

The second field trial was represented by surveys carried out in a corn *(Zea Mays)* field, with very young plants at around 2-3 months old (fig. 91). The field was not recently irrigated and the surface of the soil was much rougher compared to the previous field. Digging was possible at the site and the depth at which the root is placed was observed and noted.

The profiles covered 3 plants on a row and the method used is similar to the method used for the field trial 1. Three profiles were measured on each side of the corn row and the method consisted of an ERT with a Wenner array. The same copper electrodes were used. Compared to the previous site which had a more even surface and the area was irrigated constantly, this site had specifications representative of agricultural fields. Due to ploughing the surface consisted of many irregularities in the surface and the irrigation was scarce which made the insertion of the electrodes very difficult. Due to the nature of the electrode material, it was very easy for them to bend when inserted in this type of soil.

Figure 92. Measuring the root area of the plant in the corn field, after the survey.

Because the area was not as irrigated as the first site, lots of cracks existed in the soil due to drought; this made the contact between the soil and the electrodes very difficult. These factors affected the precision of the measurements by increasing or decreasing the distance between the electrodes which was set to be 5 cm.

4.2.1.2.1. CORN FIELD SITE RESULTS AND GENERAL REMARKS

The resistivity data from the corn field correlates very well with the position of the plants, which are positioned at 23, 68 and 105 cm (fig. 93).

A 3D interpolation was attempted for this site, which used all the 3 profiles to create an inversion model from which horizontal slices were cut at different depths (fig. 92). It can be observed from the slices that in the first layer there is a lot of variation in terms of resistivity.

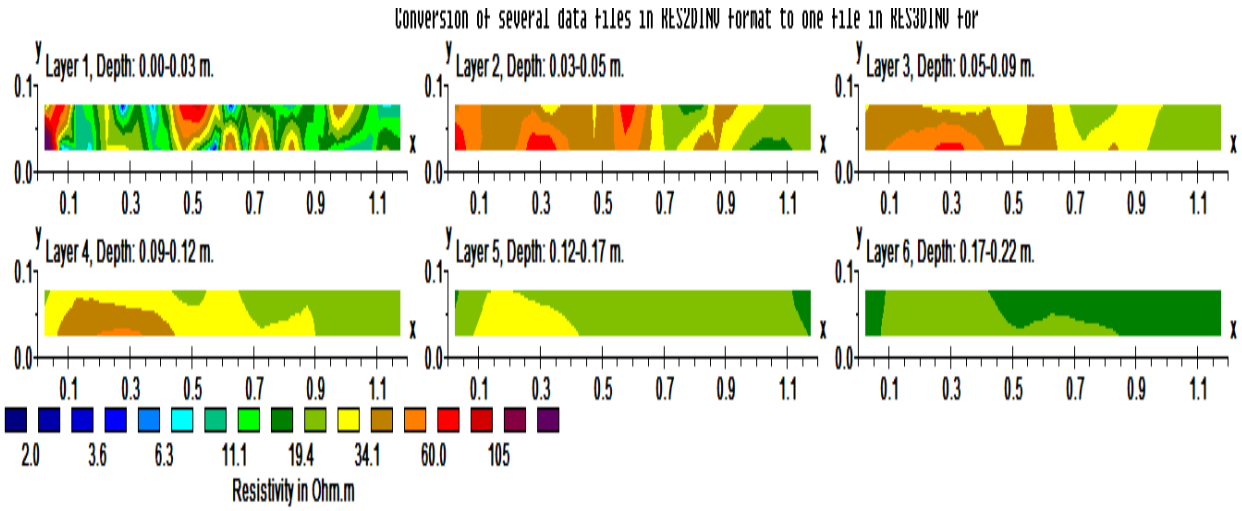

Figure 93 The image represent slices at different depths resulted from the interpolation of all the 3 profiles.

Figure 94. Image representing the position of the plants and the length of the profile measured using a measuring tape.

As it goes deeper from approximately 5 cm it can be observed that there are some higher resistivity values in the left side of the profile however there is another high resistivity area appearing in the left side close to the position of the 3rd plant (fig. 92).

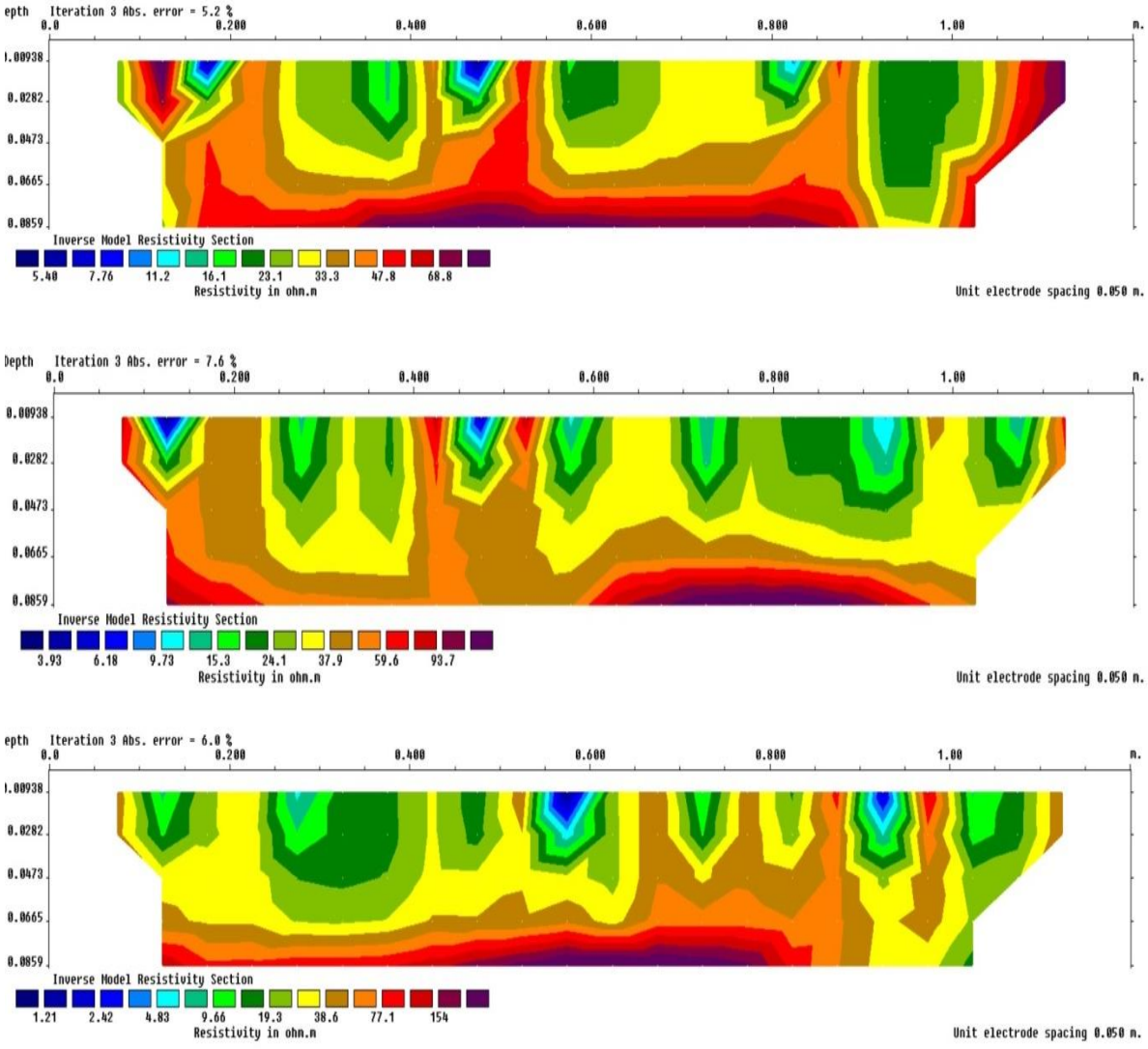

Figure 95. From up to bottom, profiles 1, 2 and 3 processed with Res2DInv. Profile no. 1 is the closest to the plants.

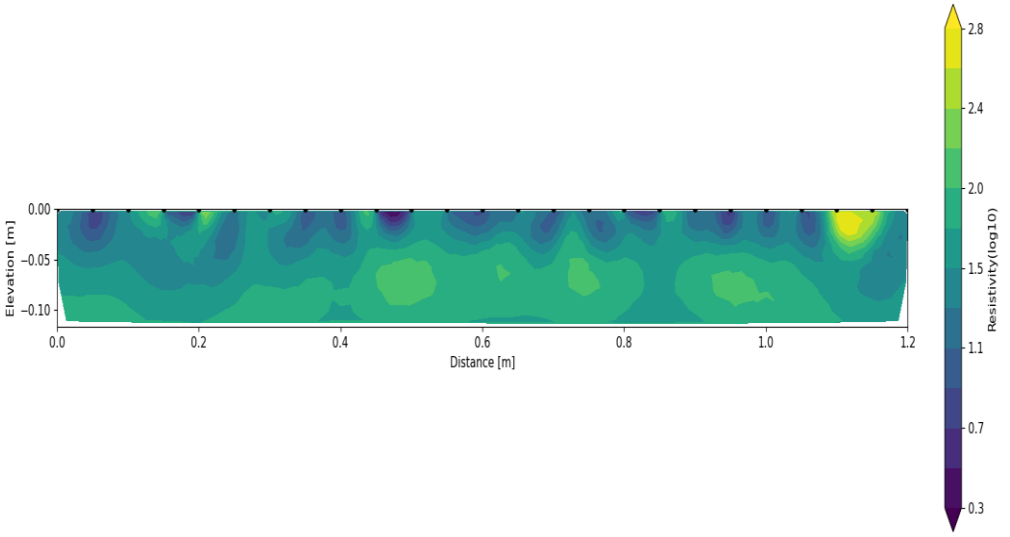

Figure 96. Corn field profile 1 processed with ResIPy. This represents the the profile closest to the plants.

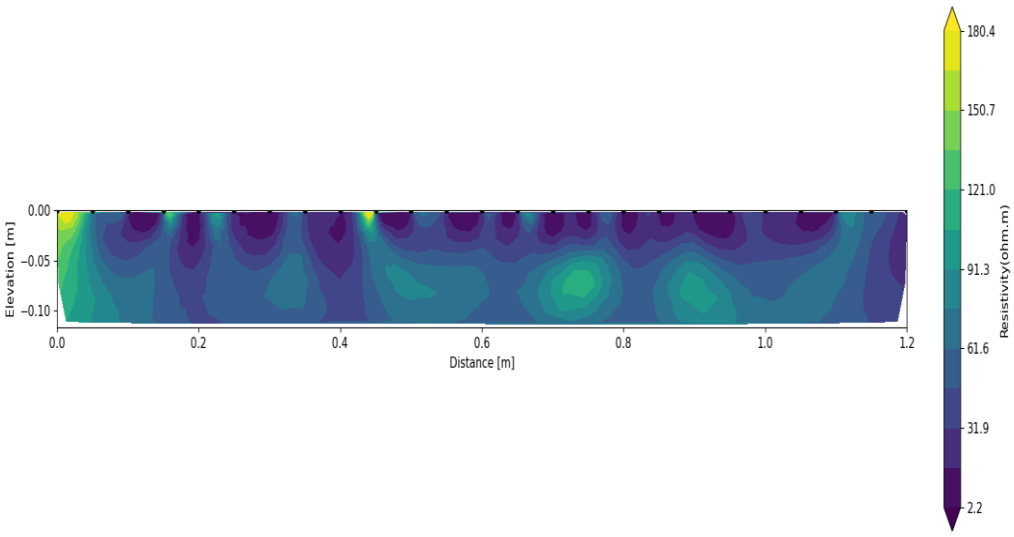

Figure 97. Corn field profile 2 processed with ResIPy.

It appears that in this situation the plants would correlate more to the resistive areas according to the data from the Res2DINV (fig. 94) whereas the data processed with ResIPy (fig. 95-97) is harder to interpret as the anomalies from the top surface appear much stronger.

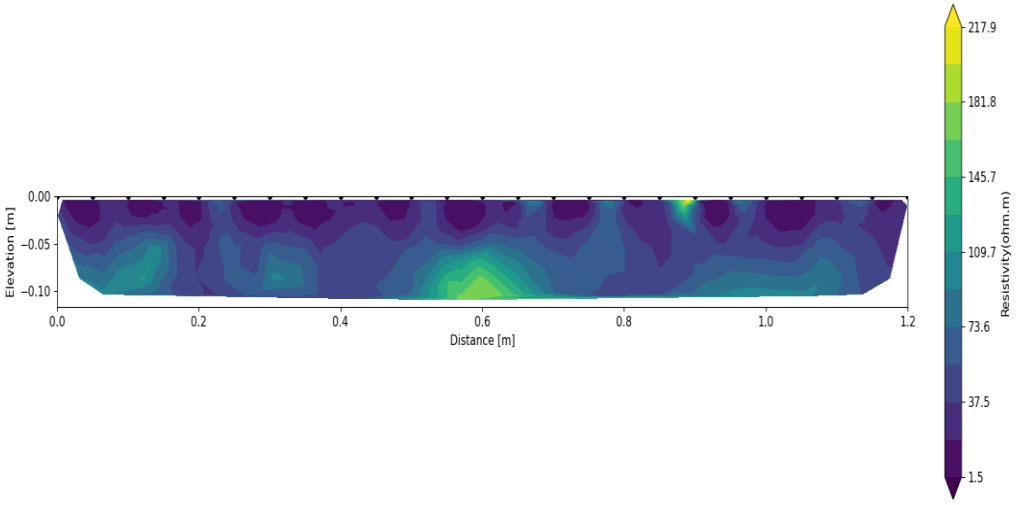

Figure 98. Corn field profile 3 processed with ResIPy. This represents the the profile furthest to the plants.

These observations are interesting, from both fields, as it is possible to explain the findings as, roots appearing more conductive than the surrounding environment when the plants have been recently watered, as they might hold more water for longer period of time compared to the surrounding area, as observed with the cabbage plants in the previous surveys. Higher resistivity areas correlate with the plants' position in the corn field which has not been

watered which is close to the findings of Amato (2009), when the soil with high root content presented much larger resistivity values compared to the bare soil.

Due to the soils being porous, from the point of view of the resistivity method, the resistivity values of most soils are dependent on the water and other solutions or materials that are filling up the pores (Reynolds, 2011). Therefore it is possible in this case that the roots are filling up space inside the soil and are making the area around them more resistive compared to the surrounding material.

4.2.1.3. DAFFODILS - WITH PROTOTYPE EQUIPMENT

For this experiment a prototype equipment which is described in chapter 3.5.2.2. was used for collecting resistivity data.

The survey carried out with the electrical resistivity prototype (fig. 98) took place in the University of Birmingham garden's during spring time when the daffodils were blooming. The plants were chosen based on the fact that they were in a natural environment but also because they come really close to plants from the agricultural sector. The 16 electrodes used were made of copper and had a length of 1 m with a diameter of 1 cm, and the distance between the electrodes was of 15cm (fig. 99). The position of the survey was chosen as to have both an area with plant roots from the daffodils and to have a plain normal area only covered with grass. Choosing this type of setting was made based on the decision to see a contrast between the area with plants and the area with no plants. This way it should allow to

highlight the plant root area of the plants and increase the certainty of their appearance in the resistivity section.

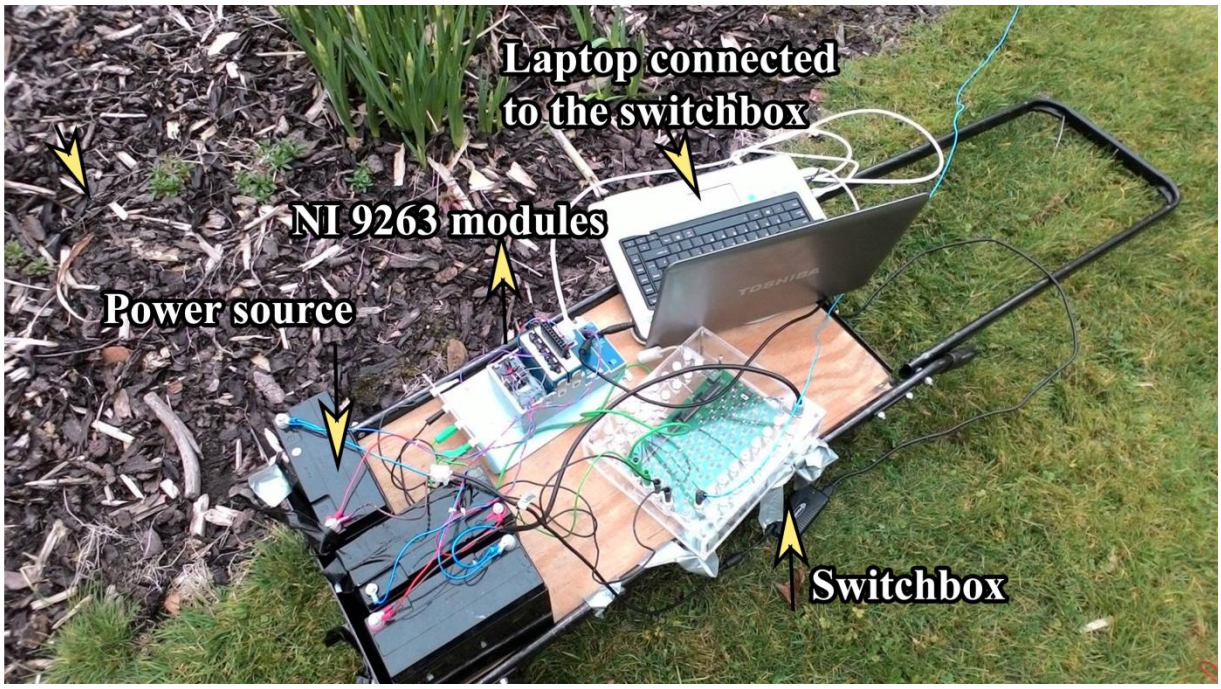

Figure 99. The prototype equipment can be seen in the image, with the laptop, switch box, chassis and batteries.

The profile had a length of 2.25 m and the plants appear at the 1.34 m, 1.85 m and 2.2 m on the tape (fig. 99). Knowing the exact position of the plants on the profile allows for better correlation of the anomalies with the plant root position.

After the survey was finished, some digging was carried really close to the plants in order to understand the stratification, depth of the roots and physical parameters, like colour and root content or soil content.

Figure 100. Example of resistivity survey with the electrical resistivity prototype.

4.2.1.3.1. RESISTIVITY PROTOTYPE SURVEY RESULTS

The observations made were: the depth of the daffodil bulb was at a depth of 14.5 cm; the grass layer at the top of the soil had a thickness of 4 cm and appeard very humid; the top 15 cm of the soil appear as containing a high level of organic matter including worms, roots and other types of insects.

The electrode arrays used in this survey are represented by Wenner array (fig. 101), dipole-dipole (fig. 100) and a new experimental configuration which is similar to dipole-dipole, but measuring all the possible combination in the dipole-dipole style (fig. 102).

The data was processed using the BERT software and it was displayed using ParaView.

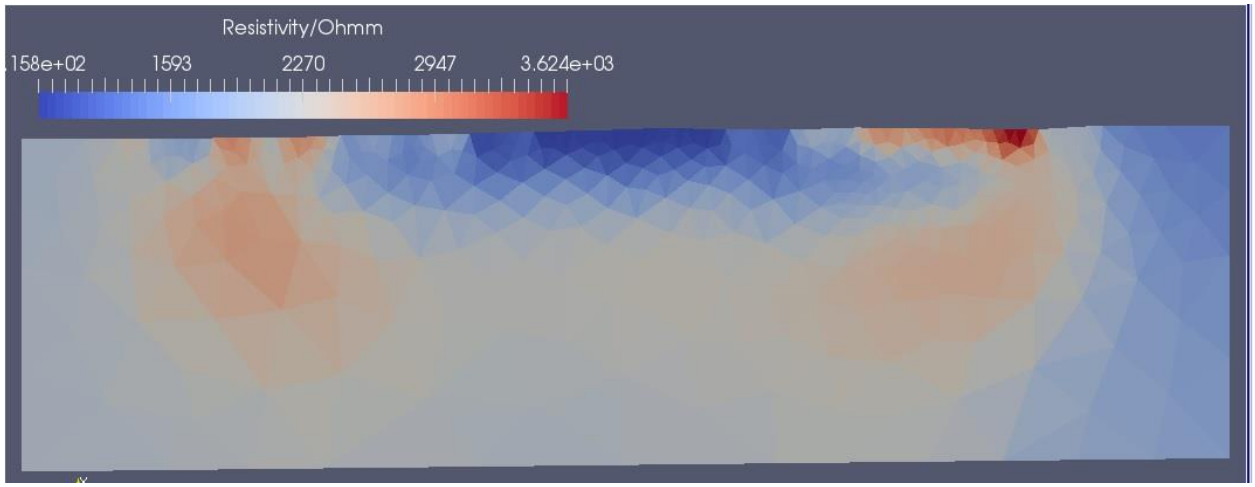

Figure 101. Represents the dipole-dipole array inversed data.

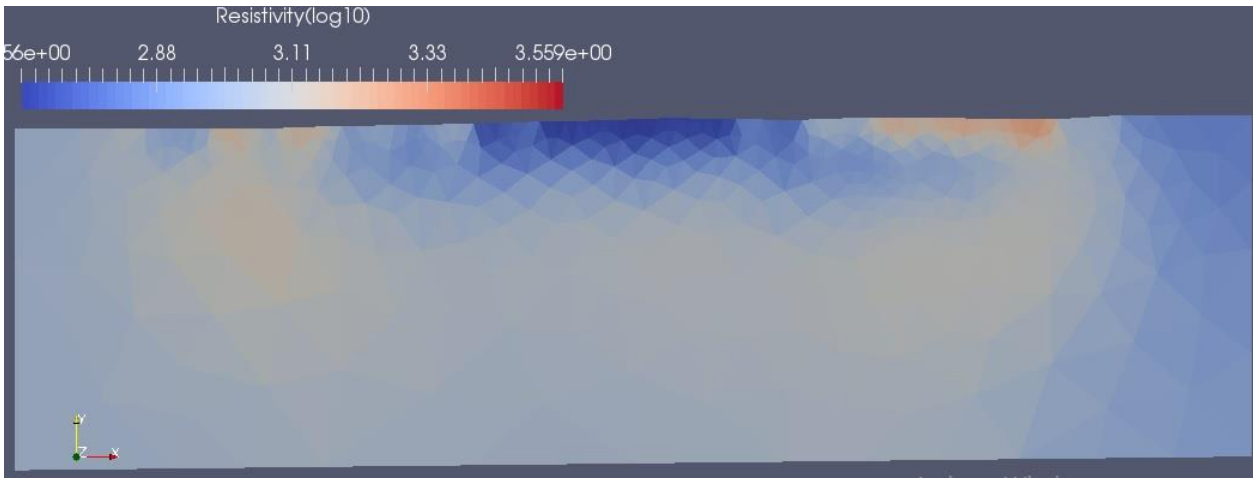

Figure 102. Represents the inversed data for the Wenner array.

The data processing was carried for all the 3 types of arrays used in the survey. The dipole array profile (fig. 100) is characterized by high resistive data on the right side of the image compared to the left side which is characterized by low resistivity values. The Wenner (fig. 101) and dipole-dipole array look very similar in shape, and position of the anomalies with the difference that in the dipole-dipole profile the anomalies look significantly stronger.

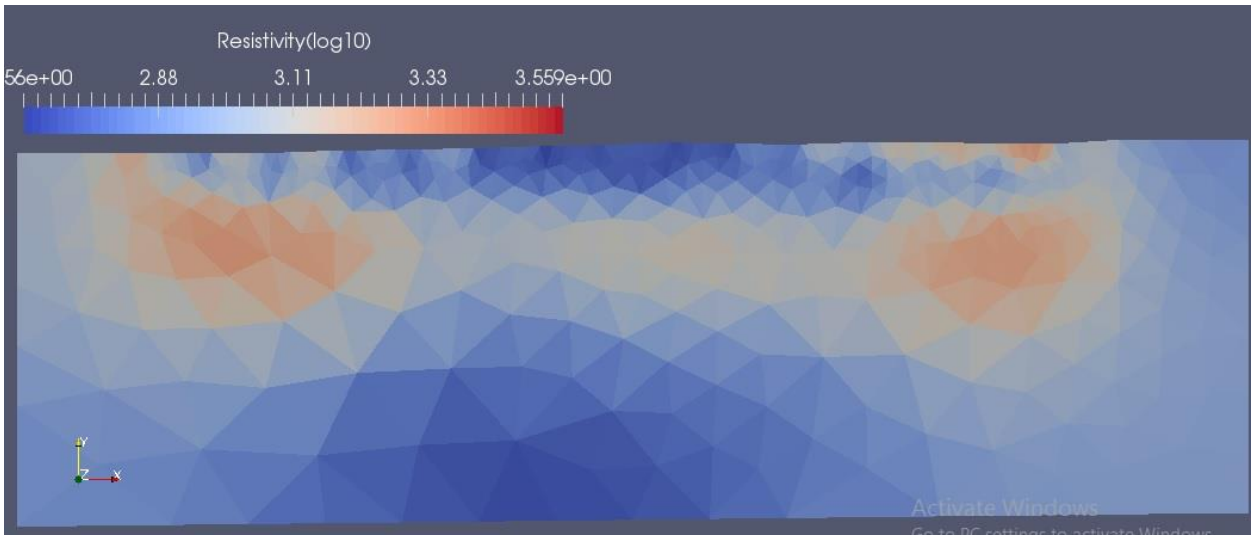

Figure 103. Represents the experimental dipole-dipole inversed data.

The experimental profile on the other hand, even though continues with the same pattern of anomalies, looks more detailed. What the experimental profile has different than the other two profiles, is the fact that it is a possibility that the electrodes effect to be visible as well very close to the surface.

4.3.2. RESISTVITITY - INDOOR SURVEYS

The arrays used for the large plastic boxes, consisted of the classical Wenner, Wenner-Schlumberger and Dipole-Dipole, but having the ability to modify the code with specific arrays, an optimized type of array was also used.(Schwartz, Schreiber and Yan, 2008; Loke, Wilkinson and Chambers, 2010). The positions of the plants in the box are at 18, 38 and 58 cm or in terms of relating them to the position of the electrodes, the plants are positioned as

follows: the first plant is between electrodes 4-5, Second plant between electrodes 8-9 and the third plant between electrodes 12-13.

4.3.2.1. RESISTIVITY – INDOOR SETTING NO. 2 CONTAINER

The following 2 surveys are carried in the container with soil type 2 (very loamy-peaty, high organic material content) in which the 3 tomato plants have grown the setting is covered in full detail in chapter 3.4.1.2. From left to write, the first two plants are still healthy but the third plant has died. After the surveys were carried, the plants were removed from the boxes in order to see the differences between the roots. The roots of the first two living plants, are still quite fine, very moist, and very fragile. The extent of the roots was very difficult to follow, as the thin tomato roots were breaking very easily. It has been observed however that there existed a more concentrated area close to the tip of the main root. The third plant, which has died, showed a difference in root texture. The roots seemed much woodier, and drier than and not as fine as the roots of the still living plants.

4.3.2.1.1. INDOOR SETTING NO. 2 RESISTIVITY SURVEY RESULTS

While the position of the roots might not be exact, compared to the surveys in transparent soil where the exact position of the roots and depth is known, the position of the plants is fixed. The second set of surveys was carried at about 24 hours after watering the plants with fertilizer and 3L of water. The fertilizers consisted of: Ccompound fluit fertilizer NPK 2-2.5-

4.5, Nitrogen total (N): 2.0%, Phosphorus pentoxide (P2O5) total: 2.5%, Potassium oxide (K2O) total: 4.5%.

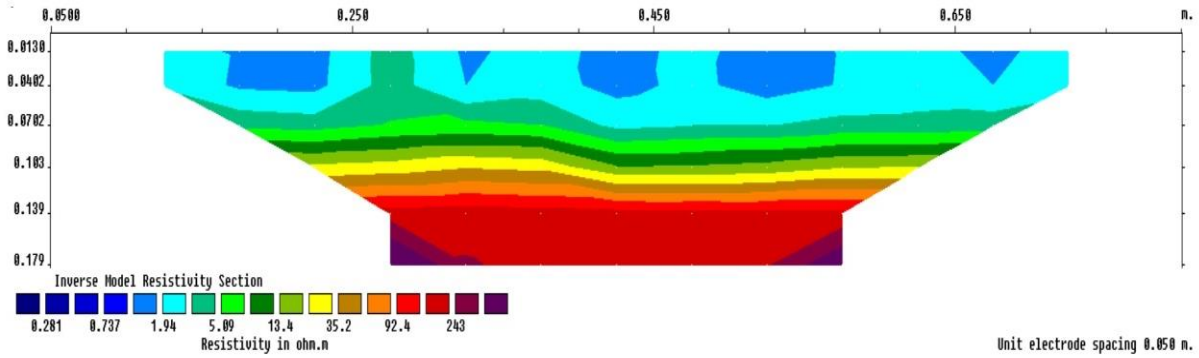

Figure 104. Image representing profile no. 3 with Schlumberger array and processed with Res2DINV. The survey was conducted before adding water.

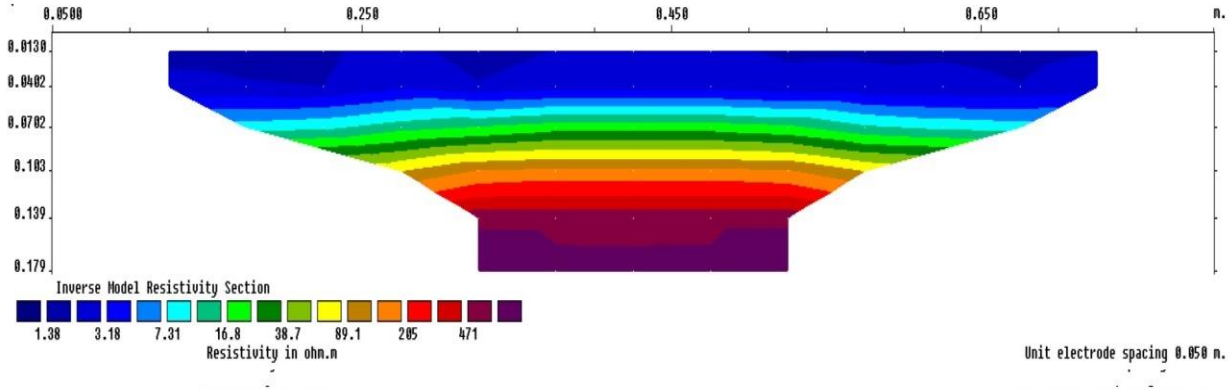

Figure 105. Image represents profile no. 3 with Wenner array and processed with Res2DINv.The survey was conducted before adding water.

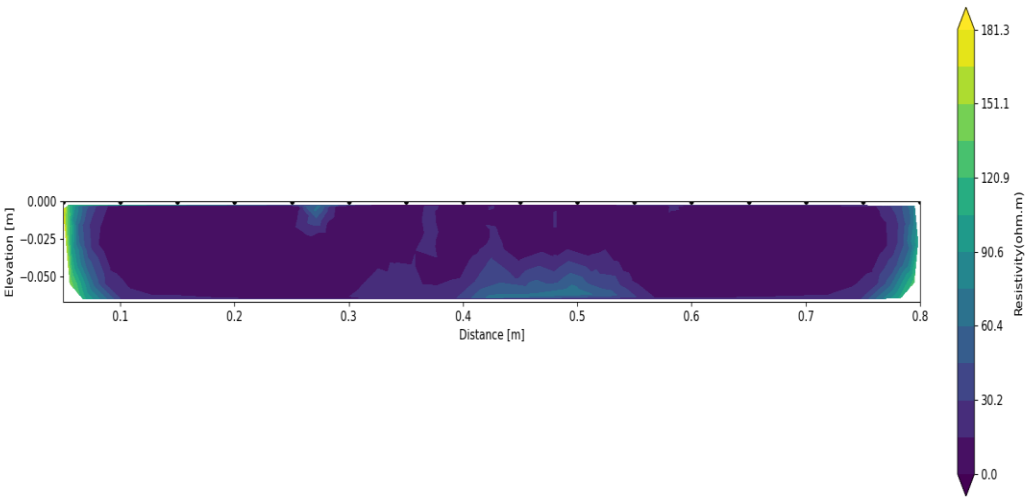

Figure 106. Profile no. 3 with the Wenner array processed with ResIPy. The survey was conducted before adding water.

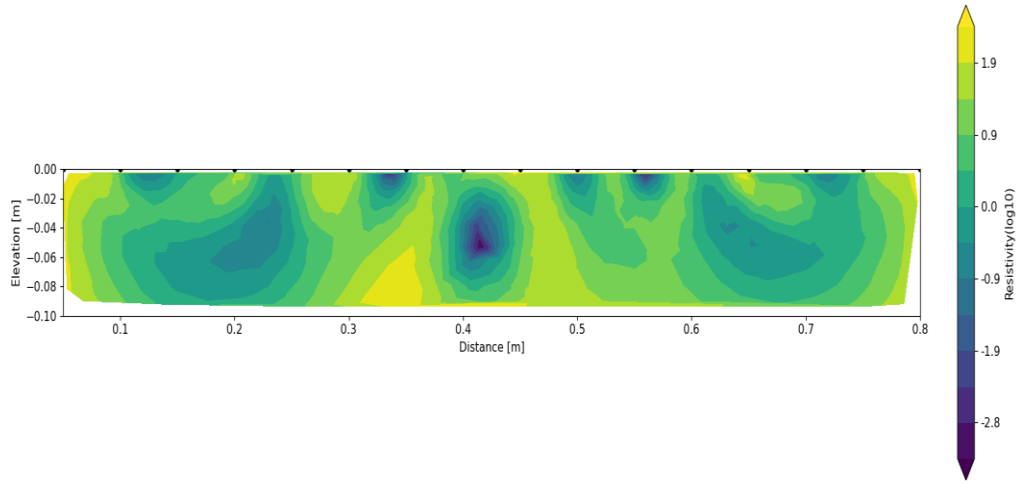

Figure 107. Profile no.3 with the Schlumberger array, using a logarithmic scale to visualize the data. The survey was conducted before adding water. Using a linear (non-logarithmic) scale to visualize the data.

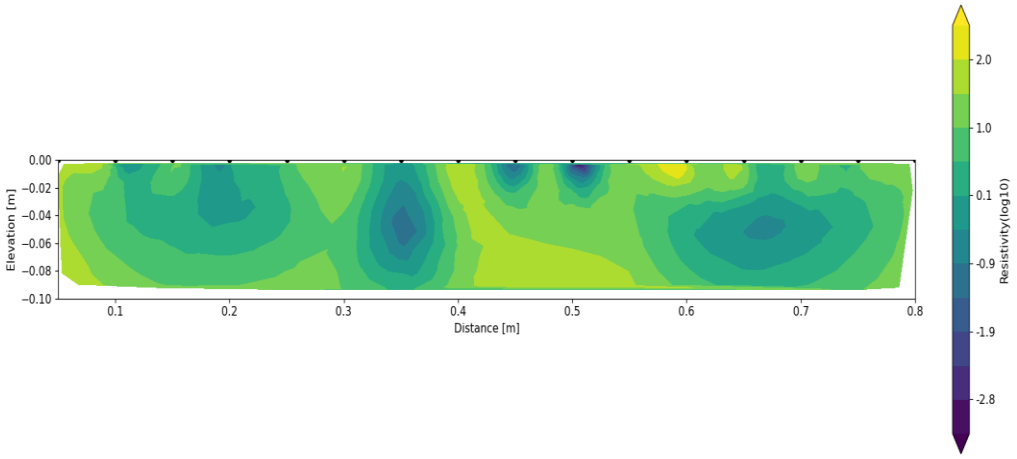

Figure 108. Profile no. 3 with Schlumberger array after watering the plants, processed with ResIPy. Using a logarithmic scale for visualizing the data.

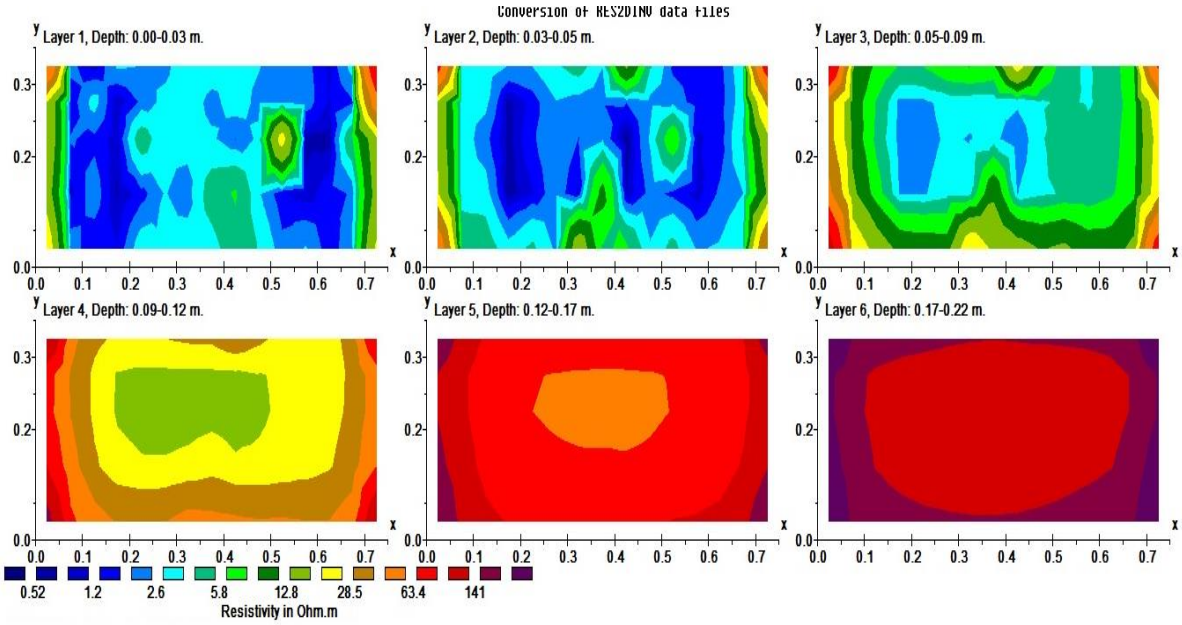

Figure 109. Image representing the horizontal slices resulted from the interpolation of all the 6 profiles with Schlumberger array. Survey carried out after the plants have been watered.

It can be observed in layer 3 (fig.108), a the 0.05-0.09 depth, 3 areas appearing in the central and left side, which seem to have lower resistivity values, whereas the anomaly on the right side, even though the values are still low compared to the surrounding environment, it presents higher resistivity values compared to the middle and left side.

At greater depths, in layer 4 (fig.108), due to the reduced number of data points with depth given by the Schlumberger array, there still seem to be an area in the middle with low resistivity values, which appears to be dominant in the central and left side but not on the right side. The anomaly seems to be connected this time which is probably due to the reduced data points in the area. The area on the right side still presents values of resistivity compared to the middle and left side.

At deeper levels, as the data points are decreasing even more, there is no more reliable information below 12 cm.

The information from layer 3 and 4 can be explained such as that, after the plants have been watered, even though time was allowed for the water to drain, the root area of the plants seems to be holding more moisture around it, therefore reducing the resistivity values in the soil in that particular area. This is an aspect similar to what has been observed in the data from the outdoor surveys in the agricultural fields.

The anomalies on the right side of the horizontal sections, appearing with higher resistivity values, but still lower compared to the surrounding environment, might be explained by the delayed drainage in the area caused by the roots, as the roots might still be able to hold some moisture in the area.

However, these represent just some of the data from the numerous surveys that were carried out in the box with 3 plants, and after a thorough analysis part of the data has been removed as inconclusive and part of the data has not been presented due to the redundancy in the results throughout multiple surveys.

4.3.2.2. TRANSPARENT SOIL CONTAINER RESISTIVTY SURVEYS

The surveys in the box containing transparent soil are presented below, as several surveys were conducted using two different types of plants with different roots.

4.3.2.2.1. SPRING ONION PLANTS SURVEYS AND RESULTS

The next survey consisted of the same transparent container as the previously described, only the plants changed (fig. 109 - 110). No fertilizer was added to the gel solution. Being able to see the exact location of the buried part of the plant area and where the positions of the roots are, the survey design was changed. Due to these factors, another profile was set going right through the middle of the box but also getting very close to the roots up to a point where the actual roots of the spring onion plants were between electrodes.

As can be seen in figure 111, the position of the plant root area is visible, especially the bulb area, whereas the white fine roots don’t appear as clear in the image. The roots appear in the top 10 cm of the transparent soil. The surveys were carried using the array_slayer_g software on the tablet connected to the switchbox.

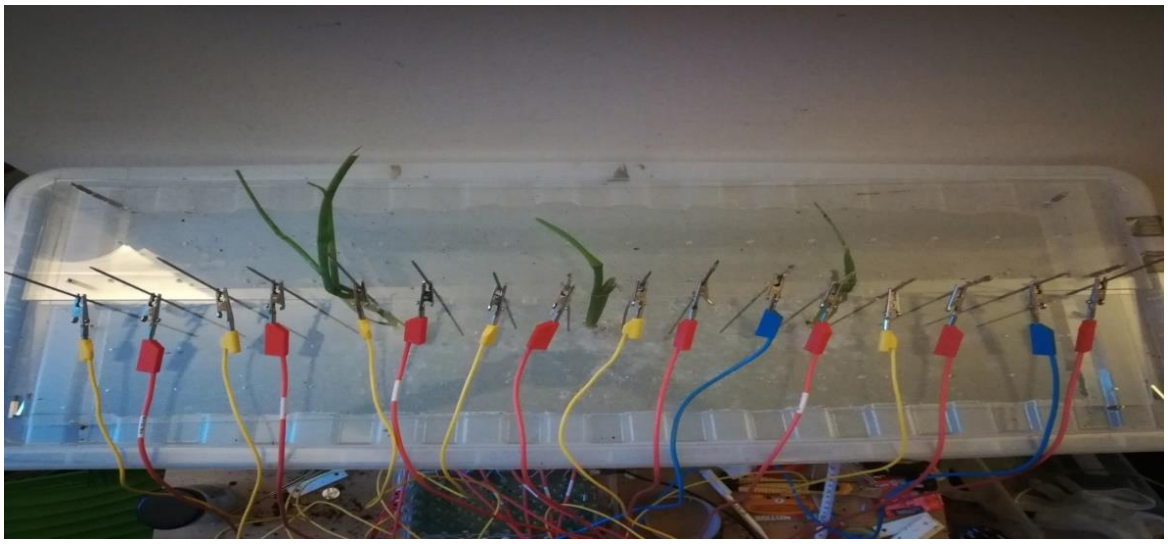

Figure 110. The above image represents the profile in the middle of the box right on the line of the plants. Survey from the box with transparent soil and spring onion plants.

Figure 111. Left - The green onion plant roots used in the transparent box. Right, the green onion plants, which were planted in the transparent gel box, and the visibility of the roots through the gel.

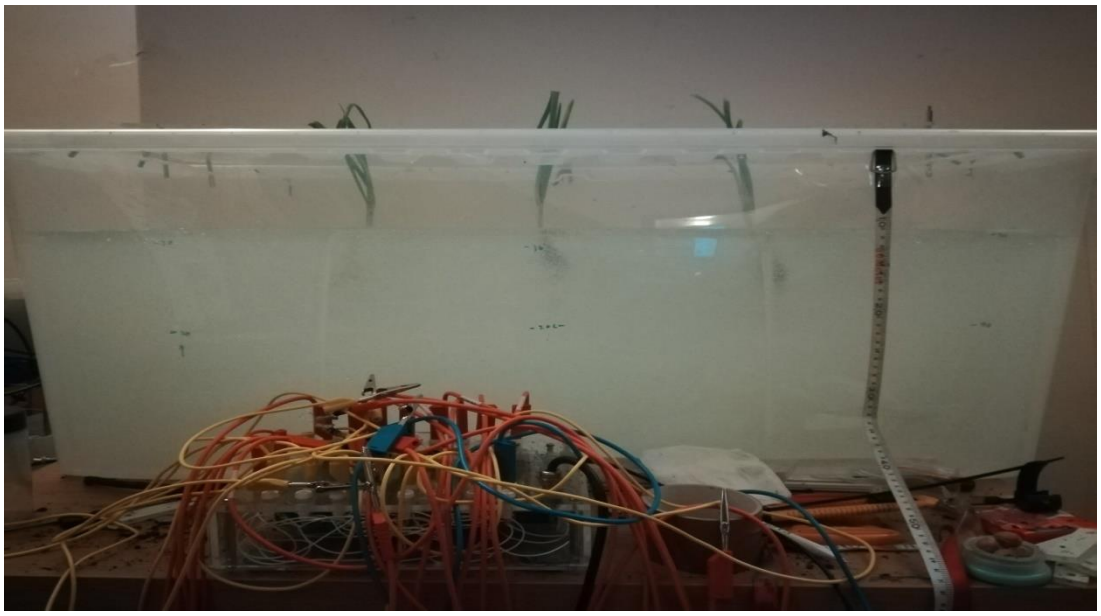

Figure 112. the lateral view of the transparent soil box with the green onion plants.

A number of 3 profiles were surveyed, with the first profile in line with the roots, and the other two profiles on each side of the middle profile at a distance of 2.5cm. The number of electrodes used is 16 at a distance of 5 cm in-between.

The arrays used were: Dipole-Dipole, Wenner, Schlumberger and Optimized array. The data processing was carried using the RES2DINV software.

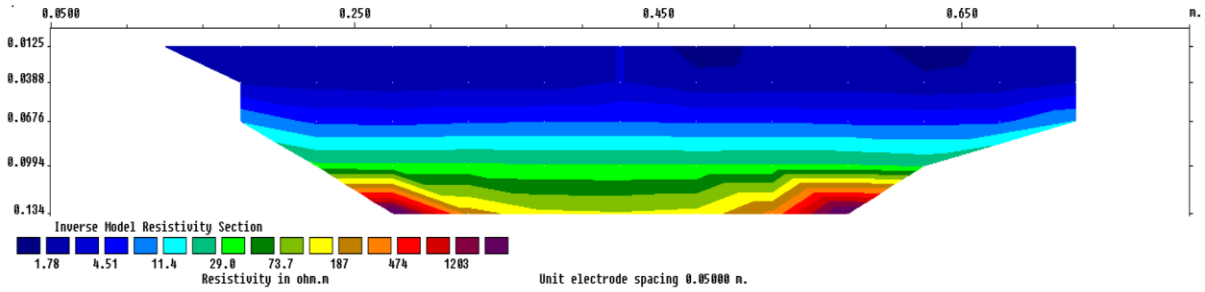

Figure 113. Profile no. 3 using dipole-dipole array and processed with Res2DINV.

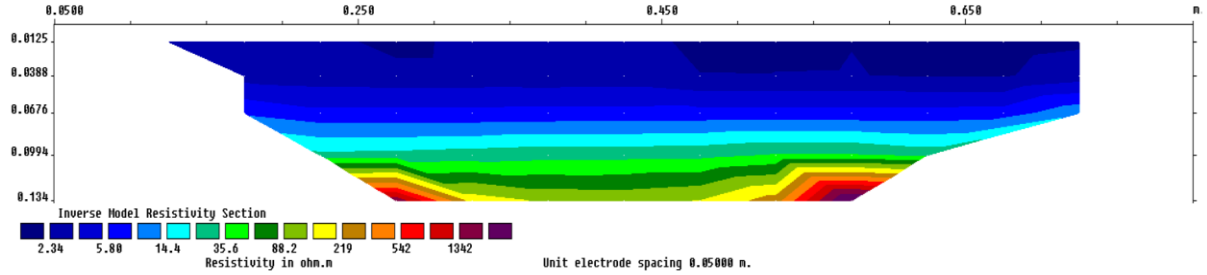

Figure 114. Profile no. 4 using dipole-dipole array and processed with Res2DINV.

In the 2D inversion profile using the dipole-dipole array (fig. 112-113), 3 offseted with 1 step areas appear in the place where the plant roots were. There areas are characterized by low-resistivity values. In this profile there appear small lower resistivity areas very close to the surface which corresponds with the position of the electrodes, which is interpreted as the electrode effect due to the small distance between the measured points and the high number of points measured due to the specifications of the dipole-dipole array.

4.3.2.2.2. TOMATO PLANTS IN TRANSPARNT SOIL SURVEY AND RESULTS

The tomato plants used for this survey were added to the environment at a mature stage (fig. 114). The plant roots were washed and inserted into the transparent soil.

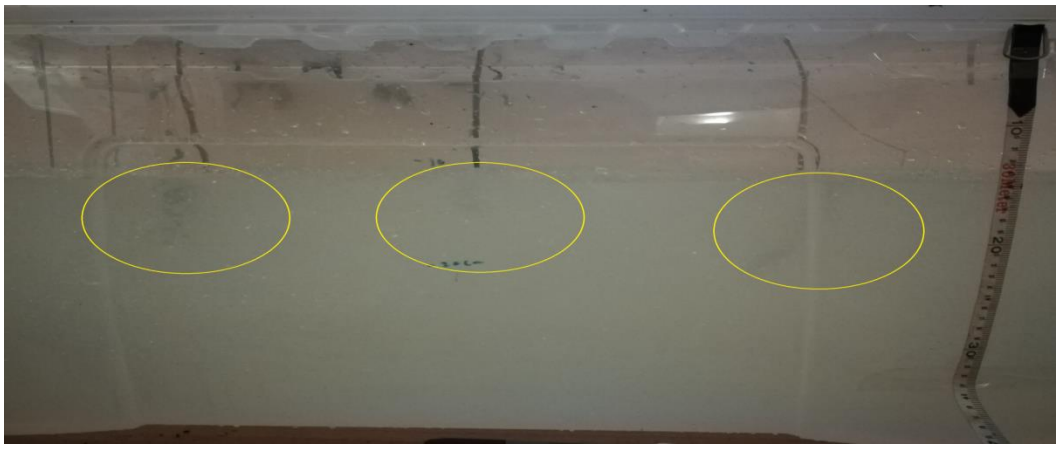

Figure 115. The tomato roots visible in the transparent soil.

For this setting 6 profiles were created with a similar profile that goes through the middle of the box where the roots are positioned between the electrodes. The middle profile is at a distance of 2.5 cm between profiles on each side of it, and all the other profiles are at a distance of 5 cm. This setting was chosen, to include a middle profile, which was accessible due to being able, not only to see the exact position of the roots but also inserting the plants at desired position in the box.

The surveys consisted of resistivity measurements with dipole-dipole, wenner, schlumberger and optimized array, using the code on the tablet and the switchbox to control the electrodes.

2D resistivity inversion profiles were created using the RESIPY software (fig. 115-116) and 3D inversion horizontal slices were created with the help of RES3DINV (fig. 117-119). The 2D resistivity sections show different characteristics which are mostly due to the type of array used. The Wenner array which has the least data points, with a higher density of points closer to the surface and decreases with depth, offers the least amount of information about the position of the plant root areas, but it makes the electrode effect very much visible. With the

increase in data numbers from one array to another, the effect of the electrodes seems to dissipate and other objectives start to contour.

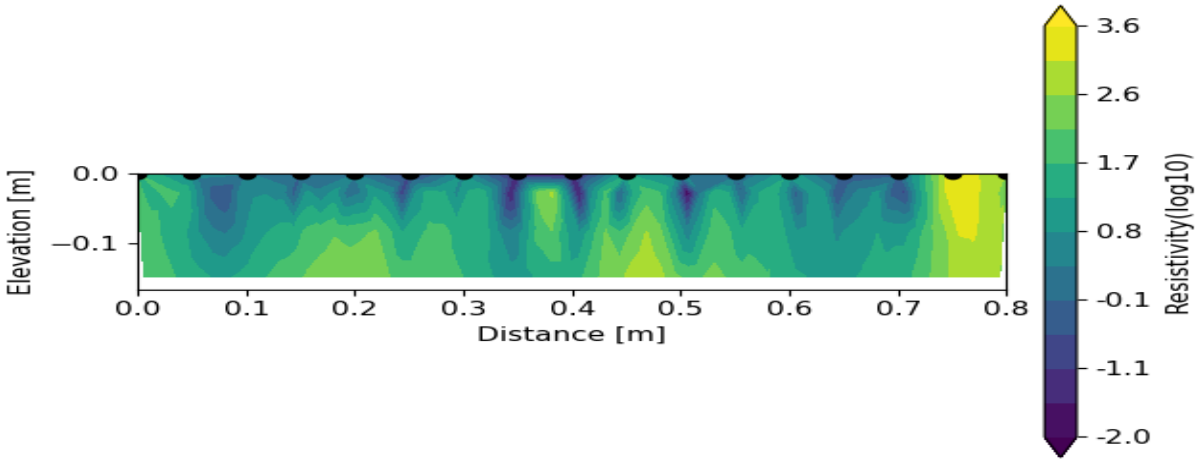

Figure 116. 2D inversion profile created in RESIPY with resistivity values on a logarithmic scale. The array used for this section is Wenner for the middle profile.

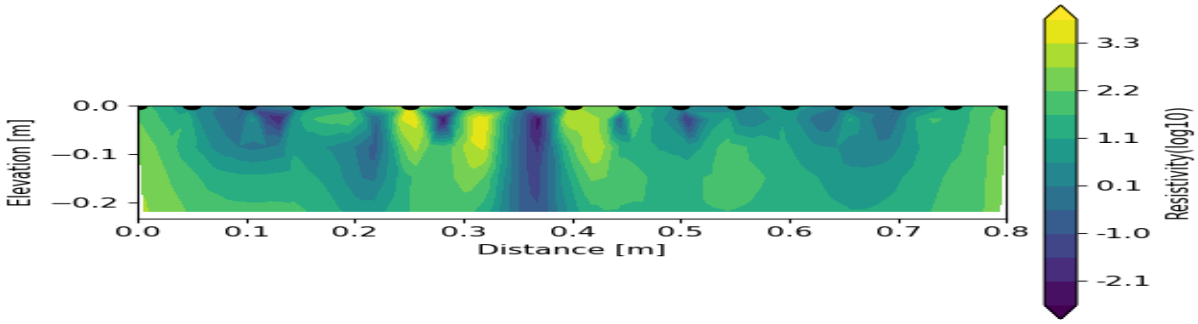

Figure 117. 2D inversion profile created in RESIPY with resistivity values on a logarithmic scale. The array used for this section is Schlumberger for the middle profile.

Schlumberger still show the effect of the electrodes which appears as really low resistivity areas. Because the whole environment is very conductive due to the high water content of the soil type, the root areas are expected to appear as slightly more resistive than the environment.

In both Schlumberger and Dipole sections, there appear small resistive areas at the surface that overlaps with the position of the plants.

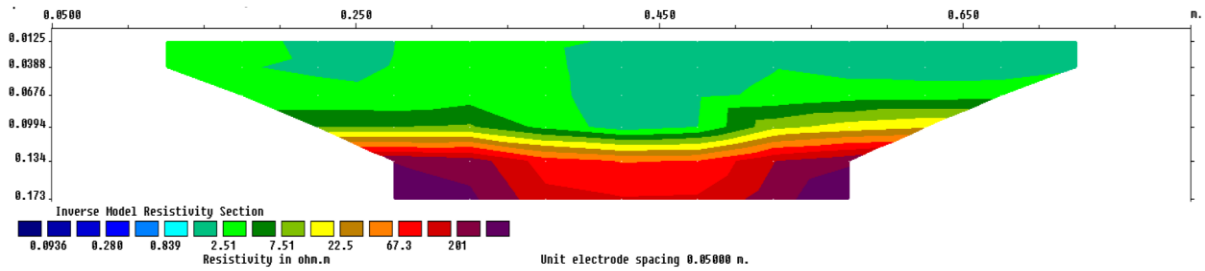

Figure 118. Profile no. 3 with Schlumberger array processed in Res2DINV.

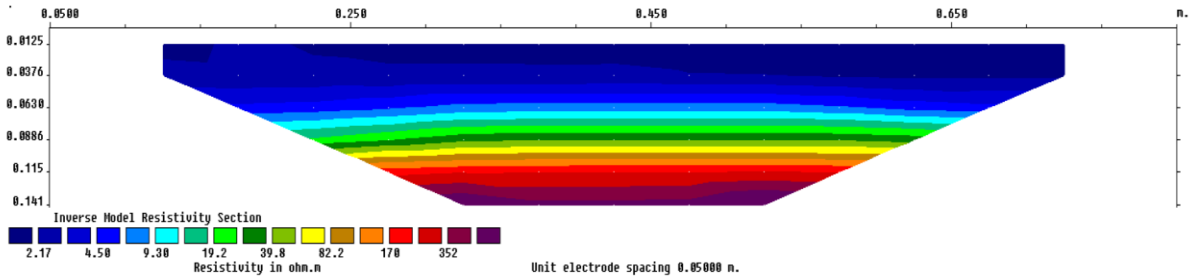

Figure 119. Profile no. 3 with Wenner array processed in Res2DINV.

After analysing the data it has been observed that compared to the real soil, in transparent soil it is difficult to highlight any specific areas that would correlate with the position of the plants, even though there appear to be some variations in the transparent soil in terms of resistivity values. However, when comparing the data from the box with transparent soil and

the plants with the box with transparent soil and no plants, there are some features that can be observed. The resistivity values of the box without the plants appear as smaller for the whole box compared to the box which had the plants in.

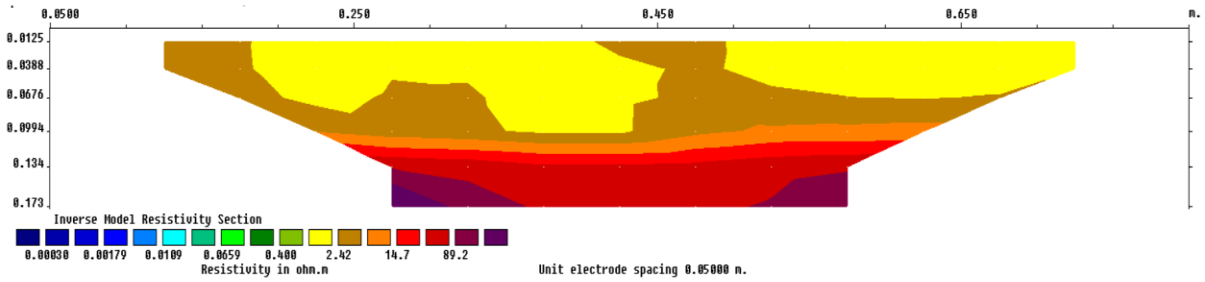

Figure 120. Profile no. 3 with Schlumberger array, processed with Res2DINV. Survey was carried out in the transparent soil without any plants.

This is interesting in particular because, as it has been observed in the synthetic models with homogenous environments, it appears that the roots that have a very different resistivity value compared to the soil, affect the value of the whole resistivity section, usually by increasing the values. This happens even if the soil has a smaller resistivity value, which appears in sections with higher values after the forward models were generated. Therefore, based on these observations and resistivity sections resulted from these surveys, it is possible that, even though singular features cannot be observed around the root areas of the plants, differences still appear in the transparent soil which are pointing out that the plants are there and are changing the resistivity values for the whole section. Another observation is related to the resistivity values from the transparent soil. It appears, based on the values resulted from the empty box, that the resistivity values are generally low and would correspond to values between 2.42 and 14.7 Ωm. Compared to normal soils, the transparent soil has similar values

to clays according to Telford et al. (1990) and according to Peck et al. (1974) these would have similar values to both clays and saturated silts.

4.3.2.2.3. TUBES WITH TRANSPARENT SOIL SURVEYS AND RESULTS

In order to carry resistivity surveys in the tubes, the Matlab codes that controlled the switchbox and the types of arrays, needed to be modified. Different types of arrays needed to be adapted and developed for this type of surveys. The arrays developed were based on (Werban, Al Hagrey and Rabbel, 2008), which describes different types of borehole surveys in which the electrodes considered are placed on two parallel vertical profiles (fig. 120). The arrays used are the following:

- Alfa-vc (a), which is similar with the wenner array with the electrode order CPPC (where C is current electrode and P is potential electrode);
- Beta-vc (b), which is similar to dipole dipole with the electrode order CCPP;
- Beta-l (c), which uses two opposite profiles and takes the top points from as the current electrodes and the next points below them as the potential electrodes.

The data processing proved to be much more difficult due to the unusual setting of the arrays and to the low number of measured points compared to normal borehole surveys.

The transparent soil used in the tubes has the same properties and represents the same transparent gel used in the boxes (fig. 122).

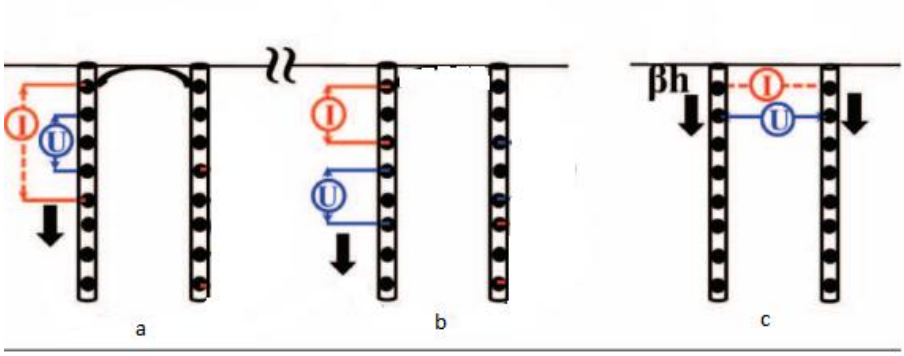

Figure 121 Image reproduced after Hagrey et al 2008. A – represents the alfa-vc array, b – the beta-vc array, and c – the beta-l array.

The fact that the quantity of water was much more enhanced compared to the boxes (fig. 122), it allowed for a very high degree of transparency, in which the plant with the roots were fully visible. All of the arrays described above were used for the surveys in the transparent soil tube.

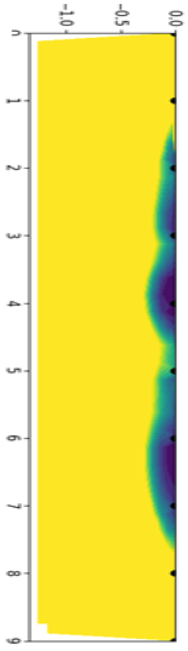

Figure 122 Inversion of the data from the alpha array. The data is not at scale.

.Figure 123. Left – the visibility of the tomato root in the tube filled with transparent soil. Right – the tube with transparent soil and no plant, with very high transparency level.

After processing the data for the alfa-vc arrays in the transparent soil tube with one plant in the middle of the tube which reached up to the 4th electrode, it appears that the data resulted more likely due to the low resistivity area really close to the side of the tube (fig. 121), or in the resistivity section, really close to the surface, represent the effect of the electrodes.

4.3.2.2.4. INDOOR SETTING NO. 1 RESISTIVITY SURVEYS

The following resistivity surveys took place in the indoor setting no. 1 transparent containers, fully described in chapter 3.4.1.1. Both surveys presented bellow used 10 electrodes on each of the four parallel profiles, due to the size of the limited size of the container, with the same distance of 5 cm in-between and electrodes made of a stainless steel alloy (tent pegs).

Different conditions have been tested and multiple sets of data collected with arrays like Wenner, Schlumberger, dipole-dipole and multiple combinations of electrodes, however only the most representative ones have been selected.

4.3.2.2.4.1. INDOOR SETTING NO. 1 RESISTIVITY RESULTS

Container no. 2 with 1 plant

The soil box 1 which contained a mixture of different types of top soil, with low organic material content only contained 10 electrodes with a distance of 5 cm in-between and 4 profiles, due to the sizes of the box.

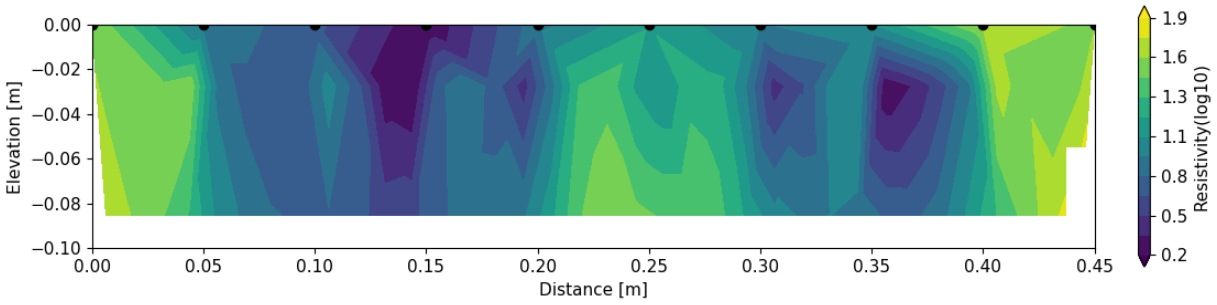

Figure 124. Profile no. 2 closest to the plant using Wenner array.

The profile no. 2, which is one of the inner profiles closer to the plant area (fig. 123) used Wenner array and was processed using RESIPY. The Wenner array which has the least amount of data points makes the resistivity sections hard to be reliable. But even so, in this section, close to the plant, the area that coincides with the position of the plant, appears in the resistivity section to have higher resistivity values. The water wasn't spread regularly when watering the plant and the resistivity section might reflect the spread of water rather than the root area (more on this limitation described in chapter 3.4.1.1.).

Container no. 1 with 3 plants

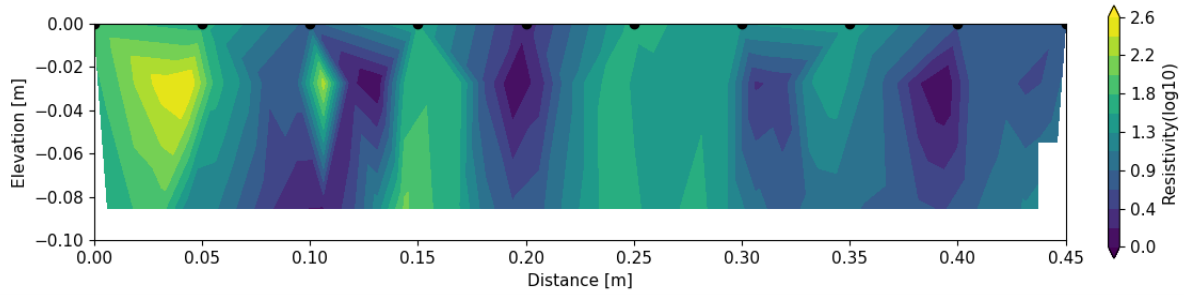

Figure 125. Profile no. 2 closest to the plant using Wenner array.

The box containing 3 plants, with similar size as the previous one, used also 10 electrodes at a distance of 5 cm between profiles and electrodes. Similarly, the array used was Wenner and the data was processed with RESIPY. Even though the number of points for Wenner is much lower than other profiles, it is interesting to see similarities between the profile in the container with 3 plants (fig. 124) and the profile in the box with only one plant. What they both share in common is the fact that the position of the plant corresponds with higher resistivity values. In this box as well, the water was not equally spread, so this might affect the accuracy of the data.

4.3.2.2.5. WOODEN CONTAINER WITH SURVEY AND RESULTS

The setup of the wooden container, including dimensions, type of soil and plants is fully described in chapter 3.4.1.4. An innovative attempt was carried out to apply a type of electrical survey “borrowed” from archaeology to measuring plant roots. Specifically, the

twin probe array was deployed to measure the subsurface area around a tomato plant in a controlled environment. It is believed this method has not been previously trialled in the literature for the study of roots.

The twin-probe array represents an array usually used in the archaeological surveys which displays the resistance values instead of the usual resistivity values (Gafney & Gater, 2010).

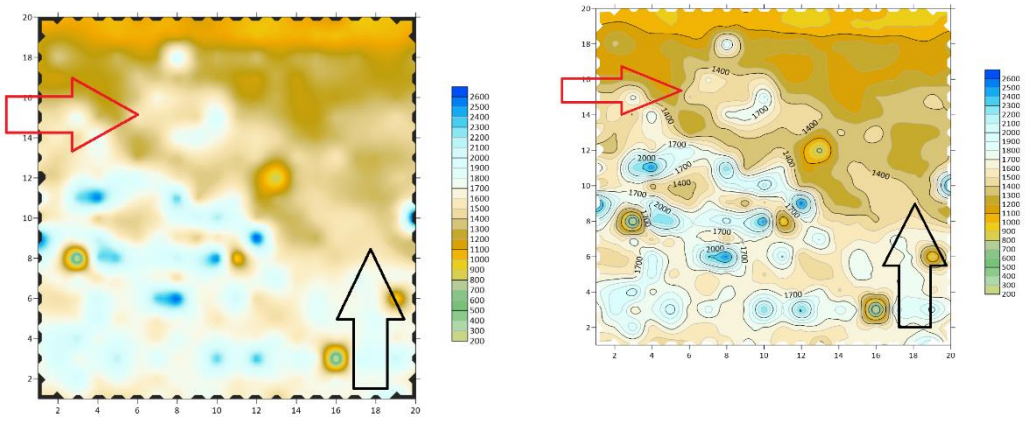

Figure 126. Contour maps created in Surfer of the twin-probe array survey, the arrows are highlighting areas of interest. The images are not at scale.

In terms of displaying the data, the twin probe array is similar to Wenner array in creating horizontal images of the subsurface compared to the ERT vertical sections (Gafney & Gater, 2010). The twin-probe array is a variation of pole-pole array, in which two electrodes (one current and one potential – C1 and P1) are fixed and two mobile electrodes (C2 and P2), which are moved from one point to the other for every point. The survey is carried in a zig-zag grid pattern on the whole surface of the area of interest. In the twin-probe array the important factor is represented by the distance between the two electrodes, and this is the value that should be chosen depending on the desired depth. The fixed electrodes should be at

an infinite distance in theory, but in practice it shouldn't be less than 30 times the distance between the electrodes (Gafney & Gater, 2010). According to Gafney (2010) a distance between the electrodes of 0.5 m reaches a depth of approximately 0.75 m. In this survey, the chosen distance between the electrodes was 2 cm which should reach a depth of around 3-4 cm, and the fixed electrodes have been set at a distance of 60 cm. The grid started at the left bottom corner and the points were measured every 2 cm, and the parallel profiles at 2 cm.

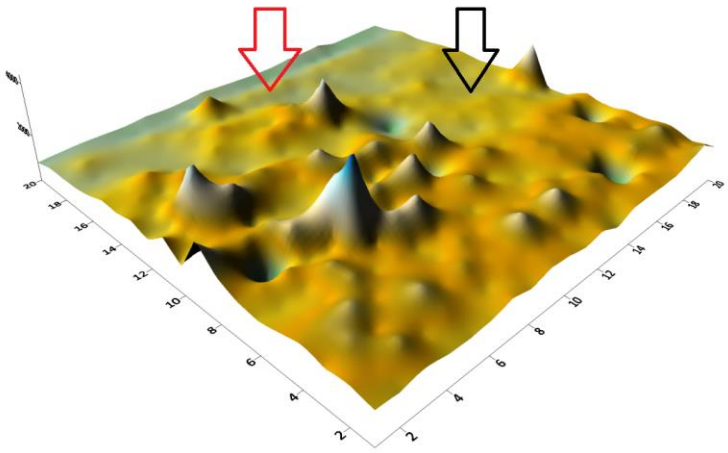

Figure 127. Image representing a 3D surface map of the 2D data. On the Z axis the values represent resistance values. Image created in Surfer. Arrows highlight areas of interest. The image is not at scale.

The area chosen includes one tomato plant as it can be seen in figure 125 and an area on the right side which has a higher moisture content visible from the surface. This area has been chosen to understand if the plant root can be visible in any way; the moisture side is used as a control to understand how the anomalies would be highlighted with the survey.

The electrodes (fig. 129) used in the survey are upholstery needles of 10 cm length and 2 mm in diameter.

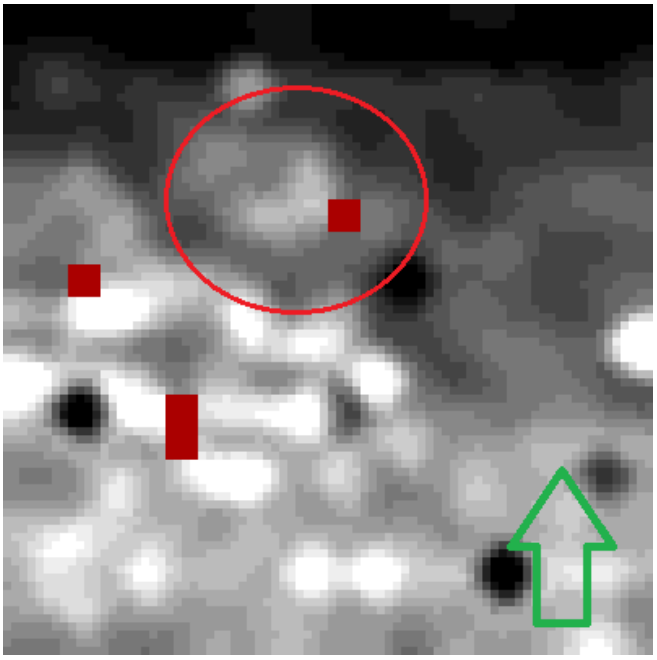

Figure 128. Image resulted from processing the data in Snuffler, with red circle is highlighted the approximate area of the tomato plant, and with green arrow is highlighted the area with higher moisture content visible on the surface. The image is not at scale.

The data was processed with the open-source software Snuffler which displays the resistance values and allows for simple filters and interpolation to be added in order to process the data. The red pixels (fig. 127) represent points with anomalous values that go outside the normal range of values. Snuffler usually displays data in a way that focused on highlighting contrasts.

The same data was processed in Surfer, where contour maps have been created after the anomalous values have been removed (fig. 125). A 3D surface visualization model (fig. 126) was also created, which has on z axis the resistance to be able to highlight any contrasts that might not be visible in the 2D horizontal sections.

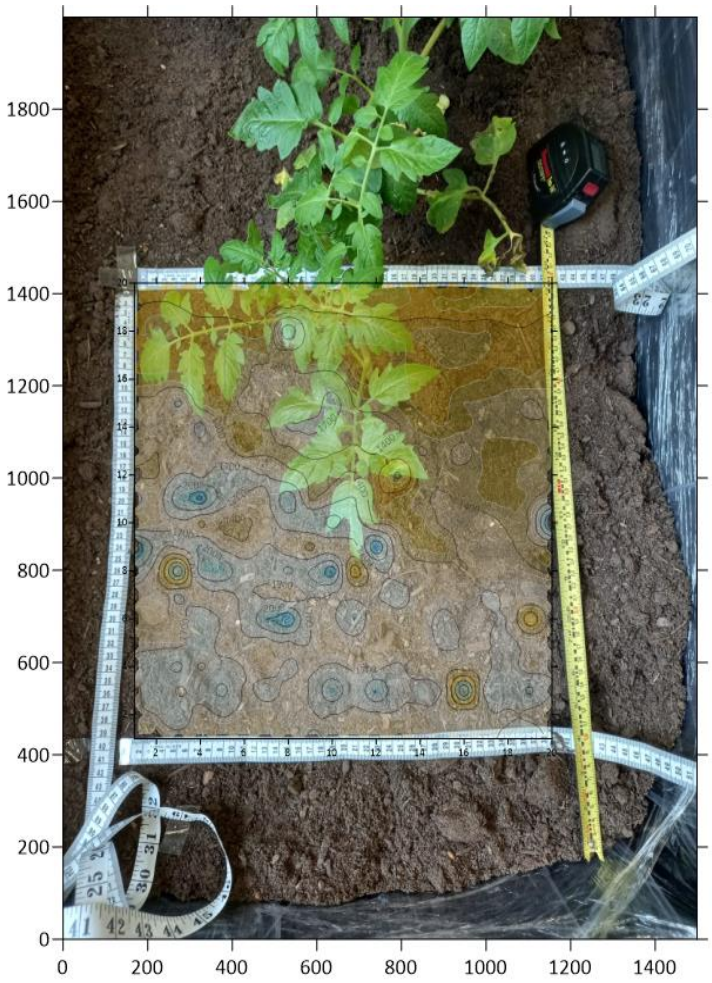

Figure 129. Overlapping the contour map with resistance values resulted from processing the data in Surfer on the actual image of the grid from the experimental box where the twin-probe survey took place. The image is not at scale.

After overlapping the processed images with the actual photograph (fig. 128) and based on the information regarding the position of the plant and the higher moisture area, there are some features of interest that can be observed in the twin-probe array survey.

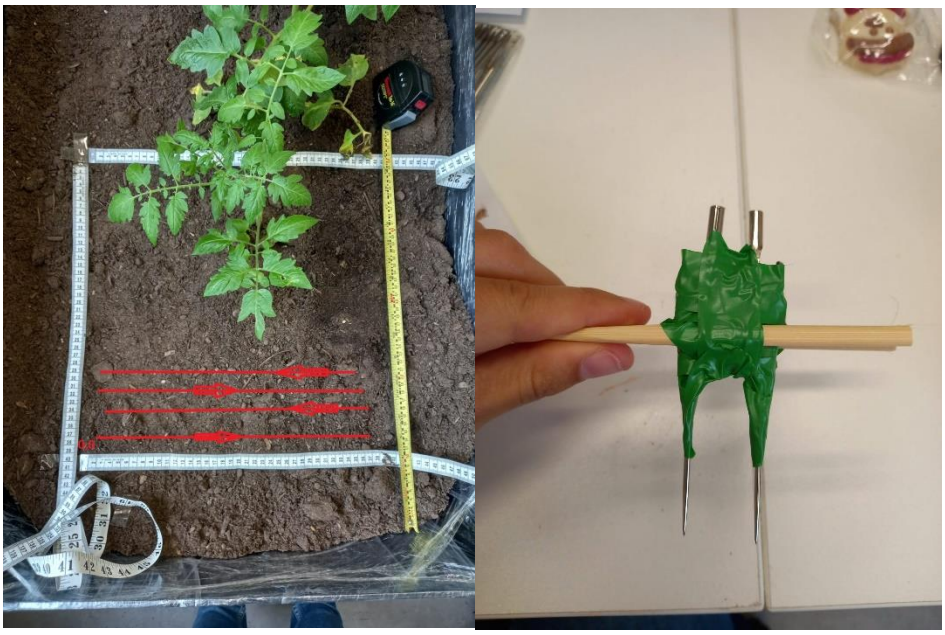

Figure 130. Left - image representing the direction of the twin-probe profiles and the 0,0 start point of the gird. The image is not at scale. Right – the electrodes at a fixed distance of 2 cm between them.

The area highlighted with a red arrow or red circle in the Snuffler image (fig. 127), corresponds to the position of the tomato plant, but it is larger in size compared to the real position, and it represents a higher resistivity area compared to the values surrounding it. The area highlighted with black and green arrows represent the starting area (from down to up) of the area with high moisture content visible from the surface.

4.3.3. RESISTIVITY SYNTHETIC MODELS

Resistivity synthetic models have been created using ResIPy software, with a variety of parameters and designs. The models are very useful as a first step, to understand how to adapt the experiments in a way that the data resulted from the resistivity surveys will provide useful

information but they can also be used for a different purpose: for a better understanding of certain aspects from the surveys, such as limitations, interferences, and so on. Two versions of the same model have been created an ideal model, with finer mesh and low noise percentage, and another model with higher noise percentage and coarser mesh to create much more realistic forward models that would come close to data from the actual surveys.

However, producing a realistic shape of the root remains challenging, and a straightforward way to do so does not exist. Therefore, a simplified version of the root area was used instead.

4.3.3.1. MODEL NO. 1

This model represents a very simplistic approach, with 3 plant root areas in the form of rectangles of approximately 5 x 5 cm, with 2 contrasting resistivity values for the soil and the roots respectively. The shape and position were chosen based on the information and measurements from previous experiments. The number of electrodes is 16, which is the same number of electrodes used in the real surveys (fig. 131), with a distance between the electrodes of 5 cm. The simplistic model of the roots is based on the plants that were transplanted from the propagator trays into the experimental box (fig 130).

The resistivity values chosen for the forward model (fig. 132) are 20 Ωm for the roots and 100 Ωm for the soil, and the values are based on the values mentioned by Hagrey (2011). The 20 Ωm corresponds to conductive root zones and was chosen because the roots of the plants chosen in the experiment are the conductive sap flowing roots (Hagrey, 2011). The value for the soil corresponds to the maximum value for top soils as described by Telford (1976).

Figure 131. Image representing the plants grown in the propagator trays ready for transplanting in the experimental box.

Figure 132. Image with the plants after they have been transplanted in the experimental box ready for surveying.

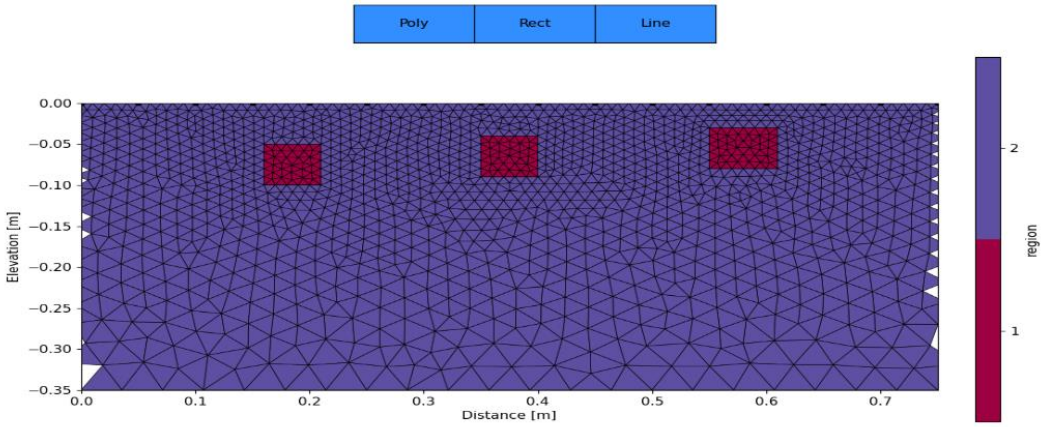

Figure 133. The forward model created with the rectangles representing the roots with a resistivity of 20 Ω m, in a 100 Ω m soil.

A variety of arrays have been used on this model: Wenner, Schlumberger, dipole-dipole and a combination of both Wenner and dipole-dipole (fig. 133-136).

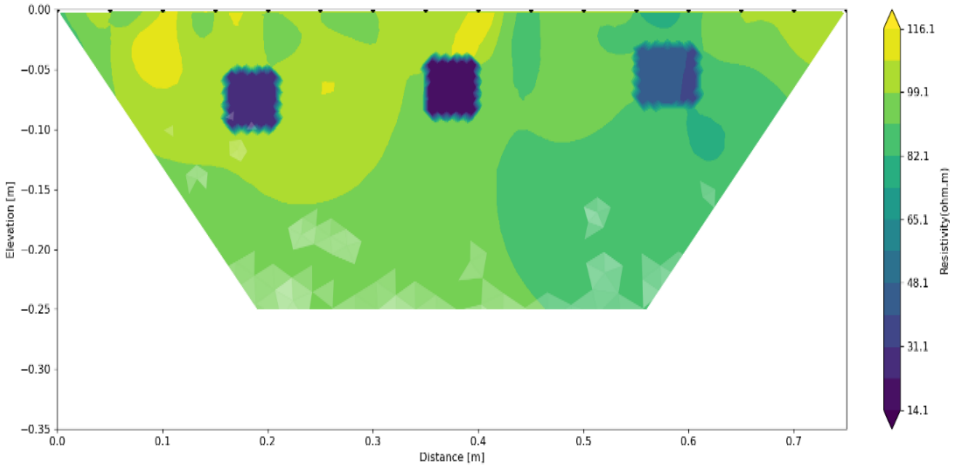

Figure 134. Image representing the model no. 1 with the Wenner array.

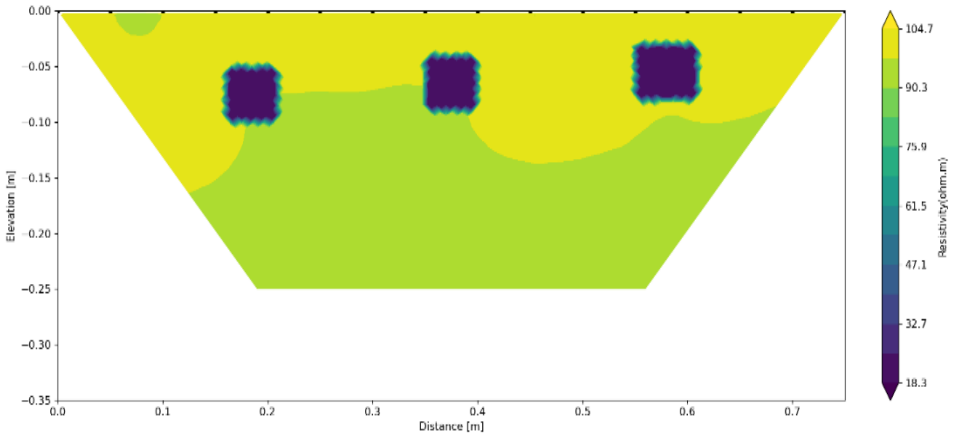

Figure 135. Image representing the model no. 1with the dipole-dipole array.

What can be observed from the images is that the Wenner array (fig. 133) and the Schlumberger array (fig. 136) are introducing some artefacts in the data and variations with shapes unrelated to the shapes of the plants.

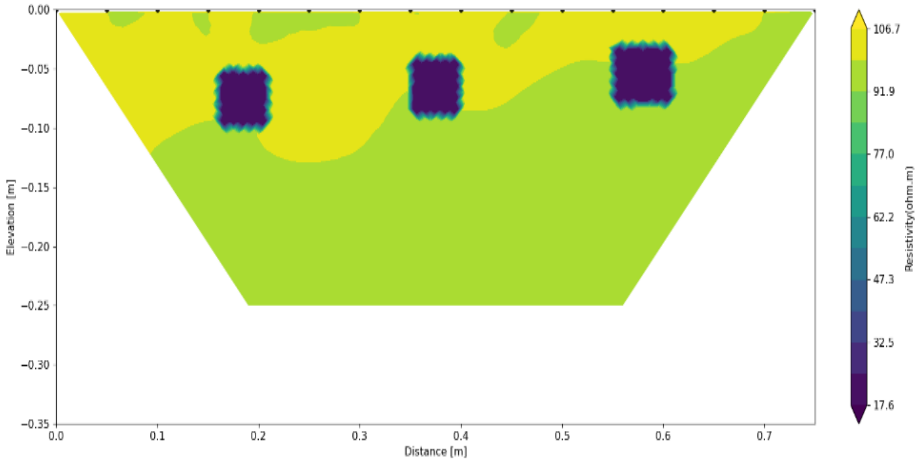

Figure 136. Image representing the model no. 1 with the combination of both Wenner and dipole-dipole arrays.

The range of resistivity value of the top soil for both arrays seems to get a bit lower (70 – 105 Ωm) compared to the range of values in the dipole-dipole (90 – 106 Ωm) array. The combination of the Wenner and dipole-dipole array (fig. 135) seems to have the least amount of artefacts at the surface and variations of top soil resistivity values inside the model, showing a higher resistivity area on top of the model (104.7 Ωm) and lower resistivity values for the lower half of the model, under the roots (approx. 97 Ωm).

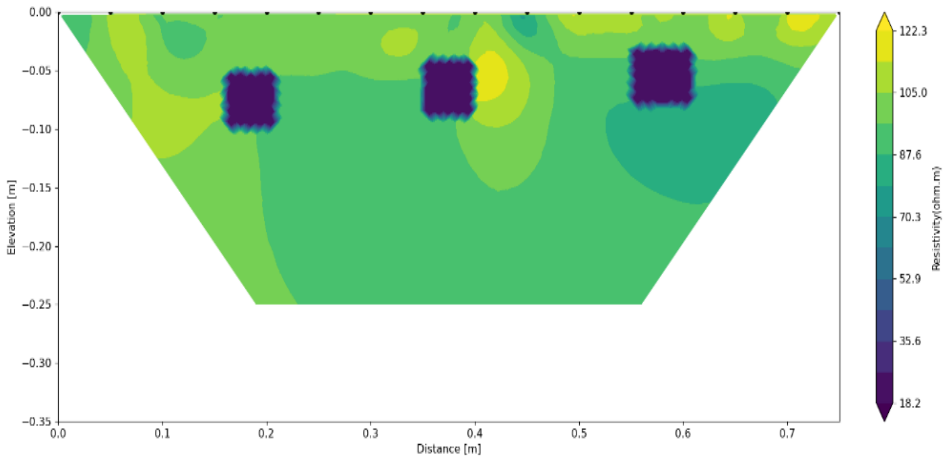

Figure 137. Image representing the model no. 1 with the Schlumberger array.

4.3.1.2. MODEL NO. 2

In this scenario, the modelled plant root areas (fig. 138) were based on the plants that were dug out of the experimental boxes (fig. 137), after surveys have been carried out on them.

Figure 138. Image representing the plants removed from the boxes after surveys have been carried to measure and analyse the shape and size.

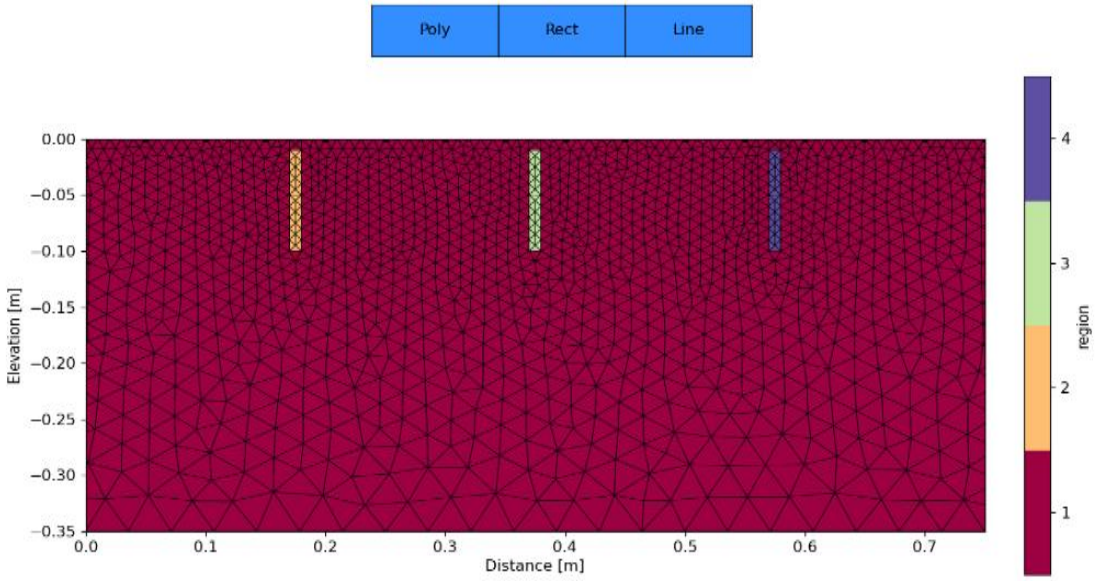

Figure 139. The forward model and the 3D meshed used. Even though the rectangles appear as 4 regions, all the 3 rectangles have the same resistivity value of 20 Ω m, and the resistivity of the soil of 34.89 Ω m.

These tomato plants have grown and have developed in the box (fig. 137), thus allowing them to have a more natural spread of the roots compared to the plants grown in the propagator trays and transplanted in the box. Because the roots of the tomato plant have a very fine structure, some of the roots couldn't be saved, and the only roots remaining are the ones closer to the tap root. Therefore, the shape of the roots chosen for the forward model is represented by a finer and longer rectangle of 3 x 10 cm (fig. 138).

Even though the roots have spread inside the box, the largest volume of roots is still the one closest to the tap root. The resistivity values chosen for this model are 20 Ω m for the roots, and 34.89 Ωm for the soil. The resistivity value for the roots is the same as for the previous model based on the models by Hagrey (2011), as for the soil, the value was chosen to represent the soil described and used in experiments by Amato (2009) as a silt loam soil with 1.12% organic matter content which comes close to the type of soil used in the experimental setting in which the tomato plants have grown before being dug out.

The purpose of the experiment was to see if a finer model of the roots close to the size of the tap root of the plant would be visible when it shares a resistivity value closer to the soil's resistivity value.

The same number of electrodes has been used to represent the same setting used in the experiments, with 16 electrodes at a distance between them of 5 cm.

The forward model goes through inversion in order to get an image as close as possible to real world inversion data and to be able to understand how these features look in terms of resistivity values and arrays used.

Four arrays and combinations of arrays have been tested: Wenner, Schlumberger, dipole-dipole and a combination of Wenner and dipole-dipole.

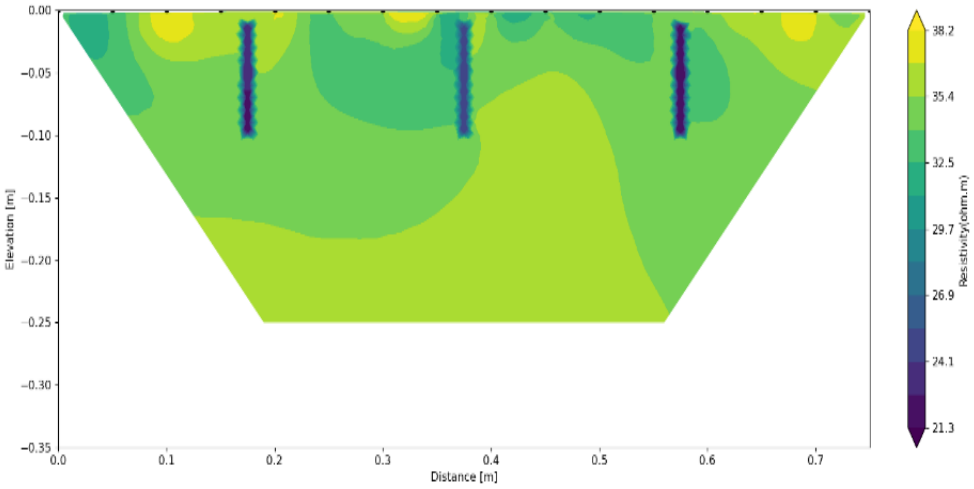

Figure 140. Image representing the model with the Wenner array.

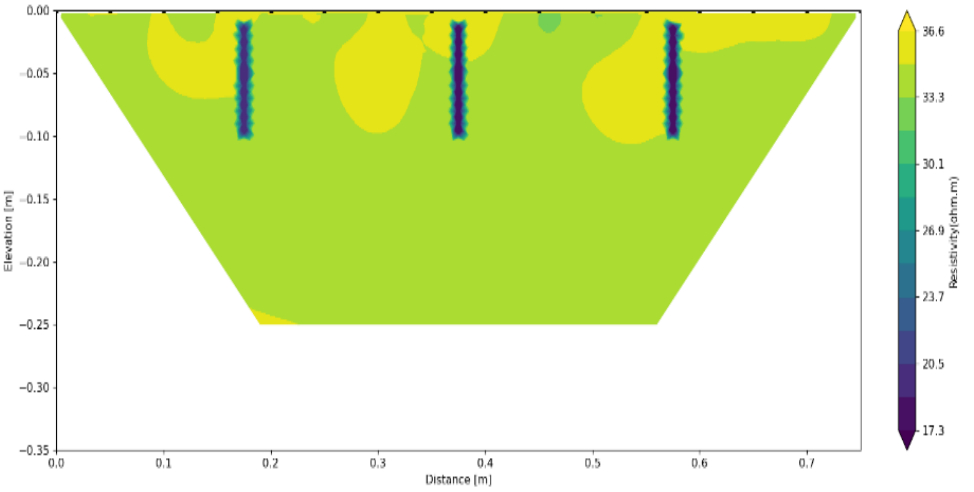

Figure 141. Image represents the model with the Wenner and dipole-dipole combined array.

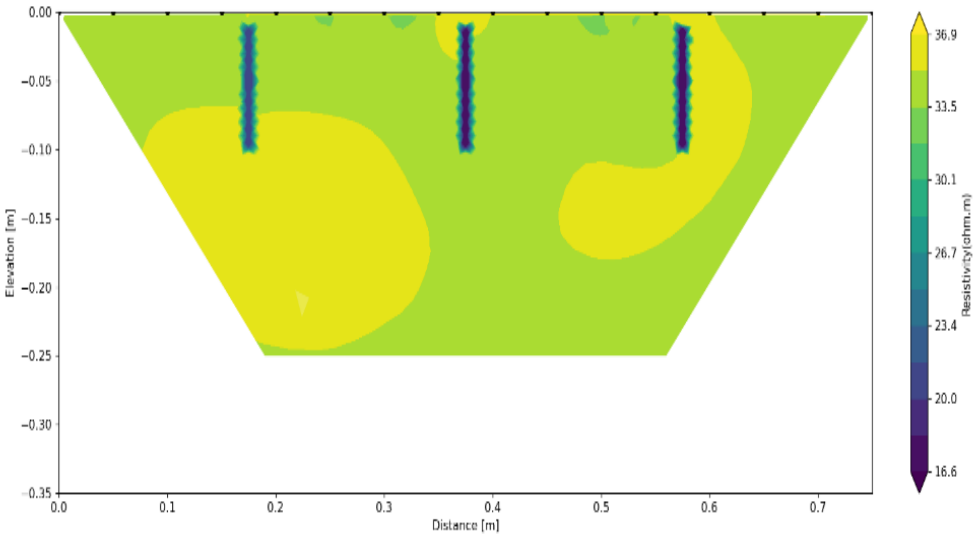

Figure 142. Image representing the model with the Schlumberger array.

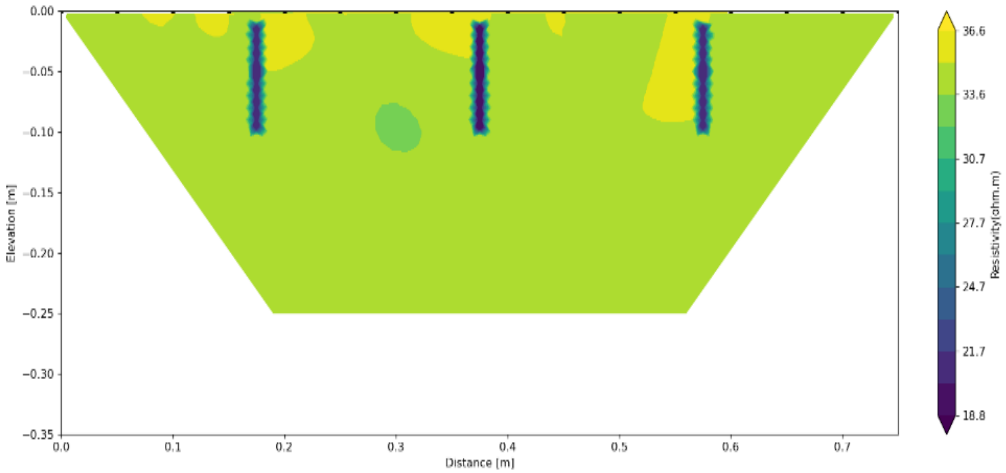

Figure 143. Image representing the model with the dipole-dipole array.

It can be observed from the resulted models that Schlumberger (fig. 142) and Wenner (fig. 139) represent the arrays which display more artefacts in the resistivity models, with Wenner array presenting a minimum resistivity range of values of around 30 – 35 Ωm in the soil

surrounding the roots compared to the other arrays (33 – 36 Ωm). In the model showing the combination of Wenner and dipole-dipole arrays, the resistivity value of the soil seems to be around 34 Ωm with an increasing value around the roots of around 36 Ωm. However, all models (fig. 140-143) other than the simple Wenner one appear to produce positive contrasts around the negative contrasts associated with the roots. These positive anomalies can be quite problematic, as they can obfuscate the root area and create the illusion of a positive resistivity area. This could explain some of the uncertainty observed in results both in this work and in the existing literature. Meanwhile, the Wenner models seemed to produce the least amount of strong, positive resistivity anomalies, which may suggest that while the Wenner ERT has fewer datapoints than its counterparts, it could in fact be preferable for this type survey.

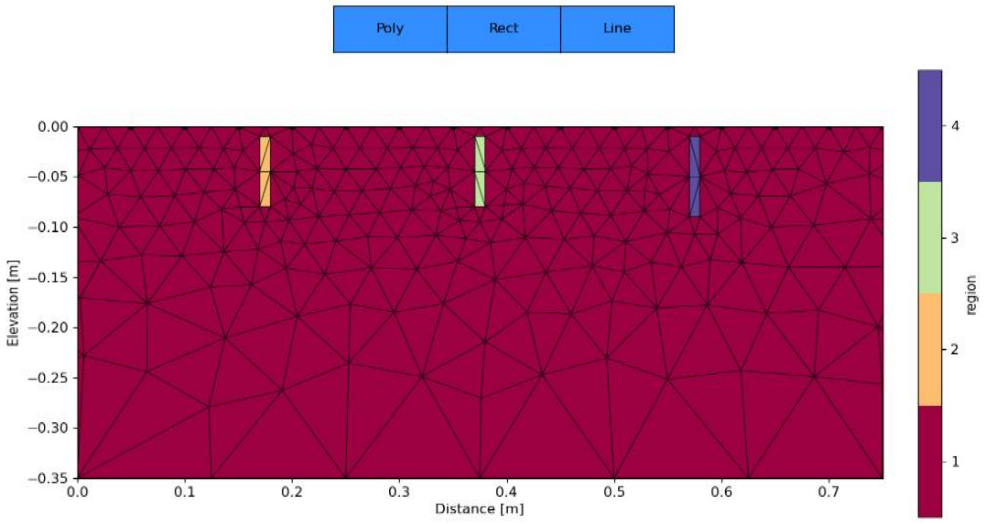

Figure 144. The model uses same resistivity parameters for soil and roots but the mesh is much coarser and the noise is up to 3%, to create a situation more realistic and more similar to what is likely to be encountered in real surveys.

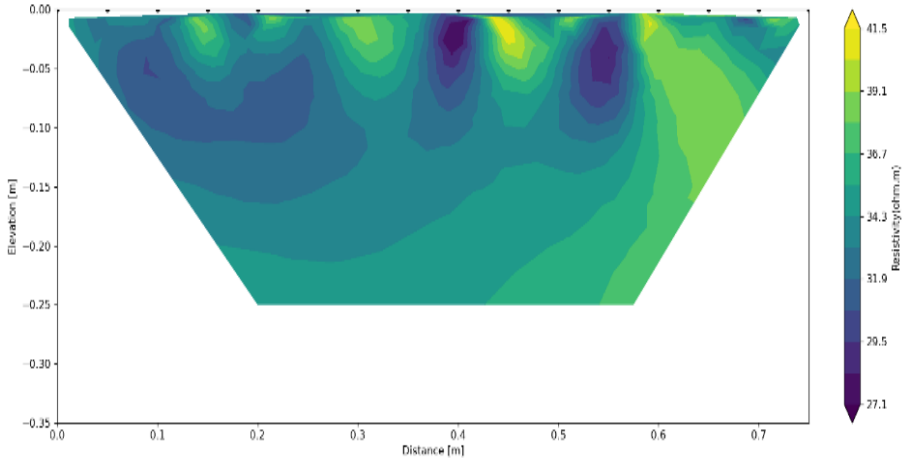

Figure 145. Representation of the Wenner array for the model that uses rectangles to highlight the roots, and a coarse mesh with 3% noise.

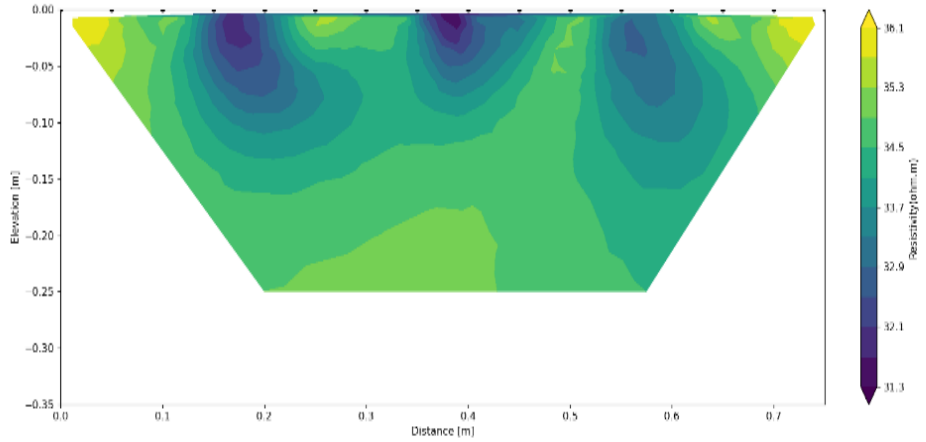

Figure 146. Image representing the model with the dipole-dipole array.

After these ideal models have been created, further models with the same parameters in terms of resistivity values were developed, but with a coarser mesh and a 3% noise compared to the 2% noise recommended and used with the previous models, are created (fig. 144). These parameters should allow for a more realistic perspective of what the real data may look like.

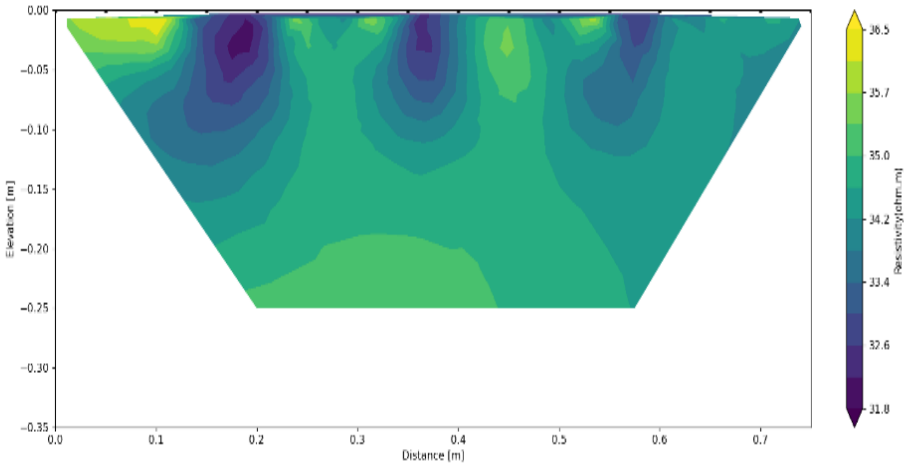

Figure 147. The forward model using both Wenner and dipole-dipole arrays.

It can be observed from the models (fig. 145-147) that the anomalies of the roots are much fainter from the models that use 3% noise and a coarser mesh compared to the models using 2% noise and a finer mesh. Another observation is that the Wenner (fig. 145) array alone seem to show just two of the roots well contoured,the ones on the right side, however the one of the left side is not as distinguishable in terms of shape and resistivity value. The dipole-dipole array (fig. 146) seems to show all the root areas but the shapes of the roots are less clear for all of the models.

4.3.1.3. MODEL NO. 3

The 3rd model tries not only to get to a shape closer to the root area of the tomato roots used in the experiments but it also uses closer resistivity values for the soil and the roots, which produces a fainter contrast. The shape used for the roots is a polygon with a resistivity value

of 30 Ωm (fig. 148) which is the value resulted from the experiments for the middle part of the root area described by Hagrey (2011).

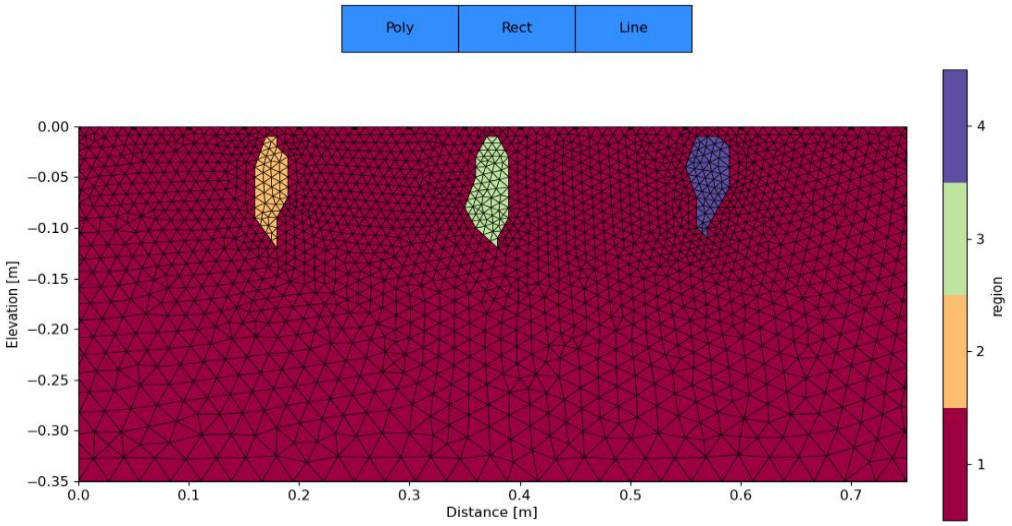

Figure 148. Image representing the forward model with the roots in the form of irregular polygons, with resistivity values for the roots of 30 Ωm and 34.89 Ωm for the soil.

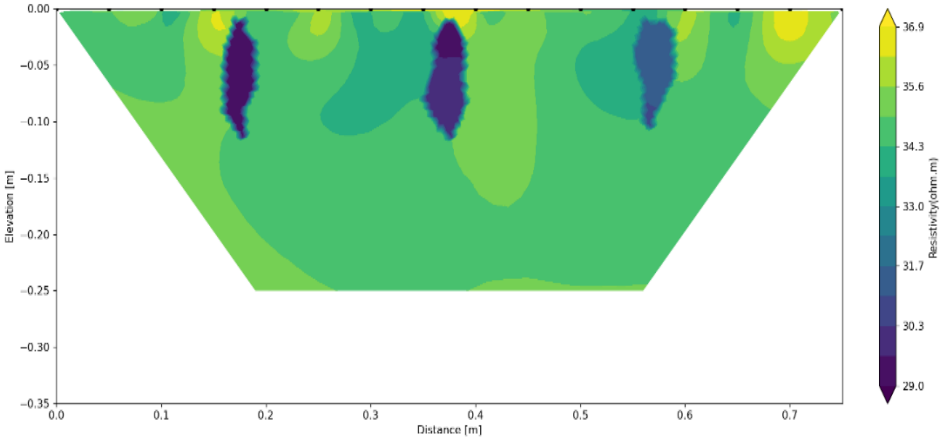

Figure 149. Image representing the model with the Wenner and dipole-dipole array

The resistivity value for the soil is the same as the one used, 34.89 Ωm in the previous model based on the silt loam with a small fraction of organic matter described by Amato (2009). The purpose was to see what the differences are when using a irregular shape, much closer to the aspect of the root area from the plants in real world, when the root area and the soil share closer resistivity values.

The same number of electrodes was used, with the same distance between them, 16 electrodes with 5 cm in-between.

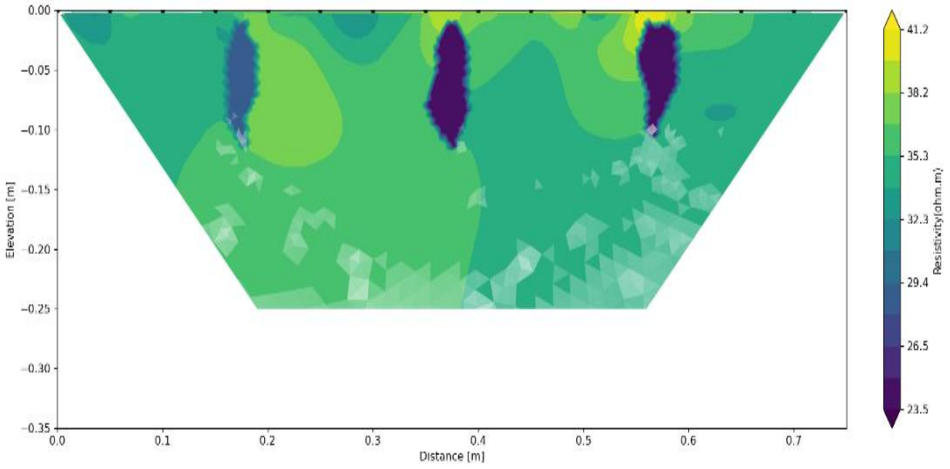

Figure 150. The model using the Wenner array.

It can be observed from the images (fig. 149-152) that the root area would still be distinctive even though their values might change and they might be visibly different. For example, in the model using the Schlumberger array (fig. 151), it appears that the left root has a higher resistivity (38.4 Ωm) value compared to the other two (27.7 – 31.3 Ωm), which is not the case. The model with the Wenner array (fig. 150) would show a similar aspect with the left root appearing with a resistivity much lower (32.3 Ωm) compared to the other two (23.5 Ωm).

There would be much higher variations inside the soil as well for the Wenner and Schlumberger array, compared to previous models.

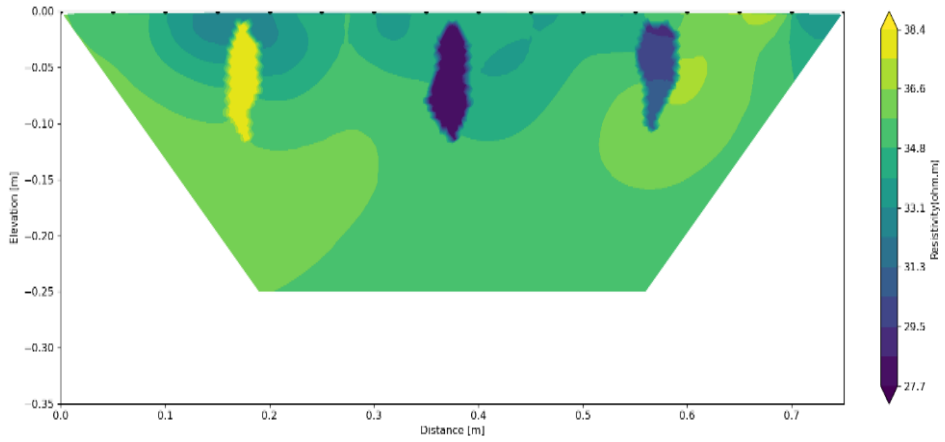

Figure 151. Image representing the Schlumberger array.

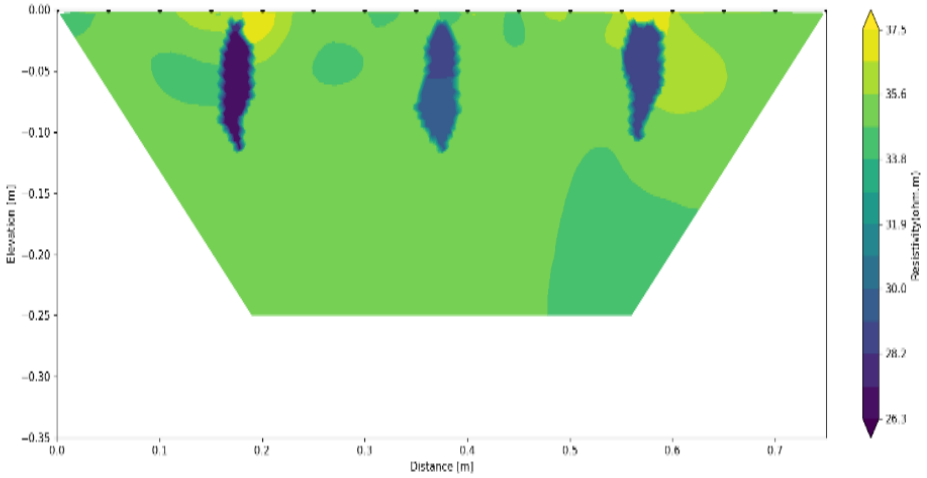

Figure 152. Model created with the dipole-dipole array.

The following forward model is based on the same model but with different parameters in terms of meshing and forward modelling. The resistivity values are the same 30 Ωm for the roots and 34.89 Ωm for the soil. The mesh used is much coarser and the noise level

introduced in the model is 3% compared to the previously used 2% level (fig. 153). These parameters have been chosen in order to create models much closer to the data from the surveys.

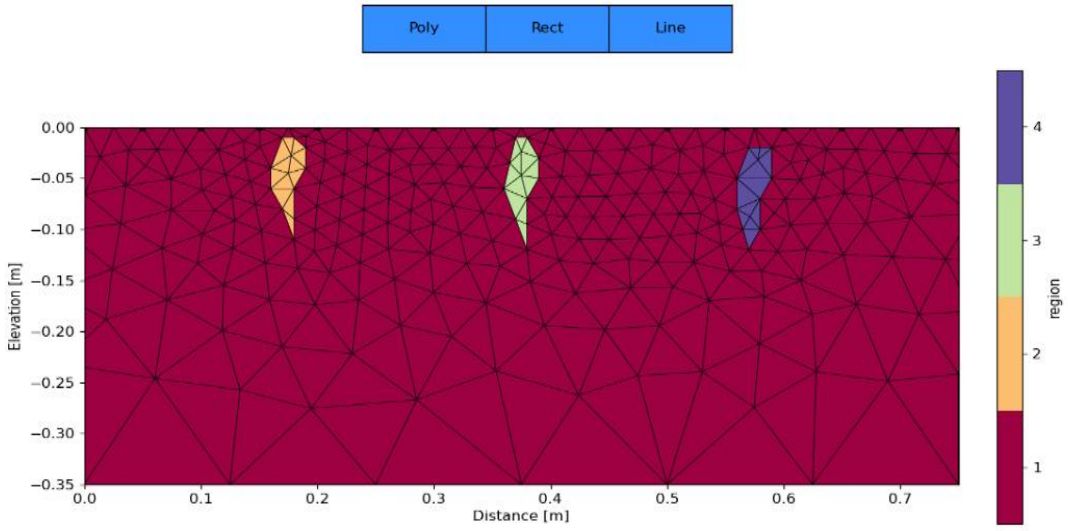

*Figure 153. Image representing the model with a coarser triangular mesh and resistivity values of 30 Ω*m *for the roots and 34.89 Ω*m *for the soil.*

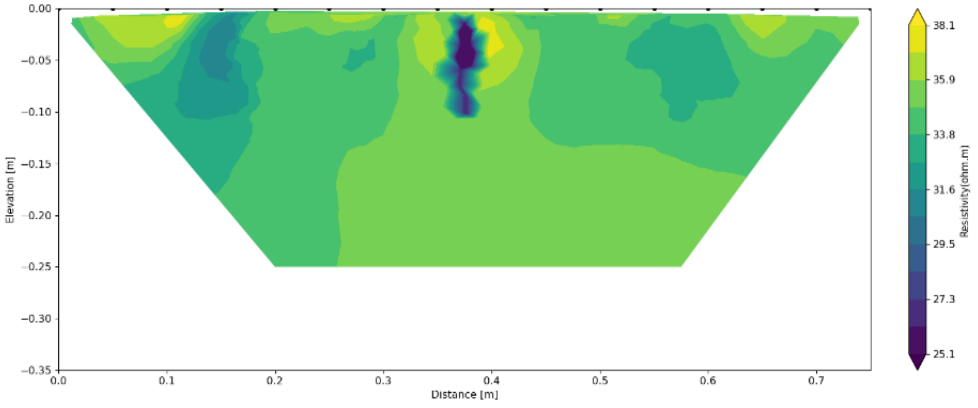

Figure 154. The model with the coarser mesh and 3% noise with the dipole-dipole array.

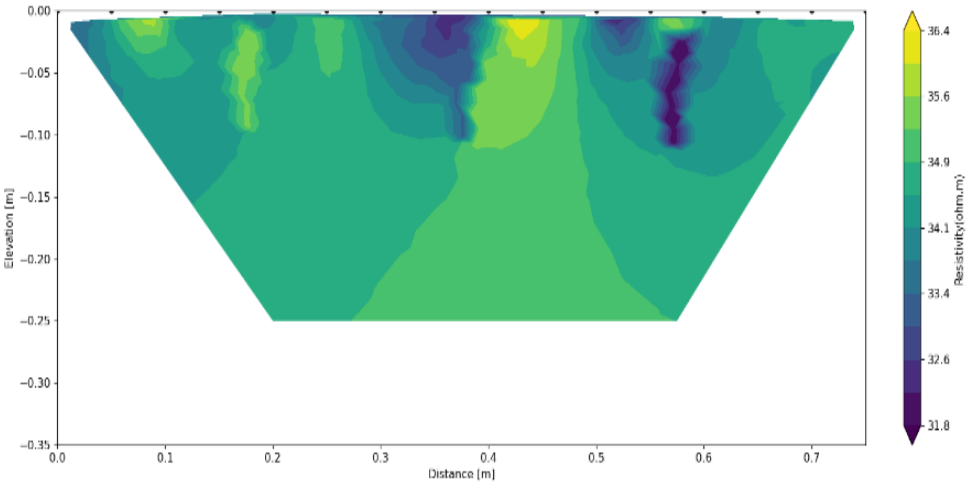

Figure 155. The model with coarser mesh and 3% noise with the Wenner array.

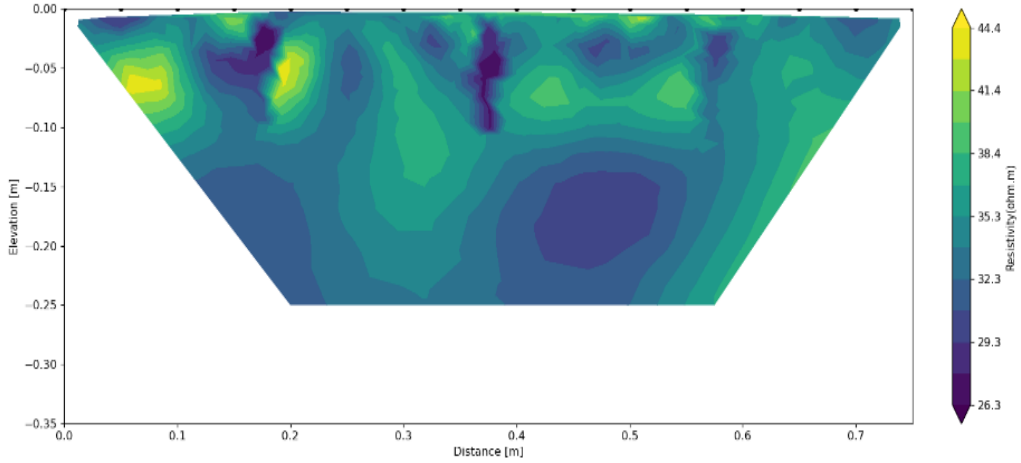

Figure 156. The model with coarser mesh and 3% noise with both Wenner and dipole-dipole arrays.

As the soil is not homogeneous throughout the whole experimental box, as there might be different levels of compactness, or elements like organic matter may not be evenly spread throughout the whole soil, etc., it is necessary to introduce a higher noise percentage. What can be observed from the models is that the anomalies from the roots are becoming very faint

and in some of the arrays some root areas would be more visible than in others. The model which includes both Wenner (fig. 155) and dipole-dipole (fig 154) array seems to include more detail regarding the roots, whereas the dipole-dipole alone seems to show a stronger anomaly in the middle with the ones on the laterals appearing faint. The model which combines both Wenner and dipole-dipole arrays (fig. 156), seems to have a larger range of resistivity values and more variation inside the soil. In sum, all the models the roots seem to lose their shape and are far less distinguishable.

4.3.1.4. MODEL NO. 4

For this model, irregular shapes have been chosen to represent the roots (fig. 157). What is different for this model compared to the previous ones is that the roots represent resistivity values higher compared to the surrounding soil.

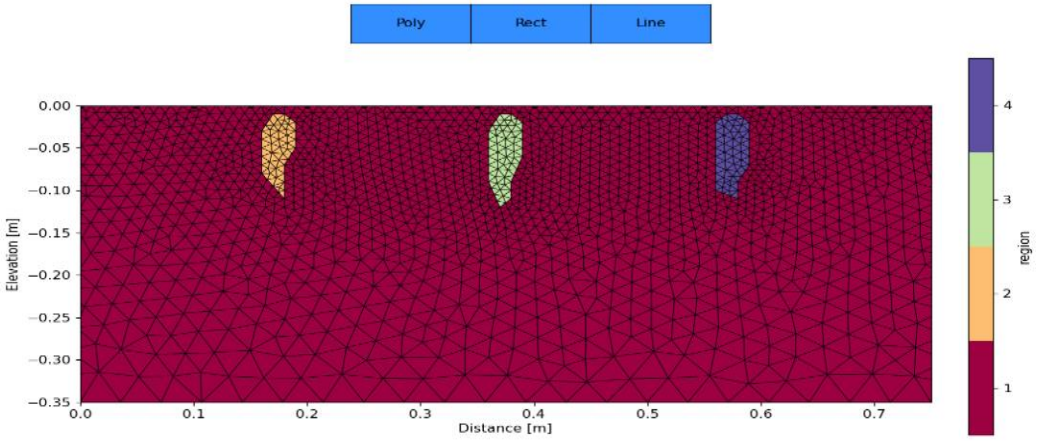

Figure 157. The forward model with fine mesh which was used with 2% noise.

The value for the soil (100 Ωm) represents the maximum value for the top soil as described by Telford (1976) and the value for the roots, 108.69 Ωm actually represents a value of a type of rooted soil described and tested in experiments by Amato (2009).

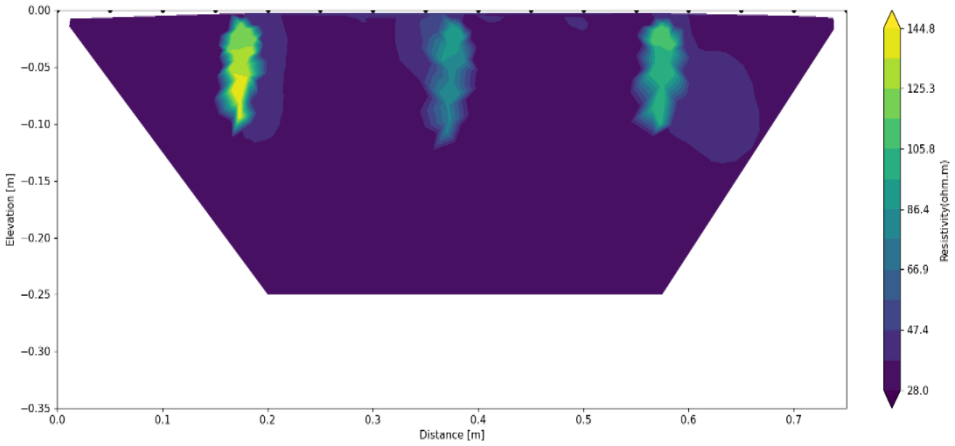

Figure 158. Forward model using the fine mesh and 2% noise and the Wenner array.

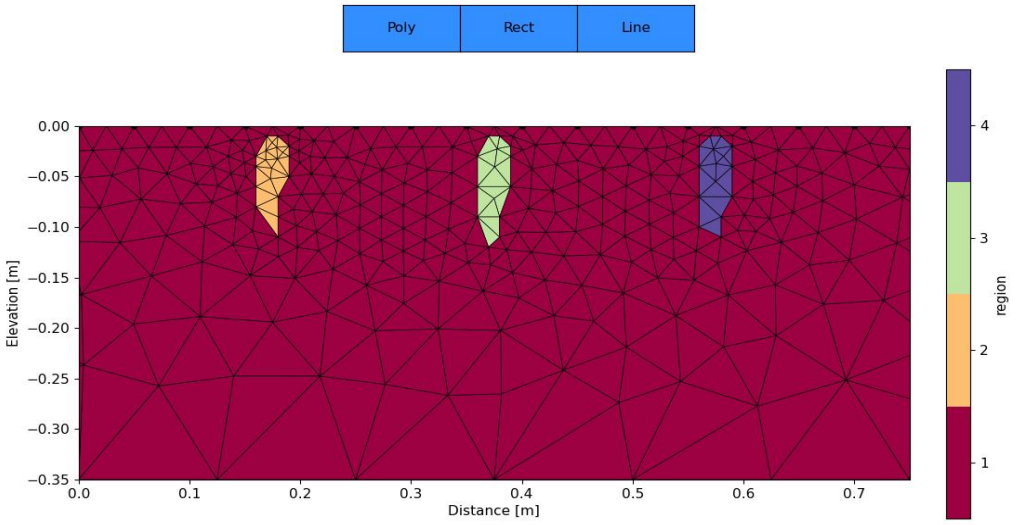

Figure 159. Image representing the coarse mesh for the forward model which was used with a 3% noise to create a model closer to the data from the experimental surveys.

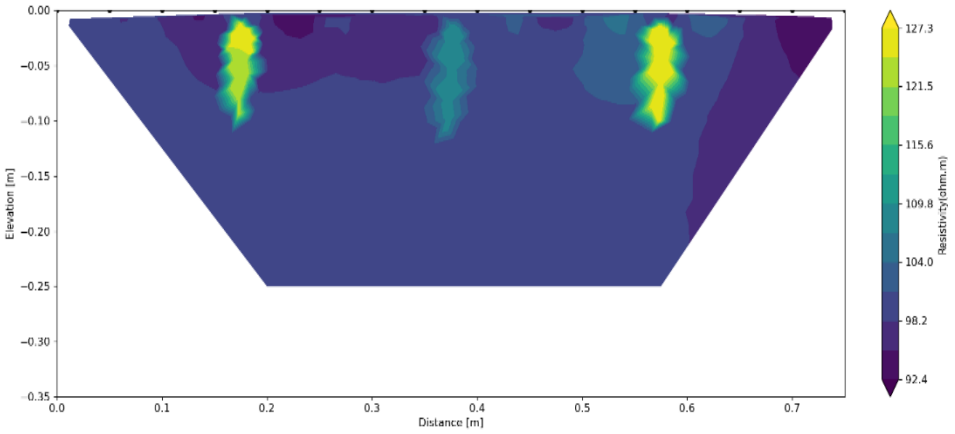

Figure 160. Forward model using the coarse mesh with 3% noise and Wenner array.

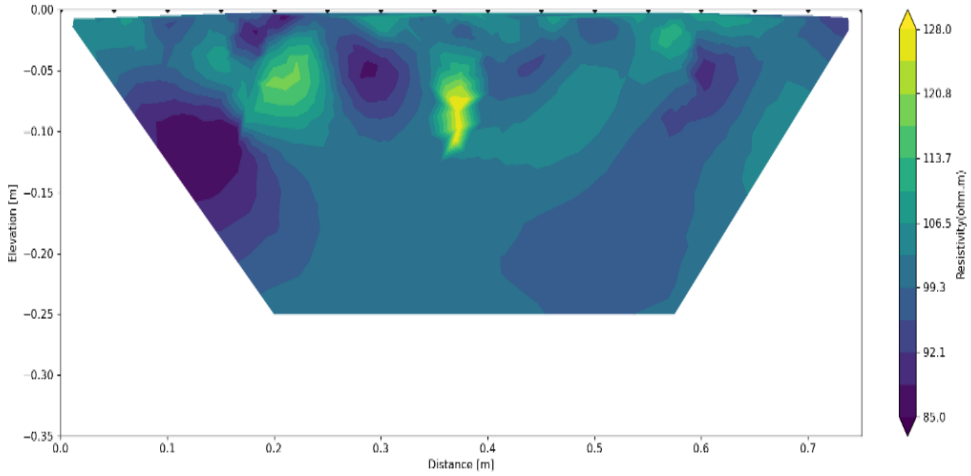

Figure 161. Forward model using the coarse mesh with 3% noise and dipole array.

Higher resistivity values of the roots compared to the soil seem to be less visible in the models using the dipole-dipole array (fig. 161-162), the root area losing their shape in some areas of the model, with Wenner (fig. 158, 160) showing more information regarding the roots position and shape. This is slightly different when compared to previous models where

usually the dipole-dipole array or the combination of dipole-dipole array and Wenner appeared to show more information.

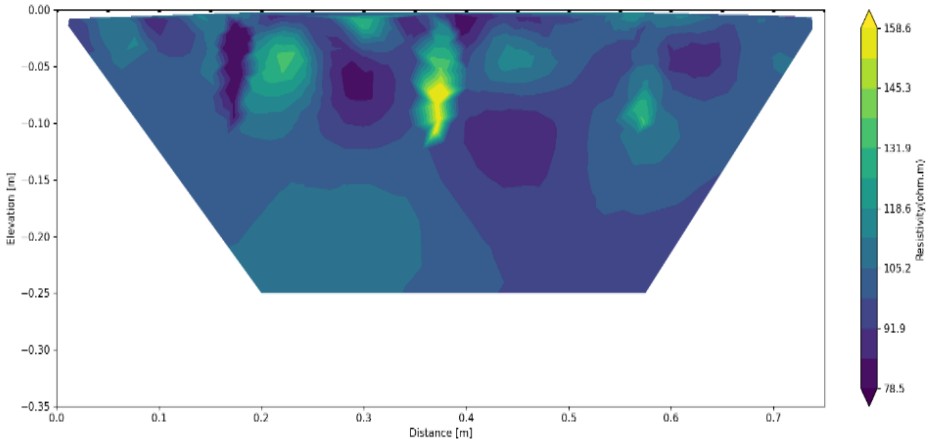

Figure 162. Forward model using the coarse mesh with 3% noise and a combination of both dipole-dipole and Wenner array.

4.3.1.5. MODEL NO. 5

The last model presents forward models with irregular shapes for the roots and resistivity values for the roots much higher compared to the resistivity of the soil. The resistivity value of the roots is the same as the one used for the previous model, 108.69 Ωm, and the resistivity of the soil is 34.89 Ωm which represents the soil described by Amato (2009) and used in the previous forward models. The forward models and types of meshes are similar to the ones presented in the 4th model. Having high resistivity roots is a common aspect, and according to Hagrey (2011) the value of the resistivity roots can go up to 500 Ωm, but here, a lower resistivity value was chosen, in order to try to get any variations from the models.

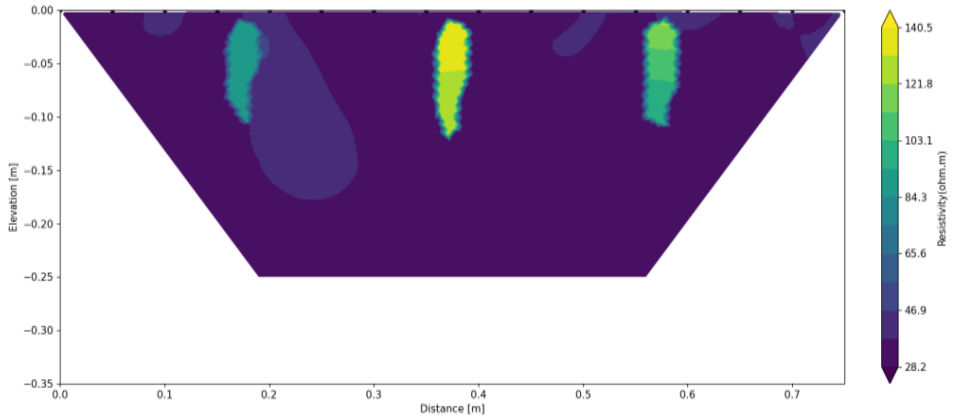

Figure 163. Forward model with fine mesh and 2% noise and the Wenner array.

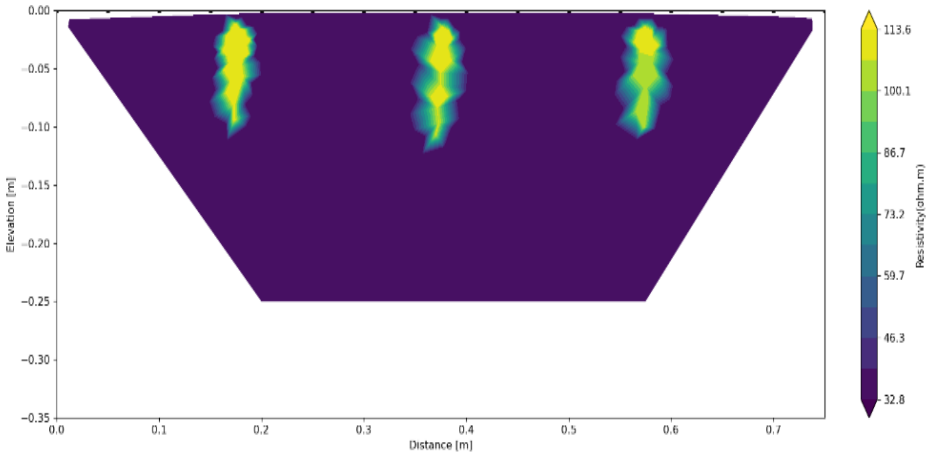

Figure 164. Forward model with coarse mesh and 3% noise and dipole-dipole array.

Most of the models look the same for different arrays (fig. 163-164), and the contrast is too strong to show any other information apart from the artefacts, even when inserting more noise.

Overall, the series of models has proven its utility in understanding the type of geoelectrical contrast that can be encountered. However, it is important to note that real data will not look

nearly as “clean” as these results, and the detectable contrasts are expected to be far less pronounced, if they are detectable at all.

4.3.1.6. MODEL NO. 6 - FOR PROTOTYPE EQUIPMENT

A resistivity model was created for a theoretical setting. The software packages used for the resistivity model consist of Gmsh software which has the role to create geometrical parameters and two types of mesh (triangular and rectangular).

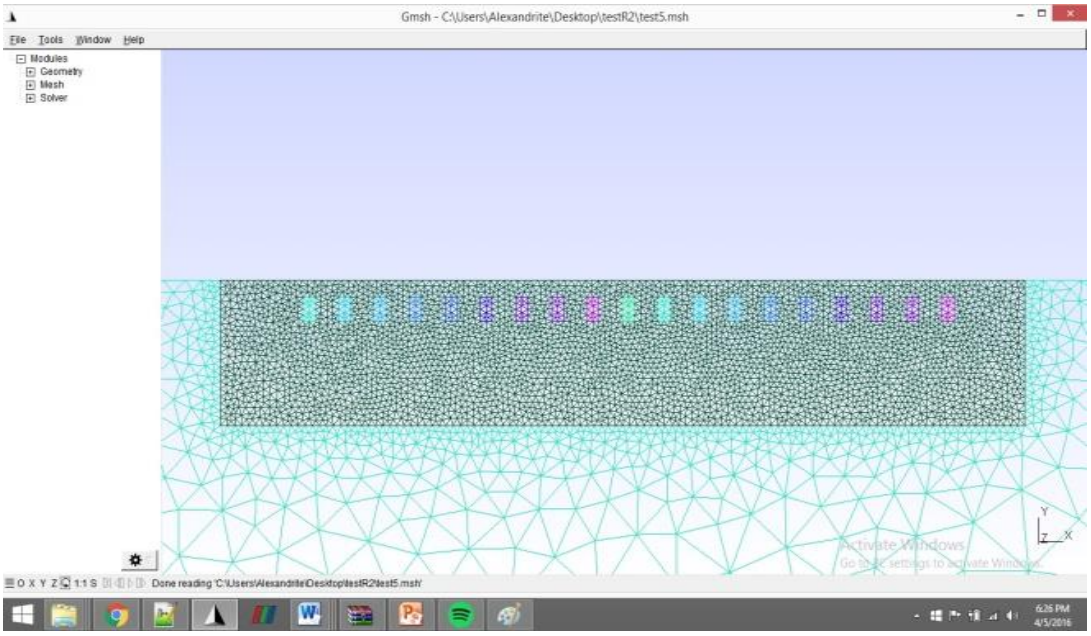

Figure 165. The generated mesh with Gmsh and the representation of the geometry of electrodes, the media, and the objects represented with rectangles.

And the second software is represented by the R2 software (Binley, 2012) for forward models which represents a precursor of the GUI interfaced software, ResIPy, which was used for data processing for other surveys and the previously presented models.

To be able to create a 2-dimensional finite element mesh for a forward resistivity model several steps were followed, like defining electrodes, mesh booundaries, creating lines and points and generating the mesh.

Before creating the triangular mesh a design of the environment and the objects needs to be created in order to define some important parameters. First step would be represented by defining the objects which will be introduced in the model, in this case is represented by 19 plant roots (only the root part) at a distance between them of 10 cm and a depth of 7 cm. These parameters were chosen based on the resistivity survey of the daffodils in natural environment. The roots are represented as rectangles of 5x10 cm and the distance between the electrodes was chosen to be of 20 cm with a number of 16 electrodes that cover a single profile with the length of 3m. Because the maximum depth usually in theory is used AB/2 but in reality is most of the time less than that (AB/4-AB/6) where AB are the electrodes that inject the current therefore sometimes are also named current electrodes or C1 and C2 for this model the chosen depth was set to be 60cm.

After clarifying the physical parameters the geometry of the model was created, starting with the electrodes, than the objects and ending with the boundary of the medium and also the Neumann boundary. After setting everything and following the steps as presented above a 2D triangular mesh for the whole model was generated.

The file generated by the Gmsh software (fig. 165) is in format .msh and needed to be converted in a .dat file format in order to be used in the R2 software.

In order to generate the actual forward models in R2, the software needs 2 or 3 files depending on the mesh type. The first file is the data input file R2.in which almost all of the information about the objective and electrodes can be found.

The variables used to define the file for creating the forward model contain information related to: the title of the file or header, mesh_type , scale, resistivity values and other specific parameters.

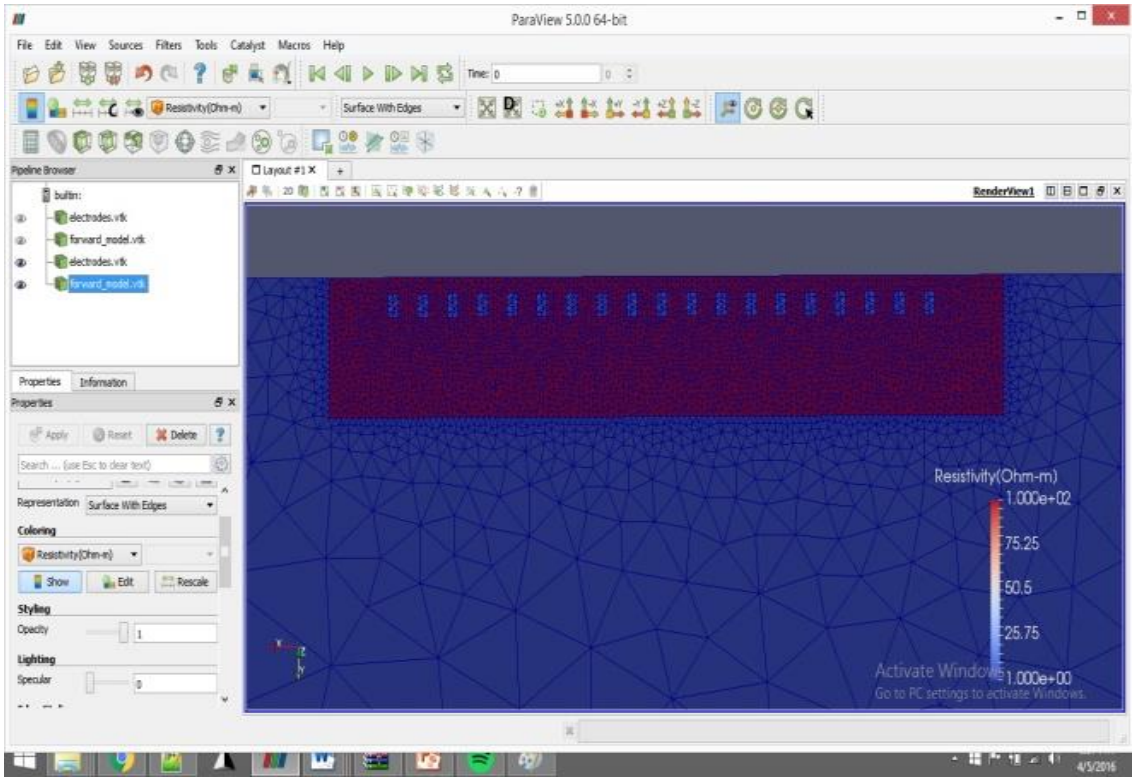

Figure 166. Representation of the forward model generated by R2 and visualized in ParaView. In the image we can also see the triangular mesh that overlays the model.

The files resulted from running the software, electrodes.vtk and forward_model.vtk can be opened in ParaView to visualize the forward model. The electrodes.dat file generates the value of the apparent resistivity at every measurement which will be used for generating the inverse model.

After the forward model was created (fig 166) the data needed to be inverted in order to get as close as possible to the data from a real setting and to better understand how the anomalies of the synthetic data behave and are to be visualized in a resistivity section when all the parameters and objectives are known. In order to do this a file needs to be created with apparent resistivity values at every given point, depending on the array type used.

For creating the inversion of the forward model, 3 files are to be used from which the previous protocol.dat and the mesh.dat which were described above and the R2.in file which represents the input file of the data and should contain the followings:

The triangular mesh and a mesh.dat file contain the coordinates and other details regarding the geometry of the model, described previously.

For the inverse model some extra parameters need to be defined, like data type (normal or logarithmic), tolerance, number of iterations, etc.

The last part of the line contains details about the electrodes and the triangular nodes where they are found in the triangular mesh.

The result data from this model (fig. 167) shows an area of low resistivity which coincides with the rectangles with low resistivity values, and the anomaly is surrounded by high

resistivity values which represent the value chosen for the environment. It can also be observed that on the right part of the survey there is an area with low resistivity values which appear much closer to the surface compared to the rest of the profile. This happens even though the rectangles have the same exact position and the same resistivity value.

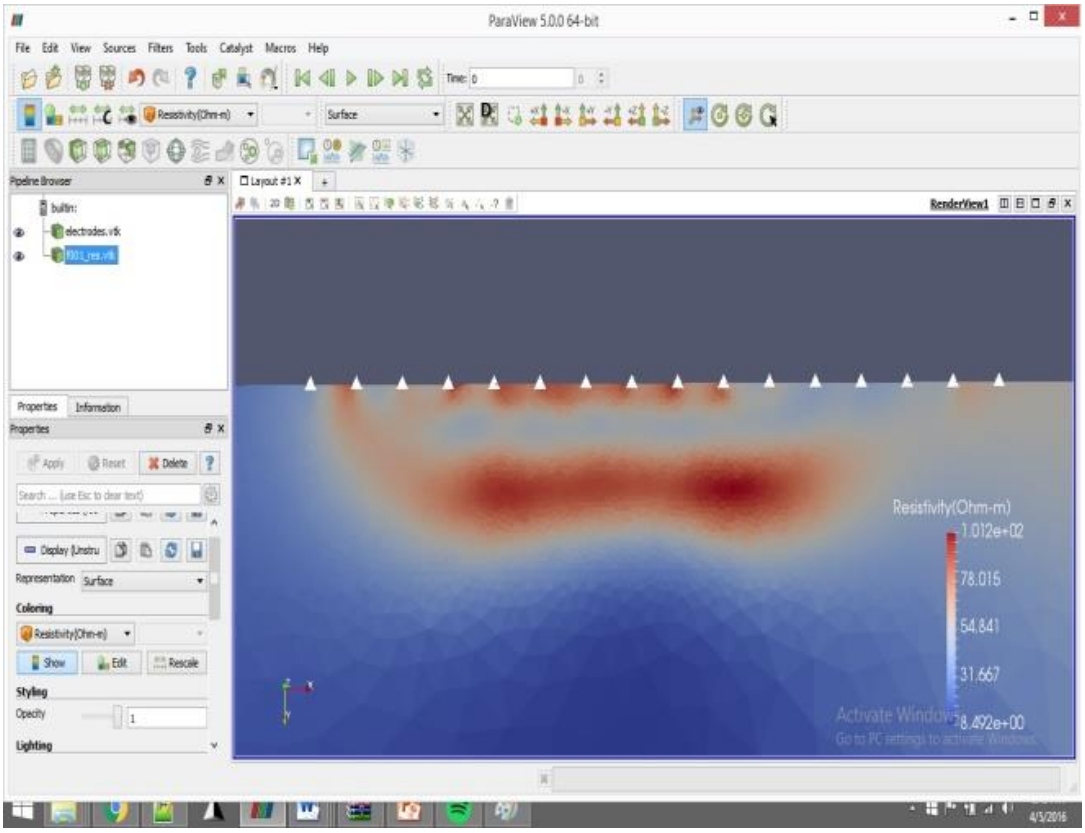

Figure 167. the result of the inverse model. With white triangles are represented the electrodes. Visualization using ParaView.

The effect may be due to the characteristics of the dipole-dipole array and represents very interesting information about how, even in a homogenous environment with known variables, the array affects the visibility and even position of different objects in the surveyed environment.

5. CONCLUSIONS AND DISCUSSION

5.1. DISCUSSION

As the thesis represents a multidisciplinary approach on the study of the agricultural roots with the use of geophysical methods, this section has been split in different sections focusing on different methods more in depth and to allow for an easier structure to facilitate readability.

Ground penetrating radar surveys

Using high frequency antennas is not very much covered in literature when it comes to the analysis and detection of plant roots of different origins and sizes, and the studies which use the higher frequencies usually stop at 2 GHz antennas, however applied to tree roots which are much coarser and definite in terms of shape, size and path (Cui *et al.*, 2010). Similarly the 1.5 GHz antenna has been used to show that in sandy soils it is possible to detect roots of as low as 2 to 3 mm in diameter when antennas of 1.5 GHz were used (Wielopoiski *et al.*, 2000), if the permittivity contrast exists, as it had been showed through repetitive studies on permittivity analysis (Mihai *et al.*, 2019) of the roots (of the trees) that is very easy for these to fall in ranges closer to those of many types of soils.

However in the thesis it a much higher frequency antenna has been tested, the 4 GHz antenna along with a 1.5 GHz antenna which was more often used in other studies, with the purpose of increasing the resolution of data collection and managing to catch as much information as possible. This has been proved to be challenging in both indoor and outdoor surveys. For

example, doing surveys close together is difficult in achieving a high level of precision and correlation of the data, especially on uneven ground which is the case in agricultural environments, and seeing the plant's root area is much harder because of ground unevenness.

Research shows that GPR can usually identify individual large, woody roots, focusing mainly on trees or plants with similar root types. For other plants, especially those common in agriculture with fibrous roots, the goal is more about finding root areas and correlating these with the position of the plants visible at the surface for validation, rather than identifying each root. However, these root zones are often just seen as areas with soil and roots or roots taking up water, not as living environments with complex interactions. For example, when it has been tested in the indoor settings which had three plants with one of the plants which died, it appears that even before and after watering the plant there still appears to be a significant reflective area appearing in the data for the areas which correspond to the living plants but not to the area where the plant which died is. It is known that organic matter increases the permittivity values of a soil, and even though the dead plant was adding to the organic matter content, the living roots were showing much higher permittivity values overall which were significant in the results. However a faint reflective area where the dead plant was slightly more highlighted in the vertical radargrams (even though at a low intensity by comparison), this was not as visible in the slices, indicating that the presence of the extra organic matter increases the permittivity but the moisture surrounding the root water uptake area plays a greater role when it comes to GPR surveys.

In both indoor and outdoor surveys it appears that, at least in the horizontal slices, the areas in the GPR data closer to the known position of the plants to highlight the root area by high reflectivity area, changing from positive to negative amplitude with depth.

Individual roots have not been identified; however root areas have been identified in the majority of the plants surveyed in both indoor and outdoor surveys. In some instances where the plants are really close together, they create a layer at the surface which is characterized by a higher reflectivity, visible in the vertical radargrams, and only occasionally isolated hyperbolas have been noticed (in the case of the Pampas grass for example) however this might be also cause by the proximity of the survey to the plants and issues with the top shielding of the antenna. However as profiles were carried out at different intervals, as there is higher reflectivity with an individual aspect corresponding to the position of the grass plants, these areas could be easily correlated.

The 4 GHz antenna shows much more attenuation below 3 ns however seems to provide useful data for the very top layer where usually the higher density of the root area is, however both antennas manage to show areas which can be described as root zone area corresponding to the surveyed plants.

Ground Penetrating Radar Synthetic Models

Creating synthetic models has the advantage of creating a variety of scenarios at a faster pace and testing different situation which can provide explanations for what can be seen in the actual surveys.

In this case testing different combination of soil/root permittivity allowed to better understanding in which instances there are higher chances of detecting root areas (or roots) in different types of soils. As it is already discussed many times in the literature review, from the point of view of the permittivity values it so happens that in many cases the roots share similar permittivity values to those of the soil they are surrounded in, therefore making their detection more difficult however there are instances and cases when the detection could be achieved given the "ideal" situation tested in the models. It appears that roots with higher permittivity compared to the soils have higher chances of detection with both 1.5 and 4 GHz antennas. Situations where the soil had a permittivity of 4.54 and the roots of 26 for example allowed for the best realistic situations in which these roots can be visibly detected. Therefore it can be said, at least from this point of view, that in brown soils with silty loam texture (similar to what has been used in the experiments for example) as described by Zhou et al, 2019, roots of 6 mm diameter roots (in this situation of a Sycamore tree as described by Mihai et. al 2019). Some cases do poorly, for example in situations where the same root is added to the same type of soil however the moisture content increases slightly from 18% to 26%, the root is almost undetectable.

There are also limitations to these models, as the soils used have been homogeneous which is rarely the case in natural environments, which have different porosity levels for example, or different types of organic matter, and so on.

However these examples provide a good overview on the potential detection of the roots in different types of soils from the point of view of the permittivity values.

Resistivity surveys

In terms of applying the resistivity method to the plant root detection and analysis, normally the simplified view in terms of resistivity values is that the dry roots appear to have higher resistivity values of about 100 Ωm whereas the more younger roots appear to have lower resistivity values of about 50 Ωm (al Hagrey, 2007), which is probably more valid for individual roots, however fibrous fine roots growing in the soil appear to behave differently than individual roots only. Therefore it has been observed that the root area in natural environment is very much related to the presence of water or recent precipitation. For example in the corn field it has been observed that the low resistivity anomalies correlated with the position of the plants whereas in most of the experiments carried out after the plants have been watered, it appears that the root area correlated with the known position of the plant at the surface highlights a lower resistivity area. The resistivity method is normally dependent on the content of water in pores and pore size and material fill, therefore this situation can be interpreted as follows: the region of soil which yields higher content of roots but very low water content would have a decreased resistivity value compared to the surrounding environment however when water has been previously present, and even after the drainage of the water from the root area, the roots tend to hold more water for longer period of time surrounding them (similar to what can be seen in the GPR data) there for decreasing the resistivity value in the soil mass.

However resistivity data appears to be affected by the size of the electrodes even more as the distance between the electrodes is as small as 5 cm, and their effect is more pronounced in the data processed with the ResiPy software compared to the Res2DINV software, affecting the

clarity and detection in many instances, of the topmost layer which normally contain the higher density of the roots (adapted this way due to irrigation practices).

It also appears in general that some arrays appear to add more uncertainty in the data than it is necessary, therefore arrays which contain more data points appear to have more artifacts and be more ambiguous in interpretation compared for example with the Wenner array which has a lower density of points.

In many instances the roots appear to not be exactly highlighted perfectly below the position of the known plant (even if the position of the roots has been validated by digging after the survey to properly locate them), an aspect which is influenced by the horizontal sensitivity of the specific arrays. It is also notable, the fact that in many instances the roots of the plants, especially as in agricultural environments (and it was replicated in the experimental settings) the plants are close together (in this case at 20 cm apart), they sometimes have a tendency of influencing the resistivity values, by lowering the overall value of the whole top layer – and this has been compared to surveys where there were no plants in the container, which shows the influence the roots have on the general resistivity of the soils.

Resistivity Synthetic Models

Creating synthetic resistivity models allows for a better understanding of different situations in which the roots can be detected in different types of soil and in which situations there appear to be limitations this specific method in terms of highlighting the root area.

Different shapes of the root area have been tested with slightly different sizes based on the observations made through the experiments. Having the option of adding noise to the data allows for the models to create images closer to what can be seen in the actual resistivity data collected in the experimental settings where normally the soil has a more homogeneous aspect compared to the natural environments. It appears in some of the models, depending also on the electrode array used not only on the values used, that some arrays would add more artefacts, whereas some arrays would connect the anomalies from the roots forming layer like anomalies (for example the dipole-dipole array). There are instances where the root areas are not very well represented in the resulted models, as it is the case when the resistivity value of the soil (34 Ωm)gets closer to that of the root (36 Ωm), however, most probably due to the fact that even though slightly but still a bit higher, the resistivity of the root still allow for identification of areas which are correlated with the position of the roots, however the shape looks slightly larger than the actual size of the roots and the anomalies' resistivity values are just slightly different than those of the layer they are forming.

Compared to the GPR models, where higher permittivity of the roots compared to that of the soil, would've made the detection of the roots almost not possible, in the case of the resistivity surveys, the roots still appear to be visible in both scenarios (soil < root < soil), as long as there is a slight contrast the resistivity would still detect and highlight a lower/higher resistivity area surrounding the root area, even if it means to change the resistivity of the whole layer in which these are found; and this even in homogeneous environments, so it is only sensible to assume how this are affecting data in natural environments which are more complex, even more.

Transparent soil

Using transparent soils in the experiments has shown some overall advantages in general related to the better correlation between the real position of the roots with the actual resistivity data. Even though challenging to handle the advantages are obvious, however it does have limitations in growing the plant in the transparent soil environment. As initially the intent was to grow the plant fully in the transparent soil container and to allow for a natural development of the roots, with the purpose of creating a setting which comes as close as possible to the natural environment, this couldn't be achieved due to the high water content and lack of nutrients. The initial intent would've been to control the chemical parameters of the soil with the use of fertilizers however that was not possible.

Creating the transparent soil especially at a lower cost has been proved to be challenging, especially as there are no protocols for this particular type of transparent soil with the purpose to grow plants in it and to conduct geophysical surveys. Normally the type of soil is being used in geotechnical studies (Iskander, 2011) and the way it is created is directly from the less available and more expensive powder form, whereas is this case because a more natural texture with different particle size was desired, perfecting the technique proved to be challenging and the addition of fertilizer affecting the stability of the final solution of the gel. Overall in the data it has been observed that from a geophysical point of view, in terms of resistivity values (as the transparent soil has been tested without any plants in it as well) range between 1-15 Ωm which by comparing to different types of soils and soil like materials from natural environments, it appears to hold a similar resistivity value to the wet-to-moist clayey and silty soils (Hunt, 2005) therefore not negatively impacting the surveys.

Comparing the data from the transparent soil experiments with plants to those without plants, there seem to be an interesting aspect appearing – the presence of the plant roots appears to allow for the appearance of a layer of low resistivity which corresponds with the position of the plants, an aspect similar to what has been observed in the synthetic models, especially as the transparent soil represents an environment, which from the point of view of the resistivity values comes as close as possible to a homogeneous environment (similar to those in the synthetic models.

Therefore from a general geophysical perspective it appears that the roots of the agricultural (and some ornamental) plants have a more complex relationship to the soil, moisture and surrounding environment in general. And even though root zone areas have been detected and described from both points of view (resistivity and ground penetrating radar methods) it is significant that these are considered active environments which appear to change characteristics and reflectivity in the case of GPR surveys, and resistivity values in the case of geoelectrical surveys but taken into consideration as a whole system rather than individual roots.

5.2. CONCLUSSIONS

In general, geophysics can be applied in agriculture for a number of different purposes, but when it comes to plant root detection and characterization, the amount of information that geophysical methods can provide is not entirely clear. In addition, data from indoor,

controlled environments (as is often the case in the published literature) can create misleading, overly optimistic expectations.

The geophysical method which can provide the best amount of detail in general is GPR especially with the increase in antenna frequency (1.5 GHz and 4 GHz antennas used). However, in addition to the well-known challenges of GPR (such as its inability to provide clear data in some types of soil like clays for example), agricultural surveys provide other extra challenges as well. Some of these are practical. For instance, carrying out closely spaced profiles, especially while manoeuvring the antenna on an uneven soil surface, can be challenging, and these irregularities can affect the data. With surveys carried out in time mode, ensuring an even speed by hand can be challenging, while with surveys carried out in distance mode, the wheels from the antennas proved to be affected by very small changes in the micro topography of the of the area. Uneven soil also caused imperfect antenna coupling, which affects the data even more, making it harder to achieve high levels of precision and to correlate the anomalies in the data with the actual location of the individual plants.

In the literature it has been show that resolving individual roots is generally possible in the case of coarse, woody roots, when applying the GPR method, most of the studies focusing on trees or on plants (even though from the agricultural spectrum) with non-fibrous roots (which are more common for a large variety of agricultural plants). In the other cases, the main focus would be detecting the root area rather than resolving individual roots, however simplifying what the root zone area represents, and being treated as a mass or of only soil and roots, or roots absorbing water, not as active biological environments with complex interactions.

Unlike individual coarse, woody roots that generally appear as hyperbolae on radargrams, the root areas in more fibrous root systems, often appear in the form of a higher reflective layer or area in the vertical radargrams, and as high reflective areas in slices which appear to be changing from positive to negative amplitudes with depth. As the roots areas usually hold more water around them, it has been observed that these reflections coincide with the position of the plants; therefore the specific high reflective areas could be actually due to the increase in moisture content in the mass of soil in the top layer where the root density is high. Controlled environment experiments (where the position of the plants and roots, relative to the GPR profile, was known) helped in showing what type of radargram responses root areas can produce, which facilitated the detection of such signal in natural environments. Measurements carried out in a laboratory setting also helped establish a radargram baseline that was useful in understanding and interpreting data from realistic situations.

However, in real-world environments, it was much more difficult to visualize the root area of the plants, due to slight inhomogeneities from the ground, buried objects such as rocks or roots from other plants, organic matter, and other sources of noise. While the overall quality of the data and the signal-to-noise ratio can be improved through suitable processing, the above-mentioned elements can still affect the quality of the data when surveying with high-frequency antennas. The 1.5-4 GHz frequency interval appears to be a useful one for the task of studying agricultural plant roots. The antennas work well to complement each other: the 4 GHz antenna has better resolution, but it is more vulnerable to any inhomogeneities or sources of noise and more prone to signal attenuation.

Therefore in most surveyed areas, a root area could be detected, even in the case of very fine and condensed roots (as was the case with grass or wheat plants, where both antennas showed the area of the roots) which appears to correspond to the position of the plants and the roots; however, if the plants are too closely spaced to one another, then it can becomes impossible to differentiate between the effect of the roots of individual plants (for instance, in surveyed areas where plants were spaced at a distance of around 10 cm or even less; even in these cases, it was impossible to detect some elements of a root area, though it was not clear which plant was producing the effect) these creating a higher reflectivity layer in the radargrams. Furthermore, it is not always clear if this area represents the roots themselves or is rather an area where the roots are changing the physical parameters of the soil around them. The root area differentiates usually as a humid area compared to the surrounding environment, which can be an important aspect in delimitating the root area in real-world situations.

Compared to the GPR surveys, the ERT surveys proved to be much more flexible without being significantly affected by the rough surface of the agricultural top soil. Using different types of electrodes with a small diameter 4-5 mm made it possible to reduce the distance between the electrodes, going down to as little as 5 cm. At the same time, however, using such a short distance between the electrodes made the data challenging. The conventional Resistivity Inversion software (Res2DINV) tended to produce inversions with large errors, while the open-source software ResIPy tended to produce an electrode effect that is visible on the resistivity sections, which affected the top 2-3cm of the resistivity imaging profile even for the electrodes with the diameter as low as 2.5mm (the electrodes used in the surveys from the tube with one profile of electrodes, filled with soil).

All types of trialled arrays had both advantages and disadvantages, and it is not always clear which one is recommended; for example – if data acquisition time is a constraint, then Wenner could be a consideration as it has fewer datapoints and provides comparable quality, and it appeared highlight overall areas of interest related to the known position of the plant. The optimized array used in this study, added extra points of measure, compared to the Schlumberger survey, but while creating the inversion profiles, not in all cases the data showed useful information compared to Schlumberger and Dipole-Dipole data. Therefore in this case, where the electrodes are close together and the anomalies and objective are on the very low size, more data points does not necessarily bring more useful data, rather affect the data compared to the more simple arrays.

Having a lab-built relay board which was connected to the commercial geophysical equipment, offered an advantage in the flexibility of creating the arrays, and also in programming different parameters like acquisition time and order of the arrays to be measured, allowing for consecutive surveys to be carried out automatically, as well as flexibility in choosing pairs of electrodes in any configuration possible. The electrical resistivity meter prototype, proved to offer valuable information, even though the data presented a high degree of difficulty in processing. The high advantage of the equipment was the fact that it highly reduced the acquisition time significantly compared to commercially available equipment, and providing large sets of data acquired at different frequencies and with a multitude of combinations of arrays at the same time. However, more surveys in the same setting, and comparison to commercial equipment will be needed in order to highlight the degree of quality of the data.

Unlike individual tree roots, which produce resistive anomalies as described in the literature, the data presented in the thesis showed that there is a level of complexity to the understanding of how the agricultural plants and their roots (and root areas) behave from the point of view of the resistivity surveys. In many instances the plant roots often appear in the resistivity sections as a conductive area, or a low resistivity area, which is reasonable considering the root water uptake area which usually surrounds the roots. In most surveys carried out, this seems to be the case in wet soils, or soils that have been irrigated recently. This is likely due to the fact that the plant roots used in the experiment represent very fine roots which create an absorption area around them, keeping moisture, lowering the resistivity of the surrounding material (soil). However, in very dry soils, where there has been no prior watering or rain, and no moisture around, the effect of the roots themselves becomes more pronounced, and the root area starts to appear as a more resistive anomaly. It is therefore important to have an understanding of the soil context in which the survey is carried out.

The type of the soil used in experiments also played a very important role in defining the root area in the resistivity sections. For example soils containing a large amount of organic matter made the data interpretation more difficult compared to the more resistive and compact soil with a lower amount of organic matter, most probably due to the overall increase in organic matter throughout the soil material which doesn't leave room for contrasts.

In most cases, the type of algorithm used for geoelectrical inversion produced similar results, but in some cases it seemed that the RES2DINV and RES3DINV had the highest percentage of error when calculating the inversion models, whereas RESIPY and BERT which are on the open-source educational side of software, sometimes had lower errors, most probably due to

the discretization models used. BERT software proved to be a useful option in this kind of study, where it allowed for flexibility in analysing non-conventional data, and works very well with different types of non-standard arrays which were explored in the thesis. Experimental, lab-based surveys also proved a useful tool for geoelectrical measurements, and yet again, the selection of soil is important. In addition to ERT, profiling (with methods similar to the twin probe array used in archaeology) may be useful, though this was only briefly explored.

A novel approach in regards to the soil use for geoelectrical surveys is represented by the creation and use in the experiments of the transparent soils. The gel-like soil, allowed flexibility regarding the position of the plants and allowed the survey data to be better correlated with the actual position of the plant roots, in the indoor experimental setting.

After experimenting with different types of potential transparent soils used in other areas of research, it has been concluded that the transparent soil made from the super absorbent polymers commercially known as aqua beads, represents a more suitable environment for growing the plants in order to carry geophysical surveys. The gel like solution resulted from preparing the transparent soil from the aqua beads mimics very closely the soil structure, allowing the plants to develop the roots in a way closer to the natural environments. However due to the lack of nutrients in the transparent soil there is a necessity for fertilizer use in order to keep the plants healthy for longer periods of time which comes with its own challenges. The use of fertilizer has been proved to be difficult in this situation, as the type of fertilizer used reacted with the transparent gel solution and separated the water from the aqua-beads dust, therefore not allowing for a full development of the roots in this environment as desired.

In terms of geophysical properties of the transparent soil, as this has only been used in the geolectrical surveys, resulted from the numerous collected data that the transparent soil possess similar resistivity values to what appear to be wet clays.

Overall the transparent soil proved to be very useful in the study, as it allowed better correlation between the resistivity data and the actual position of the plants. It also allowed flexibility when working with the plants, as these could be arranged in any position with the roots spread in the soil as wished, and a great novel environment to be explored in future experimental geophysical surveys with great potential.

Synthetic models, both in ERT and in GPR, represent an important tool for this type of study. A great range of situations and scenarios can be simulated with relative ease, offering information regarding the type of contrast that can be detected, the type of signal that can be expected, and the limitations of the methods. However, it is important to note that these are ideal situations, and even with the addition of distortions such as added noise and different discretisation models, they are still much higher quality than what can be expected from real data. Overall the models managed to show a large variety of instances and to test different combinations of root/soil properties, be it permittivity in the case of GPR data or resistivity. Even though, at least in the case of the resistivity survey, many types of root shapes have been used, the models created for the soil are simplistic and overall homogenous, but even so they manage to highlight some features which were noted in the actual surveys as well – represented by roots which affect a whole layer in terms of resistivity values in some instances, and to project the influence of resistivity array and the artefacts included in the data

with such small differences between resistivity values and distances between electrodes adding ambiguity and offering explanations for the data collected in real world environments.

Creating electrical devices, like the IoT automatic irrigation system had the advantage of spreading equal amounts of water on the surface of the soil in the experimental setting, which played an important role in removing uncertainties that might have occurred due to the unequal spread and quantity of the water in the indoor environment. The other part of the system consisted of the humidity sensor, which offered information about the level of dryness of the soil or humidity, which helped with interpreting the geophysical data. Incorporating these devices and resulted advantages and data, allowed for more controlled surveys and better interpretation of the resulted geophysical data.

Overall it can be concluded that when it comes to using geophysical methods, more specifically resistivity and ground-penetrating-radar, in real world agricultural settings for the plant root detection and analysis, the mind-set in which this is treated in the literature should be shifted from the idea that the plant roots and plant environments are static objects of certain shapes, sizes and parameters (just like objects in civil engineering for example), as it was shown and treated in most of the geophysical studies on plant roots; but rather, the plant root area especially on smaller, agricultural (and even some ornamental plants as it was shown in the paper) in actual agricultural environments represents a living active environment, which changes constantly depending on the conditions in the soil and environment. The focus should be made on the root zone area rather than the actual individual roots, a level which proved to be difficult to achieve even in indoor experimental and controlled environments, and more than the root zone it should be treated as a root zone in certain specific conditions which, from

the point of view of geophysical methods, their parameters not only change with the conditions in soil, but the roots themselves change the parameters of the soil they are part in depending on how dense they are how wet or dry the soil is at the moment of surveying; and in many instances both the roots and the surrounding soil share similar geophysical parameters. All of these can be better explored through a multidisciplinary approach which has also been approached in this thesis, for analysing and finding solutions for a very complex subject, widely debated and not fully understood in the literature.

5.3. FUTURE WORK

Much of the uncertainty in this field stems from a limited understanding of the relevant biophysical properties of plant roots. The lack of direct permittivity or geoelectrical measurements directly on the roots complicates the assessment of their geophysical parameters and soil-water-root relationship. Moreover, the complex geometry of plant roots introduces additional challenges. Therefore improving and prioritising direct root measurements could significantly improve geophysical survey insights.

For resistivity surveys specifically, exploring optimised arrays and custom-made equipment is a promising direction. Moreover, establishing larger and more voluminous indoor environments could play a role in improving boundary effects encountered in the indoor surveys in this study. Further investigation into geoelectrical mapping and non-contact resistivity measurements is also important, offering a non-invasive approach to data collection, as well as complementing these with less conventional geophysical methods, such

as TDR surveys, could bring additional valuable insights, helping with a better understanding of the GPR and resistivity data.

Investigating various soil types with detailed compositional analysis could refine data quality and interpretation accuracy as well as comprehensive bio-chemical and physical soil analyses could significantly improve the application of geophysical methods, lowering their limitations and improve applicability.

The exploration of transparent soil as a material for testing geophysical methods represents a novel approach, which could better be improved and experimented with for improved testing protocols, not only limited to applications on better correlations between the plant roots and geophysical anomalies, but with any other types of objectives and geophysical anomalies.

As IoT automation continues to develop, using smart sensors to monitor geophysically-relevant parameters or even carry out geophysical measurements could be an important development. For the acquisition of GPR surveys to improve precision, an automation using IoT devices or other similar equipment likely represents the next step, in which the GPR antennas are carried at constant speed and in automated paths to improve precision. This way it is possible to remove the user errors and improve the clarity and quality of the data.

Currently, efforts are directed towards developing more accurate 3D root models which closely mimic the real-world parameters and geometry of roots, aiming to refine the geophysical models created in this study. Integrating plant root modelling with geophysical techniques, alongside machine learning and automation, presents numerous opportunities for a deeper comprehension of this complex but fascinating issue.

REFERENCES

Allred, B. *et al.* (2016) 'Agricultural Geophysics', pp. 1–4. doi: 10.4133/sageep.29-001.

Amato, M. *et al.* (2008) 'In situ detection of tree root distribution and biomass by multi-electrode resistivity imaging', (Pollen 2007), pp. 1441–1448.

Amato, M. *et al.* (2009) 'Multi-electrode 3D resistivity imaging of alfalfa root zone', *European Journal of Agronomy*, 31(4), pp. 213–222. doi: 10.1016/j.eja.2009.08.005.

Amato, M. *et al.* (2011) 'In situ detection of tree root distribution and biomass by multielectrode resistivity imaging', *Tree Physiology*, 28(8), pp. 1441–1448. doi: 10.1093/treephys/28.8.1441.

Anderson, W. P. and Higinbotham, N. (1976) 'Electrical resistances of corn root segments.', *Plant physiology*, 57(2), pp. 137–41. Available at: http://www.ncbi.nlm.nih.gov/pubmed/16659437%0Ahttp://www.pubmedcentral.nih.gov/articlerender.fcgi?artid=PMC541978.

André, F. *et al.* (2012) 'High-resolution imaging of a vineyard in south of France using ground-penetrating radar, electromagnetic induction and electrical resistivity tomography', *Journal of Applied Geophysics*, 78, pp. 113–122. doi: 10.1016/j.jappgeo.2011.08.002.

Benedetto, A., Tosti, F., Bianchini Ciampoli, L., D'Amico, F. D. (2016) 'An overview of ground-penetrating radar signal processing techniques for road inspections', Elsevier, pp. 1–26.

Annan, A. P. (2009) *Ground Penetrating Radar (GPR) Principles*, *Ground Penetrating Radar*

Theory and Application. doi: 10.1016/B978-0-444-53348-7.00001-6.

Archie, G. E. (2003) 'The Electrical Resistivity Log as an Aid in Determining Some Reservoir Characteristics', *SPE Reprint Series*, (55), pp. 9–16. doi: 10.2118/942054-g.

Attia, S. (2007) 'Geophysical imaging of root-zone , trunk , and moisture heterogeneity', 58(4), pp. 839–854. doi: 10.1093/jxb/erl237.

Benedetto, A. (2010) 'Water content evaluation in unsaturated soil using GPR signal analysis in the frequency domain', *Journal of Applied Geophysics*. Elsevier B.V., 71(1), pp. 26–35. doi: 10.1016/j.jappgeo.2010.03.001.

Bengough, A. G. *et al.* (2006) 'Root responses to soil physical conditions; growth dynamics from field to cell', *Journal of Experimental Botany*, 57(2 SPEC. ISS.), pp. 437–447. doi: 10.1093/jxb/erj003.

Besson, A. *et al.* (2004) 'Structural heterogeneity of the soil tilled layer as characterized by 2D electrical resistivity surveying', *Soil and Tillage Research*, 79(2 SPEC.ISS.), pp. 239–249. doi: 10.1016/j.still.2004.07.012.

Binley, A. and Slater, L. (2020) *Resistivity and Induced Polarization*, *Resistivity and Induced Polarization*. doi: 10.1017/9781108685955.

Blanchy, G. *et al.* (2020) 'ResIPy, an intuitive open source software for complex geoelectrical inversion/modeling', *Computers and Geosciences*. Elsevier Ltd, 137, p. 104423. doi: 10.1016/j.cageo.2020.104423.

Borden, K. A. *et al.* (2014) 'Estimating coarse root biomass with ground penetrating radar in a tree-based intercropping system', *Agroforestry Systems*, 88(4), pp. 657–669. doi:

10.1007/s10457-014-9722-5.

van Breemen, N., Mulder, J. and Driscoll, C. T. (1983) ‘Acidification and alkalinization of soils’, *Plant and Soil*, 75(3), pp. 283–308. doi: 10.1007/BF02369968.

Brillante, L. *et al.* (2015) ‘The use of soil electrical resistivity to monitor plant and soil water relationships in vineyards’, *Soil*, 1(1), pp. 273–286. doi: 10.5194/soil-1-273-2015.

Bucciarelli, B. *et al.* (2021) ‘Phenotyping seedlings for selection of root system architecture in alfalfa (Medicago sativa L.)’, *Plant Methods*. BioMed Central, 17(1), pp. 1–13. doi: 10.1186/s13007-021-00825-3.

Butnor, J. R. *et al.* (2001) ‘Use of ground-penetrating radar to study tree roots in the southeastern United States’, *Tree Physiology*, 21(17), pp. 1269–1278. doi: 10.1093/treephys/21.17.1269.

Butnor, J. R. *et al.* (2003) ‘Utility of Ground-Penetrating Radar as a Root Biomass Survey Tool in Forest Systems’, *Soil Science Society of America Journal*, 67(5), pp. 1607–1615. doi: 10.2136/sssaj2003.1607.

Christensen, N. B. and Sørensen, K. (2001) ‘Pulled array continuous electrical sounding with an additional inductive source: An experimental design study’, *Geophysical Prospecting*, 49(2), pp. 241–254. doi: 10.1046/j.1365-2478.2001.00257.x.

Cigna, F. *et al.* (2012) ‘Remote Sensing of Environment Monitoring land subsidence and its induced geological hazard with Synthetic Aperture Radar Interferometry : A case study in Morelia , Mexico’, 117, pp. 146–161. doi: 10.1016/j.rse.2011.09.005.

Conyers, L.B. (2004) Ground-Penetrating Radar for Archaeology, Alta Mira Press, Walnut

Creek, 203 p.

Corwin, D. L. and Lesch, S. M. (2005) ‘Apparent soil electrical conductivity measurements in agriculture’, 46, pp. 11–43. doi: 10.1016/j.compag.2004.10.005.

Daniels, D.J. (2004) Ground Penetrating Radar, 2nd edition. IET Radar, Sonar, Navigation and Avionics Series 15.

Dahlin, T. (1996) ‘2D resistivity surveying for environmental and engineering applications’, *First Break*, 14(7), pp. 275–283. doi: 10.3997/1365-2397.1996014.

Dahlin, T. and Zhou, B. (2004) ‘A numerical comparison of 2D resistivity imaging with 10 electrode arrays’, *Geophysical Prospecting*, 52(5), pp. 379–398. doi: 10.1111/j.1365-2478.2004.00423.x.

Degroot-Hedlin, C. and Constable, S. (1990) ‘Occam’s inversion to generate smooth, two-dimensional models from magnetotelluric data’, *Geophysics*, 55(12), pp. 1613–1624. doi: 10.1190/1.1442813.

Delgado, A. *et al.* (2017) ‘Ground penetrating radar: A case study for estimating root bulking rate in cassava (Manihot esculenta Crantz)’, *Plant Methods*. BioMed Central, 13(1), pp. 1–11. doi: 10.1186/s13007-017-0216-0.

de Dorlodot, S. *et al.* (2007) ‘Root system architecture: opportunities and constraints for genetic improvement of crops’, *Trends in Plant Science*, 12(10), pp. 474–481. doi: 10.1016/j.tplants.2007.08.012.

Downie, H. *et al.* (2012) ‘Transparent Soil for Imaging the Rhizosphere’, *PLoS ONE*, 7(9), pp. 1–6. doi: 10.1371/journal.pone.0044276.

Drake, T. *et al.* (2016) 'The cultivation of arabidopsis for experimental research using commercially available peat-based and peat-free growing media', *PLoS ONE*, 11(4), pp. 1–16. doi: 10.1371/journal.pone.0153625.

Duarte, M. D. R. and Debur, M. D. C. (2004) 'Characters of the leaf and stem morpho-anatomy of Alternanthera brasiliana (L) O. Kuntze, Amaranthaceae', *Revista Brasileira de Ciencias Farmaceuticas/Brazilian Journal of Pharmaceutical Sciences*, 40(1), pp. 85–92. doi: 10.1590/S1516-93322004000100013.

S.A. Elias (2013) Geosciences: The Study of the Solid and Molten Parts of the Earth and How They Interact with Our Environment, Reference Module in Earth Systems and Environmental Sciences, Elsevier. https://doi.org/10.1016/B978-0-12-409548-9.05354-9.

Fageria, N. K., Baligar, V. C. and Li, Y. C. (2008) 'The role of nutrient efficient plants in improving crop yields in the twenty first century', *Journal of Plant Nutrition*, 31(6), pp. 1121–1157. doi: 10.1080/01904160802116068.

Fan, C. C. and Chen, Y. W. (2010) 'The effect of root architecture on the shearing resistance of root-permeated soils', *Ecological Engineering*. Elsevier B.V., 36(6), pp. 813–826. doi: 10.1016/j.ecoleng.2010.03.003.

Galagedara, L. W. *et al.* (2005) 'Field studies of the GPR ground wave method for estimating soil water content during irrigation and drainage', 301, pp. 182–197. doi: 10.1016/j.jhydrol.2004.06.031.

Gebbers, R. and Adamchuk, V. I. (2010) 'Precision Agriculture and Food Security', *Science*, 327(5967), pp. 828 LP – 831. doi: 10.1126/science.1183899.

Geuzaine, C. (2009) ‘Gmsh : A 3-D Finite Element Mesh Generator with Built-in Pre- and Post- Processing Facilities Gmsh : a three-dimensional finite element mesh generator with built-in pre- and post-processing facilities’, (February 2021). doi: 10.1002/nme.2579.

Ginsburg, H. and Laties, G. G. (1973) ‘Longitudinal electrical resistance of maize roots’, *Journal of Experimental Botany*, 24(6), pp. 1035–1040. doi: 10.1093/jxb/24.6.1035.

Goodman, D. *et al.* (2006) ‘Correcting forTopographyand theTilt of Ground-penetrating Radar Antennae’, 161(March), pp. 157–161. doi: 10.1002/arp.284.

Guo, S. *et al.* (2022) ‘Root System Architecture Differences of Maize Cultivars Affect Yield and Nitrogen Accumulation in Southwest China’, *Agriculture (Switzerland)*, 12(2). doi: 10.3390/agriculture12020209.

Hei, V. A., Fisher, A. N. D. J. I. and Friend, D. J. C. (1967) ‘Daylength on the’, 45(526).

Hirano, Y. and Dannoura, M. (2009) ‘Limiting factors in the detection of tree roots using ground-penetrating radar’, pp. 15–24. doi: 10.1007/s11104-008-9845-4.

Huisman, J. A. *et al.* (2001) ‘Soil water content measurements at different scales : accuracy of time domain re ¯ ectometry and ground-penetrating radar’, 245, pp. 48–58.

Hunt, R. E. (2005), “Geotechnical Engineering investigation” Hand book second edition, pp 56-63.

Jol, H. M. and Smith, D. G. (1995) ‘Ground penetrating radar surveys of peatlands for oilfield pipelines in Canada’, *Journal of Applied Geophysics*, 34(2), pp. 109–123. doi: 10.1016/0926-9851(95)00018-6.

Jones, S. B., Wraith, J. M. and Or, D. (2002) ‘Time domain reflectometry measurement principles and applications’, *Hydrological Processes*, 16(1), pp. 141–153. doi: 10.1002/hyp.513.

Khele, V. V. N., Shaikh, A. A. and Ramshetti, R. S. (2009) ‘Dielectric properties of black soil with organic and inorganic matters at microwave frequency’, *Indian Journal of Radio and Space Physics*, 38(2), pp. 112–115.

Klotzsche, A. *et al.* (2018) ‘Measuring Soil Water Content with Ground Penetrating Radar : A Decade of Progress’, (2017). doi: 10.2136/vzj2018.03.0052.

Koganti, T. *et al.* (2017) ‘Mapping cation exchange capacity using a Veris-3100 instrument and invVERIS modelling software’, *Science of the Total Environment*, 599–600, pp. 2156–2165. doi: 10.1016/j.scitotenv.2017.05.074.

Kohlbeck, F. and Mawlood, D. (2009) ‘Computer program to calculate resistivities and layer thicknesses from Schlumberger soundings at the surface, at lake bottom and with two electrodes down in the subsurface’, *Computers and Geosciences*, 35(8), pp. 1748–1751. doi: 10.1016/j.cageo.2009.03.001.

Kufa, T. and Burkhardt, J. (2013) ‘Studies on root growth of Coffea arabica populations and its implication for sustainable management of natural forests’, *Journal of Agricultural and Crop Research*, 1(1), pp. 1–10. Available at: http://sciencewebpublishing.net/jacr/archive/2013/July/pdf/Kufa and Burkhardt.pdf.

Kumar, V. *et al.* (2005) ‘Cover crop residues enhance growth, improve yield, and delay leaf senescence in greenhouse-grown tomatoes’, *HortScience*, 40(5), pp. 1307–1311. doi:

10.21273/hortsci.40.5.1307.

Lawal, A. U., Nasiru, R., and Garba, N. N. (2019) ‘Correlation Between Dielectric Constant and Ph for Soil Types in the Southern Part of Katsina State, Nigeria’, *FUDMA Journal of Sciences (FJS*, 3(2), pp. 364–369.

Leitner, D. *et al.* (2014) ‘Recovering root system traits using image analysis exemplified by two-dimensional neutron radiography images of lupine’, *Plant Physiology*, 164(1), pp. 24–35. doi: 10.1104/pp.113.227892.

Liu, X., Dong, X. and Leskovar, D. I. (2016) ‘Ground penetrating radar for underground sensing in agriculture : a review **’, (2008), pp. 533–543. doi: 10.1515/intag-2016-0010.

Loke, M. H. (2013) ‘Tutorial : 2-D and 3-D electrical imaging surveys’, *Geotomo Software Malaysia*, (July), p. 127. Available at: http://seisweb.oma.be/bibadmin/uploads/pdf/COURSENOTES.pdf.

Loke, M. H., Acworth, I. and Dahlin, T. (2003) ‘A comparison of smooth and blocky inversion methods in 2D electrical imaging surveys’, *Exploration Geophysics*, 34(3), pp. 182–187. doi: 10.1071/EG03182.

Loke, M. H., Wilkinson, P. B. and Chambers, J. E. (2010) ‘Fast computation of optimized electrode arrays for 2D resistivity surveys’, *Computers and Geosciences*. Elsevier, 36(11), pp. 1414–1426. doi: 10.1016/j.cageo.2010.03.016.

Lynch, J. (2016) ‘Root Architecture and Plant Productivity’, *Plant Physiology*, 109(1), pp. 7–13. doi: 10.1104/pp.109.1.7.

Lynch, J. P. and Brown, K. M. (2012) ‘New roots for agriculture: Exploiting the root

phenome', *Philosophical Transactions of the Royal Society B: Biological Sciences*, 367(1595), pp. 1598–1604. doi: 10.1098/rstb.2011.0243.

McCutcheon, M. C. *et al.* (2006) 'Effect of Soil Water on Apparent Soil Electrical Conductivity and Texture Relationships in a Dryland Field', *Biosystems Engineering*, 94(1), pp. 19–32. doi: 10.1016/j.biosystemseng.2006.01.002.

Meister, R. *et al.* (2014) 'Challenges of modifying root traits in crops for agriculture', *Trends in Plant Science*. Elsevier Ltd, 19(12), pp. 779–788. doi: 10.1016/j.tplants.2014.08.005.

Melo, L. B. B. de *et al.* (2021) 'Effect of compaction on the relationship between electrical resistivity and soil water content in Oxisol', *Soil and Tillage Research*, 208(November 2019). doi: 10.1016/j.still.2020.104876.

Mihai, A. E. *et al.* (2019) 'Direct measurements of tree root relative permittivity for the aid of GPR forward models and site surveys', Near Surface Geophysics, pp. 1–31.

Milsom, J (2011) Field Geophysics 4th edition. John Wiley and Sons Incs.

Özdemir, C. *et al.* (2014) 'A review on migration methods in b-scan ground penetrating radar imaging', *Mathematical Problems in Engineering*, 2014. doi: 10.1155/2014/280738.

Paglis, C. M. (2013) 'Application of electrical resistivity tomography for detecting root biomass in coffee trees', *International Journal of Geophysics*, 2013(1). doi: 10.1155/2013/383261.

Petersen, T. and al Hagrey, S. A. (2014) 'Numerical and Experimental Mapping of Root Zone Using Surface and Borehole Resistivity Tomography', *Near Surface 2009 - 15th EAGE European Meeting of Environmental and Engineering Geophysics*, 76(2). doi: 10.3997/2214-

4609.20147063.

Pierik, R. L. M. and Steegmans, H. H. M. (1975) ‘ANALYSIS OF ADVENTITIOUS ROOT FORMATION IN ISOLATED STEM EXPLANTS OF RHODODENDRON possible much sooner than experiments with cuttings in vivo . The a m o u n t of space and time taken by in vitro experiments is much smaller than when using in vivo techniq’, 3.

Quinta-Ferreira, M. (2019) ‘Ground Penetration Radar in Geotechnics. Advantages and Limitations’, *IOP Conference Series: Earth and Environmental Science*, 221(1). doi: 10.1088/1755-1315/221/1/012019.

Rasol, M. Pais, J.C. Pérez-Gracia, V. Solla, M. Fernandes, F.M. Fontul, S. Ayala-Cabrera, D. Schmidt, F. Assadollahi, H.. (2022). GPR monitoring for road transport infrastructure: A systematic review and machine learning insights. Construction and Building Materials, 324: 126686.

Reynolds, J.M (1997) An Introduction to Applied and Enviornmental Geophysics. Chichester: John Wiley and Sons Ltd, 1st edition.

Reynolds, J.M (2011) An Introduction to Applied and Environmental Geophysics. Wiley Blackwell, 2nd edition.

Robbins, N. E. and Dinneny, J. R. (2018) ‘Growth is required for perception of water availability to pattern root branches in plants’, *Proceedings of the National Academy of Sciences of the United States of America*, 115(4), pp. E822–E831. doi: 10.1073/pnas.1710709115.

SASAKI, Y. (1992) ‘Resolution of Resistivity Tomography Inferred From Numerical

Simulation', *Geophysical Prospecting*, 40(4), pp. 453–463. doi: 10.1111/j.1365-2478.1992.tb00536.x.

Schiefeibeina, J. W. and Benfeyb, P. N. (1991) 'The Development of Plant Roots: New Approaches to Underground Problems', 3(November).

Schwartz, B. F., Schreiber, M. E. and Yan, T. (2008) 'Quantifying field-scale soil moisture using electrical resistivity imaging', *Journal of Hydrology*, 362(3–4), pp. 234–246. doi: 10.1016/j.jhydrol.2008.08.027.

Schwarz, D., Thompson, A. J. and Kläring, H. P. (2014) 'Guidelines to use tomato in experiments with a controlled environment', *Frontiers in Plant Science*, 5(NOV), pp. 1–16. doi: 10.3389/fpls.2014.00625.

Seladji, S. *et al.* (2010) 'The effect of compaction on soil electrical resistivity: A laboratory investigation', *European Journal of Soil Science*, 61(6), pp. 1043–1055. doi: 10.1111/j.1365-2389.2010.01309.x.

Shima, H., Sakashita, S. and Kobayashi, T. (1996) 'Developments of non-contact data acquisition techniques in electrical and electromagnetic explorations', *Journal of Applied Geophysics*, 35(2–3), pp. 167–173. doi: 10.1016/0926-9851(96)00018-3.

Smith, S. and de Smet, I. (2012) 'Root system architecture: Insights from Arabidopsis and cereal crops', *Philosophical Transactions of the Royal Society B: Biological Sciences*, 367(1595), pp. 1441–1452. doi: 10.1098/rstb.2011.0234.

Society, E. and Society, E. (2014) 'A Tentative Classification of Root Systems Author (s): William Austin Cannon Source : Ecology , Vol . 30 , No . 4 (Oct ., 1949), pp . 542-548

Published by : Ecological Society of America Stable URL : http://www.jstor.org/stable/1932458 .', 30(4), pp. 542–548.

'Soil Water Content Estimation Using High-Frequency Ground Penetrating Radar _ Enhanced Reader.pdf' (no date).

Szalai, S. and Szarka, L. (2008) 'On the classification of surface geoelectric arrays', *Geophysical Prospecting*, 56(2), pp. 159–175. doi: 10.1111/j.1365-2478.2007.00673.x.

Szymanski, D. (2013) *Arabidopsis thaliana: The Premier Model Plant, Brenner's Encyclopedia of Genetics: Second Edition*. Elsevier Inc. doi: 10.1016/B978-0-12-374984-0.00088-7.

Tabe, K., Iskander, M. and Honma, S. (2011) 'Transparent aquabeads to visualize flow in porous material', *Advanced Materials Research*, 239–242, pp. 2602–2605. doi: 10.4028/www.scientific.net/AMR.239-242.2602.

Tan, H. S. (1981) 'Microwave measurements and modelling of the permittivity of tropical vegetation samples', *Applied Physics*, 25(3), pp. 351–355. doi: 10.1007/BF00902994.

Tang, L. *et al.* (2011) 'Root Architecture Modeling and Visualization in Wheat', pp. 479–490.

Thomas, G. and Carsten, R. (2019) 'Boundless Electrical Resistivity Tomography BERT 2 – the user tutorial', pp. 1–70.

Thomas, G., Carsten, R. and Spitzer, K. (2006) 'Three-dimensional modelling and inversion of dc resistivity data incorporating topography – II . Inversion', pp. 506–517. doi: 10.1111/j.1365-246X.2006.03011.x.

Tracy, S. R. *et al.* (2012) 'Quantifying the impact of soil compaction on root system architecture in tomato (Solanum lycopersicum) by X-ray micro-computed tomography.', *Annals of botany*, 110(2), pp. 511–519. doi: 10.1093/aob/mcs031.

Tronicke, J. and Hamann, G. (2014) 'Vertical radar profiling : Combined analysis of traveltimes , amplitudes , and reflections', 79(4).

Turner, A. J., Arzola, C. I. and Nunez, G. H. (2020) 'High pH stress affects root morphology and nutritional status of hydroponically grown rhododendron (Rhododendron spp.)', *Plants*, 9(8), pp. 1–12. doi: 10.3390/plants9081019.

United Nations, Department of Economic and Social Affairs, Population Division (2022). World Population Prospects 2022: Summary of Results. UN DESA/POP/2022/TR/NO. 3.

Verdoliva, S. G. *et al.* (2021) 'Controlled comparisons between soil and hydroponic systems reveal increased water use efficiency and higher lycopene and β-carotene contents in hydroponically grown tomatoes', *Scientia Horticulturae*. Elsevier B.V., 279, p. 109896. doi: 10.1016/j.scienta.2021.109896.

Wang, B. J. *et al.* (2014) 'Interspecific interactions alter root length density , root diameter and specific root length in jujube / wheat agroforestry systems'. doi: 10.1007/s10457-014-9729-y.

Wang, Z. *et al.* (2015) 'Effects of different management systems on root distribution of maize', (275), pp. 21–28. doi: 10.4141/CJPS-2014-026.

Warren, C., Giannopoulos, A. and Giannakis, I. (2015) 'An advanced GPR modelling framework : the next generation of gprMax', pp. 0–3.

Werban, U., Al Hagrey, S. A. and Rabbel, W. (2008) 'Monitoring of root-zone water content in the laboratory by 2D geoelectrical tomography', *Journal of Plant Nutrition and Soil Science*, 171(6), pp. 927–935. doi: 10.1002/jpln.200700145.

Wielopoiski, L. *et al.* (2000) 'Imaging Tree Root Systems In Situ Co2 currently sequestering , directly from the of atmospheric carbon dioxide (C02), due to tree root systems in situ . The method is non-', 4084, pp. 642–646.

Xihong, C. U. I. *et al.* (2010) 'Modeling tree root diameter and biomass by ground-penetrating radar', (January 2021). doi: 10.1007/s11430-010-4103-z.

Zhang, X. *et al.* (2019) 'Evaluation of a ground penetrating radar to map the root architecture of HLB-infected citrus trees', *Agronomy*, 9(7), pp. 1–21. doi: 10.3390/agronomy9070354.

APPENDICES

Appendinx A: Representing the dielectric constant and conductivity in mS/m for various materials. (Daniels J. D, 2004).

Material type	Dielectric Constantant	Conductivity in mS/m
Acrylic glass	2.7 - 3.7	1.0E-14
Asbestos	3 - 4.8	1.0E-6 - 0.0001
Asphalt - dry	2 - 4	0.1 - 1
Asphalt - wet	6 - 12	10 - 100
Basalt - wet	8	4 - 8
Clay - dry	2 - 6	2 - 100
Clay - wet	5 - 40	100 - 1000
Coal - dry	3 - 4	1 - 10
Coal - wet	7 - 9	10 - 100
Concrete - dry	4 - 10	0.1 - 10
Concrete - wet	10 - 25	10 - 100
Cultural layer - fresh water	65 - 75	0.1 - 10
Dolomite	6 - 8	0.2 - 3

Granite - dry	4 - 6	1.0E-5 - 0.001
Granite - wet	6 - 8	1 - 10
Limestone - dry	4 - 8	1.0E-6 - 0.001
Limestone - wet	7 - 9	10 - 100
Marsh land	12	0.006 - 0.012
Peat	60 - 75	40 - 300
Permafrost	3 - 8	0.01 - 10
Plastic PE	2.2 - 2.4	1.0E-11 - 1.0E-14
Plastic PVC	3 - 3.4	1.0E-7 - 1.0E-9
Quartz	4.2 - 5	2.0E-11 - 4.0E-9
Salt - dry	5 - 6	0.01 - 1
Sand - dry	2 - 6	0.0001 - 1
Sand - dry coastal	6 - 10	0.002 - 2
Sand - wet	15 - 30	1 - 10
Sandstone - dry	2 - 5	1.0E-5 - 0.001
Sandstone - wet	5 - 10	0.1 - 10
Sea chalk - fresh water	45 - 55	0.1 - 10
Shale - dry	4 - 9	1 - 10
Shale - saturated	7 - 16	1 - 100
Silt - dry	3 - 30	1 - 50
Silt - saturated	10 - 40	100 - 400
Snow	6 - 12	0.001 - 0.01
Soil - average	9	1

Soil - clayey - dry	4 - 10	10 - 100
Soil - clayey - wet	10 - 30	50 - 1000
Soil - frozen	6	0.1 - 0.5
Soil - loamy - dry	4 - 10	0.1 - 1
Soil - loamy - wet	10 - 30	10 - 100
Soil - sandy - dry	4 - 10	0.1 - 10
Soil - sandy - wet	10 - 30	10 - 100
Water - distilled	80	0.005 - 0.05
Water - fresh (0 °C)	88	0.1 - 1
Water - fresh (18 °C)	81	0.001 - 10
Water - ice - fresh	3.5 - 4	0.1 - 5
Water - ice - salt	4 - 8	10 - 100
Water - salt/sea	80 - 81	400 - 30000
Wood - dry	2 - 5	1.0E-14 - 1.0E-12
Wood - wet	10 - 30	0.1 - 1

Appendix B: Matlab and Arduino codes

One of the codes used for controlling the switch box for the resistivity measurements. It allows flexibility to the user by inserting the actual position of the electrodes for the points that need measuring. It displays the position of the electrodes, and at the end of the survey it also generates a file with the position of the electrodes in an .xls converted from electrode position to distance in cm.

```
%Run the program several times for several profiles/ERTs
clear
iteration=0;
no_of_measurements=0;
load handel.mat;
while(1)
iteration=iteration+1;

%Close the port so it's ok after each profile

if exist('RS232Port','var')
   fprintf('It looks like the COM port is still open!\nTrying to close it...\n');
   try
      fclose(RS232Port);
   catch ME
      fprintf('I was unable to close the port!\n');
```

```
    end
end


%You can change the number of electrodes accordingly up to 30
NumberOfElectrodes = 18;


%% Generate an array of data collection connections


A = [1  1   1   1   1   1   1   1   1   3   3   3   3   3   3   3   5   5   5   5   5   5   7   7   7   7   7   9   9   9   9   11  11  11
13  13  15  ]
B = [2  2   2   2   2   2   2   2   2   4   4   4   4   4   4   4   6   6   6   6   6   6   8   8   8   8   8   10  10  10  10  12  12
12  14  14  16  ]
M = [3  4   5   7   9   11  13  15  17  5   7   9   11  13  15  17  7   9   11  13  15  17  9   11  13  15  17  11  13  15  17
13  15  17  15  17  17  ]
N = [4  5   6   8   10  12  14  16  18  6   8   10  12  14  16  18  8   10  12  14  16  18  10  12  14  16  18  12  14  16
18  14  16  18  16  18  18  ]
%iteration thingie
x = 1;


%Select only positions lower than the number of electrodes
pos = [A; B; M; N];
pos_invers = pos';
for i = 1:37
    if (A(i)<=NumberOfElectrodes)
        if(B(i)<=NumberOfElectrodes)
```

```
        if(M(i)<=NumberOfElectrodes)
          if(N(i)<=NumberOfElectrodes)
          A_n(x)=A(i);
          B_n(x)=B(i);
          M_n(x)=M(i);
          N_n(x)=N(i);
          x=x+1;
          end
        end
      end
   end
end
pos_n = [A_n; B_n; M_n; N_n];
num_pos = numel(pos_n)/4;


%Assign positions to the ERT array
ElecrodePositions = zeros(10000,4);
ElecrodeIndex = 0;
for ArrayIncrement = 1:num_pos;                    %Distance between electrodes
   C1Electrode = A_n(ArrayIncrement);
   C2Electrode = B_n(ArrayIncrement);
   P1Electrode = M_n(ArrayIncrement);
   P2Electrode = N_n(ArrayIncrement);
   ElecrodeIndex = ElecrodeIndex + 1;


        ElecrodePositions(ElecrodeIndex,1) = C1Electrode;          % Position of C1 current injection
electrode
```

```
            ElecrodePositions(ElecrodeIndex,2) = C2Electrode;               % Position of P1 voltage sensing
electrode
            ElecrodePositions(ElecrodeIndex,3) = P1Electrode;               % Position of P2 voltage sensing
electrode
            ElecrodePositions(ElecrodeIndex,4) = P2Electrode;               % Position of C2 current injection
electrode


end


% Reduce size of the array
ElecrodePositions = ElecrodePositions(1:ElecrodeIndex,:);



Comment3 = '';


XlRange_A = 'A1';
xlswrite('test-elec-pos.xlsx', ElecrodePositions);
matrix_from_xls = xlsread('test-elec-pos.xlsx', 'A1:D34');
old_values = [1:18];
new_values = [0:0.05:0.8];
new_matrix = changem(matrix_from_xls, new_values, old_values);
sheet = 1;
xlswrite('test2-elec-pos.xlsx',new_matrix);



%% Initialise switching network communication
```

```
RS232Port =
serial('COM3','BaudRate',9600,'DataBits',8,'Parity','none','StopBits',2,'FlowControl','none','Terminator','CR/LF');

% Open Port
fopen(RS232Port);

fprintf(RS232Port,'reset\n');

%% Display to user the position of the electrodes to be connected
PreviousElectrodePositions = zeros(1,4);

for ElecrodeIndex = 1:length(ElecrodePositions)
   pause(0.6);
   %If commercial device is changing rows, needs a bigger pause
   %This is done for X=30 meters, 4 measurements/meter
   no_of_measurements=no_of_measurements+1;
   if mod(no_of_measurements,120) == 0
   beep
   pause (20);
   end

   % Draw a picture
   Figure1Handle = figure(1);
   set(Figure1Handle,'Color','w')

   OutlinePositionsX = 1:NumberOfElectrodes;          % X Positions
```

```
OutlinePositionsY = zeros(size(OutlinePositionsX));     % Y Positions
plot(OutlinePositionsX,OutlinePositionsY,'k+','MarkerSize',15,'LineWidth',2)
xlim([0 NumberOfElectrodes+1]);
ylim([-1.6 +1.6]);

C1 = ElecrodePositions(ElecrodeIndex,1);
C2 = ElecrodePositions(ElecrodeIndex,2);
P1 = ElecrodePositions(ElecrodeIndex,3);
P2 = ElecrodePositions(ElecrodeIndex,4);

hold on
% Use red markers for current injection and blue markers for voltage sense
plot(C1,0,'ro','MarkerSize',15,'LineWidth',2)
plot(C2,0,'ro','MarkerSize',15,'LineWidth',2)
plot(P1,0,'bs','MarkerSize',15,'LineWidth',2)
plot(P2,0,'bs','MarkerSize',15,'LineWidth',2)
% Use text to lable the electrodes
text(C1,-0.2,'C1','HorizontalAlignment','center')
text(C2,-0.2,'C2','HorizontalAlignment','center')
text(P1,0.2,'P1','HorizontalAlignment','center')
text(P2,0.2,'P2','HorizontalAlignment','center')
% Add block for current injection
line([C1 C1],[0 1],'LineWidth',2,'Color','r')
line([C2 C2],[0 1],'LineWidth',2,'Color','r')
BoxX1 = C1 + (C2-C1-2)/2;
BoxX2 = BoxX1 + 2;
line([C1 BoxX1],[1 1],'LineWidth',2,'Color','r')
```

```
line([BoxX2 C2],[1 1],'LineWidth',2,'Color','r')
line([BoxX1 BoxX2 BoxX2 BoxX1 BoxX1],[0.7 0.7 1.3 1.3 0.7],'LineWidth',2,'Color','r')
text(BoxX1+1,1.1,'Signal','HorizontalAlignment','center')
text(BoxX1+1,0.9,'Generator','HorizontalAlignment','center')
% Add block for voltage sense
line([P1 P1],[0 -1],'LineWidth',2,'Color','b')
line([P2 P2],[0 -1],'LineWidth',2,'Color','b')
BoxX1 = P1 + (P2-P1-0.8)/2;
BoxX2 = BoxX1 + 0.8;
line([P1 BoxX1],[-1 -1],'LineWidth',2,'Color','b')
line([BoxX2 P2],[-1 -1],'LineWidth',2,'Color','b')
line([BoxX1 BoxX2 BoxX2 BoxX1 BoxX1],[-0.7 -0.7 -1.3 -1.3 -0.7],'LineWidth',2,'Color','b')
text(BoxX1+0.4,-1,'RX','HorizontalAlignment','center')
hold off


% Control switching network - switch relays on if there is to be a change
if ElecrodePositions(ElecrodeIndex,1) ~= PreviousElectrodePositions(1),
    RelayMessage = ['c1,' num2str(ElecrodePositions(ElecrodeIndex,1)) ',on\n'];
    fprintf(RS232Port,'%s',RelayMessage);
    pause(0.6);
end
if ElecrodePositions(ElecrodeIndex,2) ~= PreviousElectrodePositions(2),
    RelayMessage = ['p1,' num2str(ElecrodePositions(ElecrodeIndex,2)) ',on\n'];
    fprintf(RS232Port,'%s',RelayMessage);
    pause(0.6);
end
if ElecrodePositions(ElecrodeIndex,3) ~= PreviousElectrodePositions(3),
```

```
    RelayMessage = ['p2,' num2str(ElecrodePositions(ElecrodeIndex,3)) ',on\n'];
    fprintf(RS232Port,'%s',RelayMessage);
    pause(0.6);
end
if ElecrodePositions(ElecrodeIndex,4) ~= PreviousElectrodePositions(4),
    RelayMessage = ['c2,' num2str(ElecrodePositions(ElecrodeIndex,4)) ',on\n'];
    fprintf(RS232Port,'%s',RelayMessage);
    pause(4);
end


if ElecrodeIndex < length(ElecrodePositions),
    % Control switching network - switch relays off if there is to be a change
    if ElecrodePositions(ElecrodeIndex,1) ~= ElecrodePositions(ElecrodeIndex+1,1),
        RelayMessage = ['c1,' num2str(ElecrodePositions(ElecrodeIndex,1)) ',off\n'];
        fprintf(RS232Port,'%s',RelayMessage);
        pause(0.1);
    end
    if ElecrodePositions(ElecrodeIndex,2) ~= ElecrodePositions(ElecrodeIndex+1,2),
        RelayMessage = ['p1,' num2str(ElecrodePositions(ElecrodeIndex,2)) ',off\n'];
        fprintf(RS232Port,'%s',RelayMessage);
        pause(0.1);
    end
    if ElecrodePositions(ElecrodeIndex,3) ~= ElecrodePositions(ElecrodeIndex+1,3),
        RelayMessage = ['p2,' num2str(ElecrodePositions(ElecrodeIndex,3)) ',off\n'];
        fprintf(RS232Port,'%s',RelayMessage);
        pause(0.1);
    end
```

```
        if ElecrodePositions(ElecrodeIndex,4) ~= ElecrodePositions(ElecrodeIndex+1,4),
            RelayMessage = ['c2,' num2str(ElecrodePositions(ElecrodeIndex,4)) ',off\n'];
            fprintf(RS232Port,'%s',RelayMessage);
            pause(0.001);
        end
    end
    PreviousElectrodePositions = ElecrodePositions(ElecrodeIndex,:);
end


fprintf('This has been profile number:')
disp(iteration);
sound(y);
%% Clear the tasks


% Close the switching network comms - close serial port
fclose(RS232Port);
clear('RS232Port');
beep
beep
beep
master_profile=input('Do you want to carry out another ERT, yes / no [Y]:','s')
    if master_profile=='no'
    break
    end


end
```

f

Code example that was used for controlling the irrigation system, in Arduino IDE. In this example, the code checked the level of humidity with one of the humidity sensors, and depending on the result the system automatically started the pump.

```
int digitalSensor = 2;
int pumpPin = 8; //the relay pin


void setup() {
  pinMode(digitalSensor, INPUT);
  pinMode(pumpPin, OUTPUT);
}


void loop() {
  if(digitalRead(digitalSensor) == HIGH){
    digitalWrite(pumpPin, HIGH);
    delay(1500);
    digitalWrite(pumpPin, LOW);
  }
```

```
  delay(1000); // 1hour

}
```

Appendix C: Conferences and Workshops Accepted Abstracts

7th IGSC – International Student Conference 2016, Katowice, Poland

The Integration of Models in Urban GPR Studies – Case Studies

Alexandra G. Gerea[1], Andrei E. Mihai[2]

[1,2]School of Electronic, Electrical and Computer Engineering, University of Birmingham

Summary

In recent years, Ground Penetrating Radar (GPR) has emerged as a versatile and reliable method for nearsurface geophysical studies. Especiall in urban areas where the survey conditions and objectives are very specific, GPR has shown considerably good results. As the method is used more and more, the integration of forward models becomes important to have a finer idea of the method's possibilities and limitations.

Introduction

In recent years, the use of geophysical techniques for environmental and engineering studies has grown significantly, and the methods themselves have gained much more acceptance. As a result, there is a growing demand for geophysical studies, especially in urban and construction areas. The diversity of the potentially applicable methods has also grown and methods have become much more specialized. A range of shallow geophysical techniques can be used to study the subsurface, faults in infrastructure and a host of physical parameters.

Detailing all the methods used goes beyond the scope of this paper, as only GPR is addressed directly. GPR is an electromagnetic technique. The method operates on a simple principle: electromagnetic waves emitted from a transmitter antenna are reflected by buried objects with different electromagnetic parameters and detected at another antenna, the receiver. The two way travel time is recorded. The principles of the method are based on Maxwell's equations for electromagnetic wave propagation. GPR data is presented in the form of time-distance plots analogous to conventional seismic reports. The central frequency is a key aspect of the equipment, as it directly affects both the resolution and the depth penetration. Because urban studies are rarely concerned with the deeper parts of the subsurface, a higher frequency is desired as it provides a better resolution.

Methodology

The use of GPR in urban studies has been described thoroughly and is no longer limited to the academic world (Conyers, 2004; Dojack, 2012). However, there doesn't seem to be any "magical recipe" for data processing and the limits and possibilities of the method are still a topic of hot debate. For urban studies, frequencies of over 400 MHz are generally needed, and ideally, over 700 MHz. For finer objectives, frequencies well over 1 GHz and even 2 GHz can be used. The typical processing flow includes some form or combination of gain, DC shift, background removal and band pass, but the effectiveness of processing flows can vary widely from case to case. Here, several profiles were acquired in urban areas, on solid surfaces, where most other geophysical methods would have been ineffective. Various objectives are observed and described, proving the effectiveness of the method, butalso highlighting its limits.

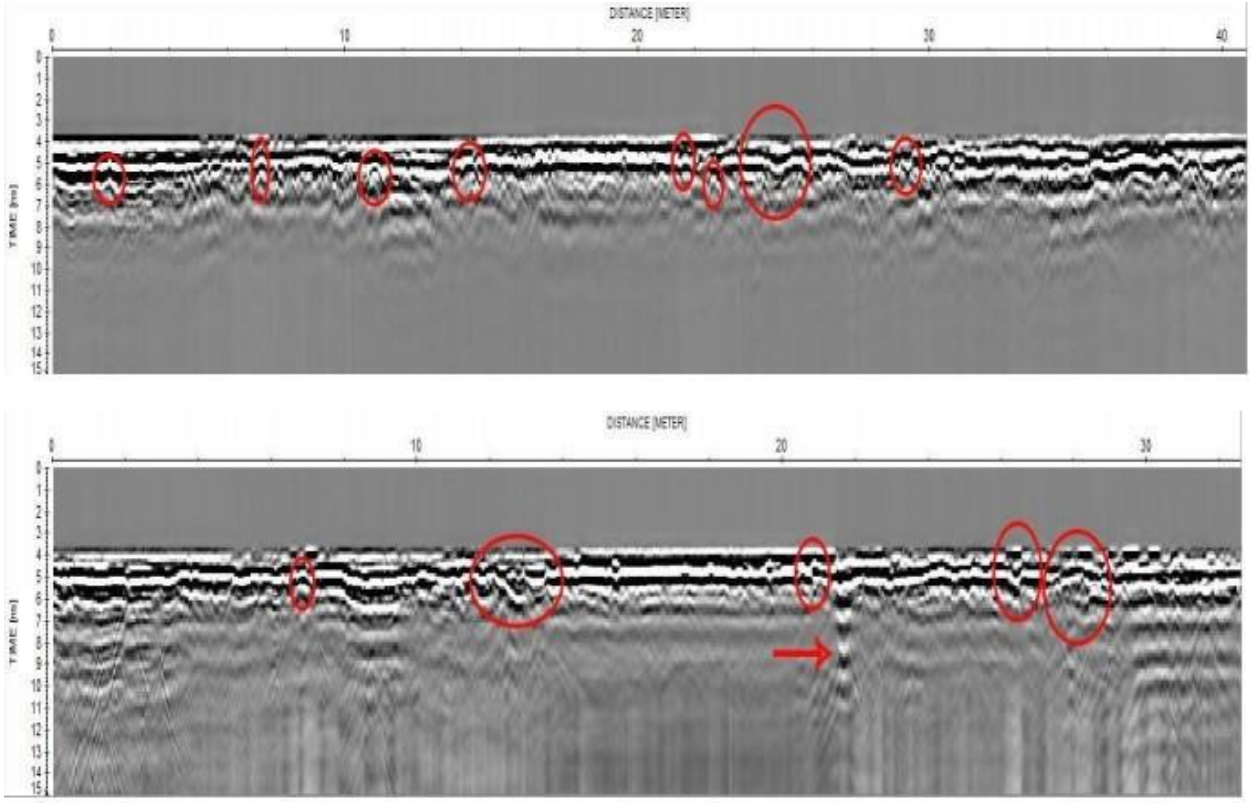

Figure 1 *Example of GPR surveys acquired on asphalt, with a 700 MHz antenna.*

Several discontinuities and interactions with tree roots can be observed. Also, forward models were constructed with an open-source software, gprMax. (Warren et al, 2015; Giannopoulos, 2005); gpr-Max is a freely-available set of electromagnetic wave simulation based on the finite-difference timedomain (FDTD) numerical method. It was originally written in the 1990s, but has since been rewritten in Python and offers faster computational times and improved user experience. The analytical solution of GPR's forward problem is a

difficult, almost impossible problem (Giannopoulos, 2005). The solution proposed by gpr-Max is an elegant, but it is a computing intensive approach.

The models are created by the users by assigning the parameters of the geometrical shapes (rectangles, triangles, circles) and assigning the dielectric parameters. The user also defines the characteristics of the antenna, the size of the discretization cells and the antenna stepping. Simple models were generated initially, followed by more complex simulations to aid GPR surveys planning and interpretation.

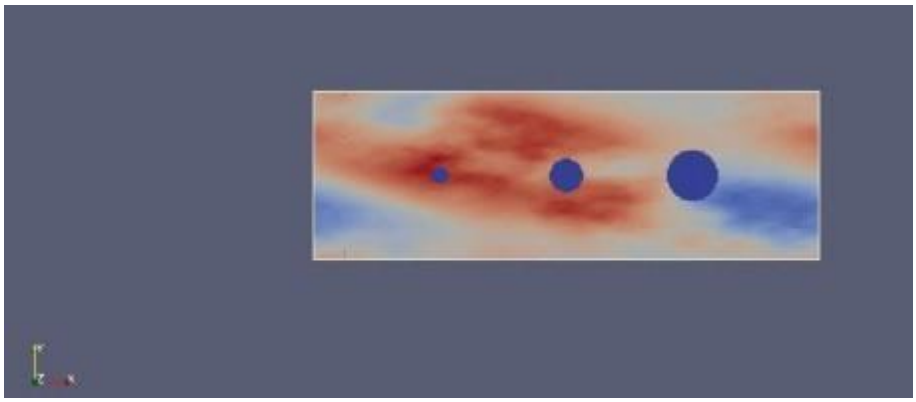

Figure 2 *Three metal pipes of different sizes modelled in a 60 x 20 cm box filled with a fractal model of soil, with various sand-clay relations.*

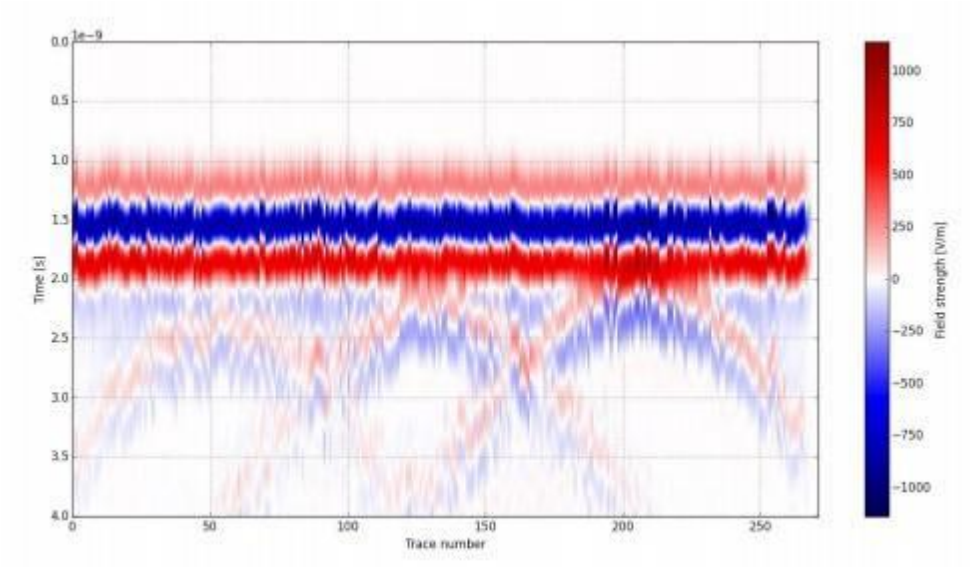

Figure 3 *The radargram of the above-presented model, in the case of a 1/1 clay-sand ratio.*

Conclusions

GPR has been integrated for a few years into subsurface urban research, but there is still debate regarding the survey design, processing and general interpretation. Forward models are a valuable tool to help better understand the potential and limitations of the method in an urban setting. Of course, there is a set of distinct differences between forward models and real-life data, but with the design of more and more complex models, GPR data can be better understood and even predicted (to an extent). Especially with the growth of processing power, the creation of more complex models becomes possible, simulating the natural world acceptably and providing valuable information at no cost.

References

Biddle P.G. (1998). Tree Root Damage to Buildings. Willowmead Publishing Ltd.

Conyers, L. B. (2004). Ground Penetrating Radar in Archaeology. AltaMira Press.

Day R. W. (1991). Damage of structures due to tree roots. Journal of Performance of Constructed Facilities, Vol. 5, 200-207

Dojack, L. (2012). Ground Penetrating Radar: Theory, Data Collection, Processing, and Interpretation: A guide for Archaeologists.

Giannopoulos, A. (2005). Modelling ground penetrating radar by GprMax, Construction and Building Materials, 19(10), 755-762.

Jim C. Y. (1998). Urban soil characteristics and limitations for landscape planting in Hong Kong. Landscape and Urban Planning. Vol. 40, 235-249.

Jol, M. H. (2011). Ground Penetrating Radar: Theory and Applications. Elsevier.

Warren, C., Giannopoulos, A., & Giannakis I. (2015). An advanced GPR modelling framework – the next generation of gprMax, In Proc. 8th Int. Workshop Advanced Ground Penetrating Radar

Abstract COST Action on GPR in London, UK.

Tree root detection in urban environment using GPR

Case study: Braga, Portugal

Alexandra G. Gerea[1], Andrei E. Mihai[2], Luis Gonçalves[3]

[1,2]School of Electronic, Electrical and Computer Engineering, University of Birmingham

[3]Department of Earth Sciences, Universidade do Minho

Abstract

The paper presents a study carried in the campus of the University of Minho in order to detect tree roots in urban environments. For this study, eight different areas were chosen with different types of surfaces (soil, concrete, pavement, soil in a flooded area, soil near a building, asphalt, etc.) and different types of trees (palm tree, cork tree, olive tree, etc.). We've used a 400MHz antenna which should offer more details in the very upper layers. According to Dobson (1995), 80-90% of the tree roots should be found in the first 60cm, even for trees up to 20m.

Methodology

For the data acquisition we've used a 400MHz antenna. Prior to data collection surveys we have determined the spatial parameters of the trees(diameter, type, etc.); and the interfering objects, surface properties (soil, concrete, etc.).

For the survey, the profiles were in one or two directions with distances between profiles of 20cm and 15 cm. For data visualization and processing the programs ReflexW, Reflex 2D Quick, Reflex 3D scan and GPR Slice were used. Through processing we've used different types of filters but the best combination of filters was : gain function (linear:1, exponenttial:2), butterworth bandpass (200-600MHz).

Results and Conclusions

The 400MHz antenna offers valuable information regarding the tree root detection in urban environments but it also has its limitations when it comes to detail. It is very difficult to differentiate tree roots of different types of trees. Even though some of the measurements were carried on soil surfaces because of the various works for the modification of the landscape affect the visibility of the roots. On the concrete surfaces because of the rebar in the sidewalks, etc., the signal attenuated so much that it was impossible to see anything under the concrete layer. The data from the cubic stone pavement surface offered the least information about tree roots, even though the tree diameters were higher than 60-70cm.

EAGE - Near Surface Geoscience Conference & Exhibition, September 2018, Porto, Portugal

Geophysics Applied in Precision Agriculture – Experimental Resistivity Studies for Plant Root Detection and Analysis

Alexandra G. Gerea[1], Andrei E. Mihai[2]

[1,2]School of Electronic, Electrical and Computer Engineering, University of Birmingham

Introduction

The population of the world it is said to rise up to 9 billion people by 2050, which means that there will be a higher demand of food and a bigger stress in the agricultural area. In order to asses a complex global issue, we need to understand and find solutions through more than one perspective, and this is possible by a multidisciplinary approach. This study tries to integrate well-known geophysical methods, adapt them for a new target, much smaller and in much more detail than before, with the help of electrical engineering and a better understanding of the environment. By building new equipment to complement the pre-existent commercial one, and also by understanding different aspects of the plant biology and behaviour in agricultural environments, we can improve the way we use our resources in a more sustainable way for a better future.

The resistivity method is widely known in the geophysical prospection, giving very useful data information on a large scale. The aim of this study is to conduct new experiments with higher precision and building new complementary equipment in which we can detect the plant

roots extent with more accuracy, their behaviour in natural environments by carrying tests in both laboratory and agricultural fields. We've been able to create ERT (electrical resistivity tomography) with electrode arrays both classical and new experimental types, using flexible equipment created in the laboratory and Matlab programming. We've developed new test settings for the experiments in order to minimize the human errors and come up with high quality data and a more precise interpretation compared to previous studies on plant root detection using resistivity measurements (Hagrey et al, 2008).

Equipment

The geophysical equipment used for this study consists of a commercial resistance meter from RM Frobisher and for the electrical resistance tomography we also used a switch box designed and created in our laboratory, which gives us the possibility to manipulate different parameters and also different types of configurations. The electrodes used for the experiments are 15cm long, with a diameter of 2.5mm and are made of stainless steel.

Figure 1 *Left – three of the test boxes with tomato plants; the box in the middle has one plant and the one on the right has three plants. Right – one of the boxes with one tomato plant, water and fertilizers. In both images, part of the equipment can be seen, the resistance meter (left) and the switch box (right).*

In order to detect information regarding the humidity level of the soil, we were able to create an Arduino device that measure the levels of humidity in different parts of the box and stores the data on a micro SD card. Collecting this kind of data is very important in order to understand how the water parameter affects resistivity measurements, the degree of detail, and types of anomalies. For a complete monitoring of the well-being of the plants tested in the laboratory we've been able to create a Raspberry Pi system that takes pictures at a pre-established interval. This device is very useful in order to understand how the plant develops throughout the study and how it is affected by different environmental parameters

(high/low levels of water, luminosity exposure, fertilizers, etc.). Correlating the data from the devices described above, represents a very important step in the data interpretation of the resistivity sections, and to minimize the errors as much as possible.

Data acquisition

Direct measurements

Before starting the geophysical measurements, several direct measurements in different agricultural fields have been carried. The process was invasive and consisted in measuring from the surface, distances between plants for different types of crops, and depth and behaviour of the roots. In order to to do the depth measurements it required to dig in several places in different parts of the field (margin, and closer to centre). It was observed from the measurements that mature agricultural plants are very close together this way being very hard to differentiate between individual plants. The maximum area of influence in depth for the plants was up to 20cm and the area covered by the roots goes up to approximately 10cm. A layer of roots can be delimited visually after the digging was done. The distance between the plants varies very much depending on the type of the crop. These information is very important in order to better understand how to properly use the equipment, what kind of modifications should be done and to understand what kind of anomalies we should expect

from the data. Also this information helped with shaping the setting of the laboratory experiments.

Laboratory experiment

For the experiments in the laboratory, we selected tomato plants, which were grown in the laboratory from seed, in order to have a better control of the fertilizer content, type of soil used and watering system evaluation. After the plants developed enough, (minimising the risk of plants not adapting to the new test environment) they were transplanted in the test boxes.

The electrode array used in these experiments were: Wenner, Schlumberger, Dipole-dipole and an experimental array aimed to provide optimum subsurface information (Stummer et al. 2004). All the electrodes were placed in the box at the same time and the measurements were controlled using Matlab via a switch box created in the laboratory.

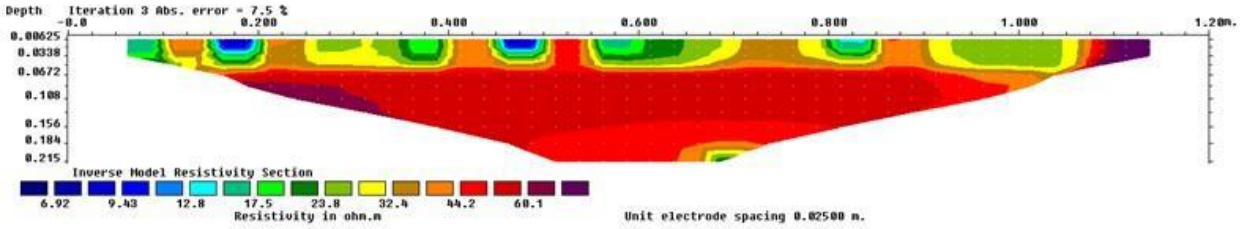

Figure 2 *Above – inverted resistivity ERT profile in an agricultural corn field. Plant position at 0.2m, 0.6m and 1m. The electrode array used was Wenner with a distance between the electrodes of 5cm.*

For a better understanding of the plant root extent we had test boxes with only one plant, placed in the centre of the box, with layers of different types of soil. Another box filled with water and fertilizers that contained only one plant, was also used for a better correlation of the resistivity data with the exact place of the plant roots. Also, because in normal agricultural settings the plants are very close to each other, therefore making it harder to differentiate the roots for individual plants, we were able to set a box with three plants on the same profile with a distance of approximately 20cm. In order to keep electrodes in place, in the exact same

place every time we took measurements, we developed different acrylic, transparent plates with a pre-set configuration of electrodes, which acted as a cap for the boxes, always connected in the same place. The distance between the electrodes for all the

experiments was 5cm and the distance between profiles of 5cm as well.

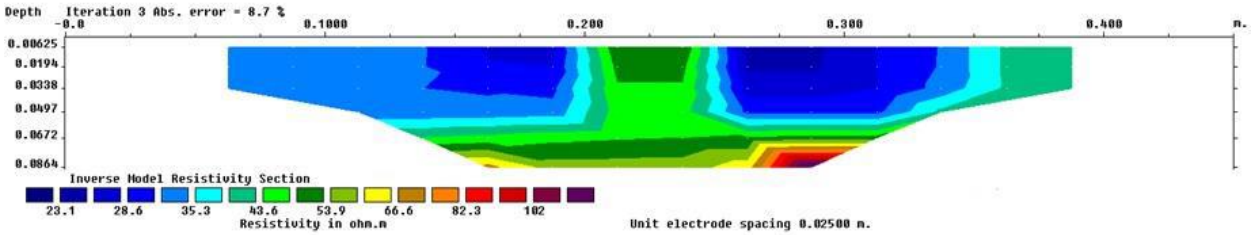

Figure 3 *Down – inverted resistivity profile in the test box with one tomato plant and soil. The plant's position is at 0.22m. The electrode array used was Wenner with a distance between the electrodes of 5cm.*

Field work

For a better understanding of the limitations of the method, more data was collected in natural

agricultural environments. Several profiles were carried in a corn and cabbage field. The electrodes used for the study were made of copper, and 3 profiles were carried parallel on each side of the plants profile line at a distance between the profiles of 5cm with a distance between the electrodes of 5cm as well.

Data processing and discussions

For data processing the software used for the inversion of the data was Res2DInv, and for creating 3D models and horizontal slices we've used Res3DInv with visualisation in ParaView. The data was correlated and calibrated with the position of the plants and with the depth of each layer of soil depending on the case. The processing of the data was carried for each profile and for each type of array separately and compared to different combinations of electrode array, for example: Schlumberger and the experimental array (Stummer et al, 2004).

It was observed from the data, that there are significant differences between different types of plants, experimental and natural environment, before or after the plant was watered and the number of the plants. For the box whit only one plant there is a significant anomaly (fig3) that correlates very well with the position of the plant, before the plant was watered.

In the agricultural field, after facing many challenges regarding the contact between the electrodes and

the aeration of the top soil (due to ploughing), and was expected to see different anomalies than the ones in the controlled environment in laboratory. Therefore, (fig2) the anomalies can easily correlate with the exact place of the plants, but because of the unevenness of the soil and other perturbations from natural environments, other anomalies with the same parameter appeared on the resistivity section. The plants in the agricultural field were watered regularly (every day). Also we were still able to differentiate a level at the top that differentiates in parameters from the much deeper ones, of a thickness of approximately 7cm.

Conclusions

An innovative experimental approach was presented for a better understanding of how to apply geophysical methods in agricultural environments. By creating new complementary equipment that allowed us to be more flexible in data acquisition style and parameters, which resulted in being able to use non-standard electrode arrays in a very time efficient mode. Doing measurements in both experimental controlled environments in the laboratory and in a natural agricultural field, we were able to understand the limitations of the data when it comes to the natural environments. We were able, in the laboratory to minimise the errors that might occur due to human errors regarding the position of the electrodes and switching of the electrodes while doing ERT's (electrical resistivity tomography). The natural environment it represents a bigger challenge due to the mechanical characteristics of the soil, which can interfere with the quality of the data. Even though it was challenging to work in these kind

of environments, we were still able to differentiate at least a level of the plant root extent area.

Acknowledgements

We would like to give our special thanks to Phil Atkins and Farzad Hayati for helping us through guidance, support and building the electrical equipment. We would also like to thank to Paulina Anastasiu for supporting our research and also to the COST TU1208 Action.

References

Stummer, P., Maurer, H. and Green A.G. [2004] Experimental design: Electrical resistivity data sets

that provide optimum subsurface information. Geophysics, 69, 120-139.

Werban, U., Hagrey, S.A. and Rabbel, W. [2008] Monitoring of root-zone water content in the laboratory by 2D geolectrical tomography. Journal of Plant Nutrition and Soil Science, 171, 927-935.

Hagrey, S.A. [2012] Geophysical Imaging Techniques. [2012] Measuring Roots. Springer Verlag, Berlin Heidelberg, 151-189.

Wilkinson, P.B., Meldrum, P.I., Chambers, J.E., Kuras, O. and Ogilvy, D. [2006] Improved strategies for the automatic selection of optimized sets of electrical resistivity tomography measurements configurations. Geophysical Journal International, 167, 1119-1126.

Reynolds, J.M. [2011] An Introduction to Applied and Environmental Geophysics – 2nd ed. Wiley- Blackwell. 289-346

Hagrey, S.A. [2007] Geophysical imaging of root-zone, trunk, and moisture heterogeneity.

Journal of Experimental Botany, 58, 839-854.

Hagrey, S.A. and Petersen, T. [2011] Numerical and experimental mapping of small root zones using optimized surface and borehole resistivity tomography. Geophysics, 76, 25-35.

Michot, D., Benderitter, Y., Dorigny, A., Nicoullaud, B., King, D. and Tabbagh, A. [2003]

Spatial and temporal monitoring of soil water content with an irrigated corn crop cover using

surface electrical resistivity tomography. Water Resources Research, 39, 1-20.

Abstract EAGE 2019 Near Surface Geophysics, Hague, Netherlands.

Integrating Resistivity and GPR Data for Plant Root Study in Indoor Agricultural Environments

Alexandra G. Gerea[1], Andrei E. Mihai[2]

[1,2]School of Electronic, Electrical and Computer Engineering, University of Birmingham

Introduction

With the ongoing climate conditions continuing to change, the agricultural sector will be one of the most affected areas, needing to adapt to the new conditions in order to produce more food for the increasing world population.

The use of geophysical methods in agriculture is no longer a novelty, as it is already widely deployed, helping farmers and plant growers improve their crops (Allred et al. 2008; Hagrey 2007). However, it still leaves plenty of room for improvement, especially in the area of precision agriculture.

Using geophysical methods in precision agriculture can improve our understanding of how different factors impact the data, improving survey design and data interpretation in an efficient way. The potential usability is significant: geophysical data can be used to optimize water (Michot et al. 2003; Werban et al. 2008) and fertilizer consumption, as well as to assess other relevant soil and plant parameters, creating a more sustainable approach to agriculture.

For a better understanding on how to apply geophysical methods in plant root detection and agriculture, an indoor experimental setting was created. In the previous version of this setup (Gerea and Mihai, 2018), the size of the boxes was unsuitable for GPR data acquisition, so a new setup was designed to enable the correlation of integration of GPR and resistivity data.

Experimental setting

The setting for the experiments consists of 2 indoor plastic boxes with a volume of 133 liters, measuring 88x29x40 cm. The boxes were uniformly filled with compost and tomato plants were grown from seed inside the boxes. Tomatoes were chosen for their ability to resist under stress and more severe conditions (conclusion based on previous tests with a various number of different types of agricultural plants). Two acrylic plates were designed and used for fixing the position of the resistivity electrodes. The plates allow the easy removal and insertion of electrodes while maintaining a fixed position, thus ensuring that no positioning errors were made.

Both types of surveys, resistivity and GPR were carried to mimic different conditions such as drought, high-water percentage and the use of fertilizers.

Acrylic tubes with a length of 1m and an inner diameter of 144mm were also used for this study. The purpose of the tubes was to be able to collect vertical resistivity data for single plants, using a combination of experimental arrays, similar to borehole surveys, using variations of the classical arrays described by Hagrey (2011). The tubes were only used for resistivity surveys so far.

In order to have an equal spreading of the water quantity (as areas with more/less water interfere with the results) an automatic micro-irrigation system was developed using an IoT (Internet of Things) system featuring readily available electronic devices and environmental sensors (humidity, luminosity, temperature).

Resistivity surveys

The resistivity equipment consists of a combination of commercial and custom equipment. A four-electrode resistance meter from RM Frobisher was used in conjunction with a switch box was designed and created in the laboratory, for the purpose of deploying an electrical resistivity tomography (ERT) using various types of regular and irregular electrode configurations. The electrodes used for the experiment were made of stainless steel with a length of 40cm and at a fixed position of 5cm apart. A dataset of 6 profiles consisting of 16 electrodes is presented here (Figure 3).

Electrode configurations used in this study, were: Wenner, Dipole-Dipole, Schlumberger (Figure 1) and an optimized survey array (Stummer et al. 2004; Wilkinson et al. 2006).

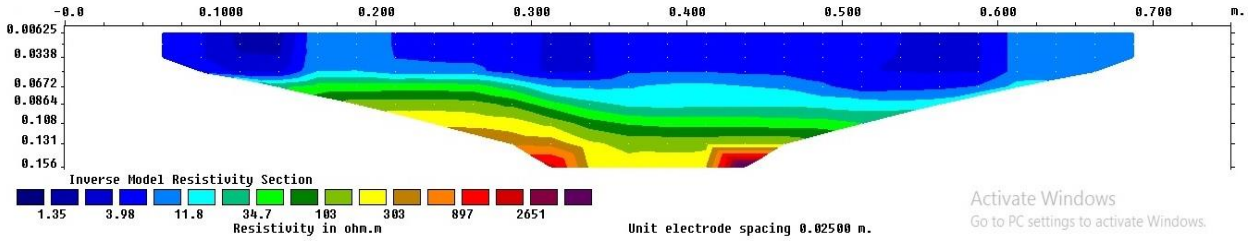

Figure 1 *Resistivity section in one of the boxes with young plants (2 months old) using a Schlumberger array. The unit electrode spacing appears as 0.025 as a discretization unit was used.*

Data processing was carried with two resistivity processing software: the commercial Res2DInv and Res3DInv. Thanks to the flexibility of the surveys, especially the surveys from the tubes, an open-source resistivity inversion software was also used, BERT, and for the visualization of the data another open-source software was used, ParaView.

GPR surveys

The equipment used for the GPR surveys consists of a UTSI GPR equipment with two different antennas from the same company, a 4GHz and a 1.5GHz antenna. Before starting the surveys in the boxes with the GPR system, several surveys were carried in the botanical gardens in the Birmingham area, for a better understanding of what to expect and how to properly use and plan the GPR surveys for the indoor systems. The use of the method in the botanical gardens allowed the surveys to be carried for various types of plants, with different types of roots.

***Figure 2**. Example of the GPR system used in the box with 3 tomato plants*

Figure 3. Example of the acrylic plates and the electrodes already inserted and ready for survey.

The measurements were carried out in time mode, not using the wheels provided as they were adding unnecessary extra length to the antenna and reducing the surveyable surface. In addition, the wheels are quite sensitive to these types of surfaces, especially the wheels from the 4GHz antenna (Figure 2), and were reducing the quality of the data, as they weren't able to roll properly.

The distance between the profiles used for this survey was 2.5cm. The dimensions of the box and the antenna only allowed 6 profiles to be carried in the box, 3 on each side of the plants. Measuring tapes were fixed to the box in order to ensure precision and create profiles as continuous and straight as possible. Only surveys in one direction were carried out.

For the GPR data processing the software used was ReflexW for 2D visualization and processing and creating 3D slices and interpretation. Different sequences of data processing were used, starting with a classical approach but adapting depending on the visibility degree of the reflections.

Conclusions and Discussions

This study represents a very thorough experimental study in which high-frequency GPR and ERT were used in order to understand the use of geophysical methods in agricultural environments. The experimental setup offers a high degree of flexibility regarding the environment, being able to control important parameters such as water and fertilizer content.

Knowing these parameters offers a deeper understanding of the potential and limitations of the methods, as well as the degree of precision that can be achieved in different conditions. In turn, this leads to a better understanding and interpretation of geophysical data in an agricultural context.

Building custom lab equipment to improve the data acquisition process and to be able to control different parameters such as acquisition time and electrode configuration also represents a great advantage and improvement when it comes to time efficiency, integration of the data and interpretation.

The resistivity data is capable of highlighting the root areas of the tomato plants in the boxes, even for plants as young as 2 months old. An example of the inverted data using Res2DInv software can be seen in Figure 1, where the position of the plants is correlated with low resistivity values. This result was expected as the survey was developed during a period of 5 days since not watering the plants. As the water drains to the bottom of the box and the top surface of the soil becomes dryer, the root zone area creates a contrast with the surrounding environment due to the high moisture content of the roots and in the very close vicinity.

The processing flow is important, and must be adapted to the environmental setting. Compared to classical surveys, it leaves much less room for error. For instance, gain function plays a very important role in all the GPR sections, whereas bandpass filters were not nearly as useful compared to surveys carried outside.

Compared to the resistivity data, the GPR data appears to show a horizontal layer in which the root zones normally appear, which are characterized by a horizontal level with many fine

hyperbolas. The depth to which the reflections are visible coincides with the depth derived from the resistivity values. Several small reflections coincide with the position of the plants.

The use of IoT devices, even relatively simple ones, made the setup cheaper and more reliable, increasing the precision of the data and offering important information, through environmental sensors. This offers an important context for interpreting geophysical data, and is also important in a practical context, where the deployed geophysical methods must be cost-effective to be successfully implemented.

Both geophysical methods proved to be working very well on such a small scale, after several modifications were made to the equipment and adaptations to the processing flow. It still represent a very fast and useful tool in understanding what happens in the hidden half of the plant growth. Even though more research is required, so far it is possible to conclude that both methods can detect the root zone area of the plants. Also, both geophysical methods can offer useful information regarding different parameters of the subsurface, like water and fertilizer content and is able trough monitoring to highlight water drainage and fertilizer spreading patterns

References

Allred,J.B., Daniels, J.J, Ehsani, M.R.[2008] Handbook of Agricultural Geophysics. Taylor and Francis.

Gerea, A. and Mihai, A. [2018] Geophysics Applied in Precision Agriculture – Experimental Resistivity Studies for Plant Root Detection and Analysis. 24th European Meeting of Environmental and Engineering Geophysics 2018. (Abstract)

Hagrey, S.A. [2007] Geophysical imaging of root-zone, trunk, and moisture heterogeneity. Journal of Experimental Botany, 58, 839-854.

Hagrey, S.A. and Petersen, T. [2011] Numerical and experimental mapping of small root zones using optimized surface and borehole resistivity tomography. Geophysics, 76, 25-35.

Michot, D., Benderitter, Y., Dorigny, A., Nicoullaud, B., King, D. and Tabbagh, A. [2003] Spatial and temporal monitoring of soil water content with an irrigated corn crop cover using surface electrical resistivity tomography. Water Resources Research, 39, 1-20.

Stummer, P., Maurer, H. and Green A.G. [2004] Experimental design: Electrical resistivity data sets that provide optimum subsurface information. Geophysics, 69, 120-139.

Werban, U., Hagrey, S.A. and Rabbel, W. [2008] Monitoring of root-zone water content in the laboratory by 2D geolectrical tomography. Journal of Plant Nutrition and Soil Science, 171, 927-935.

Wilkinson, P.B., Meldrum, P.I., Chambers, J.E., Kuras, O. and Ogilvy, D. [2006] Improved strategies for the automatic selection of optimized sets of electrical resistivity tomography measurements configurations. Geophysical Journal International, 167, 1119-1126.

International Geoscience Student Conference 2019, Uppsala Sweden.

High frequency GPR measurements in indoor experimental precision agriculture studies

Alexandra G. Gerea[1], Andrei E. Mihai[2]

[1,2]School of Electronic, Electrical and Computer Engineering, University of Birmingham

By 2050 the world's population will rise up to 10 billion people, which means that more food will need to be provided to feed the people under tougher climate conditions. Some areas are already affected by these climate conditions and by excessive agriculture. Creating agricultural environments in areas unsuitable for sustainable growth of the crops regarding high temperatures, drought, severe winds, and other climatic phenomena, will only contribute to more instability in the agricultural sector. A multidisciplinary approach to solving this complex problem is desirable, and this study focuses on integrating geophysical methods, agricultural studies and Internet of Things electronics. Geophysical methods have been used successfully in agricultural and environmental studies, but they are usually used on a very large scale.

In this study, we are trying to adapt the methods in order to have a higher precision on a smaller scale and to better understand the behavior of the roots of the agricultural plants and how different types of climatic conditions might affect both the geophysical data interpretation and the behavior of the plants. The boxes used for the experiments contain three

agricultural plants (tomatoes), and carefully selected types of soil. They were calibrated in the same way for all the measurements, to improve the precision of the results. Knowing the exact position of the plants and soil parameters, represents a high degree of precision and this aspect improves significantly the interpretation process.

The equipment used for the experiments is from Utsi Electronics and consists of two different high-frequency antennas, 1.5GHz and 4GHz, and the control unit. Internet of things devices were created in order to control different parameters in the boxes, like temperature, humidity, and luminosity. The data from the electrical equipment was used in order to better correlate and interpret the GPR data. The data was processed and analysed using ReflexW suite. For a better understanding of the limitations of the method, and for a better development of the experimental setting, measurements in natural environments were also carried.

Using a controlled environment, where relevant parameters (e.g. water content) were known, we were able to identify areas of root water uptake zone and detail about how these parameters affect the visibility of the roots. We implement a high degree of precision and detail, while also maintaining a practical perspective, employing geophysical methods that can reliably be implemented in an agricultural scenario.

Environmental Sensors – Determination of Plant Root Extent in Breeding New Varieties of Cash Crops

Alexandra G. Gerea[1], Andrei E. Mihai[2]

[1,2]School of Electronic, Electrical and Computer Engineering, University of Birmingham

Abstract

According to the UN statistics, by 2050 the population of the world will rise up to 9 billion people, which means 70% more food needs to be produced in order to feed them, under tougher climate conditions. This study focuses on using geophysical methods in precision agriculture by studying plant roots extend in different types of crops. It is important to study plant roots extent in agricultural environments in order to learn and understand more about the plant growth, root biomass changes (and other characteristics) and soil function. These factors are very important for a better understanding of the changes that occur in the environment and also the climate. This study tries to find a way in which agricultural plant roots could be identified in natural environments using non-invasive geophysical methods in order to help future studies in botany, agriculture, and climatology. Also, with this study, we try to find out what other information and parameters regarding plant roots we could find. Different from other studies regarding plant root detection using geophysical methods, this research has a different approach by using different and innovative ideas for the experiments and also creating very accurate synthetic models. The aim of the whole study is to understand what the limitations of the existing geophysical equipment are and how it can be improved in order to be able to give the most useful data that fits our research objective. Therefore, several

experimental types of equipment have been created in order to improve the pre-existent geophysical equipment so that it can adapt to this new target which is the study of plant roots.

Appendix D: Scientific Journal Publications

Near Surface Geophysics 2019

Mihai, A.E., Gerea, A.G., Curioni, G., Atkins, P., Hayati, F. (2019). Direct measurements of tree root relative permittivity for the aid of GPR forward models and site surveys:. Near Surface Geophysics, 17(3), 299-310. 10.1002/nsg.12043

Direct measurements of tree root relative permittivity for the aid of GPR forward models and site surveys

Andrei E. Mihai Alexandra G. Gerea Giulio Curioni Philip Atkins Farzad Hayati

ABSTRACT

Ground penetrating radar has been used extensively in near-surface studies to detect underground objects and features typically located within a few metres beneath the surface. In urban areas, ground penetrating radar is widely used to study buried utilities such as pipes and cables. A more recent and unconventional application of ground penetrating radar is the detection of tree roots, which can interact negatively with the human infrastructure in a number of ways. However, the geophysical study of tree roots has proven quite challenging and site-specific. Most tree roots (even coarse roots) have a small diameter and are hard to resolve through geophysical methods. In addition, the sheer amount of potential variability regarding the tree species, age, size, health and the subsurface environment (e.g., soil or a man-made material such as concrete or asphalt) makes it very hard to implement a one-size-fits-all approach. This is where robust, easily customizable forward models can be of assistance, indicating the range of detectable geophysical contrast and the limitations of the

method, as well as the suitable antenna frequencies. Here, a vector network analyser with a commercial open-ended coaxial probe was used to take direct measurements of the relative permittivity of freshly cut tree root segments at frequencies from 50 MHz to 3 GHz. The results were used as inputs to ground penetrating radar forward modelling using gprMax open source software, depicting various realistic scenarios which could be encountered in actual field surveys. The developed models help better understand the applicability, potential and limitations of ground penetrating radar surveys for detecting tree roots in different environments, aiding the development of future surveys. The notable variability in the tree roots is a significant consideration for surveys and forward models.

Danubius 2017

Mihai, A.E., Gerea, A.G., Micu, A. (2017), Application of geophysical methods in archaeological studies. Case study Negrilesti area, Galati county, Danubius, XXXV, Galați, 2017, pp. 9-31 .

Application of geophysical methods in archaeological studies. Case study Negrilesti area, Galati county

Andrei Mihai[1], Alexandra Gerea[2], Alexandru Micu[3]

[1,2] University of Birmingham, [3]University of Bucharest

Geophysical methods see more and more successful use in archaeological research. Their purpose is to create cross sections and maps to highlight archaeological elements below surface, which can then more easily be pinpointed either for excavation or conservation. The Negrilești-Curtea Școlii (Negrilești-School Yard) site, first investigated over 30 years ago, produced many archaeological evidence spanning from the early Neolithic all through to the modern age. Considering the large quantity of such evidence over a wide area, geophysical methods are ideally suited to study the subsoil and identify areas with archaeological potential. In total, seven distinct areas were studied, three of which were in the school yard proper and make the object of this paper. Following data acquisition, processing, and interpretation, we created maps and other materials representative of geophysical prospecting. All areas showed soil disturbances that can serve as indicators of archaeological potential. In some cases, these indicators pointed strongly to the existence of archaeological structures

buried in the subsoil.For example, ground penetrating radar and resistivity measurements suggest the presence of man-made structures (Fig. 7, Fig. 8), potentially archaeological in nature, in one of the areas (S2). In another area (S1), we see a highly-constrasting area that stands out from its surroundings (Fig. 4, Fig. 6). The nature of this anomaly was not initially clear judging from geophysical methods alone, but later digs confirmed it was indeed archaeological.Overall, our prospecting revealed significant anomalies that warrant more thorough research.

Appendix E: Abstracts and papers I have co-authored

Mihai, A.E., Gerea, A.G.(2016). Detecting Tree Roots In An Urban Environment With A 400 MHz GPR Antenna:. SAGEEP 2016 - 29th Annual Symposium on the Application of Geophysics to Engineering and Environmental Problems

Mihai, A.E., Gerea, A.G.(2018). The Use of Geophysical Methods in Identifying Tree Roots in Urban Areas. 24th European Meeting of Environmental and Engineering Geophysics. 10.3997/2214-4609.201802620

Mihai, A.E., Gerea, A.G., Atkins, P. (2019). The Use of Resistivity to Complement GPR Surveys on Tree Roots in Urban Areas. 25th European Meeting of Environmental and Engineering Geophysics. 10.3997/2214-4609.201902402

Mihai, A.E., Gerea, A.G (2017).The use of Ground Penetrating Radar to detect tree roots in an urban setting - Geophysical Research Abstracts Vol. 19, EGU2017-6867, 2017 EGU General Assembly 2017.

Appendix F: Full list of conferences and workshops I have participated in and/or presented paper/abstract.

COST Action TU1208 - Training School on Ground Penetrating Radar for road pavement assessment and detection of buried utilities, 2015 London, UK.

COST Action TU1208 - Aristotle University of Thessaloniki Training School on Numerical modelling of Ground Penetrating Radar using gprMax, 2015 Thessaloniki, Greece.

COST Action TU1208 - Training School on Non-destructive testing techniques for civil engineering, 2016 Barcelona, Spain.

7th International Geoscience Student Conference – IGSC 2016, Katowice, Poland

9th International Geoscience Student Conference – IGSC 2019, Uppsala, Sweden

24th European Meeting of Environmental and Engineering Geophysics – 2018, Porto, Portugal

25th European Meeting of Environmental and Engineering Geophysics – 2019, Hague, Netherlands

Euroscience Open Forum - ESOF 2018, Toulouse, France.

Appendix G: Data example codes for resistivity data processing

BERT file example: for a Wenner array survey, with 16 electrodes, the x and z position of each electrode, the number of data. The second part of the file consists of lines which contain the position of each electrode A, B, M, N for each measured point followed by the resistance value.

16# Number of electrodes

x z position for each electrode

0.05 0

0.1 0

0.15 0

0.2 0

0.25 0

0.3 0

0.35 0

0.4 0

0.45 0

0.5 0

0.55 0

0.6 0

0.65 0

0.7 0

0.75 0

0.8 0

35# number of data

a b m n rho

1	4	2	3	8.7996
2	5	3	4	13.2756
3	6	4	5	8.2581
4	7	5	6	11.4982
5	8	6	7	9.2458
6	9	7	8	11.1132
7	10	8	9	8.4239
8	11	9	10	9.9627
9	12	10	11	9.0971
10	13	11	12	12.8337
11	14	12	13	10.0563
12	15	13	14	8.2459
13	16	14	15	14.1668

1	7	3	5	13.1601
2	8	4	6	12.39
3	9	5	7	11.502
4	10	6	8	10.4644
5	11	7	9	11.7911
6	12	8	10	11.9678
7	13	9	11	11.2931
8	14	10	12	14.856
9	15	11	13	14.3497
10	16	12	14	10.7942
1	10	4	7	14.7771
2	11	5	8	15.2337
3	12	6	9	14.4876
4	13	7	10	15.1969
5	14	8	11	15.3741
6	15	9	12	17.3826
7	16	10	13	17.4522
1	13	5	9	19.5444
2	14	6	10	18.7404

3	15	7	11	19.0707
4	16	8	12	20.7536
1	16	6	11	22.8802

RES3DINV example file: in which the path of every file containing the resistivity profile is given, and the position of the file in the x, y grid.

Conversion of RES2DINV data files

Number of files to collate

3

File 1 parameters

Name of data file in RES2DINV format

C:\Users\Alexandrite\Desktop\RESISTIVITY DATA\date-cu-codul-tableta-array-slayer-g\2019-12-28-bis\dip_p3.dat

X and Y location of first electrode along this line

0.0, 0.0

Line direction (0=X,1=Y)

0

Line sign (0=positive,1=negative)

0

File 2 parameters

Name of data file in RES2DINV format

C:\Users\Alexandrite\Desktop\RESISTIVITY DATA\date-cu-codul-tableta-array-slayer-g\2019-12-28-bis\dip_p3_4.dat

X and Y location of first electrode along this line

0.0, 0.5

Line direction (0=X,1=Y)

0

Line sign (0=positive,1=negative)

0

File 3 parameters

Name of data file in RES2DINV format

C:\Users\Alexandrite\Desktop\RESISTIVITY DATA\date-cu-codul-tableta-array-slayer-g\2019-12-28-bis\dip_p4.dat

X and Y location of first electrode along this line

0.0, 1.0

Line direction (0=X,1=Y)

0

Line sign (0=positive,1=negative)

0

Name of output file in RES3DINV format

C:\Users\Alexandrite\Desktop\RESISTIVITY DATA\date-cu-codul-tableta-array-slayer-g\2019-12-28-bis\dip_3D.dat

End of file

RESIPY and RES2DINV file example – where the distance between the electrodes is set to 0.05, the resistivity array used is Schlumberger-Wenner with code 7, 102 measured points, number of electrodes 4. Every line represents the number of electrodes used for that specific measured point, with the position of the electrodes and the resistance value.

Mixed array

0.05

11

7

Type of measurement (0=app.resistivity, 1=resistance)

1

102

1

0

4 0.1 0 0.8 0 0.35 0 0.55 0 20.6787

4	0.1	0	0.25	0	0.15	0	0.2	0	8.5699
4	0.15	0	0.3	0	0.2	0	0.25	0	12.9097
4	0.2	0	0.35	0	0.25	0	0.3	0	11.3959
4	0.25	0	0.4	0	0.3	0	0.35	0	10.8077
4	0.3	0	0.45	0	0.35	0	0.4	0	11.3672
4	0.35	0	0.5	0	0.4	0	0.45	0	13.001
4	0.4	0	0.55	0	0.45	0	0.5	0	8.598
4	0.45	0	0.6	0	0.5	0	0.55	0	14.5629
4	0.5	0	0.65	0	0.55	0	0.6	0	11.1638
4	0.55	0	0.7	0	0.6	0	0.65	0	12.4418
4	0.6	0	0.75	0	0.65	0	0.7	0	8.5304
4	0.65	0	0.8	0	0.7	0	0.75	0	14.8068
4	0.05	0	0.3	0	0.15	0	0.2	0	2.9804
4	0.1	0	0.35	0	0.2	0	0.25	0	6.7649
4	0.15	0	0.4	0	0.25	0	0.3	0	5.7226
4	0.2	0	0.45	0	0.3	0	0.35	0	4.5194
4	0.25	0	0.5	0	0.35	0	0.4	0	5.2585
4	0.3	0	0.55	0	0.4	0	0.45	0	6.0499
4	0.35	0	0.6	0	0.45	0	0.5	0	2.7204

4	0.4	0	0.65	0	0.5	0	0.55	0	6.5473
4	0.45	0	0.7	0	0.55	0	0.6	0	4.537
4	0.5	0	0.75	0	0.6	0	0.65	0	4.1488
4	0.55	0	0.8	0	0.65	0	0.7	0	2.6234
4	0.05	0	0.4	0	0.2	0	0.25	0	3.0842
4	0.1	0	0.45	0	0.25	0	0.3	0	2.0699
4	0.15	0	0.5	0	0.3	0	0.35	0	1.7159
4	0.2	0	0.55	0	0.35	0	0.4	0	1.274
4	0.25	0	0.6	0	0.4	0	0.45	0	1.7298
4	0.3	0	0.65	0	0.45	0	0.5	0	1.1613
4	0.35	0	0.7	0	0.5	0	0.55	0	2.6829
4	0.4	0	0.75	0	0.55	0	0.6	0	0.5346
4	0.45	0	0.8	0	0.6	0	0.65	0	1.0458
4	0.05	0	0.5	0	0.25	0	0.3	0	0.522
4	0.1	0	0.55	0	0.3	0	0.35	0	0.0843
4	0.15	0	0.6	0	0.35	0	0.4	0	0.4533
4	0.2	0	0.65	0	0.4	0	0.45	0	0.364
4	0.25	0	0.7	0	0.45	0	0.5	0	3.306
4	0.3	0	0.75	0	0.5	0	0.55	0	0.3514

4	0.35	0	0.8	0	0.55	0	0.6	0	1.3496
4	0.05	0	0.6	0	0.3	0	0.35	0	2.0005
4	0.1	0	0.65	0	0.35	0	0.4	0	1.864
4	0.15	0	0.7	0	0.4	0	0.45	0	1.8186
4	0.2	0	0.75	0	0.45	0	0.5	0	4.6666
4	0.25	0	0.8	0	0.5	0	0.55	0	1.5408
4	0.05	0	0.7	0	0.35	0	0.4	0	2.9252
4	0.1	0	0.75	0	0.4	0	0.45	0	2.546
4	0.15	0	0.8	0	0.45	0	0.5	0	5.3747
4	0.05	0	0.8	0	0.4	0	0.45	0	3.1617
4	0.05	0	0.35	0	0.15	0	0.25	0	13.8714
4	0.1	0	0.4	0	0.2	0	0.3	0	16.3362
4	0.15	0	0.45	0	0.25	0	0.35	0	14.4908
4	0.2	0	0.5	0	0.3	0	0.4	0	15.0811
4	0.25	0	0.55	0	0.35	0	0.45	0	15.1896
4	0.3	0	0.6	0	0.4	0	0.5	0	13.9528
4	0.35	0	0.65	0	0.45	0	0.55	0	14.0831
4	0.4	0	0.7	0	0.5	0	0.6	0	15.7243
4	0.45	0	0.75	0	0.55	0	0.65	0	13.739

4	0.5	0	0.8	0	0.6	0	0.7	0	12.9645
4	0.05	0	0.45	0	0.2	0	0.3	0	12.1055
4	0.1	0	0.5	0	0.25	0	0.35	0	12.357
4	0.15	0	0.55	0	0.3	0	0.4	0	10.8649
4	0.2	0	0.6	0	0.35	0	0.45	0	11.5011
4	0.25	0	0.65	0	0.4	0	0.5	0	9.124
4	0.3	0	0.7	0	0.45	0	0.55	0	10.3861
4	0.35	0	0.75	0	0.5	0	0.6	0	11.2702
4	0.4	0	0.8	0	0.55	0	0.65	0	10.4238
4	0.05	0	0.55	0	0.25	0	0.35	0	9.2036
4	0.1	0	0.6	0	0.3	0	0.4	0	8.963
4	0.15	0	0.65	0	0.35	0	0.45	0	9.2472
4	0.2	0	0.7	0	0.4	0	0.5	0	6.7718
4	0.25	0	0.75	0	0.45	0	0.55	0	7.4468
4	0.3	0	0.8	0	0.5	0	0.6	0	9.6194
4	0.05	0	0.65	0	0.3	0	0.4	0	7.0508
4	0.1	0	0.7	0	0.35	0	0.45	0	8.1614
4	0.15	0	0.75	0	0.4	0	0.5	0	5.6667
4	0.2	0	0.8	0	0.45	0	0.55	0	6.5491

4	0.05	0	0.75	0	0.35	0	0.45	0	6.9071
4	0.1	0	0.8	0	0.4	0	0.5	0	5.1625
4	0.05	0	0.5	0	0.2	0	0.35	0	19.694
4	0.1	0	0.55	0	0.25	0	0.4	0	19.062
4	0.15	0	0.6	0	0.3	0	0.45	0	19.1112
4	0.2	0	0.65	0	0.35	0	0.5	0	16.8249
4	0.25	0	0.7	0	0.4	0	0.55	0	17.614
4	0.3	0	0.75	0	0.45	0	0.6	0	17.0831
4	0.35	0	0.8	0	0.5	0	0.65	0	19.0034
4	0.05	0	0.6	0	0.25	0	0.4	0	16.584
4	0.1	0	0.65	0	0.3	0	0.45	0	16.9158
4	0.15	0	0.7	0	0.35	0	0.5	0	14.4651
4	0.2	0	0.75	0	0.4	0	0.55	0	15.1412
4	0.25	0	0.8	0	0.45	0	0.6	0	15.2682
4	0.05	0	0.7	0	0.3	0	0.45	0	14.848
4	0.1	0	0.75	0	0.35	0	0.5	0	13.1934
4	0.15	0	0.8	0	0.4	0	0.55	0	14.4355
4	0.05	0	0.8	0	0.35	0	0.5	0	12.6293
4	0.05	0	0.65	0	0.25	0	0.45	0	22.763

4 0.1 0 0.7 0 0.3 0 0.5 0 21.4673

4 0.15 0 0.75 0 0.35 0 0.55 0 21.7302

4 0.2 0 0.8 0 0.4 0 0.6 0 22.059

4 0.05 0 0.75 0 0.3 0 0.5 0 19.3503

4 0.05 0 0.2 0 0.1 0 0.15 0 12.3449

4 0.05 0 0.8 0 0.3 0 0.55 0 26.9222

0

0

0

0

0

Appendix H: example file for gprMax 2D GPR models

comands:

python3 -m gprMax newmodels/template.in -n 300, 40 traces

python3 -m tools.outputfiles_mergehdf5 model_Bscan_2D 40, all traces in one file

python3 -m tools.plot_hdf5_Bscan model_Bscan_2D_all.out Ez, inverse hdf5-bscan,for Ez field

#title: 1.5GHz antenna model of 3 roots with stem

#domain: 0.60 0.20 0.002

the size of the domain x y z. upper area with air

#dx_dy_dz: 0.002 0.002 0.002

discretisation

#time_window: 4e-9

time in seconds

#time_step_limit_type: 2D

#pml_cells: 10 10 0 10 10 0

negative x,y,z positive x,y,z

#material: 20 0 1 0 soil

material: relative perm, conductivity, rel perm, magnetic loss, name

#material: 9 0 1 0 test_material

#material: 6 0 1 0 stem

#material: 15 0 1 0 root

#waveform: ricker 1 1.5e9 my_ricker

type of waveform(ricker, gaussian, gaussiandotnorm...), amplitude, frequency Hz, name

#hertzian_dipole: z 0.020 0.170 0 my_ricker

polarization (x,y,z), x, y, z of antenna, name

#rx: 0.060 0.170 0

receiver x y z

#src_steps: 0.002 0 0

#rx_steps: 0.002 0 0

increments for moving source

#box: 0 0 0 0.6 0.170 0.002 soil

x y z pentru lower left corner si x y z pentru upper right

box: 0 0 0 0.240 0.100 0.001 test_material

#box: 0.100 0.180 0 0.120 0.200 0.002 stem

#box: 0.090 0.130 0 0.130 0.180 0.002 root

#box: 0.300 0.180 0 0.320 0.200 0.002 stem

#box: 0.290 0.130 0 0.330 0.180 0.002 root

#box: 0.500 0.180 0 0.520 0.200 0.002 stem

#box: 0.490 0.130 0 0.530 0.180 0.002 root

soil_peplinski: 0.05 0.95 2.0 2.66 0.001 0.25 my_soil

sand fraction, clay fraction, soil density, sand density, clay water, sand water, identifier

fractal_box: 0 0 0 0.6 0.2 0.002 1.5 1 1 1 50 my_soil my_fractal_box

x,y,z lower left, x,y,z upper right, fractal dimension(0-3), fractal weight x,y,z, number of materials for distribution, identifier mixing model, identifier fractal box

#geometry_view: 0 0 0 0.60 0.20 0.002 0.002 0.002 0.002 alexandrabasic n

x y z lower left, x y z upper right, discretisation x y z, file name, n or f